Characterization of Physical and Functional Interactions Between the Chromatin Assembly Factor 1, CAF-1, and Homologous Recombination Factors During DNA Repair

Dingli Dai

Caractérisation des interactions physiques et fonctionnelles entre le facteur d'assemblage de la chromatine, CAF-1, et des facteurs de la recombinaison homologue au cours de la réparation de l'ADN

Thèse de doctorat de l'Université Paris-Saclay
préparée à l'Université Paris-Sud

École doctorale n°577, Structure et Dynamique
des Systèmes Vivants, (SDSV)
Spécialité de doctorat: Sciences de la vie et de la santé

Thèse présentée et soutenue à Orsay, le 21 décembre 2018, par

Dingli Dai

Composition du Jury :

Simon Saule Directeur de Recherche, Institut Curie (UMR 3347)	Président
Stefania Francesconi Chercheur, Institut Pasteur (CNRS)	Rapporteur
Jean-Pierre Quivy Chercheur, Institut Curie (UMR 3664)	Rapporteur
Constance Alabert Directeur de Recherche, University of Dundee (School of Life Sciences)	Examinateur
Françoise Ochsenbein Directeur de Recherche , CEA, (I2BC)	Examinateur
Sarah Lambert Directeur de Recherche, Institut Curie (UMR3348)	Directeur de thèse

Université Paris-Saclay
Espace Technologique / Immeuble Discovery
Route de l'Orme aux Merisiers RD 128 / 91190 Saint-Aubin, France

Université Paris-Saclay
Institut Curie- Section de Recherche

THÈSE
Pour obtenir le grade de

Docteur en Sciences de L'Université Paris-Saclay
École doctorale « Structure et dynamique des systèmes vivants »

Présentée et soutenue par
Dingli DAI
le 21 décembre 2018

Caractérisation des interactions physiques et fonctionnelles entre le facteur d'assemblage de la chromatine, CAF-1, et des facteurs de la recombinaison homologue au cours de la réparation de l'ADN

Jury

Prof. Simon Saule	Président du Jury
Dr. Stefania Francesconi	Rapporteur
Dr. Jean-Pierre Quivy	Rapporteur
Dr. Constance Alabert	Examinateur
Dr. Françoise Ochsenbein	Examinateur
Dr. Sarah Lambert	Directeur de thèse

N° INE : 0JJ0DQ06P53

Characterization of physical and functional interactions between the chromatin assembly factor 1, CAF-1, and homologous recombination factors during DNA repair

Acknowledgement

From the beginning until today, I have spent three years and seven months on the journey of PhD thesis at Institut Curie. This has been a momentous period in my life as I have learnt so much from it. Now it is the time to express my gratitude to the people who have helped me, supported me and influenced me.

First, I would like to give my thanks to all the jury members:

Prof. Simon Saule, for accepting being the president of the jury.

Dr. Jean-Pierre Quivy and Dr. Stefania Francesconi, for reading and correcting my manuscript.

Dr. Constance Alabert and Dr. Françoise Ochsenbein, for their willingness to be the examiners of my PhD thesis.

I would like to thank my supervisor, Dr. Sarah Lambert, for giving me the opportunity of doing my PhD thesis in her lab, for always inspiring me with great new ideas and for all the comments on my manuscript. The knowledge and scientific skills I have obtained under her supervision are tremendous.

I would like to thank all the previous and current members of Team LAMBERT. Especially Louise Dupoiron, Julien Hardy and Karine Fréon , for their great work on my project.

Karol Kramarz, Charlotte Audoynaud, and Ana Silva, for always charging me with positive attitude.

Vincent Pennaneach and Anissia Ait Saada, for all the kind help they gave me.

I would like to thank all the people from the unit.

Especially Dr. Mounira Amor-Guéret, for accepting me in UMR 3348.

Claire Lovo from the Plateforme IBiSA d'Imagerie Cellulaire et Tissulaire and Patricia Duchambon from Plateforme Production Protéines Recombinantes, for helping me so much with their great professional skills.

Rosine, Tania, Dorothée, Hélène, Alina, Géraldine, Virginie, Åsa, Domi, Meng-er, Sudarshan and Kamila, for all the help from them and happy moments with them.

I would like to give my special thanks to ANR (Agence Nationale de la Recherche), for funding my PhD thesis

I deeply thank my beloved families and friends, for they were always listening to me when I was at my lowest point. Without you, I would not have made it.

Table of Contents

Abbreviations

alt-NHEJ: alternative Non- Homologous End-Joining

Asf1: anti silencing function 1

BER: base excision repair

BIR: break-induced replication model

BLM: Bloom Syndrome RecQ like helicase

CAF-1: chromatin assembly factor1

CO: crossing-over

CPDs : cyclobutane-pyrimidine dimers

CPT: camptothecin

DDR: DNA damage response

D-loop: displacement loop

dNTP: deoxyribonucleotides

DSB: double strand break

DSBR: double-strand break repair

dsDNA:double strand DNA

EMSA: electrophoretic mobility shift assay

FRET: fluorescence resonance energy transfer

HJ/dHJ: (double) Holliday Junctions

HR: homologous recombination

HU: hydroxyurea

Hyg: hygromycine

ICL: Inter-strand Cross-link repair

IDLs: insertion-deletion loops

JM: joint molecules

Kan: geneticine

MCM: Mini-chromosome Maintenance Complex

MMR: mismatch repair

MMS: methyl methanesulfonate

MRX: Mre11-Rad50-Xrs2

Nat: nourseothricin

NCO: non-crossing-over

NER: nucleotide excision repair

NHEJ: non-homologous end joining

PCNA: proliferating cell nuclear antigen

PCR: polymerase chain reaction

PIP: PCNA Interacting Protein

PTMs: post-translational modifications

RDR: recombination-dependent replication

RFB: replication fork barrier

RFC: replication factor C

Rtf1: Replication Termination Factor 1

RTS1: Replication Termination Sequence

RMPs: recombination mediator proteins

RPA: replication protein A

SCE: sister chromatid exchange

SDSA: synthesis-dependent strand annealing

SSA: single strand annealing

ssDNA: single strand DNA

TCR: transcription-coupled repair (NER)

TLS: Translesion Synthesis

UV: Ultraviolet radiations

WHD: winged helix domain

Abstract

DNA is constantly exposed to both endogenous and exogenous genotoxic insults. Multiple DNA repair mechanisms are exploited to guard the genome and epigenome stability. Homologous recombination (HR) plays a major role in repairing DNA double strand breaks (DSBs) and restarting stalled replication forks under replicative stress. These two processes are both coupled to chromatin assembly. The chromatin assembly factor 1 (CAF-1) is a highly conserved histone chaperone known to function in a network of nucleosome assembly coupled to DNA repair and replication, by depositing newly synthesized histone $(H3\text{-}H4)_2$ tetramers onto the DNA. The fission yeast CAF-1 complex consists of three subunits: Pcf1, Pcf2 and Pcf3. CAF-1 has been previously reported to act at the DNA synthesis step during the process of recombination-dependent replication (RDR) and protects the D-loop from disassembly by the RecQ helicase family member, Rqh1. In this study, we addressed the role of CAF-1 during homologous recombination-mediated DNA repair in fission yeast.

Using *in vivo* and *in vitro* approaches, we validated interactions within a complex containing Rqh1, CAF-1, PCNA, and Histone H3. We showed that Rqh1 interacts with both Pcf1 and Pcf2 independently of each other, and the Pcf1-Rqh1 interaction is stimulated by DNA damage. We developed an *in vivo* chromatin binding assay to monitor the association of CAF-1 to the chromatin upon DNA damage. We observed that replication stress but not double strand break favors CAF-1 association to the chromatin. We identified that several HR factors are required for CAF-1 association to the chromatin upon replication stress. In support of this, we have identified physical interactions between Pcf1 and HR factors, including RPA and Rad51. Our data suggest that CAF-1 would associate to the site of recombination-dependent DNA synthesis through physical interactions with HR factors. Put together, this work contributes to strengthening the role of CAF-1 coupled to DNA repair, and reveals the crosstalk between HR factors and chromatin assembly.

Résumé

L'ADN est constamment exposé à des insultes génotoxiques endogènes et exogènes. Plusieurs mécanismes de réparations de l'ADN sont mis en œuvre pour préserver la stabilité du génome et de l'épigénome. La recombinaison homologue (RH) joue un rôle central dans la réparation des cassures double brin de l'ADN (CDBs) et le redémarrage des fourches de réplication en réponse à un stress réplicatif. Ces deux processus sont tous deux couplés à l'assemblage de la chromatine. Le facteur d'assemblage de la chromatine 1 (CAF-1) est un chaperon d'histone conservé au cours de l'évolution qui fonctionne dans le processus d'assemblage des nucléosomes couplé à la réparation de l'ADN et à la réplication, en déposant sur l'ADN les tétramères d'histones $(H3\text{-}H4)_2$ nouvellement synthétisés. Chez la levure *Schizosaccharomyces pombe*, le complexe CAF-1 est constitué de trois sous-unités, Pcf1, Pcf2 et Pcf3. Il a été montré que CAF-1 agit dans l'étape de synthèse de l'ADN durant le processus de réplication dépendante de la recombinaison (RDR) et protège le désassemblage des D-loops par l'hélicase Rqh1, membre de la famille des hélicases RecQ. Dans cette étude, nous avons adressé le rôle de CAF-1 pendant la réparation de l'ADN par recombinaison homologue chez la levure *Schizosaccharomyces pombe*.

En utilisant des approches *in vivo* et *in vitro*, nous avons validé des interactions protéines-protéines au sein d'un complexe contenant Rqh1, CAF-1, PCNA, et l'Histone H3. Nous avons montré que Rqh1 interagit avec Pcf1 et avec Pcf2 indépendamment l'un de l'autre, et que l'interaction Rqh1-Pcf1 est stimulée par des dommages à l'ADN. Nous avons mis en place une méthode d'analyse d'association de CAF-1 à la chromatine en réponse aux dommages à l'ADN. Nous avons observé qu'un stress réplicatif, mais pas l'induction de cassures double brin de l'ADN, favorise l'association de CAF-1 à la chromatine. Nous avons identifié plusieurs facteurs de la RH nécessaire pour l'association de CAF-1 à la chromatine en réponse à un stress réplicatif. De plus, nous avons mis en évidence des interactions physiques entre Pcf1 et des facteurs de la recombinaison homologue, parmi lesquels RPA et Rad51. Nos données suggèrent que CAF-1 pourrait s'associer aux sites de synthèse d'ADN dépendent de la recombinaison via son interaction avec des facteurs de la RH. L'ensemble des données de cette étude contribuent à renforcer le rôle de CAF-1 couplé à la réparation de l'ADN, et révèlent une interconnexion entre les facteurs de la RH et l'assemblage de la chromatine.

Résumé en français

L'ADN est constamment exposé à des insultes génotoxiques endogènes et exogènes. Plusieurs mécanismes de réparations de l'ADN sont mis en œuvre pour préserver la stabilité du génome et de l'épigénome. La recombinaison homologue (RH) joue un rôle central dans la réparation des cassures double brin de l'ADN (CDBs) et le redémarrage des fourches de réplication en réponse à un stress réplicatif. Ces deux processus sont tous deux couplés à l'assemblage de la chromatine. Le facteur d'assemblage de la chromatine 1 (CAF-1) est un chaperon d'histone conservé au cours de l'évolution qui fonctionne dans le processus d'assemblage des nucléosomes couplé à la réparation de l'ADN et à la réplication, en déposant sur l'ADN les tétramères d'histones $(H3\text{-}H4)_2$ nouvellement synthétisés. Chez la levure *Schizosaccharomyces pombe*, le complexe CAF-1 est constitué de trois sous-unités, Pcf1, Pcf2 et Pcf3. Il a été montré que CAF-1 agit dans l'étape de synthèse de l'ADN durant le processus de réplication dépendante de la recombinaison (RDR) et protège le désassemblage des D-loops par l'hélicase Rqh1, membre de la famille des hélicases RecQ. Dans cette étude, nous avons adressé le rôle de CAF-1 pendant la réparation de l'ADN par recombinaison homologue chez la levure *Schizosaccharomyces pombe*.

En utilisant des approches *in vivo* et *in vitro*, nous avons validé des interactions protéines-protéines au sein d'un complexe contenant Rqh1, CAF-1, PCNA, et l'Histone H3. Nous avons montré que Rqh1 interagit avec Pcf1 et avec Pcf2 indépendamment l'un de l'autre, et que l'interaction Rqh1-Pcf1 est stimulée par des dommages à l'ADN. Nous avons mis en place une méthode d'analyse d'association de CAF-1 à la chromatine en réponse aux dommages à l'ADN. Nous avons observé qu'un stress réplicatif, mais pas l'induction de cassures double

brin de l'ADN, favorise l'association de CAF-1 à la chromatine. Nous avons identifié plusieurs facteurs de la RH nécessaire pour l'association de CAF-1 à la chromatine en réponse à un stress réplicatif. De plus, nous avons mis en évidence des interactions physiques entre Pcf1 et des facteurs de la recombinaison homologue, parmi lesquels RPA et Rad51. Nos données suggèrent que CAF-1 pourrait s'associer aux sites de synthèse d'ADN dépendant de la recombinaison via son interaction avec des facteurs de la RH. L'ensemble des données de cette étude contribuent à renforcer le rôle de CAF-1 couplé à la réparation de l'ADN, et révèlent une interconnexion entre les facteurs de la RH et l'assemblage de la chromatine.

Dommages à l'ADN et réponse cellulaire

Les stress exogènes et endogènes sont constamment rencontrés par une cellule tout au long de sa vie. En conséquence, des dommages à l'ADN sont potentiellement présents sur tous les chromosomes, ce qui entraîne l'accumulation de mutations et augmente donc le risque d'instabilité du génome. L'instabilité du génome n'est pas seulement une caractéristique des cellules cancéreuses, elle est également la cause de nombreuses maladies humaines. Pour préserver l'intégrité, les cellules ont développé des réseaux complexes en réponse aux dommages causés à l'ADN, appelés «Réponse aux dommages causés à l'ADN». La réponse aux dommages de l'ADN (DDR) inclut la régulation et la coordination de multiples voies comprenant les points de contrôle du cycle cellulaire, les voies de réparation de l'ADN, les mécanismes de tolérance aux dommages de l'ADN et la dynamique de la chromatine pour influer en fin de compte sur le destin des cellules (Giglia-Mari et al., 2011). La réponse aux dommages de l'ADN est étroitement régulée pour garantir l'élimination définitive des lésions de l'ADN.

Dommages à l'ADN et voies de réparation

Pour contrer les conséquences néfastes des dommages causés à l'ADN, les cellules ont utilisé plusieurs voies de réparation de l'ADN pour corriger les dommages causés à l'ADN. Les voies de réparation de l'ADN comprennent: la réparation par excision de base (BER), le mécanisme prédominant pour réparer les bases endommagées, entraînant une distorsion mineure de la structure de la double hélice de l'ADN; la réparation par excision de nucléotides (NER), une voie polyvalente pour éliminer les adduits d'ADN volumineux tels que les dimères de pyrimidine induits par les UV-C; la réparation des mésappariements (RMA), qui joue un rôle important dans l'élimination des bases mal incorporées lors de la réplication de l'ADN; et la réparation de la double rupture de l'ADN, qui contient deux mécanismes importants: la recombinaison homologue (HR) et la jonction d'extrémité non homologue (NEHJ) (Dexheimer, 2013).

Recombinaison homologue (HR)

La recombinaison homologue (HR) joue un rôle vital dans le maintien de la stabilité du génome. Au-delà de la réparation par DSB, la recombinaison homologues est également impliquée dans d'autres processus cellulaires importants.

Au cours de la méiose, la formation programmée de DSB est répartie le long des chromosomes, via la catalyse d'un complexe de topoisomérase contenant la protéine spécifique de la méiose conservée au cours de l'évolution (Keeney et al., 1997). Les DSB déclenchent ensuite la recombinaison entre les chromosomes paternel et maternel afin de promouvoir l'échange d'informations génétiques. La recombinaison méiotique est

essentielle à la génération de la diversité génétique et à l'évolution moléculaire, elle contribue également à assurer un alignement correct des paires de chromosomes homologues sur le fuseau (Baudat et al., 2013; Davis et Smith, 2001).

Le rôle de la recombinaison homologue dans la réparation de l'ADN

Plusieurs modèles de réparation DSB par HR ont été proposés, tels que la réparation classique à double brin (DSBR), le recuit par brin dépendant de la synthèse (SDSA), le recuit à simple brin (SSA) et la réplication induite par rupture (BIR). La plupart de ces modèles reposent sur une étape de résection de l'ADN dans le sens de 5 'à 3', une étape de recherche d'homologie, une étape d'invasion de brin médiée par la recombinase Rad51 et la formation d'une structure à boucle en D (boucle de déplacement).

Le rôle de la recombinaison homologue dans la réplication de l'ADN

La réplication complète et fidèle de l'ADN est essentielle au maintien de l'intégrité du génome. L'exposition à des contraintes endogènes et exogènes, ainsi que des obstacles intrinsèques tels que les barrières de fourche de réplication (RFB) peuvent interférer avec les mécanismes de réplication de l'ADN, conduisant à un arrêt de la fourche de réplication (Lambert et Carr, 2013). Le non-maintien de l'intégrité de la fourche de réplication peut entraîner une augmentation des mutations génétiques, un réarrangement génomique et même une létalité.

Les contraintes de réplication peuvent entraîner le blocage de la progression des fourches de réplication (arrêt de la fourche). Différentes perturbations de la réplication arrêtent la fourche de réplication de différentes manières, notamment des fourches bloquées et des

fourches dysfonctionnelles / effondrées. Un blocage de réplication se produit lorsque la progression du réplisome est entravée par des obstacles alors que les composants du réplisome sont conservés. Ainsi, les fourches bloquées restent compétentes pour la réplication et peuvent être reprises sans autre intervention. Considérant que les fourches dysfonctionnelles peuvent être brisées ou non, en fonction de l'association avec une rupture double brin (DSB) ou non, respectivement. Les fourches dysfonctionnelles peuvent avoir des composants de réplication de perte et nécessiter une intervention ultérieure pour être reprises (Carr et Lambert, 2013; De Piccoli et al., 2012). Quand un fourche de réplication est bloqué, il peut être sauvé par la convergence avec le fourche opposé ou par le mécanisme HR.

La recombinaison homologues constituent une voie cruciale et efficace pour le sauvetage des fourches effondrées. Le rôle de recombinaison homologues dans l'escorte des fourches de réplication comprend la protection des fourches, le redémarrage des fourches, la réparation des fourches cassées ou des lacunes post-réplicatives. Les facteurs de fréquence cardiaque favorisent la convergence des fourches et participent à la réplication dépendante de la recombinaison (RDR) pour permettre la reprise de la synthèse de l'ADN à partir de fourches arrêtées lorsqu'un fourche convergente n'est pas disponible.

Assemblage de nucléosomes à la fourche de réplication

La duplication des chromosomes doit conserver fidèlement à la fois les informations génétiques codées par l'ADN et les informations épigénétiques intégrées à la chromatine. La chromatine constitue une barrière intrinsèque à la machinerie de réplication de l'ADN. Par conséquent, les nucléosomes situés en avant de la fourche de réplication avancée sont

expulsés et les histones parentales et nouvellement synthétisées sont assemblées sur de l'ADN nouvellement répliqué par le biais d'un processus appelé assemblage de la chromatine couplée à la réplication. Du fait que le matériel ADN double pendant la réplication de l'ADN, des histones nouvellement synthétisées sont nécessaires en temps utile pour conserver le conditionnement de la chromatine et les informations épigénétiques.

En conséquence, la chromatine nouvellement répliquée est composée d'histones parentales préexistantes ainsi que d'histones nouvellement synthétisées. L'assemblage de la chromatine couplée à la réplication nécessite un réseau de facteurs chromatiniens, y compris des modificateurs d'histone chaperon et d'histone, qui opèrent des réactions séquentielles pour gérer la dynamique de l'histone sur des fourches de réplication en cours.

Les histones sont des protéines chargées positivement et ont une affinité intrinsèque pour l'ADN chargé négativement. Sans histones chaperones pour assurer l'incorporation appropriée de l'histone dans l'ADN, des histones solubles pourraient être impliquées dans la formation non spécifique d'agrégation histone-ADN. Les histones chaperones sont une classe de protéines eucaryotes hautement conservées qui se lient à des histones simples ou complexes pour favoriser leur dépôt de manière contrôlée sur l'ADN, sans faire partie du produit final (Laskey et al., 1978; Polo et al., 2006a; Ray -Gallet et al., 2002a). Les chaperons d'histones sont des protéines chargées négativement nécessaires pour escorter les histones afin d'éviter les interactions malsaines et pour assembler / désassembler la chromatine. Depuis l'élucidation de la fonction histone chaperon de la nucléoplasmine par des approches biochimiques classiques en 1978 (Laskey et al., 1978), le nombre de membres de la famille des histones chaperons ne cesse de croître. Jusqu'à présent, une variété de chaperons d'histones ont été identifiés pour fonctionner dans différents processus cellulaires et

présentant des affinités distinctes pour les variants d'histones et d'histones. Selon leurs substrats d'histones, les histones chaperons sont classées en deux familles principales: les chaperons H2A-H2B et les chaperons H3-H4 (tableau 3.1) (Gurard-Levin et al., 2014; Ramirez-Parra et Gutierrez, 2007).

Le facteur d'assemblage de la chromatine 1, CAF-1

L'identification du CAF-1 remonte à 1986, lorsque Stillman et ses collègues remarquèrent que des extraits cytoplasmiques de cellules 293T étaient capables de faciliter la réplication de l'ADN du plasmide SV40, mais aucun autre mini-chromosome n'avait été formé avant l'ajout d'extraits nucléaires de cellules 293T (Stillman, 1997). 1986). Une telle observation a conduit aux travaux suivants de Stillman et Smith, dans lesquels ils purifiaient un complexe hétérotrimérique contenant p150, p60 et p48 à partir des noyaux de cellules humaines. Ce complexe présentait l'activité d'assemblage d'histones couplées à la réplication de l'ADN, d'où le nom CAF-1 (Chromatin Assembly Factor 1) (Smith et Stillman, 1989). D'autres études ont confirmé que les trois sous-unités de CAF-1 suivaient un stoichiomerty de 1: 1: 1 lors de la formation du complexe et qu'un nouveau motif d'acétylation de la lysine était identifié sur l'histone H4 co-purifiée avec le complexe de CAF-1 (Verreault et al. , 1996). Depuis lors, de nombreuses études sur le CAF-1 ont été effectuées sur divers organismes, permettant ainsi de réaliser la haute conservation de la fonction du CAF-1, ainsi que son rôle crucial dans l'assemblage des nucléosomes lors de la réplication et de la réparation de l'ADN. Les trois sous-unités de CAF-1 sont Pcf1, Pcf2 et Pcf3 dans S. pombe.

Rôles du CAF-1 lors de la réparation de l'ADN

Outre le rôle discuté précédemment du CAF-1 dans le dépôt d'histones couplées à la réplication de l'ADN, le CAF-1 est également un acteur actif dans la restauration de la chromatine dans le réseau DDR. De plus, des études ont également mis en avant le rôle du CAF-1 dans la promotion d'événements de réparation de l'ADN au-delà de sa fonction d'histone chaperon (Baldeyron et al., 2011). Cette section sera consacrée aux activités de CAF-1 dans le contexte de la réparation de l'ADN.

Objectifs

Un rapport précédent avait identifié une interaction physique et directe entre la grande sous-unité de CAF-1, p150, de mammifère et le BLM d'hélicase RecQ, in vivo et in vitro (Jiao et al., 2004). BLM et p150 ont été trouvés co-localisés in vivo au sein de foyers nucléaires discrets en réponse à des dommages à l'ADN et au stress de réplication. De plus, BLM inhibe l'assemblage de la chromatine induite par CAF-1, associé à la réparation de l'ADN. Dans la levure à fission, le laboratoire a précédemment signalé un nouveau rôle pour CAF-1 dans la réplication dépendante de la recombinaison (RDR) (Pietrobon et al., 2014). La levure de fission CAF-1 a été trouvée en train d'agir à l'étape de synthèse de l'ADN de RDR pour protéger la boucle D du désassemblage par l'hélicase RecQ Rqh1, l'orthologue de BLM pour levures à fission. Le laboratoire a proposé que la probabilité d'instabilité chromosomique au site des fourches arrêtées résulte d'activités antagonistes du CAF-1 et du Rqh1 dans le traitement des intermédiaires de recombinaison: Rqh1 favorise le désassemblage de la boucle D et le CAF-1 contrecarre cette activité. De manière intéressante, une interaction in vivo entre Rqh1 et Pcf1 a également été identifiée, montrant que les interactions physiques et fonctionnelles entre les hélicases CAF-1 et RecQ sont conservées au cours de l'évolution.

Le modèle de travail résumant les observations précédentes est présenté à la figure 1 (Pietrobon et al., 2014). Cependant, plusieurs questions restent à résoudre: 1) quel est le rôle de l'interaction physique entre CAF-1 et Rqh1 dans le maintien de la stabilité du génome en réponse au stress de réplication, 2) Comment la CAF-1 s'associe-t-elle aux sites RDR, 3) La chromatine fonction d'assemblage du CAF-1 est-elle nécessaire pour promouvoir le RDR?

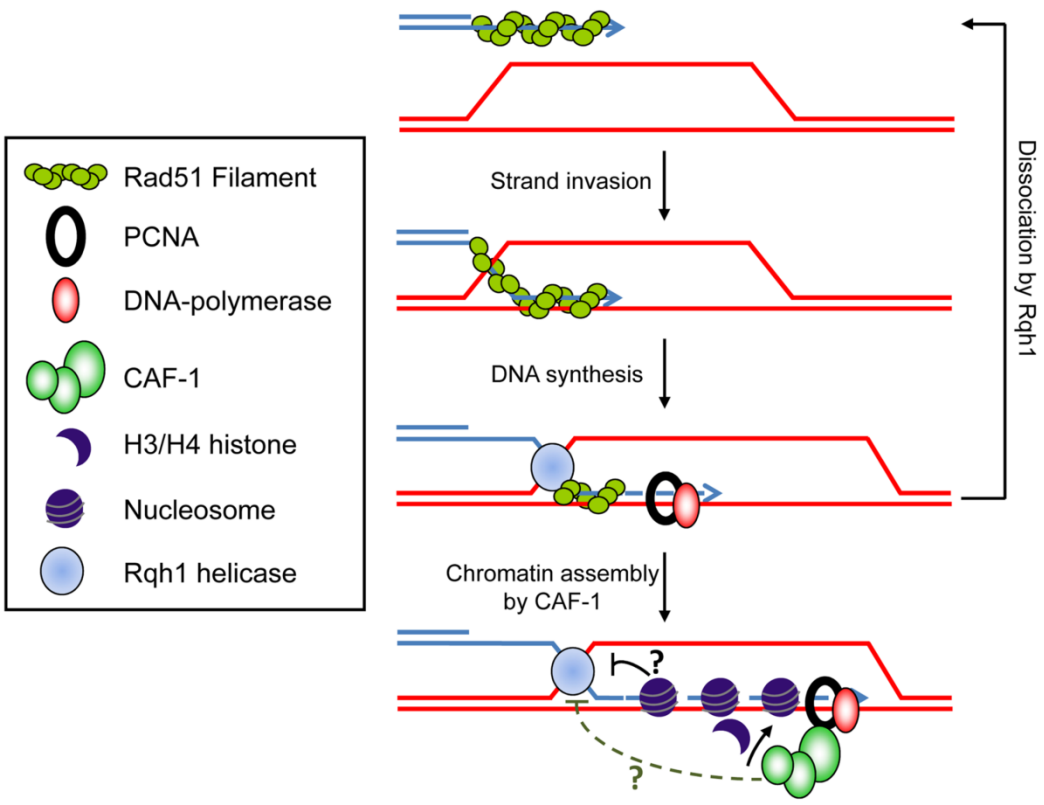

Figure 1. Modèle de travail de la stabilisation de la boucle D par CAF-1 à l'étape de synthèse de l'ADN de la réplication dépendante de la recombinaison (RDR). Le CAF-1 pourrait empêcher le désassemblage de la boucle D en favorisant le dépôt d'histones couplé à la synthèse d'ADN au cours de la RDR. L'ADN nouvellement synthétisé sur la boucle D est assemblé en chromatine et peut neutraliser l'activité de désassemblage de la boucle D de Rqh1 (ligne noire). Alternativement, CAF-1 est ciblé sur la boucle D via son interaction avec PCNA et contrecarre l'activité de Rqh1 directement ou indirectement (ligne verte en pointillés). Cependant, le ciblage

de CAF-1 sur la boucle d pourrait également être médiatisé via son interaction avec des facteurs de recombinaison homologues. Adapté de Pietrobon et al., 2014 (Pietrobon et al., 2014).

Au cours de ma thèse, j'ai contribué à répondre à ces trois questions. J'ai combiné des approches in vivo et in vitro pour caractériser l'interaction physique entre CAF-1 et Rqh1. J'ai développé un test de liaison à la chromatine in vivo pour explorer l'association entre CAF-1 et la chromatine en réponse aux dommages de l'ADN. Le test a également été utilisé pour aborder le rôle des facteurs HR dans l'association de CAF-1 à la chromatine.

Des études récentes ont fourni des données précieuses sur l'architecture du complexe CAF-1, ainsi que des informations sur les mécanismes de dépôt d'histones par CAF-1 (examiné par Sauer et al., 2018). Le CAF-1 en tant qu'histone chaperon contribue au maintien de la stabilité du génome. La carence en CAF-1 altère l'assemblage de la chromatine couplée à la réplication et entraîne l'instabilité des fourches en progression qui nécessitent un traitement par la machinerie HR (Clemente-Ruiz et Prado, 2009; Clemente-Ruiz et al., 2011; Endo et al., 2006a; Myung et al., 2003). Cependant, l'interaction entre les événements de réparation de l'ADN lors d'un stress de réplication et la restauration de la chromatine reste difficile à atteindre. Dans cette étude, la diaphonie du CAF-1 et les facteurs HR au cours du RDR ont été étudiés. Mes données ont révélé un rôle plutôt dynamique de chaque sous-unité CAF-1 dans le réseau RDR et indiquent que l'association de CAF-1 à la chromatine est obtenue par des mécanismes de régulation complexes composés de multiples facteurs de recombinaison homologues. À la lumière d'études antérieures rapportant le rôle du CAF-1 dans la stabilisation de la boucle D pendant le RDR (Pietrobon et al., 2014; Hardy et al., Publication en cours de préparation), les travaux de cette étude ont ajouté des détails sur le mécanisme de régulation du CAF. -1 dans ce contexte. Les comportements différents de chaque sous-unité CAF-1 en association avec la chromatine endommagée soulèvent également la nécessité d'étudier l'importance d'une telle divergence. En

outre, il a été rapporté que la forte expression de CAF-1 était associée à divers types de cancer, alors que le stress de réplication est une cause majeure d'instabilité du génome et est une marque des cellules cancéreuses (Gaillard et al., 2015; Polo et al., 2010). . Par conséquent, déchiffrer le rôle de CAF-1 dans le réseau RDR pourrait également offrir une valeur clinique potentielle.

Introduction

1. DNA damage and cellular response

Exogenous and endogenous stresses are constantly encountered by a cell throughout its lifespan. As a consequence, DNA damages are potentially occurring all over the chromosomes, leading to the accumulation of mutations and thus increasing the risk of genome instability. Genome instability is not only a hallmark of cancer cells, it is also a cause of many human diseases. To safeguard the integrity of the integrity, cells have developed complex networks in response to DNA damage that are referred to as the "DNA Damage Response". DNA damage response (DDR) includes the regulation and coordination of multiples pathways comprising cell cycle checkpoints, DNA repair pathways, DNA damage tolerance mechanisms and chromatin dynamics to ultimately impact cell fate (Giglia-Mari et al., 2011). DNA damage response is tightly regulated to ensure the faithful removal of DNA lesions.

1.1. Types of DNA damage and their origins

Surrounding environment and cellular metabolic processes are the sources of several types of DNA lesions with distinct toxicity. In order to maintain the cellular fitness, cells are equipped with multiple DNA repair machineries to deal with different types of DNA damage (Figure 1.1). If DNA lesions fail to be repaired or are improperly repaired, serious consequences such as gene mutations and chromosome rearrangement can occur that contribute to the development of a wide range of human diseases including cancer (Weeden and Asselin-Labat, 2018).

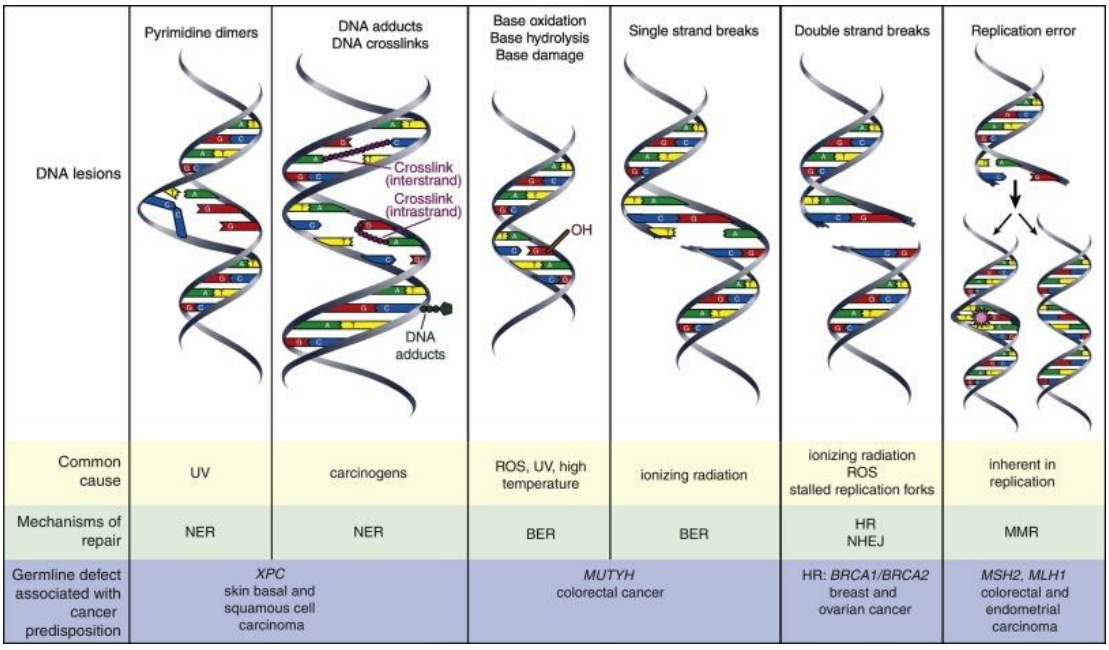

Figure 1.1. Different types of DNA lesions, their causing sources, and respective DNA repair pathways. Certain DNA lesions are found to be in association with cancer predisposition. Adapted from Weeden and Asselin-Labat, 2018 (Weeden and Asselin-Labat, 2018).

UV-C irradiation-induced pyrimidine dimers

Accounting for about 10% of the sunlight, ultraviolet (UV) light is the most common exogenous DNA damaging source. The wavelength of UV light ranges from 10 nm to 400 nm, and three classes are applied to subdivide the UV light: UVA (315-400 nm) and UVB (280-315 nm) have longer wavelengths and they can cause oxidative stress and protein denaturation to cells; while UV-C (100-280 nm) has a shorter wavelength and higher energy, thus causes more severe damages to the cell, especially to the DNA. With the protection from the stratospheric ozone layer, most of the UV-C irradiation is efficiently absorbed before reaching the earth (McKenzie et al., 2003).

UV photons damage the DNA molecules. The major harmful photoproducts includes cyclobutane-pyrimidine dimers (CPDs) which count for 75%, and to a less extent 6-4 photoproducts (6-4PPs) which count for 25% of UV-mediated DNA lesions, respectively (Ravanat et al., 2001; Sinha and Häder, 2002). Nucleotide excision repair (NER) is the dedicated DNA repair pathway for removing UV-induced DNA lesions.

DNA adducts and DNA crosslinks

DNA adducts are covalent modifications of the DNA after the exposure to reactive carcinogen chemical species. The most common environmental factor is cigarette smoke, other sources include alkylating agents, chemotherapy medications as well as endogenous metabolic intermediates (Huang et al., 2011; Swenberg et al., 1985, 2011)

DNA adducts can block DNA replication. To continue DNA replication, cells have the translesion DNA synthesis (TLS) mechanism to bypass the adducts. Translesion DNA polymerases utilized in TSL include the Y-family Pol η, κ, ι and Rev1, and the B-family Pol ζ. They are different from DNA replicative polymerases δ and ε (Yagi et al., 2017). TLS can be error-free or error-prone, which is largely dependent on the structure of DNA adducts and the polymerase involved (Basu et al., 2017; Sale, 2013). DNA adducts may also alter the regulation of gene transcription by completely or partially blocking the elongation. The removal of DNA adducts is mainly through the NER machinery (Cai et al., 2012).

DNA crosslinks can be either inter-strand or intra-strand. Main causes of these DNA lesions are found to be environmental mutagens and chemotherapeutic agents. Intra-strand DNA crosslinks can be recognized and removed by the NER pathway (Huang and Li, 2013; O'Donovan et al., 1994; Szymkowski et al., 1992). Inter-strand DNA crosslinks (ICLs) can prevent the separation of the DNA duplex and thus block the access of DNA repair and transcription machineries, and intact ICLs can lead to cell death (Noll et al., 2006). The repair of ICLs largely respects the stage of the cell cycle: during G1 phase, NER contributes to the removal of a subset of ICLs, whereas in S and G2 phase, there are also other DNA repair mechanisms involved, such as homologous recombination, TLS and Fanconi Anemia/BRCA pathway (Deans and West, 2011; Moynahan et al., 2001; Rothfuss and Grompe, 2004; Sarkar et al., 2006; Sasaki and Tonomura, 1973; Wood, 2010).

DNA single strand breaks (SSBs)

DNA single strand breaks (SSBs) arise when discontinuity occurs on one strand of the DNA duplex. Common forms of SSBs are the loss of a single nucleotide or damaged 3'- or 5'- termini (Caldecott, 2008). Given the aqueous cellular environment, DNA is undergoing spontaneous hydrolysis that gives rise to abasic AP sites (apurinic/apyrimidinic sites). In addition, AP sites also occur as repair intermediates during the process of base excision repair (BER) (Boiteux and Guillet, 2004; Lindahl, 1993). The generation of damaged 3'- or 5'- termini via the cleavage of AP sites by AP endonuclease or glycosylase- results in SSBs. Other endogenous or exogenous insults including reactive oxygen species (ROS), innate erroneous or abortive topoisomerase I (TOP I) activity and ionizing radiation (IR), and are also known to give rise to SSBs. SSBs can induce replication stress when they are encountered by replication forks in S phase, leading to the formation of replication-associated one-ended double strand break or a broken fork (Magdalou et al., 2014; Petermann et al., 2010). The repair mechanisms of SSBs may differ according to the damaging sources. However, the processes share the similarity of four basic steps: the detection of SSBs, DNA end processing, DNA gap filling and ligation.

DNA double strand breaks (DSBs)

DNA double strand breaks (DSBs) are formed by simultaneously severing the phosphor-sugar backbone of both strands of a DNA duplex in close proximity, leading to the physical dissociation of two DNA ends (Jackson, 2002). DSBs are among the most cytotoxic lesions. Unrepaired or misrepaired DSBs can lead to the process of mutagenesis, carcinogenesis and cell death (Bennett

et al., 1993; Khanna and Jackson, 2001). In metazoan, one DSB can result in the inactivation of an essential gene or trigger apoptosis (Rich et al., 2000). Additionally, DSBs are also deliberately programmed during meiosis in order to initiate meiotic crossovers between homologous chromosomes as well as to promote accurate chromosome segregation (need a ref here: Murakami and keeney 2008). During V(D)J recombination of developing lymphocytes, programmed DSBs are instrumental in creating various antigen-receptors in vertebrates (8; Schatz and Swanson, 2011). There are many factors that can bring DSBs into the genome, including chemotherapeutic drugs, IR and replication stress. The repair of DSBs mainly relies on two highly conserved pathways, namely homologous recombination (HR), and non-homologous end joining (NEHJ). The choice of which pathway to employ is largely cell-cycle regulated and the relative importance of these two pathways differs in organisms.

1.2. DNA replication stress

The maintenance of DNA replication accuracy is of paramount importance in order to guard genomic stability. DNA is duplicated in S phase, during which the chromatin structure has been primed for the accommodation of the machinery to initiate DNA replication as well as multiple replication-coupled processes. Chromatin is de-condensed by ATP-dependent remodeling factors to alter the histone occupancy by moving or ejecting histones (Falbo and Shen, 2006). At the transition of G1/S phase, certain histone modifications such as acetylation are required for the specification and activation of replication origins (Raynaud et al., 2014). The DNA duplex also needs to be separated in order to serve as the template for the replication machinery.

In eukaryotes, DNA replication is initiated with the licensing followed by the firing of multiple replication origins at which bidirectional replication forks are formed (Diffley, 2011). There are numerous obstacles on the DNA that can impede the progression of replication forks (Figure 1.2) (Lambert and Carr, 2013; Masai et al., 2010). Given the fact that there are multiple ongoing replication forks along the genome, one impeded replication fork could be rescued by another converging fork, or by firing another replication origin in close proximity. Indeed, most eukaryotic genome contain a considerable amount of dormant origins which have been licensed by the helicase Mcm2-7 (mini chromosome maintenance complex 2-7), but do not fire during normal replication. Multiple studies have provided evidences showing that these dormant origins are used as a “backup” for rescuing stalled forks and to complete DNA replication in conditions of replication stress (Ge et al., 2007; Kawabata et al., 2011; Woodward et al., 2006).

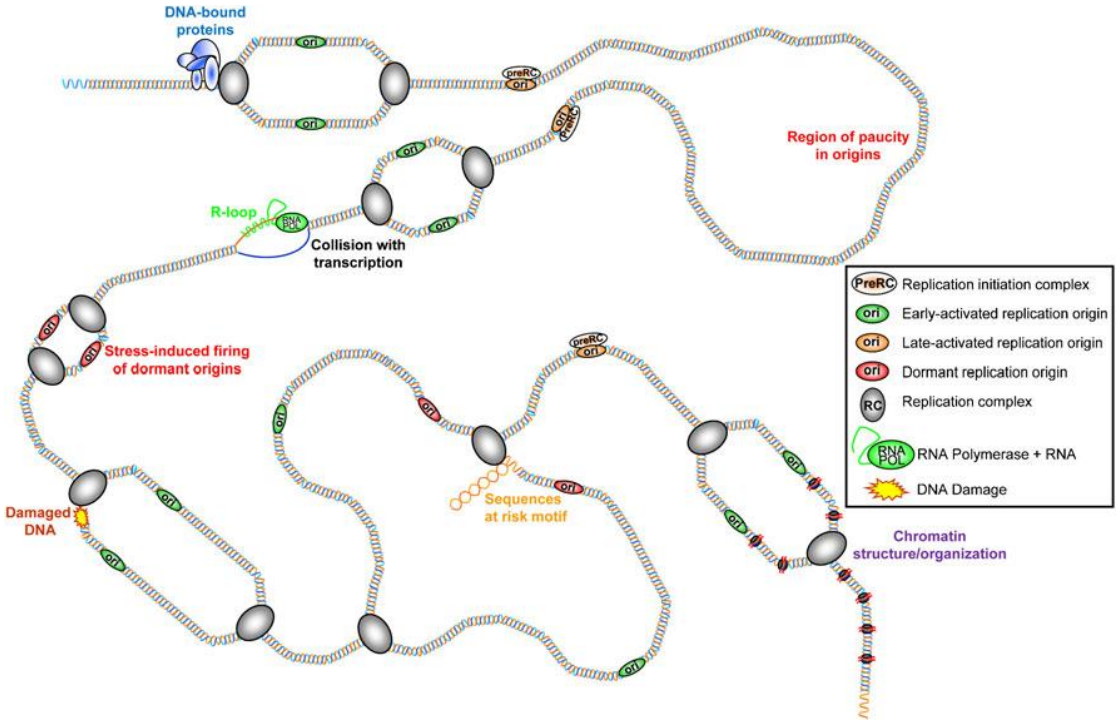

Figure 1.2. An overview of genomic obstacles encountered by the replication fork. Adopted from Lambert and Carr, 2013 (Lambert and Carr, 2013).

The transcription machinery may collide with the replication machinery causing fork stalling (Aguilera and García-Muse, 2012; Deshpande and Newlon, 1996). DNA itself can also give rise to replication fork impediments by forming secondary DNA structure such as inverted repeats, palindromic sequences, hairpins and tri-nucleotides repeats (Lobachev et al., 2007; Mirkin and Mirkin, 2007; Voineagu et al., 2008). Any unrepaired or newly introduced lesions on the DNA such as nicks on a single-strand DNA and DSBs will also hinder replication fork progression.

Genomic loci containing a paucity of replication origins are linked to sites of fragility, and they are associated with increased genome rearrangement. Such sites that are referred to as fragile sites are found to vary in different tissue types. For example, the placements of replication origins of human *FRA3B* (the most frequently expressed common fragile site localized within human chromosomal band 3p14.2) and *FRA16D* (common chromosomal fragile site localized within human chromosomal band 16q23.2) are differently fragile in lymphocytes and in fibroblasts, in a way that these loci are more fragile in lymphocytes (Letessier et al., 2011; Palakodeti et al., 2009; Le Tallec et al., 2011). In the regions associated with a paucity of replication initiation events, the replication fork needs to keep progressing for a rather long distance. Thus, there is a higher chance for the replication fork to meet more impediments, and as a result, the duplication of such region is more stress-sensitive.

The lack of dNTP triggers global replication stress. Inhibitors such as hydroxyurea (HU) which depletes the dNTP pool via the inhibition of the ribonucleotide reductase, and Aphidicolin which irreversibly inhibits DNA polymerase Pol α, slow down the velocity of replication fork and consequently lead to replication fork stalling (Vesela et al., 2017).

Replication stress is an unavoidable disturbance which needs to be resolved in order to achieve complete DNA replication in a timely and accurate manner. To this end, there are multiple approaches to ensure the continuity of replication and support its robustness. First, DNA repair mechanisms and DNA damage bypass mechanisms can minimize the risk of the encounter between replication obstacles and the fork. Secondly, the intra-S checkpoint is activated in response to DNA damage, leading to the halt of the cell cycle so that the cell has time to achieve DNA replication before entering into mitosis. Lastly, merging with a converging fork and homologous recombination-mediated replication fork processing will safeguard the completion of DNA replication (reviewed by Lambert and Carr, 2013). The chapter 2.4 will be dedicated to how homologous recombination supports the robustness of DNA replication.

1.3. DNA damage response

The DNA damage response (DDR) is activated by DNA structures resulted from DNA damage or DNA replication stress. The DDR network is orchestrated by four major groups: DNA damage sensors, signal transducers, downstream mediators, and effectors (Figure 1.3).

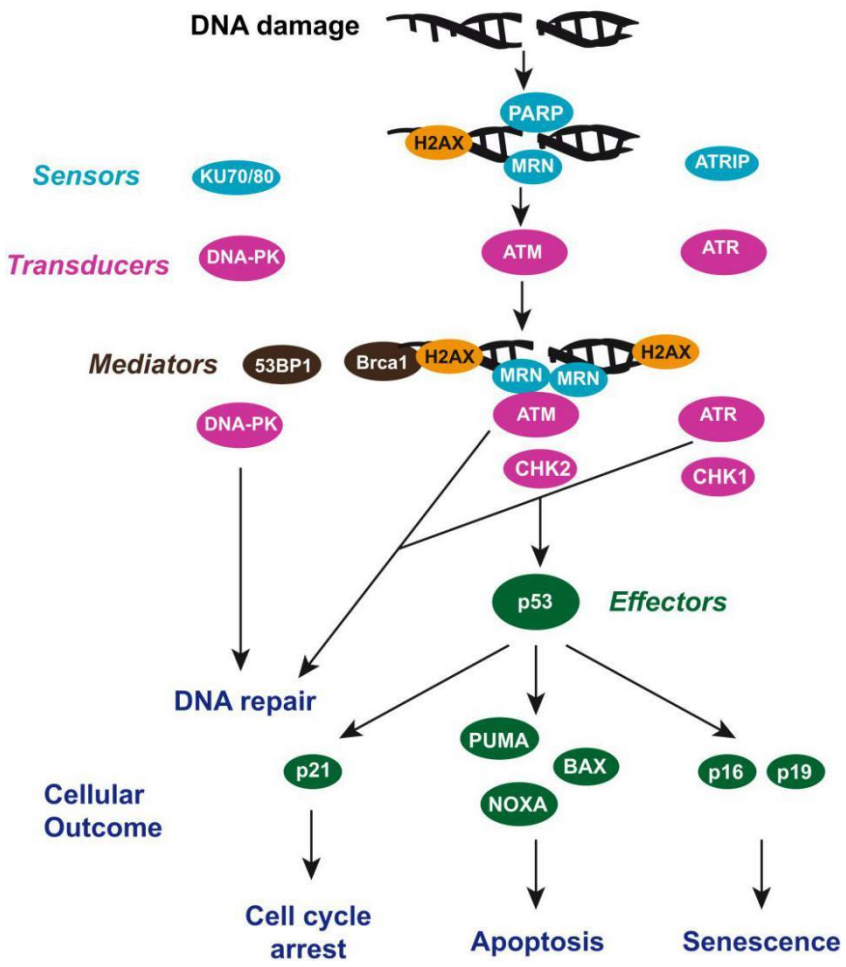

Figure 1.3. The framework of DDR signaling pathways. Adapted from Blanpain et al., 2011 (Blanpain et al., 2011).

In response to replication stress, RPA-coated single-stranded DNA (ssDNA) is the initial signal/sensor to trigger the master transducer, the ATR kinase (*Ataxia Telangiectasia and Rad3-related*) (38). In the case of DSBs, DNA lesions are sensed by the MRN complex (Mre11-Rad50-Nbs1) with ATM (*Ataxia-Telangiectasia Mutated*) and DNA-PKcs (DNA-dependent protein kinase catalytic subunit) being the major primary responding kinases. ATR, ATM and DNA-PKcs are members of the phosphoinositide-3-kinase-related protein kinase (PIKK) family, their activation involves their recruitment to damaged sites (Falck et al., 2005; Maréchal and Zou, 2013). The activation of ATM and ATR leads to subsequent phosphorylation events of many target proteins, among which is the histone variant H2AX. The phosphorylation at serine 139 of H2AX (γ-H2AX) occurs abundantly and rapidly in response to DNA damage. Thus, it has been profoundly used as the marker of DNA damage and local activation of checkpoint (Burma et al., 2001; Sharma et al., 2012; Ward and Chen, 2001).

Among all the factors involved in DDR in metazoan, the effector p53, a tumor suppressor, p53, is one of the most important players. Half of the cancers either lack p53 or have mutated versions of p53. Thus, p53 is referred to “the guardian of the genome” (Lane, 1992). The main function of p53 is to bind DNA and induce the transcription of a subset of genes in response to cellular stress (Riley et al., 2008).

DNA damage activates checkpoint pathways allowing the cell cycle to halt transiently so that DNA repair events can take place. There are three major checkpoints triggered by DNA structures, namely G1/S, intra-S and G2/M checkpoint. These distinct checkpoints control the progression of cell cycle at different phases. Nonetheless, the proteins involved are commonly shared (Wang et al., 2015).

1.4. DNA repair pathways

To counteract harmful consequences of DNA damage, cells employed multiple DNA repair pathways to correct DNA damage. DNA repair pathways consist of: base excision repair (BER), the predominant mechanism to fix damaged bases causing minor distortion of DNA double-helix structure; nucleotide excision repair (NER), a versatile pathway to remove bulky DNA adducts such as UV-C-induced pyrimidine dimers; mismatch repair (MMR), which plays an important role to rule out the misincorporated bases during DNA replication; and DNA double strand break repair, which contains two important mechanisms: homologous recombination (HR) and non-homologous end joining (NEHJ) (Dexheimer, 2013).

Base excision repair (BER)

When small base lesions are introduced to the DNA by chemical modification such as deamination, oxidation, or methylation, or via spontaneous DNA decay, the DNA duplex structure is not significantly altered. DNA lesions are recognized as the substrate by the BER pathway. The core of BER pathways is composed of four proteins: a DNA glycosylase, the DNA-apurinic/apyrimidinic endonuclease, DNA polymerase, and DNA ligase. The DNA glycosylase has the role to initiate BER by severing the N-glycosyl bond between the sugar and the base so that the damaged base is removed, and this step creates an apurinic/apyrimidinic site (AP site). The choice of which DNA glycosylase to utilize is based on the type of DNA lesion, and it also fine-tunes the subsequent steps. The resulting AP site is then incised by DNA-apurinic/apyrimidinic endonuclease 1 (APEX1), and the 5‘-deoxyribosephosphate (dRP) residue is removed by the dRP lyase, the one-nucleotide gap left behind is lastly filled up by DNA polymerase Pol β and DNA

ligase. It is noteworthy that, if DNA replication happens prior to the completion of BER, point mutation could still be introduced into the genome (Figure 1.4) (Krokan and Bjørås, 2013).

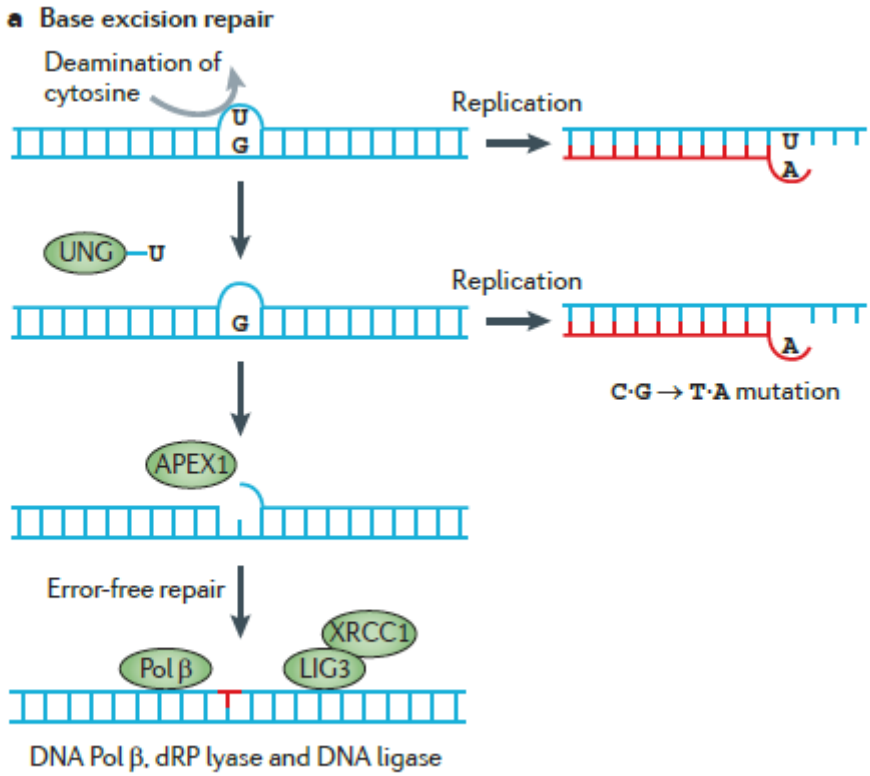

Figure 1.4. Model of repairing a deaminated cytosine by BER. The DNA Uracil-DNA glycosylase (UNG) is used here to remove the uracil residue. Adapted from Helleday et al., 2014 (Helleday et al., 2014).

Nucleotide excision repair (NER)

In contrast to BER, the substrates of NER are bulky DNA helix-distorting lesions such as pyrimidine dimers, 6–4 photoproducts and cisplatin-DNA intra-strand crosslinks. There are two sub-pathways of NER depending on the context in which it takes place: the global genome NER (GG-NER) and transcription-coupled NER (TC-NER). Multiple enzymes are involved in NER to recognize a wide range of thermo-dynamically DNA duplex-destabilizing lesions. In the case of TC-NER, the NER is triggered by RNA polymerase stalling at the lesion via the help of TC-NER specific factors CSA (Cockayne syndrome group A) and CSB (Cockayne syndrome group B). Likewise, if the process of NER is interrupted by DNA replication at this step, mutations will be introduced (Helleday et al., 2014). Core NER factors are shared by both TC-NER and GG-NER in the following steps. Two incisions are made on both sides of the DNA lesion enabling the

removal of a 24 to 32-nucleotide oligo containing the DNA lesion, the gap is later filled in by polymerase Pol δ, Pol ε or Pol κ (Figure 1.5) (Laat et al., 1999; Schärer, 2013).

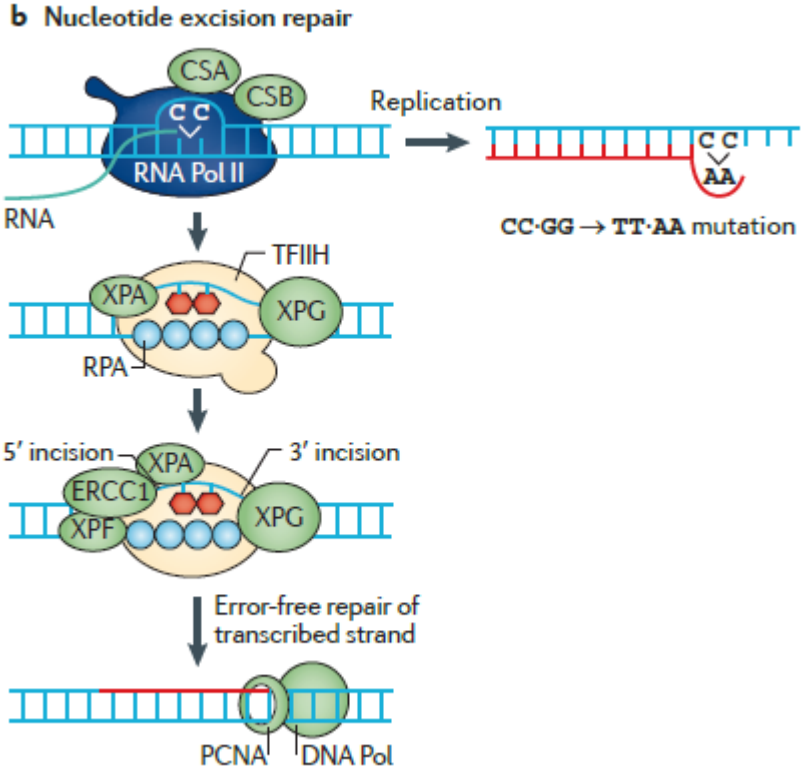

Figure 1.5. Model of TC-NER.Adapted from Helleday et al., 2014 (Helleday et al., 2014).

Mismatch repair (MMR)

Mismatch repair is a highly conserved pathway to eliminate base-base mismatches, incorrectly incorporated bases, as well as insertion/deletion loops (IDLs) resulting from polymerase slippage during DNA replication. It is essential for suppressing spontaneous mutation (Barrera-Oro et al., 2008; Huang et al., 2003). The MMR pathway is divided into three major steps. First, the substrates of MMR are recognized by the DNA mismatch recognition protein heterodimers (MSH2-MSH6 complex for recognizing base-base mismatches and small IDLs, and MSH2-MSH3 complex for recognizing large IDLs). Second the error-containing strand is then degraded by exonuclease 1 (Exo1) through its 5’ to 3’ exonuclease activity, resulting in an extensive gap on a single strand of the DNA. Third, the gap is eventually re-synthesized by the polymerase Pol δ along the DNA via PCNA interaction, and the remaining nicks are sealed by DNA ligase I (Figure 1.6) (Li, 2008a).

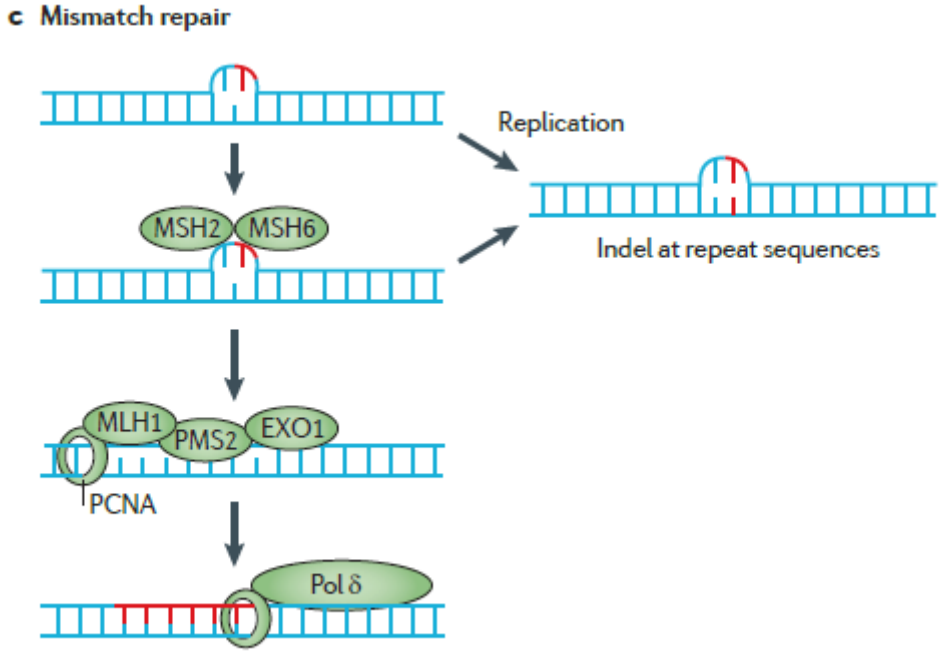

Figure 1.6. Model of MMR.Adapted from Helleday et al., 2014 (Helleday et al., 2014).

DNA double strand break repair

DSBs are among the most hazardous DNA lesions. Even a single unrepaired DSB is sufficient to cause the death of a haploid cell (Bennett et al., 1993; Nowsheen and Yang, 2012). Moreover, misrepaired DSBs are usually associated with oncogenic aberrations. There are two major mechanisms utilized by the cell to fix DSBs: homologous recombination (HR), and non-homologous end joining (NEHJ). The HR mechanism operates when a sequence of homology is present, which usually is the sister chromatid. Therefore, HR tends to be restricted to S and G2 phase. While the NHEJ pathway is active throughout the cell cycle, with an elevated activity when cells progress from G1 to G2/M phase (Dexheimer, 2013; Mao et al., 2008). The mechanism of homologous recombination will be the main focus in the next chapter.

2. Homologous recombination

The crucial roles of the two highly conserved mechanisms, namely homologous recombination (HR) and non-homologous end joining (NHEJ) in repairing DSBs, have been mentioned in the previous chapter. Besides these two major pathways, there are additional pathways involved in DSB repair such as alternative end joining (alt-EJ). The choice to repair a DSB with a given pathway impacts repair efficiency and has potential mutagenic consequences. In addition to repair DSB, the process of HR is involved in many other cellular processes, independently of DSB. In this chapter, DSB repair pathways will be introduced, and then the role of HR in cellular processes will be reviewed in more details.

Non-homologous end joining (NHEJ)

Non-homologous end joining (NHEJ) is the predominant pathways to repair DSBs throughout the cell cycle in mammalian cells. In contrast, in yeast models (both *saccharomyces cerevisiae* and *schizosaccharomyces pombe*), most of DSBs are efficiently repaired by Homologous Recombination (HR) while NHEJ plays a minor role in repairing DSB, excepted during the G1 phase (Ferreira and Cooper, 2004; Reis et al., 2012). In mammalian cells, NHEJ is involved in the repair of accidental DSBs (such as the ones induced by genotoxic drugs and gamma irradiation) as well as programmed and physiological DSBs such as the ones that initiate immunoglobulin diversity and T cell receptor rearrangement (Lieber et al., 2014). Studies carried out in mice and human have reported that dysfunctional NHEJ due to deficient DNA ligase IV (essential ligase involved in NHEJ to ligate double stranded DNA ends in an ATP-dependent reaction) leads to sensitivity to ionizing radiation, tumorigenesis, severe immunodeficiency, and developmental and growth delay (O'Driscoll et al., 2001; Pierce and Jasin, 2001; Sharpless et al., 2001).

The repair of a DSB by the classical NHEJ is divided into four steps: the recognition and detection of DSB ends, the limited resection of DSB ends, and a limited step of DNA polymerization followed by the ligation of the two DNA ends (Figure 2.1). The flexibility of DNA ends joining is featured by the configuration of the DNA ends in order to maximize the efficiency of end joining (Chang et al., 2017).

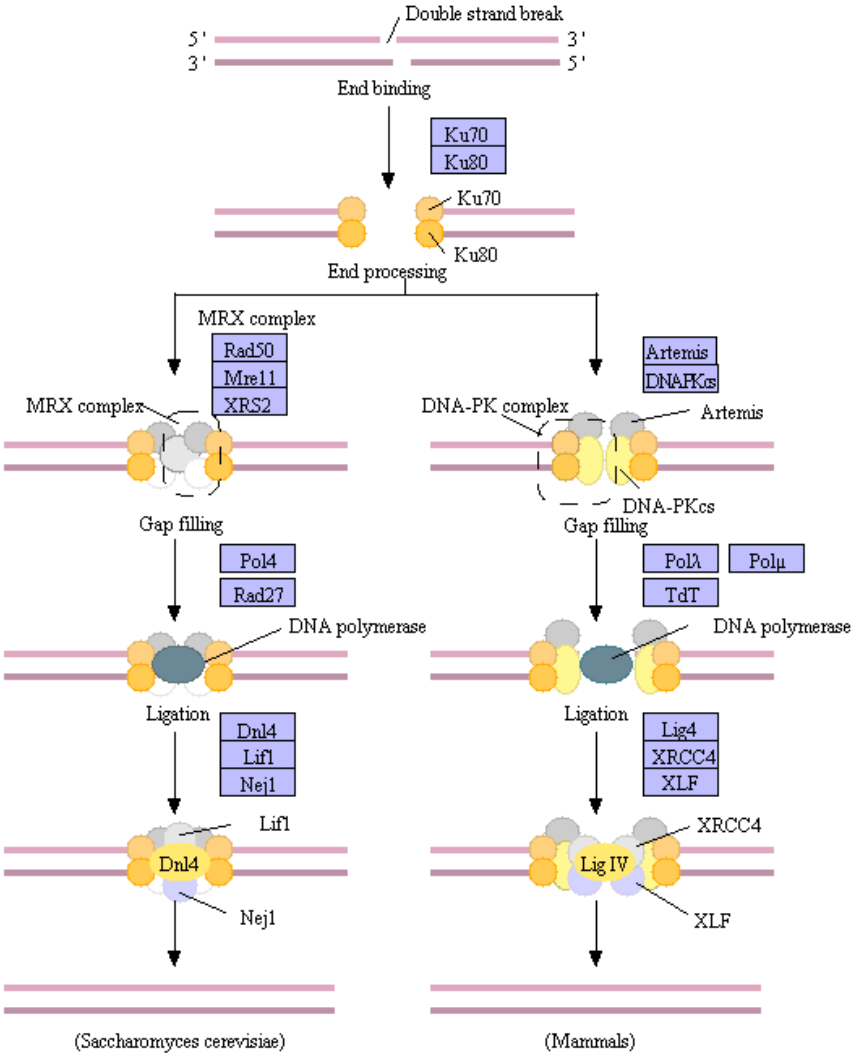

Figure 2.1. Schematic of non-homologous end joining pathway in budding yeast (left) and mammals (right). Adapted from KEGG: Kyoto Encyclopedia of Genes and Genomes.

The heterodimer Ku, composed of Ku70 and Ku80, is thought to be the first complex to be recruited at the sites of DSBs (Downs and Jackson, 2004; Walker et al., 2001). Ku is considered as a ring that encircles each DSB end. The resulting Ku-DNA complex then serves as a docking place for the recruitment of downstream nuclesase, polymerase and ligase, thereby priming the repair event (Lieber, 2008). The binding of Ku to DNA impacts on its conformation in a way that the ability of Ku to interact with the downstream repair factors are increased, such as for DNA-PKcs (DNA-dependent Protein Kinase catalytic subunit) (Yaneva et al., 1997), for the DNA polymerases Pol μ and Pol λ, for the XRCC4 (X-ray Repair Cross-Complementing protein 4) and for DNA ligase IV (Chen et al., 2000; Nick McElhinny et al., 2000). Nuclease activities are then activated. The highly conserved MRX/MRN complex (Mre11-Rad50-Xrs2 in budding yeast and Mre11-Rad50-Nbs1 in fission yeast and mammals) is the critical nuclease for resecting a wide range of dirty

DNA ends at DSBs (Moreau et al., 1999, 2001; Symington, 2014). However, the MRX complex was found to be not essential in promoting HO-induced DSB repair by HR in budding yeast, in contrast to that in fission yeast and mammalian cells (Limbo et al., 2007; Williams et al., 2008). After the trimming of DNA ends, the short gaps are filled up by the DNA polymerases Pol λ and Pol μ (Pol 4 in budding yeast) via extending termini with limited sequence homology (Bebenek et al., 2005). The repair event is finally completed by a ligation step performed by DNA ligase IV. As a result, the DNA duplex is rejoined, but the regions removed by the nuclease are lost.

Alternative end joining (alt-EJ)

Alternative end joining (alt-EJ) is a recently discovered mechanism for repairing DSBs. Alt-EJ was initially assumed to be a backup pathway which was activated only when the canonical NHEJ pathway was dysfunctional (Göttlich et al., 1998; Kabotyanski et al., 1998; Wang et al., 2003). However, subsequent studies have revealed that alt-EJ also exists redundantly with a functional canonical NHEJ (Deriano and Roth, 2013).

There are a few features of alt-EJ making it distinct from canonical NHEJ. The junctions favored by alt-EJ are frequently but not necessarily associated with microhomology (usually 3–16 nucleotides) and associated with extensive deletion compared to canonical NHEJ, reflecting a more extensive DNA-end resection. Alt-EJ is found to be 20-fold less efficient than the canonical NHEJ and more error-prone, as alt-EJ commonly leads to chromosome translocations (Simsek and Jasin, 2010; Zhu et al., 2002). To date, the molecular mechanisms that favor the use of alt-EJ instead of the classical NHEJ are not fully understood. A study in single living cells suggests a role of DNA damage-sensing in alt-EJ by PARP1 (Poly (ADP-ribose) polymerase 1), that PARP1 competes with Ku70/80 for the binding to laser microirradiation-induced DNA ends (Haince et al., 2008).

Depending on if microhomology is involved, another pathway termed microhomology-mediated end joining (MMEJ) was further identified to subdivide alt-EJ (Figure 2.2). MMEJ is shown to rely on pre-existing microhomologies around DNA ends. A major feature to mark MMEJ is the usage of LIG3 (ligase III) for DNA sealing, whereas in the alt-EJ pathway LIG1 (ligase I) is preferred (Deriano and Roth, 2013).

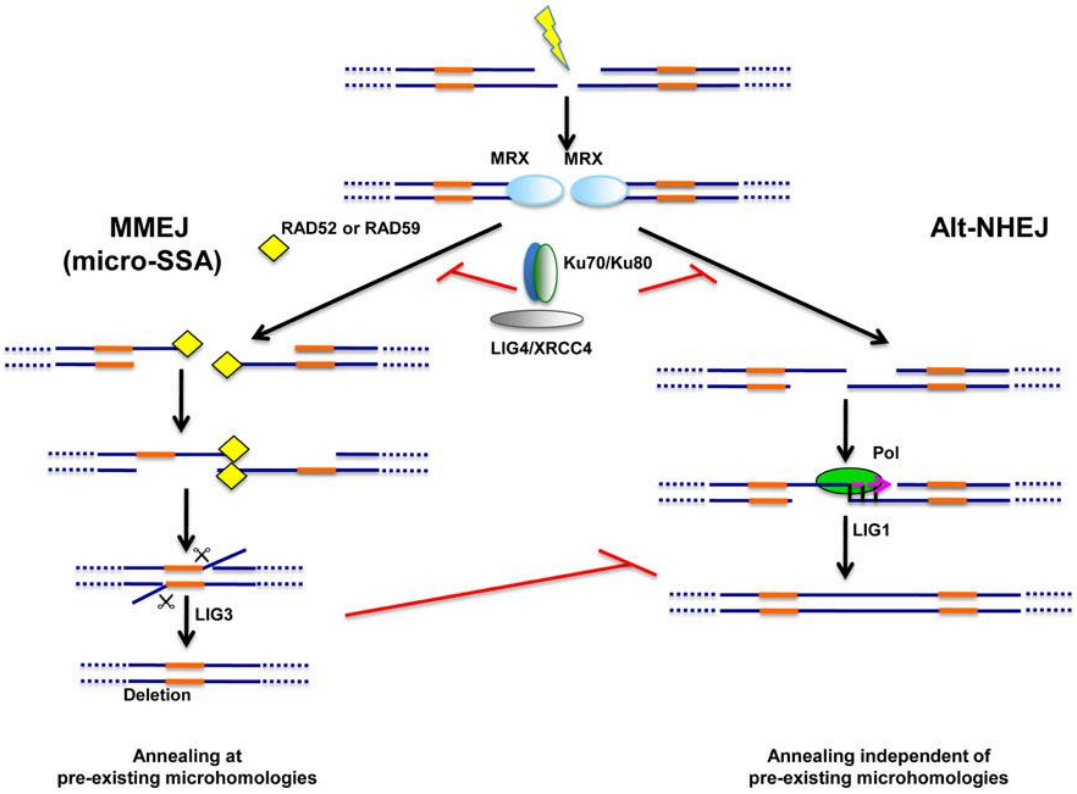

Figure 2.2. Schematic of two types of alternative end joining pathways of DSB repair. The orange DNA regions flanking the DNA break site indicate pre-existing microhomologies. Adapted from Decottignies, 2013 (Decottignies, 2013).

2.1. Homologous Recombination

Homologous recombination (HR) is playing a vital role in maintaining genome stability. Beyond DSB repair, HR is also implicated in other important cellular processes.

During meiosis, programmed DSBs formation is distributed along the chromosomes, via the catalysis of a topoisomerase complex containing the evolutionarily conserved meiosis-specific protein Spo11 (Keeney et al., 1997). DSBs then trigger the recombination between the paternal and maternal chromosomes to promote the exchange of genetic information. Meiotic recombination is key to the generation of genetic diversity and molecular evolution, it also contributes to ensuring proper alignment of homologous chromosome pairs on the spindle (Baudat et al., 2013; Davis and Smith, 2001).

Bacteria perform cell-to-cell conjugation for transferring genetic material. Bacterial conjugation requires the presence of a conjugative plasmid (for example, the F-plasmid), which is capable of integrating itself into the chromosomal DNA via HR. Upon the reception of F-plasmid into the chromosome, the cells become very efficient in gene delivery in a recombination-dependent

manner, hence they are termed as Hfr cells (high-frequency recombination cell) (Figure 2.3) (Lederberg and Tatum, 1946).

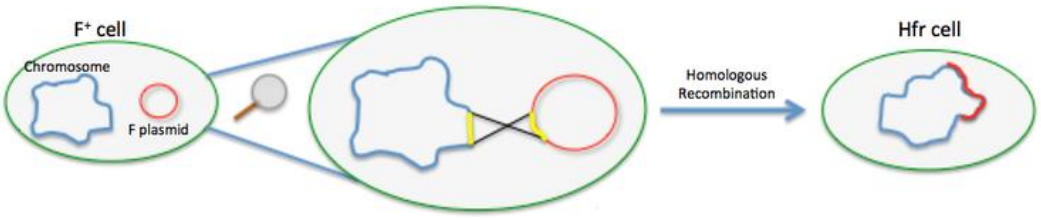

Figure 2.3. Model of the formation of a Hfr cell via recombination-dependent chromosome integration. Adapted from online source (https://en.wikipedia.org/wiki/Hfr_cell).

At telomeres, HR allows the maintenance of telomeres when the telomerase is absent, (Claussin and Chang, 2015; Tacconi and Tarsounas, 2015). Recent studies have also shown that HR has an important role in supporting the robustness of DNA replication, which will be further discussed in section 2.4.

Due to the need for homologous sequences, HR is restricted to S and G2 phase, whereas NHEJ is active throughout the cell cycle. When both pathways are active, the step of DNA end-resection impacts on repair pathway choice. The 5’ to 3’ end-resection generates a single stranded DNA with a 3' overhang which is instrumental to initiate the HR pathway and to block NHEJ (Symington and Gautier, 2011). Therefore, the cell-cycle regulation of the resection machinery is pivotal in DSB repair pathway choice.

2.2. Models of homologous recombination and the initial substrates

Several models of DSB repair by HR have been proposed, such as the classical Double Strand Break Repair (DSBR), Synthesis Dependent Strand Annealing (SDSA), Single Strand Annealing (SSA) and Break Induced Replication (BIR). Most of these models rely on a step of 5’ to 3’ DNA end resection, a step of homology search, a step of strand invasion mediated by the recombinase Rad51 and the formation of a D-loop (Displacement loop) structure.

DSB repair by HR is initiated by 5’ to 3’ resection of DSBs to generate a single-stranded DNA with a 3’ overhang. The end-resection occurs in a two-step manner: a short-range resection followed by a long-range resection. In fission yeast the short-range resection machinery involves the MRN complex (MRX in budding yeast) and the endonuclease Ctp1 (Sae2 in budding yeast and CtIP in mammals). They bind to the DNA ends and trim off a short stretch of DNA (50-100 nucleotides) from the 5’ end. The processed 5’ end is further resected (the long-range resection) by either the

exonuclease Exo1 or the Sgs1/BLM-Dna2 pathway to expose a 3' overhang single-stranded DNA, on which is coated the replication protein A, RPA (Cannavo and Cejka, 2014; Mimitou and Symington, 2008; Nicolette et al., 2010; Petrini and Stracker, 2003; T 2017; Zhu et al., 2008). Notably, in fission yeast Rqh1 (orthologue of human BLM and budding yeast Sgs1) only has a moderate role in long-range end resection (Langerak et al., 2011;; Zhang et al., 2016). The displacement of RPA is then stimulated by the recombination mediator Rad52 to load the recombinase Rad51 (Gaines et al., 2015; Plate et al., 2008; Sugiyama and Kowalczykowski, 2002; Sung, 1997a). Rad51 forms a nucleoprotein filament, which is capable of searching for homology and to perform strand invasion. The next step of HR is termed the synaptic phase, in which the presynaptic filament invades the homologous DNA duplex, pairs with its homologous strand and displaces the complementary strand resulting in the formation of a D-loop (Figure 2.4). Downstream the D-loop formation (postsynaptic phase), HR can occur via different pathways that are regulated by multiple helicases and nucleases.

Double Strand Break Repair (DSBR)

The Double Strand Break Repair DSBR pathway was initially proposed as a model to explain the repair of gapped plasmids in budding yeast (Szostak et al., 1983). To date, this model remains considered as the canonical model to explain the formation of crossover (CO) and gene convention event associated to DSB repair by HR.

In this model, the repair of the DSB includes the capture of the second DSB end in a way that the displaced strand of the donor duplex anneals with the 3' overhang ssDNA generated from the second DNA end (Figure 2.4). The capture of the second DNA end is thought to be promoted by the single strand annealing activity of Rad52 resulting in the formation of a double Holliday Junction (dHJ) (Cejka et al., 2010; McIlwraith and West, 2008; Nimonkar et al., 2009). The dHJs are then resolved either by cleavage via several resolvases, such as Mus81-Mms4 (Mus81-Eme1 in pombe), Slx4, Yen1 (Gen1 in human) to produce crossover and non-crossover (NCO) products, or are dissolved via the helicase activity of Rqh1 (the Sgs1-Top3-Rmi1 complex in budding yeast, BLM in human) to generate exclusively non-crossover products (Boddy et al., 2001; Fekairi et al., 2009; Holliday, 1964; Hollingsworth and Brill, 2004; Ip et al., 2008; Ira et al., 2003; Osman et al., 2003; Singh et al., 2009; Wu and Hickson, 2003).

The DSBR model explains the occurrence of CO and NCO events associated to the repair of meiotic DSBs. Nonetheless, mitotic COs are rare. In mitotic cells, chromosomal COs can lead to

chromosomal rearrangements which challenge genome integrity, and COs are not commonly associated with mitotic recombination event. Therefore, an alternative model was proposed: the Synthesis Dependent Strand Annealing (SDSA) model (Nassif et al., 1994).

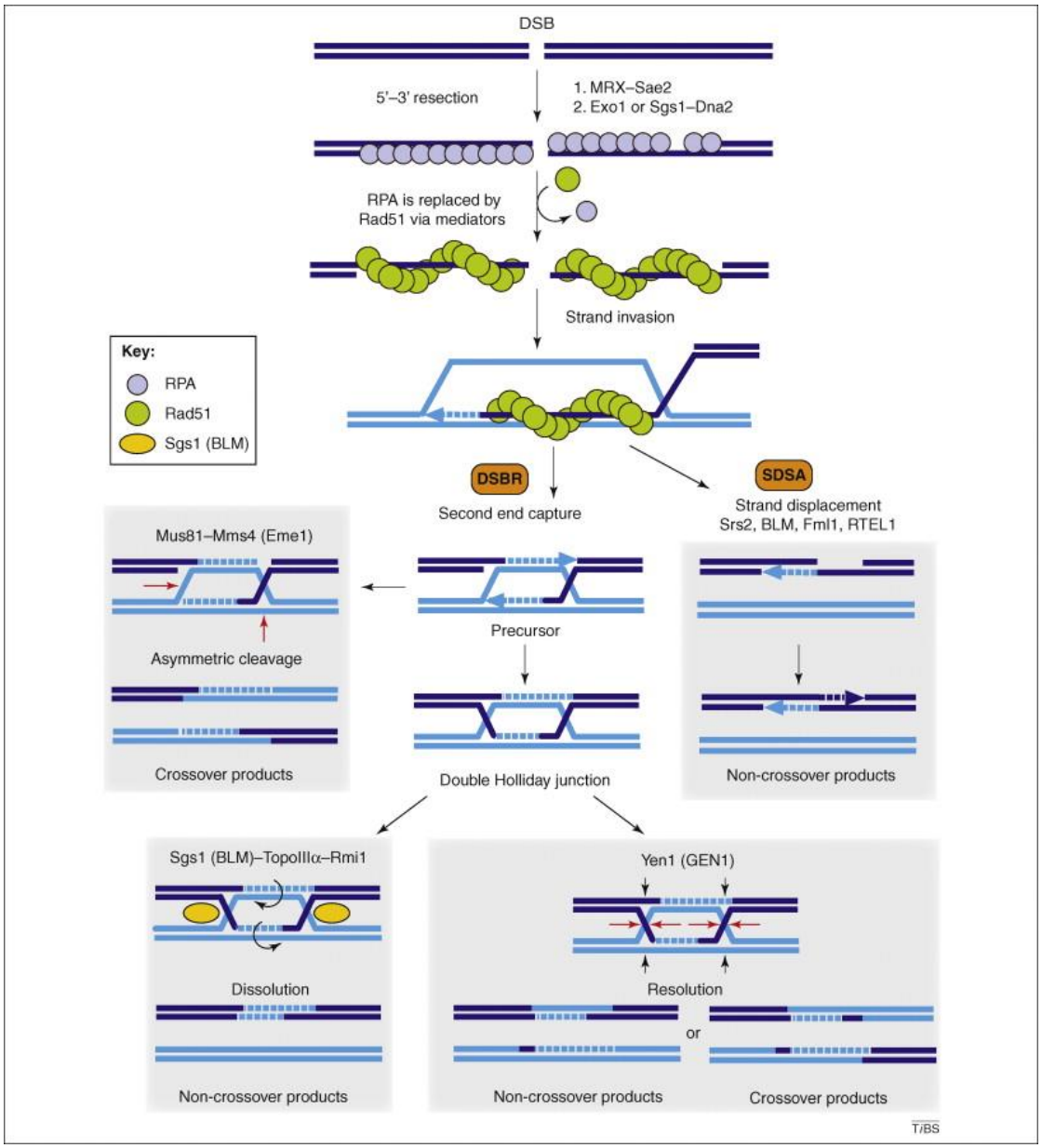

Figure 2.4. Models of double strand break repair (DSBR) and synthesis dependent strand annealing (SDSA) pathways. The initiation of both pathways is an extensive 5'-3' resection of DNA end generating a 3' overhang, which is later on loaded with recombinase Rad51 resulting in a homology search-proficient nucleoprotein filament (pre-synaptic phase). The Rad51-nucleofilament invades the homologous duplex and replaces the complementary strand leading to the formation of D-loop (synaptic phase). At the D-loop the homologous strand is used as the template for nascent DNA synthesis (post-synaptic phase). Crossover and non-crossover products are yielded according to different models. Adapted from Mimitou and Symington, 2009 (Mimitou and Symington, 2009).

Synthesis Dependent Strand Annealing (SDSA)

In the Synthesis Dependent Strand Annealing (SDSA) model, it is proposed that after the D-loop formation and a limited extension by DNA synthesis, this structure can be disassembled by the activity of helicases. The nascent strand anneals to the 5' strand at the DNA end and serves as the template allowing gap-filling by DNA synthesis and ligation (Figure 2.4) (Ferguson and Holloman, 1996; Nassif et al., 1994; Pâques et al., 1998).

The outcome of the SDSA model is the generation of exclusive NCO products which are associated with gene conversion (Nassif et al., 1994). The SDSA pathway has been implicated in both mitotic and meiotic recombination (San Filippo et al., 2008).

Single Strand Annealing (SSA)

Single Strand Annealing (SSA) is another alternative pathway to repair DSBs and exploits the presence of direct tandem repeats flanking a single DSB. SSA requires an extensive resection of DNA ends by multiple nucleases and helicases (Bhargava et al., 2016). SSA has been demonstrated to exist in a wide spectrum of organisms including yeast models, mammalian cells, higher plants such as *A. thaliana*, *D. melanogaster*, and *C. elegans*) (Lin et al., 1984; Pitt and Cooper, 2010). The mechanism of SSA has been thoroughly studied in budding yeast.

The initial step of SSA is an extensive resection of DNA in 5' to 3' direction in order to expose single stranded DNA with a 3' overhang containing direct repeats (ranging from 63 bp to 1.17 kb) (Sugawara et al., 2000). The homology allows the annealing of the two resected DNA ends by complementary base pairing. The non-annealed extremities generate 3' flap single stranded DNA strands that are then trimmed off by the Rad1-Rad10 nuclease in budding yeast (Rad16-Swi10 in fission yeast and XPF-ERCC1 in mammals) (Carr et al., 1994a; Fishman-Lobell and Haber, 1992; Ivanov and Haber, 1995). Any DNA gaps left will be filled by DNA polymerases and sealed by DNA ligase (Figure 2.5). However, the specific polymerases and ligases exploited to complete SSA are still poorly understood (Bhargava et al., 2016). The final repair product results in the deletion of one direct repeat and the intervening DNA sequence. Therefore, SSA is considered as a highly mutagenic and non-conservative DSB repair pathway (Fishman-Lobell et al., 1992; Lin et al., 1984; Maryon and Carroll, 1991).

SSA can be considered as a sub-pathway of HR as it requires sequence homology but no step of strand exchange. In yeast, SSA requires the HR factor Rad52 but not the recombinase Rad51

(Ivanov et al., 1996; Symington, 2002). During SSA, Rad52 promotes the annealing of two complementary strands (Mortensen et al., 1996).

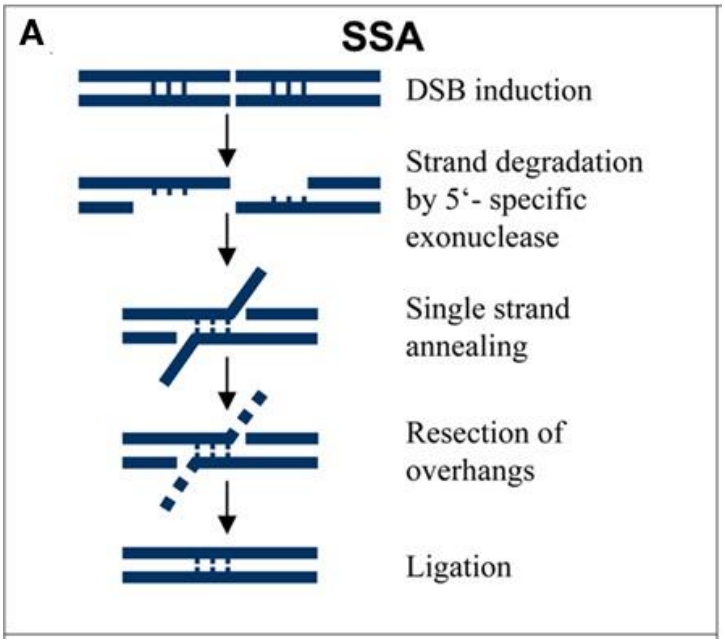

Figure 2.5. Schematic of single strand annealing. Adapted from Schubert et al., 2011 (Schubert et al., 2011).

Break-Induced Replication (BIR)

Break-induced replication (BIR) is a pathway that has been studied for several decades, and it has been reported in viruses, prokaryotes and eukaryotes in different contexts. BIR was first described as a mechanism of HR to explain very long gene conversion tract, multiple templates switching and non-reciprocal translocation (Bosco and Haber, 1998; Kraus et al., 2001; Ruiz et al., 2009).

BIR is required to repair stalled replication forks in bacteriophage T4 and *Escherichia coli*, (Heller and Marians, 2006; Mosig, 1998). In addition to restarting broken replication forks, BIR is also exploited in telomere maintenance in the absence of telomerase in yeast and human cells (Anand et al., 2013; Llorente et al., 2008; Malkova and Ira, 2013).

BIR is initiated when homologous sequence is available for only one extremity of the DSB end. For example, when a one-ended DSB is generated at a broken fork or during telomere erosion. The strand invasion in the canonical BIR pathway is Rad51-dependent (Figure 2.6). However, BIR may also occur independently of Rad51 with less efficiency (Malkova et al., 2005). BIR is classified as a sub-pathway of HR, and requires the core components of the HR machinery.

In budding yeast, BIR occurs using a migrating D-loop which can proceed hundreds of kilobases of DNA until the end of the chromosome. Major proteins involved in DNA replication were found to be required for BIR, excepted the replication initiation factors, including all three major replicative DNA polymerases (Pol α, Pol δ and Pol ε), as well as replicative DNA helicases such as Cdc45, the GINS and the Mcm2-7 complex, and the pre-RC (pre-Replication Complex) component Cdt1 (Lydeard et al., 2010). Therefore DNA synthesis during BIR has been suggested to follow a canonical semi-conservative fashion involving both leading and lagging strands synthesis, which is in contrast to that in SDSA where only the synthesis of leading strand is involved (Lydeard et al., 2007, 2010). However, recent studies have reported conflicting observations that DNA synthesis during BIR is significantly different from S-phase DNA synthesis and results in conservative inheritance of the new genetic material, indicating that BIR proceeds rather by conservative DNA synthesis without the synthesis of lagging strands (reviewed by Ait Saada et al., 2018).

Studies in budding yeast have shown that DNA synthesis rate during BIR is comparable to that of normal DNA replication (about 3kb per min) (Malkova et al., 2005). However, DNA synthesis during BIR is highly inaccurate and results in more than 1000-fold increase in mutation rate compared to normal replication (Deem et al., 2011; Saini et al., 2013).

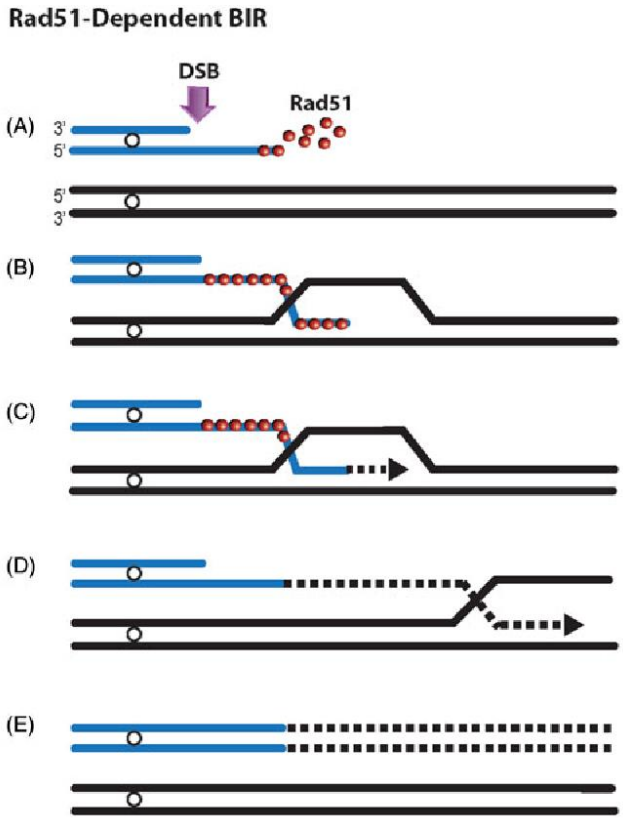

Figure 2.6. Model of canonical break-induced replication involving Rad51 (red) in eukaryotes. In this model, the 3' ssDNA (blue) generated from extensive resection of a DSB end is bound by Rad51 (A), the formation of Rad51-nucleoprotein filament is capable of searching for its homologous sequence (black) and perform strand invasion (B). Using the homologous sequence as the template, a new stretch of DNA is synthesized (black dotted line) (C). BIR replication bubble progresses with the ongoing DNA synthesis and generates a long tract of ssDNA behind the bubble (D). BIR is completed with the inheritance of a newly synthesized conservative strand (E). Adapted from Sakofsky and Malkova, 2017 (Sakofsky and Malkova, 2017).

2.3. HR factors and proteins involved in HR

During the presynaptic and synaptic step, the recombinase Rad51, which forms a nucleoprotien filament onto ssDNA, plays a central role in the search for homology. There are several mediators that impact Rad51 activity. The positive regulators facilitate the nucleation of Rad51 onto ssDNA to form the nucleoprotein filament, and promote the strand invasion step as well as D-loop formation. The negative regulators favor the disassembly of Rad51-nucleoprotein filament and destabilize the D-loop (Figure 2.7). Notably, one factor may have bidirectional effect. For example, the heterotrimeric protein RPA prevents DNA secondary structure and undergoes SUMOylation to facilitate Rad51 loading at DNA damage sites thus promoting DNA repair by HR (Burgess et al., 2007; Dou et al., 2010; Kowalczykowski and Krupp, 1987).

Nonetheless, excessive RPA may prevent the nucleation of Rad51 onto ssDNA thus impacting the presynaptic step of HR (Van Komen et al., 2002).

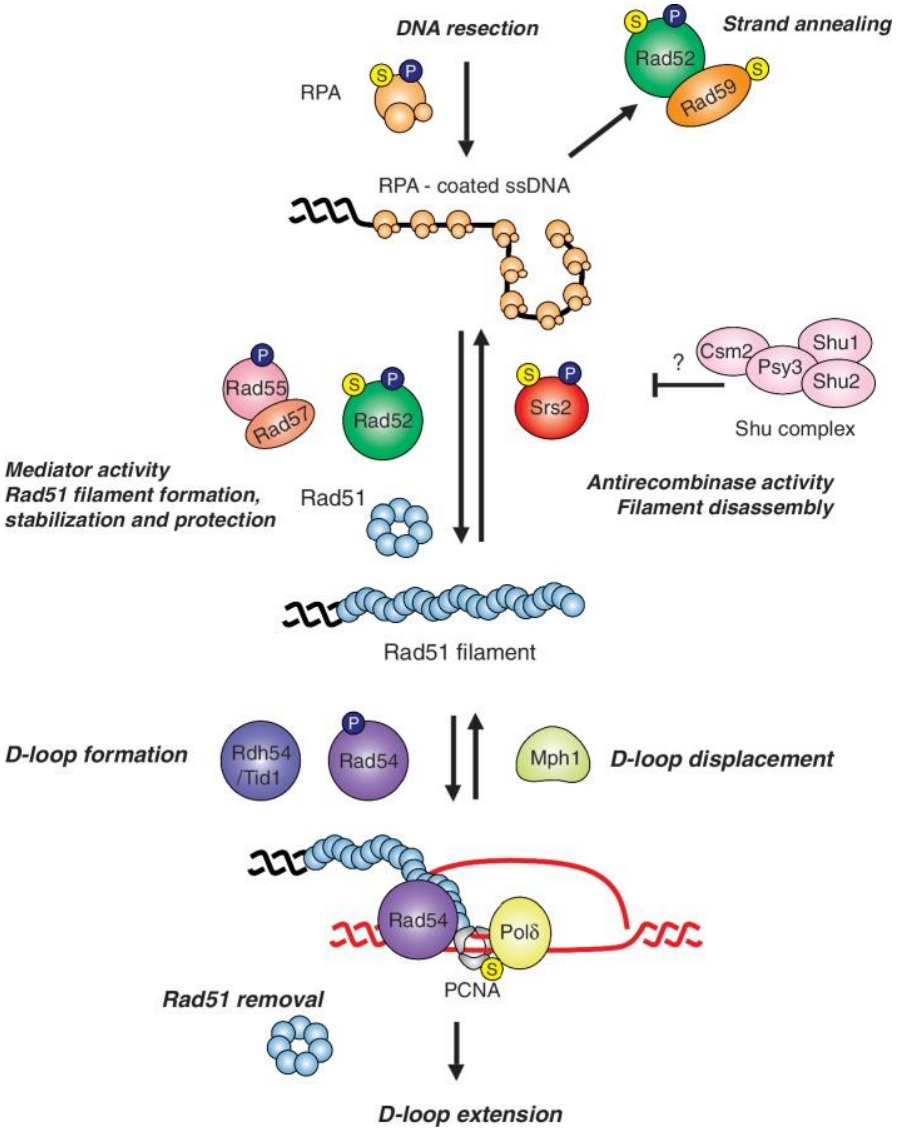

Figure 2.7. Factors that regulate the early step of HR. RPA is displaced by Rad51 via the aids from the recombination mediator protein Rad52. The other mediator proteins including Rad55 and Rad57 help to stabilize the Rad51-nucleoprotein filament against the helicase Srs2. Rad54 promotes homology search performed by the Rad51 presynaptic filament. Mph1 (Fml1 being the orthologue in fission yeast) can channel the downstream events to the SDSA pathway by unwinding D-loop intermediates. Adapted from Krejc et al., 2012 (Krejci et al., 2012).

Recombination Mediator Proteins (RMPs)

Before the loading of recombinase Rad51 to form the presynaptic filament, the ssDNA is coated by RPA which has a higher affinity for ssDNA than Rad51, thus RPA inhibits the loading of Rad51. Several proteins act to counteract the inhibition from RPA and facilitate the formation of Rad51-

nucleoprotein filament, hence they are positive players in HR and are referred to as the recombination mediator proteins (RMPs) (Table 2.1).

	Budding yeast	**Fission yeast**	**Human**
Recombinase	Rad51	Rad51 (Rhp51)	RAD51
RMPs	Rad52 Rad55-Rad57	Rad52 (Rad22) Rad55-Rad57(Rhp55-Rhp57)	RAD52 BRCA2 RAD51B-RAD51C RAD51D-XRCC2 RAD51C-XRCC3
	The Shu complex (Csm2, Psy3, Shu1, and Shu2)	Rdl1, Sws1 and Rlp1	RAD51D SWS1 XRCC2
	Rad59		
	Rad54 Rdh54	Rad54 (Rhp54)	RAD54 RAD54B RAD51AP1

Table 2.1. Recombinase and recombination mediator proteins in different organisms.

RPA is a heterotrimeric complex composed of three different subunits. They all possess four OB-(Oligonucleotide/Oligosaccharide Binding) fold domains that are well characterized to bind ssDNA in both prokaryotes and eukaryotes (Flynn and Zou, 2010). RPA has a vital role in DNA metabolic processes including DNA replication, replication restart, DNA repair, transcription, and telomere maintenance (Binz et al., 2004). Beyond acting on ssDNA during the initial stage of HR, studies in budding yeast have reported that RPA also facilitates the resection of DSB end by stimulating DNA unwinding via the helicase Sgs1 (Rqh1 in fission yeast), enhancing the 5' strand incision by Dna2, and protecting the 3'-DNA end (Cejka et al., 2010; Niu et al., 2010; Zhu et al., 2008).

Rad51 is a central player in the HR pathway, it shares structural similarities with the *E. coli* RecA and T4 UxsX proteins, and is highly conserved throughout the evolution (Bianco et al., 1998; Krejci et al., 2003; Story et al., 1993). Rad51 possesses an ATPase activity (Tombline and Fishel, 2002). The binding of Rad51 to ATP leading to a structural alteration of Rad51 is necessary for the ability of Rad51 to bind ssDNA, whereas ATP hydrolysis compromises Rad51-DNA association (Chi et al., 2006; Namsaraev and Berg, 1998). Therefore, the stability of Rad51-DNA structure can also be regulated via adjusting its ATP hydrolysis ability.

Rad51 nucleates onto ssDNA in a manner that every 6 molecules of Rad51 proteins are set on 18bp nucleotides in a helical turn, and the DNA is stretched to facilitate efficient homology search (Ogawa et al., 1993). Given the structural homology of Rad51 to *E. coli* RecA protein, it

has been suggested that like in *E. coli,* the homology search by Rad51-nucleofilament favors a "random collision" model rather than by scanning along the DNA (Sung et al., 2003). It is proposed that after the presynaptic filament invades a DNA duplex, it performs multi-point contacts with the homologous donor DNA, multiple cycles of DNA-contacting and the following release of presynaptic filament from the DNA will be repeated until the homology is found (Bianco et al., 1998; Krejci et al., 2003).

In yeast models, there are several recombination mediators including Rad52, a heterodimeric complex consisting of two Rad51 praralogues, Rad55 and Rad57, and the Shu complex (Bernstein et al., 2011; Krejci et al., 2012; Martino and Bernstein, 2016).

Rad52 facilitates the formation of the Rad51 filament by displacing RPA from ssDNA, via its interaction with Rad51 and RPA (Benson et al., 1998; New et al., 1998; Shinohara and Ogawa, 1998; Sung, 1997a)(Seong et al., 2008; Shinohara et al., 1992)(Seong et al., 2008; Shinohara et al., 1992)(Seong et al., 2008; Shinohara et al., 1992). The Rad51-binding domain and the DNA-binding domain are found at the C-terminus of Rad52, which contributes largely to its role as a mediator (Seong et al., 2008). Rad52 interacts with RPA via its middle part that helps to target Rad52 to the site of DSBs (Plate et al., 2008; Seong et al., 2008). The N-terminus of Rad52 is rather versatile: it binds to DNA and facilitates the reaction of single strand annealing, and it binds to its paralogue, Rad59. The Rad52 N-terminus contributes to the role of Rad52 in promoting SSA (Seong et al., 2008). It has been shown that Rad52 accelerates the nucleation of Rad51 onto ssDNA to displace RPA (Sugiyama and Kowalczykowski, 2002). Nonetheless, only catalytic amounts of Rad52 are found to be enough for assembling Rad51-nucleoprotein filament, raising the likelihood that RPA is not directly removed from DNA by Rad52 but rather by the nucleation of Rad51 (Sugiyama et al., 1998; Sung, 1997a; Sung et al., 2003).

Displaying ATPase activity, the paralogues of Rad51, **Rad55 and Rad57** form a heterodimer possessing ssDNA-binding ability while lacking recombinase activity (Hays et al., 1995; Sugiyama et al., 1998; Sung, 1997b). Rad55-Rad57 complex facilitates Rad51-nucleoprotein filament formation by directly interacting with Rad51 and loads Rad51 onto ssDNA coated with RPA. Rad55-Rad57 complex also reinforces the resistance of Rad51-nucleoprotein filament to the anti-recombinase Srs2, the helicase activity of which is involved in DNA duplex unwinding and disassembling D-loop (Liu et al., 2011). In support of the role of Rad55-Rad57 complex as a recombination mediator, studies have shown that Rad55-Rad57 complex adds stability to Rad51-nucleoprotein filament (Fortin and Symington, 2002; Fung et al., 2009; Malik and Symington,

2008). It is therefore suggested that the recombination-promoting function of Rad55-Rad57 complex and the anti-recombination activity of Srs2 have antagonistic effect in regulating the early stage of HR via impinging on the stability of Rad51-nucleoprotein filament.

Studies in budding yeast have led to the realization of a conserved role of **the Shu complex** in regulating the key step of HR, the assembly of Rad51-nucleoprotein filament. The budding yeast Shu complex is a hetero-tetramer consisting of two novel paralogues of Rad51, Psy3 and Csm2, along with Shu1 and Shu2 containing the SWIM (SWI2/SNF2 and MuDR, zinc ion binding) domain (Sasanuma et al., 2013; Shor et al., 2005). The fission yeast Shu complex is composed of Sws1 (SWIM domain-containing and Srs2-interacting protein 1) and two Rad51 paralogues, Rlp1 and Rdl1 (Martín et al., 2006).

The Shu complex is an important regulator of Rad51 acting in different types of HR-mediated DNA repair including replication-associated and meiotic DSB repair (Bernstein et al., 2011; Martino and Bernstein, 2016). *In vitro* pull down experiments in budding yeast have demonstrated that the Shu complex interacts with the Rad55-Rad57 dimer directly, as well as with Rad51 and Rad52, both bridged by Rad55, indicating that the Shu complex and the other recombination mediators, Rad52 and Rad55-Rad57, are coordinated in regulating Rad51 (Gaines et al., 2015; Godin et al., 2013; Xu et al., 2013). In support of this, *in vitro* data have revealed that the addition of the Shu complex to reactions containing Rad52 and Rad55-Rad57 led to a more than 2-fold stimulation in Rad51 loading onto RPA-coated ssDNA, further suggesting a direct role for the Shu complex in regulating the activity of Rad51 (Gaines et al., 2015). The role of the Shu complex in positively regulating Rad51 also involves its activity in antagonizing Srs2. Importantly, a conserved physical interaction between Srs2 and the Shu complex has been observed in both budding yeast and fission yeast (Martín et al., 2006; Uetz et al., 2000). However, the underlying mechanism of how the Shu complex negatively regulates Srs2 remains unknown.

The DNA translocase **Rad54** belongs to the Swi2/Snf2 (Switch2/Sucrose non-fermentable2) family. It plays multiple regulatory roles during all steps of the HR process. Rad54 exhibits strong ATPase and DNA supercoiling activities, which are stimulated by Rad51 (Krejci et al., 2003; Symington, 2002).

It has been reported that Rad51-nucleoprotein filament is significantly stabilized upon the binding of Rad54 (Solinger et al., 2002). During synaptic phase, Rad54 hydrolyzes ATP in a dsDNA-dependent manner to support its translocation along DNA duplex, where its movement

generates topological alterations of DNA (Van Komen et al., 2000; Krejci et al., 2003; Ristic et al., 2001). The negative supercoils behind the movement of Rad54 are thought to open the DNA duplex transiently and accommodate presynaptic filament to search for homology, thus facilitate the homologous-paring reaction (Van Komen et al., 2000). During the translocation on DNA duplex, Rad54 also promotes the removal of Rad51 from DNA duplex in the D-loop in an ATP-dependent manner (Kiianitsa et al., 2006; Sigurdsson et al., 2002; Solinger et al., 2002).

Negative regulators of HR

The DNA synthesis from the 3' end in the D-loop is mainly via the activity of DNA polymerase Pol η (Mcllwraith et al., 2005). Moreover, Pol η was found to associate to the chromatin in a PCNA-dependent manner during the repair of broken replication forks by HR in Xenopus, and genetic data in DT40 cells have shown that defect in pol η results in impaired DSB repair by HR (Hashimoto et al., 2012; Kawamoto et al., 2005). Nonetheless, a role for Pol δ in priming DNA synthesis on the D-loop has been suggested by biochemical studies, and the PCNA-interaction is also essential in this scenario (Sebesta et al., 2011). In fission yeast, it has been shown that Pol δ replicates both strands during recombination-dependent synthesis (Miyabe et al., 2015a).

Several helicase and nuclease activities are known to impact the resolution of HR intermediates (known as joint-molecules) and thus channeling HR event either toward a CO or a NCO pathway. Among them there are Srs2, FANCM (Mph1 in budding yeast and Fml1 in fission yeast) and RecQ helicases (Sgs1 in budding yeast and Rqh1 in fission yeast). These factors compete with the activities of DNA polymerases by preventing D-loop formation or disassemble D-loop, thus they are also referred to as the negative regulators (Table 2.2).

	Budding yeast	**Fission yeast**	**Human**
Negative regulators	Srs2 Mph1 Sgs1	Srs2 Fml1 Rqh1	- FANCM BLM RTEL1 RARI

Table 2.2. Negative regulators of HR.

Srs2 possesses ATPase and 3'-5' DNA helicase activities. It prevents COs during mitotic recombination by disassembling joint molecules (Fabre et al., 2002; Ira et al., 2003; Robert et al., 2006; Aylon et al., 2003). The deletion of Srs2 results in a phenotype of hyper-recombination and increased COs that is rescued by the deletion of recombinase Rad51, thus leading to the role of

Srs2 as an anti-recombinase (Chanet et al., 1996; Gangloff et al., 2000). Srs2 addresses its anti-recombinase activity by facilitating the disassociation of Rad51 from the nucleoprotein filament (Krejci et al., 2003; Veaute et al., 2003). Further studies have demonstrated that Srs2 physically interacts with Rad51 via the C-terminal region of Srs2. This interaction triggers the ATP hydrolysis within the Rad51-nucleoprotein filament leading to a weakened Rad51-DNA interaction and subsequent disassociation of Rad51 from DNA (Antony et al., 2009; Colavito et al., 2009). *In vitro* study has shown that the helicase activity of Srs2 in unwinding D-loop is stimulated by the presence of Rad51-nucleoprotein filaments on dsDNA, supporting the role of Srs2 in channeling HR to the SDSA pathway and suppressing mitotic COs (Dupaigne et al., 2008).

The human Fanconi anemia protein **FANCM** migrates the Holliday Junctions (Gari et al., 2008). The homolog of FANCM is Mph1 in budding yeast, and its orthologue in fission yeast is Fml1. Mph1 is an ATP-dependent helicase of 3'-5' polarity and works independently of Srs2 and Sgs1 (Prakash et al., 2005). Purified Mph1 unwinds the D-loop via displacing the extended primer by the polymerases Pol δ and Pol η and dissociating the invading strand from the donor DNA template, thus promotes the DSB repair to the SDSA pathway (Sebesta et al., 2011). The deletion of Mph1 leads to increased mitotic COs (Entian et al., 1999; Gari et al., 2008; Prakash et al., 2009; Schürer et al., 2004; Sun et al., 2008; Zheng et al., 2011). Similarly in fission yeast, Fml1 prevents mitotic COs by destabilizing the D-loop and promotes NCOs during meiotic recombination (Lorenz et al., 2012; Sun et al., 2008).

Studies from many organisms have established that the RecQ helicase is a vital DNA recombination and repair enzyme (Harami et al., 2017; Li and Li, 2004; Wiedemann et al., 2018). The RecQ helicase family in human is composed of 5 genes: RECQL1, RECQL4, RECQL5, BLM (Bloom syndrome protein) and WRN (Werner syndrome ATP-dependent helicase). BLM is thought to be the orthologue of *S. cerevisiae* Sgs1 and the orthologue of *S. pombe* **Rqh1**.

A major role proposed for the RecQ helicase is to prevent illegitimate recombination events such as COs, hence it contributes to maintaining genome integrity (Harami et al., 2017). Studies performed in budding yeast demonstrate that cells lacking Sgs1 exhibit a hyper-recombination phenotype which resembles to the phenotype observed in cells lacking Srs2 (Bugreev et al., 2007a; Ira et al., 2003; Mankouri et al., 2002). RecQ helicase is an essential regulator during the HR where it dismantles D-loop structures and thus channels HR events towards the SDSA pathway, and it dissolves late joint molecules such as dHJs (Adams et al., 2003; Bachrati et al., 2006; Bugreev et al., 2007a; Mimitou and Symington, 2009; Schwartz and Heyer, 2011).

Mutations in RecQ helicases are found to be associated with chromosome aberrations, increased recombination frequency, elevated sister chromatid exchanges (SCEs), as well as being the direct cause of some human diseases (such as Bloom syndrome and Werner syndrome) and the predisposition to cancer (Chu and Hickson, 2009; Singh et al., 2012). The human BLM is a pivotal player in processing replication and HR intermediates and is part of the DDR (Chu and Hickson, 2009). More specifically, mutations in human BLM can cause Bloom syndrome (BS). The phenotype of BS cells includes a slowing-down of replication fork progression, accumulated replication fork blockages, chromosomal instability and frequent SCEs (Arora et al., 2014).

The activity of unwinding paired DNA and translocating in a 3' to 5' direction is crucial for RecQ helicases during HR progression. In addition, RecQ helicases bind to and unwind several DNA structures *in vitro*, such as D-loop, replication fork, Holliday junction and G-quadruplexes. Furthermore, Sgs1 and BLM are also both implicated in the 5'-3' DSB end resection to generate the 3’ ssDNA overhang (Gravel et al., 2008), in contrast to Rqh1 which is not significantly involved in the long-rang end resection (Langerak et al., 2011; Teixeira-Silva et al., 2017; Zhang et al., 2016a).

Besides the role during HR-mediated DSB repair, studies in fission yeast have revealed that Rqh1 is also an instrumental player in limiting the likelihood of chromosomal rearrangement during recombination-dependent replication (RDR). Due to the dispersed and repeated sequences in the eukaryotic genome, RDR may lead to chromosomal aberrations, and Rqh1 has been reported to prevent such faulty RDR events (Hu et al., 2013; Lambert et al., 2010). Rqh1 limits Rad51-dependent template exchange by disassembling the D-loop at the replication fork (Lambert et al., 2010). An antagonistic activity between the histone chaperone CAF-1 and Rqh1 is proposed to impact on the resolution of the D-loop during the RDR (Pietrobon et al., 2014). Moreover, the function carried out by CAF-1 and Rqh1 together appears to be conserved, as in mammals BLM directly interacts with the large human CAF-1 subunit p150, and BLM and CAF-1 coordinate in a way to promote cell survival in response to DNA damage and replication stress (Jiao et al., 2004).

2.4. Homologous recombination supports the robustness of DNA replication

Faithful and complete DNA replication is vital for maintaining genome integrity. The exposure to endogenous and exogenous stresses, as well as intrinsic hindrances such as replication fork barriers (RFBs) can interfere with DNA replication machinery, leading to replication fork arrest (Lambert and Carr, 2013). Failure in maintaining replication fork integrity may lead to increased genetic mutations, genomic rearrangement and even lethality.

Replication stresses can lead to the blockage of the progression of replication forks (fork-arrest). Various replication disturbances arrest the replication fork in different manners including stalled forks and dysfunctional/collapsed forks. Stalling of a replication fork occurs when the progression of the replisome is hindered by obstacles yet the components of the replisome are retained. Thus, stalled forks still remain competent for replication and can be resumed without further intervention. Whereas dysfunctional forks can be broken or not, depending on the association with a double strand break (DSB) or not, respectively. Dysfunctional forks may have loss replisome components and require further intervention to be resumed (Carr and Lambert, 2013; De Piccoli et al., 2012). When a replication fork is blocked, it can be rescued by the convergence with the opposite fork or by the HR mechanism.

HR is a pivotal and efficient pathway to rescue collapsed forks. The role of HR in escorting replication forks includes fork-protection, fork-restart, repair of broken forks or of post-replicative gaps. HR factors promote fork convergence and participate in recombination-dependent replication (RDR) to allow DNA synthesis resumption from arrested forks when a converging fork is not available.

Fork protection

The initial observation of HR protecting replication forks in emerged from a study showing that the recombination mediator BRCA2 stabilizes Y-shaped DNA junctions at rDNA region (ribosomal DNA, a locus that is replicated in a unidirectional manner) upon hydroxyurea-treatment (HU, an inhibitor of the ribonucleotide reductase that leads to dNTP depletion) (Lomonosov et al., 2003). Studies in *E. coli* have shown that RecA prevents replication intermediates from degradation by the nucleases in response to UV-irradiation, revealing that HR factors also have a role in fork stabilization besides the role in restarting replication forks (Chow and Courcelle, 2004; Courcelle et al., 2003). A decreased rate of replication fork progression has also been reported in mammalian cells defective for HR, suggesting the role of HR in maintaining replication fork integrity (Daboussi et al., 2008).

The role of HR in fork protection has been supported by accumulated recent studies. Using the cell-free extracts from Xenopus eggs, without the presence of RAD51, an accumulation of MRE11-dependent ssDNA gaps in newly synthesized DNA behind replication forks as well as increased levels of leading and lagging strand uncoupling at the fork junction (a result of the Cdc45–Mcm–GINS helicase complex uncoupling) have been visualized via electron microscopy

approach (Hashimoto et al., 2010). Another study has reported that the conserved C-terminus of BRCA2, which is involved in stabilizing RAD51-nucleoprotein filament but not required for the formation of the filament, is implicated in stabilizing MRE11-mediated nascent DNA degradation upon HU treatment. This demonstrates a function of HR factors in protecting stalled replication fork in a DSB repair-independent manner (Schlacher et al., 2011). RAD51 has also been shown to promote fork resumption after short HU exposure-induced fork stalling in a way that does not trigger recombination (Petermann et al., 2010). Importantly, in fission yeast, it has also been reported that the DNA-binding activity of Rad51, but not the strand-exchange function, prevents large ssDNA gaps behind arrested forks by counteracting the exonuclease activity of Exo1 (Ait Saada et al., 2017).

The fork protection function of HR is depicted in the model shown in Figure 2.8. In this model, a transient uncoupling of the replisome and DNA polymerases occurs upon fork stalling thus creating ssDNA behind the replication fork and allowing the binding of RAD51. This can occur independently of the recombination mediator. The fork reversal is mediated by RAD51. The later BRCA2-dependent loading of RAD51 onto the reversed fork prevents the degradation of the dsDNA end from several endonucleases and helicases. The stabilization of the fork could generate a time window for the merging of the stalled fork with the converging fork, therein the stalled fork is rescued in a recombination-independent manner. However, it remains unclear whether limited end-resection is required for RAD51-mediated fork reversal and protection (Ait Saada et al., 2018).

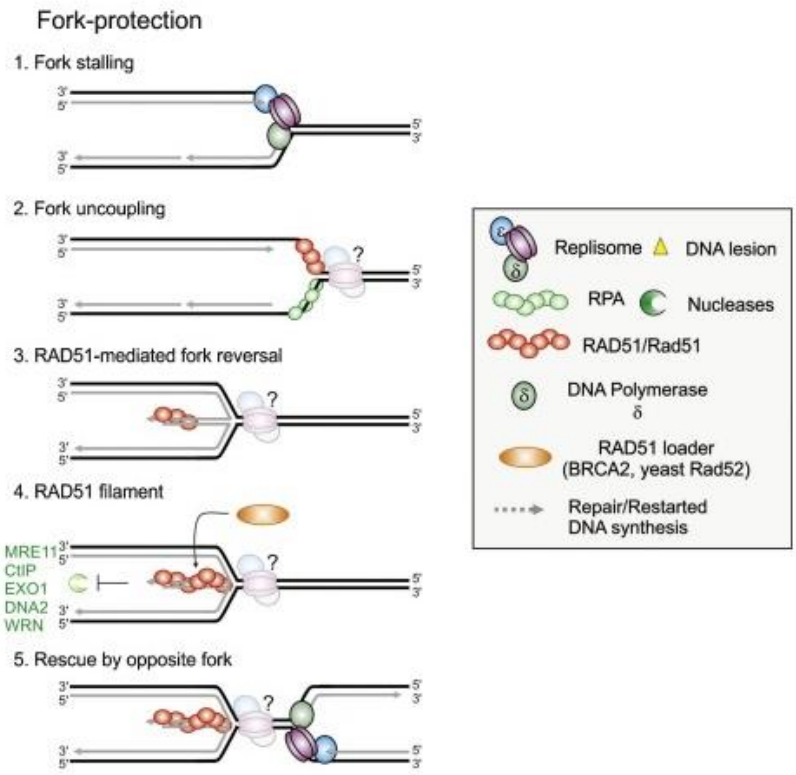

Figure 2.8. Model of the protection of a stalled replication fork by HR factors. Adapted from Ait Saada et al., 2018 (Ait Saada et al., 2018).

Fork restart

HR is exploited in restarting a collapsed fork without the presence of DSB. The studies carried out in *E. coli* have contributed to describing the mechanism of HR-mediated fork restart (reviewed in Costes and Lambert, 2013). In recent years, the application of DNA combing to study DNA replication at the single molecule level have led to a better understanding of replication restart in mammalian cells (Davies et al., 2007; Petermann et al., 2010; Tuduri et al., 2010). In fission yeast, the *RTS*1-RFB system has been used extensively in elucidating the mechanism of HR-dependent replication fork restart (Lambert et al., 2010; Mizuno et al., 2009) (Figure 2.9). The generation of ssDNA in order to accommodate Rad51 is a key step for restarting the fork at the *RTS1*. Recently, it has been elucidated that fork-resection occurs as a two-steps: the MRN complex and Ctp1 initiate a short-range resection which primes for the long-rang resection executed by Exo1 (Teixeira-Silva et al., 2017; Tsang et al., 2014). The short-range resection appears to be sufficient for fork restart (Teixeira-Silva et al., 2017). Importantly, the presence of Rad51 and Rad52 is also essential for counteracting extensive resection by Exo1 (Ait Saada et al., 2017). This is in agreement with that in mammalian cells, MRE11-mediated end resection of reversed forks requires RAD52 when BRCA2 is absent (Mijic et al., 2017). Putting

together, it suggests a role for Rad51 and Rad52 in the early recruitment of factors acting in the initial end resection events. The Rad51-nucleoprotein filament then performs strand invasion into the re-annealed parental DNA duplex forming a D-loop. Intriguingly, in contrast to the scenario of fork protection which requires the DNA-binding ability of Rad51, in the scenario of fork restart it is the strand exchange activity of Rad51 that is essential (Ait Saada et al., 2017).

The restarted fork at *RTS1* by HR is different from the canonical origin-born forks. The leading strand is synthesized by Pol ε and the lagging strand is synthesized by Pol δ within canonical forks (Kunkel and Burgers, 2008; Miyabe et al., 2011). Only Pol δ is involved in the synthesis of both strands at forks restarted by HR (Miyabe et al., 2015b). Thus the forks restarted by HR are associated with less processive DNA synthesis. The forks restarted by HR are also highly mutagenic and more error-prone than canonical replication forks (Iraqui et al., 2012; Miyabe et al., 2015b; Mizuno et al., 2013).

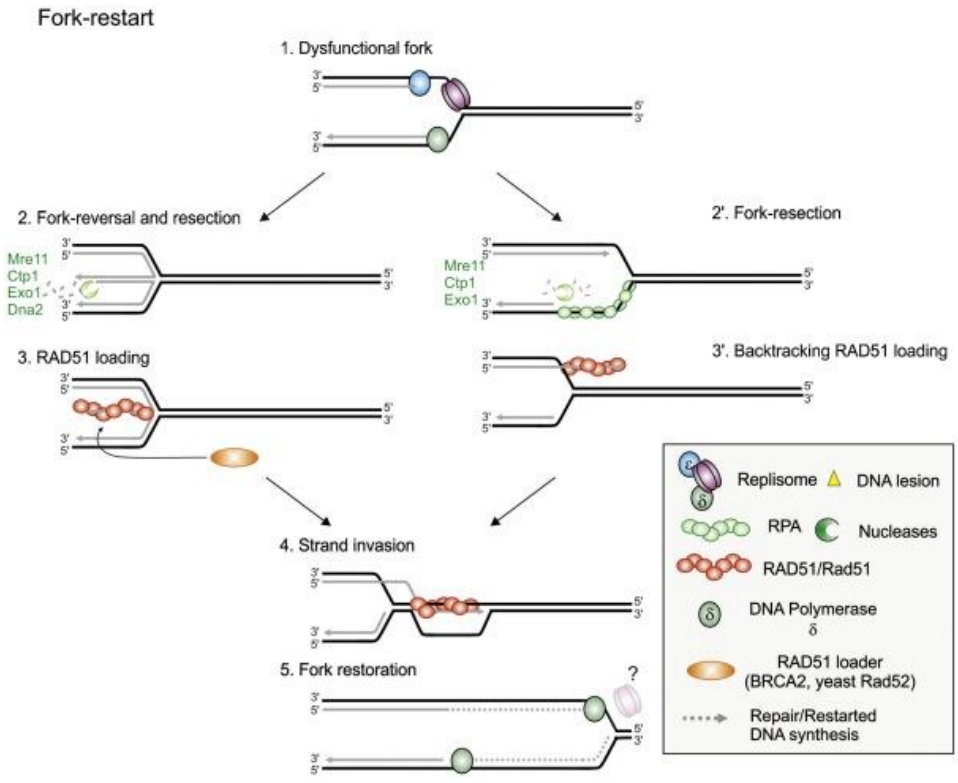

Figure 2.9. Model of restarting a DSB-free fork by HR. Adapted from Ait Saada et al., 2018 (Ait Saada et al., 2018).

Fork repair

The encounter of a nick or a gap on the passage of a replication fork results in a broken fork with a one-ended DSB. In this case, the sister chromatids are no longer physically attached to each other and the fork may be associated with an incomplete replisome (Figure 2.10). Replication-born DSBs may also occur as consequences of the presence of inter-strand crosslinks (ICLs) or high doses of the anti-cancer agents such as CPT (topoisomerase inhibitor) that lead to fork arrest and sequential cleavage by nucleases. The repair of such DSB-associated forks by HR refers to as BIR (Hashimoto et al., 2010; Moriel-Carretero and Aguilera, 2010; Räschle et al., 2008; Roseaulin et al., 2008). In budding yeast, the migration of the D-loop during BIR is mediated by the helicase Pif1 and DNA synthesis is executed by the non-essential subunit of polymerase Pol δ, Pol 32, which synthesizes DNA in a highly error-prone fashion (Lydeard et al., 2007; Saini et al., 2013; Wilson et al., 2013). Thus, BIR is highly mutagenic and is associated with genome rearrangement, as observed from different organisms (Carvalho et al., 2013; Costantino et al., 2014; Deem et al., 2011; Saini et al., 2013; Sakofsky et al., 2014; Smith et al., 2007). Notably, a recent study from budding yeast has revealed two mechanisms that contribute to limiting the mutagenic DNA synthesis during BIR. First, the timely arrival of a converging fork from the opposite direction could alleviate the extent of error-prone DNA synthesis. Second, the mutagenic DNA synthesis is limited within a few kilobases from the break as the endonuclease Mus81 could cleave the D-loop thus channeling DNA synthesis to the semi-conservative manner (Mayle et al., 2015).

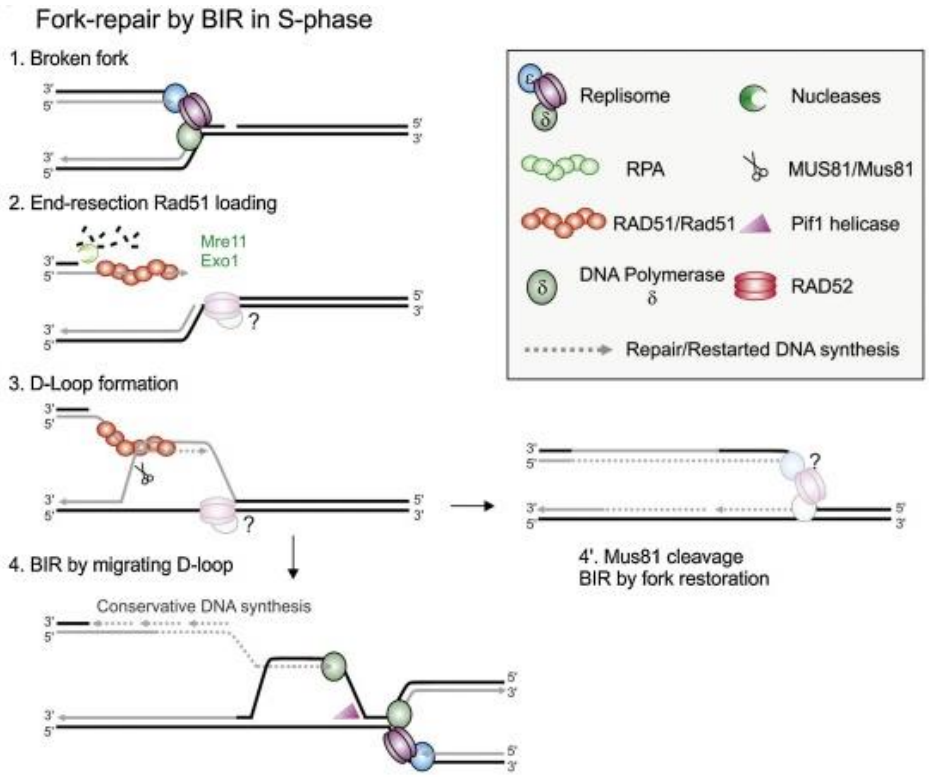

Figure 2.10. Model of restarting a broken fork associated with DSB by HR. Adapted from Ait Saada et al., 2018 (Ait Saada et al., 2018).

HR is also exploited to repair single strand gaps left behind the replication fork. Such post-replicative DNA lesions can arise when cells are exposed to UV-irradiation or MMS (DNA alkylating agent methyl methane sulfonate) leading to the uncoupling of DNA polymerases from the replisome.

In supporting the role of HR in post-replicative gaps repair, an accumulation of ssDNA gaps at/behind damaged replication forks in the absence of HR have been visualized by electronic microscopy (Hashimoto et al., 2010; Lopes et al., 2006). Specifically, it has been shown that Rad51 inhibits the accumulation of ssDNA gaps that are prevalent on damaged template behind the fork as a consequence of Mre11-dependent degradation of newly synthesized DNA strands, suggesting a role of Rad51 in protecting newly synthesized DNA and guarding continuous DNA synthesis (Hashimoto et al., 2010). Consistent with this, a study in ES (Embryonic Stem) cells has shown that large unrepaired ssDNA gaps accumulate during DNA replication when Rad51 is depleted (Choi et al., 2017). Similar observations have also been reported in other organisms. In budding yeast, the absence of Rad51 leads to the accumulation of un-replicated ssDNA gaps after MMS treatment resulting in uncompleted S phase (Alabert et al., 2009).

During the repair of post-replicative gaps, the naked DNA is coated by Rad51 to perform strand invasion into the newly synthesized sister chromatid. HR mediators Rad52, Rad55-Rad57 and Exo1 are all implicated in facilitating the strand exchange step as observed in budding yeast (Vanoli et al., 2010). DNA synthesis on the new template is mediated mainly by Pol δ, and the regulation of Pol δ is thought to involve the Rad18-Rad5-Mms2-mediated modification of PCNA (Figure 2.11) (Vanoli et al., 2010). The helicase Sgs1 is implicated in the resolution of the sister chromatid joint-molecule structure resulted from DNA synthesis (Ashton et al., 2011; Branzei et al., 2006).

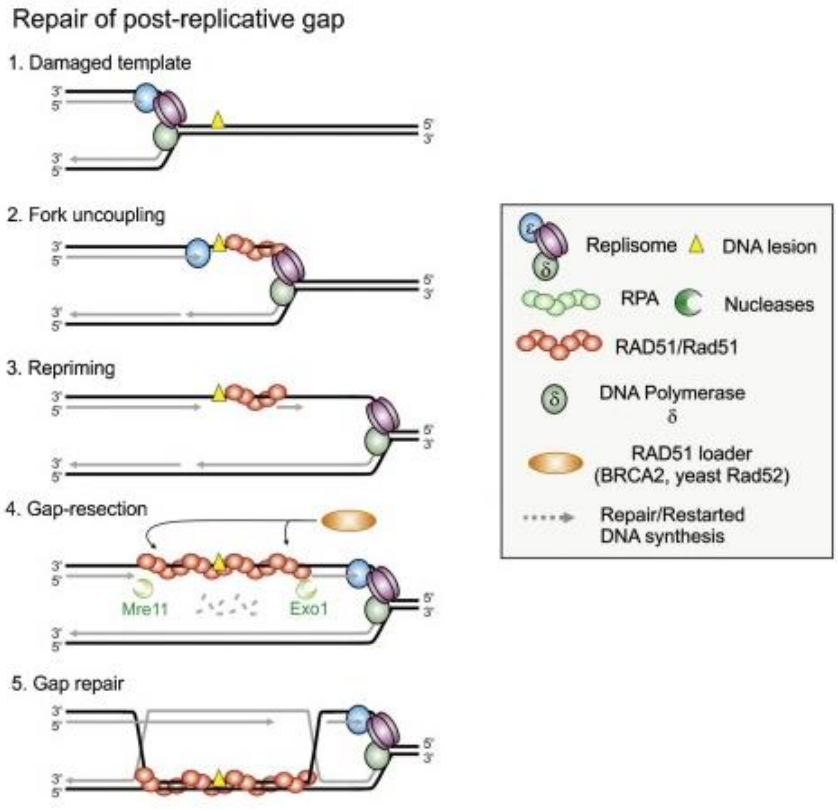

Figure 2.11. Model of repairing post-replicative gaps by HR. Adapted from Ait Saada et al., 2018 (Ait Saada et al., 2018).

3. Chromatin assembly during DNA replication

The primary structure of chromatin is a double-stranded DNA helix. The length of linearized DNA thread is way much greater than the size of any cellular compartment. Therefore, the DNA molecule must be organized in a manner that is compacted enough to fit into the nucleus while allowing its metabolism from gene expression to DNA replication and repair. There are two types of chromatin: the heterochromatin which mainly consists of inactively transcribed DNA regions, and the euchromatin which consists of actively transcribed DNA regions. Heterochromatin is defined as regions of chromatin that remain cytologically condensed and densely stained throughout the cell cycle, whereas euchromatin is de-condensed during interphase(Emil, 1928). A main difference between these two types of chromatin is that euchromatin has a less compact structure compared to heterochromatin (Eissenberg and Elgin, 2014).

The DNA molecule is packaged into chromatin via multiple levels. The first level of chromatin organization is the wrapping of the DNA around the nucleosome, the basic unit of chromatin in all eukaryotes (Kornberg, 1974; Bradbury et al., 1978). In most eukaryotic cells, a linker histone H1 (or H5 in avian species) binds to the core of a nucleosome at the site of DNA entry to form a more stable structure termed “chromatosome” (Harshman et al., 2013). The “beads on a string” structure (where the beads represent chromatosomes and the string represents DNA thread) keeps folding up to form a coiled fiber, which is reported to be 30 nm in diameter for heterochromatin, and 11 nm in diameter for euchromatin (Trojer and Reinberg, 2007). During mitosis and meiosis, the chromatin fiber is further packed in loops to form metaphasic chromosome (Figure 3.1).

Chromatin organization not only allows DNA to fit into the limited space of the nucleus, but is also instrumental to the regulation of gene expression, DNA replication and DNA repair. The chromatin fibers can cluster specific DNA regions together in an inter- or intra-chromosomal manner during transcription, creating “hotspots” of transcription activity (Brem et al., 2002; Kirst et al., 2005; Morley et al., 2004; Schadt et al., 2003). Chromatin compaction also provides an extra barrier to DNA accessibility to cellular machineries involved in DNA transcription, replication, and repair. In addition, post-translational modifications of histones and variants of histones enable the harboring of epigenetic information by the chromatin that impact chromatin dynamics and accessibility.

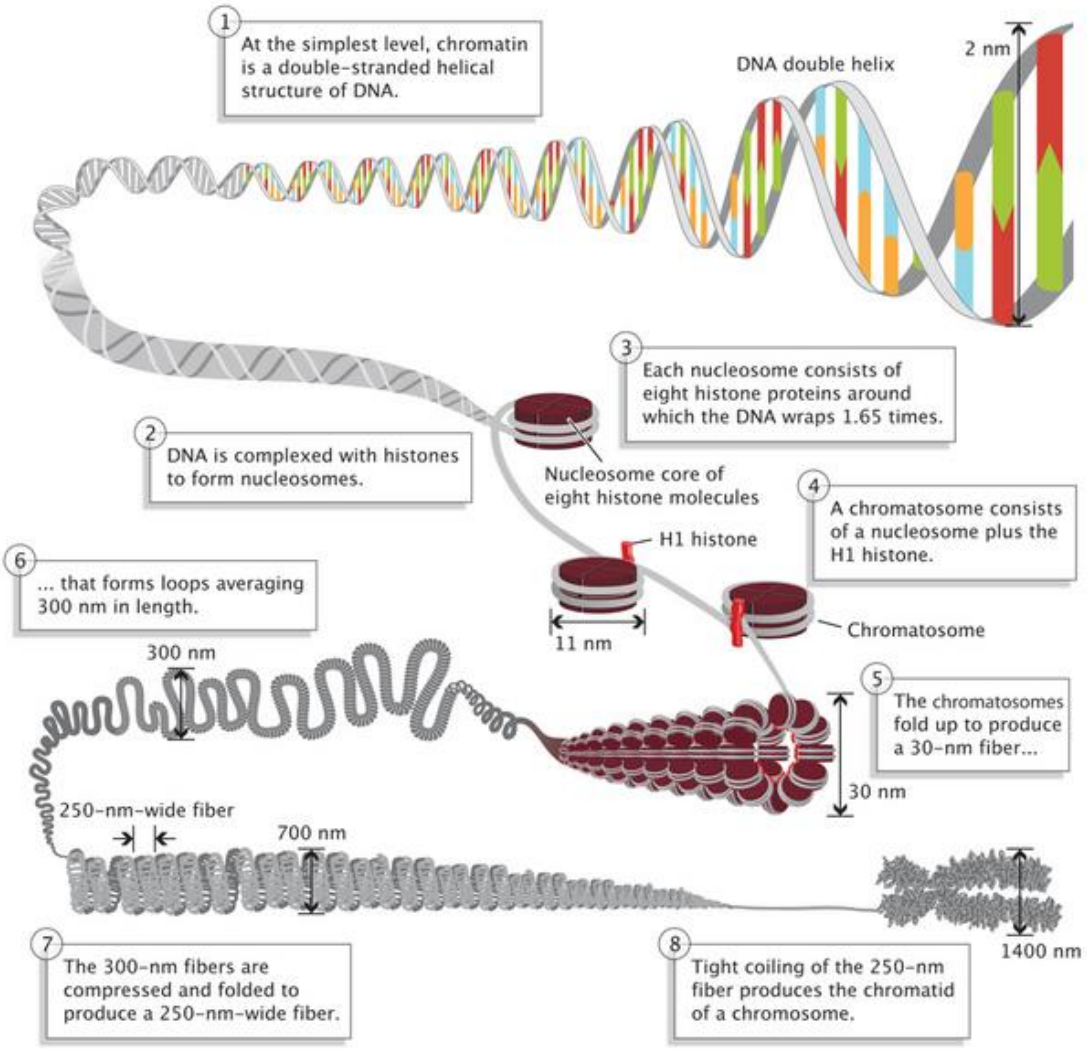

Figure 3.1. Highly complex structure of eukaryotic chromatin and levels of chromatin organization. Adapted from Pierce, Benjamin. Genetics: A Conceptual Approach, 2nd edition.

3.1. Histones and nucleosome structure

Being the fundamental unit of chromatin, the nucleosome is repeated every 160 to 240 bp along the genome (Mirzabekov, 1981). The first atomic determination of the nucleosome structure was achieved by X-ray crystallography at 2.8 Å resolution scale in 1997. This first structure showed that 146 bp of human α-satellite DNA sequence is wrapping around a *Xenopus laevis* histone octameric scaffold 1.65 times in a left-handed superhelix. Adjacent nucleosomes are connected to each other by the linker DNA in between (Luger et al., 1997). The highly alkaline histone octamer core comprises two copies each of H2A, H2B, H3 and H4 histone, in a fashion that a tetramer formed by two H3-H4 dimers is flanked by two separated H2A-H2B dimers

(Davey et al., 2002; Luger et al., 1997). The core histones have molecular weights ranging from 11 to 16 kDa, and their amino acid sequences are composed of more than 20% of lysine and arginine (Kornberg, 1974; Luger et al., 1997). In addition to the core histones, a linker histone, present in all multicellular eukaryotes, is associated with the nucleosome to increase stability and for higher orchestration of the chromatin architecture.

Regarding the primary sequences of the four core histones, H3 and H4 are found to be highly evolutionarily conserved whereas H2B and H2A are more variable (Sullivan and Landsman, 2003). In terms of protein structure, the functional domains of all four core histones can be divided into two distinct parts: a central α-helical histone fold domain and a tail domain located at the N-terminus part. The central α-helical histone fold domain comprises 80 to 90 amino acids forming a hydrophobic core, which facilitates the interactions between nucleosomal histones (Andrews and Luger, 2011). Despite differences of amino acid sequences, the histone fold domains of all core histones share a high degree of structural homology (Luger and Richmond, 1998). The N-terminal tail has a various length of 20 to 35 amino acids comprising about 20% of the total residues of a histone and is largely unstructured (Andrews and Luger, 2011). Histone tails are subjected to extensive post-translational modifications (PTMs) which are exploited in many chromatin-mediated processes. Besides the N-terminal tail, histone H2A also has a less characterized C-terminal tail, which has been suggested to stabilize the nucleosome core particles and mediate protein-protein interactions that control chromatin dynamics and conformation (Vogler et al., 2010).

The histone fold domain consists of three α-helices (α1, α2 and α3) connected by two intervening loops (L1 and L2) (Figure 3.2 b, c) (Arents and Moudrianakis, 1995; Arents et al., 1991; Luger et al., 1997). The long helix α2 is looped against by two short flanking helices α1 and α3. The histone fold domain of each histone pairs with a complementary domain from another histone in an antiparallel manner, to form the H3-H4 or H2A-H2B dimer. Two H3-H4 dimers interact with each other to form a tetramer, and in the presence of DNA, each half of the tetramer is bound by a H2A-H2B dimer, resulting in the formation of a nucleosome core octamer (Figure 3.2 a) (Arents et al., 1991; Eickbush and Moudrianakis, 1978).

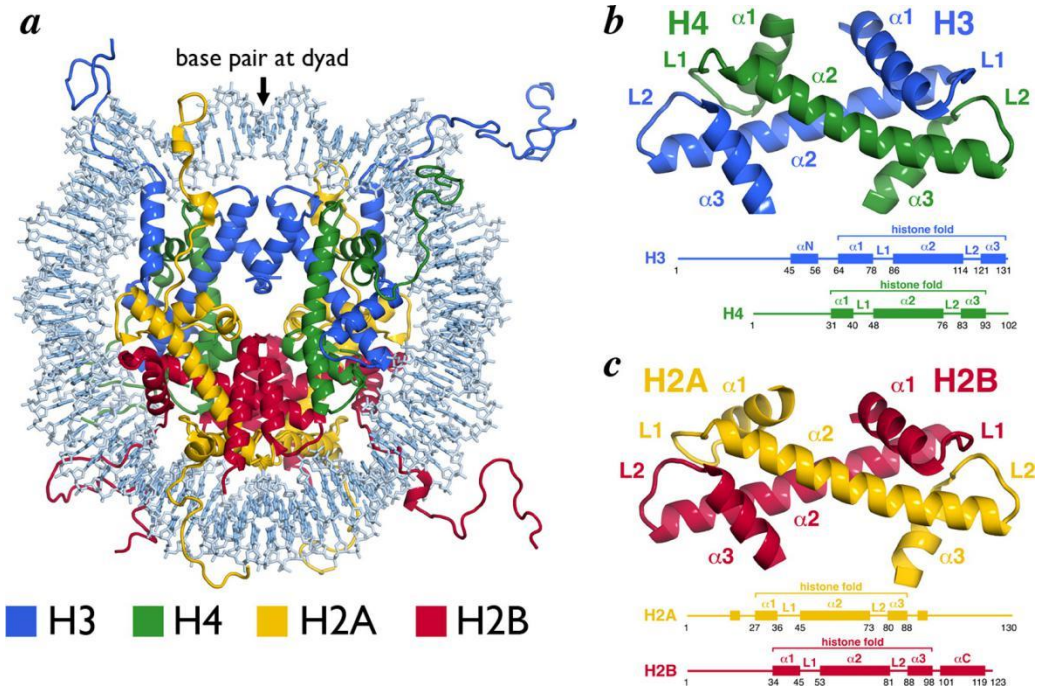

Figure 3.2. Structure of the nucleosome core particle and heterodimers formed via interaction between histone folds. (a) Structure of the nucleosome core octamer. Histones and DNA are represented in cartoon and sticks respectively, and colored as indicated. (b) H3-H4 histone-fold heterodimer. (c) H2A-H2B histone-fold heterodimer. The structure is shown on top and scheme is shown at the bottom with secondary structure elements indicated. Adapted from McGinty and Tan, 2015 (McGinty and Tan, 2015).

The N-terminal tails of histones are protruding from the nucleosome core and undergo a wide range of PTMs including methylation, phosphorylation, acetylation, ubiquitylation, and SUMOylation. PTMs on histone tails are key regulators of DNA-based processes, including transcription activity, gene silencing, DNA replication and repair. The PTMs of histones tails impact on the association with chromatin-modifying enzymes, chromatin readers and erasers in a way that the chromatin structure is locally modulated. In light of this, the concept of "histone codes" has been proposed to elucidate the mechanisms by which PTMs regulate cell fate decision (Strahl and Allis, 2000; Turner, 2000).

The core histones have further differentiated into variants throughout the evolution (Zweidler 1978). Histone variants are non-allelic isoforms of major types of histones. Histones are found in different cellular contexts in specific chromosomal regions (Talbert and Henikoff, 2010). Among the four core histones, H4 and H2B are less variant, whereas multiple variants of H3 and H2A have been identified in human somatic cells (Buschbeck and Hake, 2017; Campos and Reinberg, 2009). The discrepancy among histone variants may consist of only few amino acids substitutions in the protein sequence. Histone variants affect the structure and stability of the nucleosome

and the chromatin and thus influence the accessibility of cellular machineries to DNA (Franklin and Zweidler, 1977; Newrock et al., 1978). For instance, the mammalian histone H3 variant H3.2 differs from the main variant H3.1 by a single amino acid substitution (S96C). The H3.3 variant differs from H3.1 via five residue substitutions (A31S, S87A, V89I, M90G, and C96S) (Hake and Allis, 2006). The histone variant H3.1 is incorporated into nucleosome in a replication-dependent manner whereas H3.3 is incorporated into nucleosomes in a replication-independent manner and preferentially in transcribed regions of the genome (Ahmad and Henikoff, 2002; Orsi et al., 2009; Ray-Gallet et al., 2011a; Tagami et al., 2004). Another identified histone H3 variant is CENP-A (centromeric protein-A) which is encoded by *cnp1* in fission yeast (Huang et al., 2003). This histone variant appears restricted to the centromeric chromatin and is necessary to the centromere identity in eukaryotes (Black et al., 2004; Dunleavy et al., 2011; Sullivan et al., 2013; Palmer et al., 1987). The histone variant H2A.Z is associated to promoters and enhancers of actively transcribed genes (Billon and Côté, 2012; Guillemette et al., 2005; Talbert and Henikoff, 2017). The histone variant H2A.X is phosphorylated by checkpoint kinases in response to DNA damage and replication stress to form ϒ-H2A.X, a histone modification which is broadly used as a marker of DNA damage (van Attikum and Gasser, 2005; Kobayashi, 2004; Osley et al., 2007; Paull et al., 2000; Rogakou et al., 1998, 1999). It is noteworthy that in fission yeast, despite the existence of the histone variant H2A.Z and the histone variant CENP-A, a single histone H3 or H4 protein is encoded by three different genes: *hht1, hht2* and *hht3 for* H3, and *hhf1, hhf2* and *hhf3 for* H4 (Carr et al., 1994b; Lando et al., 2012; Matsumoto and Yanagida, 1985).

Unlike the core histones, the linker histones are the most divergent group, with numerous variants found in various types of cells during different cell stages. The linker histones are composed of 210 to 220 amino acids and do not share the structural homology of the fold domain with the core histones. However, linker histone variants in metazoans possess a conserved tripartite structure (Allan et al., 1980, 1986), consisting of a short and flexible N-terminal tail, a central globular domain (also called H15 domain) of about 80 amino acids, and a long and highly basic C-terminal tail. The H15 domain contains well conserved positively charged amino acid motifs that are important for nucleosome binding (Brown et al., 2006; Zhou et al., 2015). In addition to maintaining a higher structure of the chromatin, the linker histones have been reported to play a role in epigenetic regulation (Fan et al., 2005; Wierzbicki and Jerzmanowski, 2005). Notably, fission yeast chromatin has a more open structure and lacks the linker histones. Nonetheless, artificial addition of mammalian linker histones to reconstitute fission yeast chromatin is able to alter the chromatin fiber structure to a higher order *in vitro*,

supporting that the linker histones contribute to the positive charge of histones and fine-tune the charge balance against the negative charge of DNA, therein impacts on the chromatin structure (Prieto et al., 2012).

3.2. Nucleosome assembly at the replication fork

The duplication of the chromosomes has to faithfully maintain both the genetic information encoded by the DNA and the epigenetic information embedded in the chromatin. Chromatin constitutes an intrinsic barrier to the DNA replication machinery. Therefore, nucleosomes ahead of the advanced replication fork are evicted and both parental and newly synthetized histones are assembled onto newly replicated DNA through a process called replication-coupled chromatin assembly. Because the DNA material doubles during DNA replication, newly synthesized histones are needed in a timely manner to maintain chromatin packaging and epigenetic information.

As a consequence, the newly replicated chromatin is composed of both pre-existing parental histones as well as newly synthesized histones. Replication-coupled chromatin assembly requires a network of chromatin factors, including histone chaperone and histone modifiers, which operate sequential reactions to handle histone dynamics at ongoing replication forks (Figure 3.3).

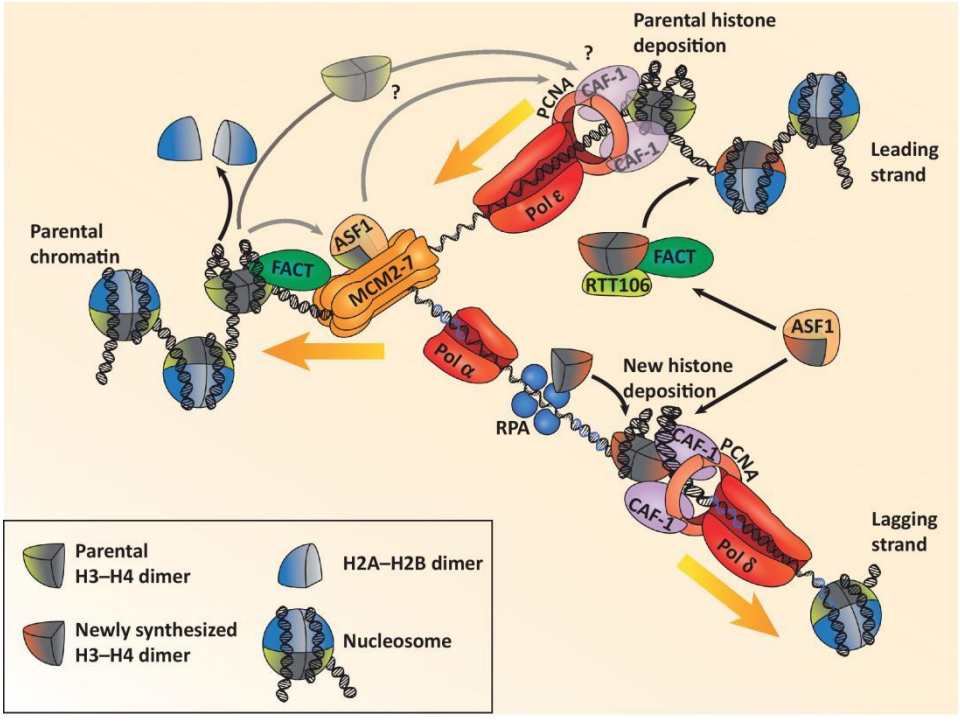

Figure 3.3. Model of nucleosome assembly at the replication fork. DNA duplex ahead of the replication fork is unwound by the helicase MCM2-7. Parental nucleosomes on the path of the replication fork are disrupted with the contribution from the histone chaperone FACT, which interacts with MCM2-7 and is thought to facilitate the progression of the replication fork. The $(H3\text{-}H4)_2$ tetramer from the disrupted parental nucleosomes could then be handed by Mcm2 and FACT. However, it remains unclear how parental $(H3–H4)_2$ tetramers are transferred behind the replication forks and deposited onto newly replicated DNA. Newly synthesized H3–H4 dimers are escorted by Asf1 and handed off to downstream histone chaperones including CAF-1 and Rtt106. Two H3-H4 dimer-containing CAF-1 complexes promote the formation of $(H3\text{-}H4)_2$ tetramer in close proximity to the DNA and deposit the tetramer onto the DNA. Additionally, Rtt106 also deposits H3-H4 dimers onto DNA in association with FACT. The trimeric RPA protein which binds the lagging strand has a role in regulating nucleosome assembly via its interaction with H3-H4 dimer as well as with histone chaperones. Adapted from Serra-Cardona and Zhang, 2017 (Serra-Cardona and Zhang, 2017).

The replication of chromatin requires the eviction of the parental nuleosomes in order to gain accessibility for the replication machinery that moves along the DNA. The MCM2-7 complex, a component of the replicative helicase, has been implicated in the complete disruption of nucleosomes to pave the way for the advancing of the replication fork (Groth, 2009). The role of MCM2-7 in nucleosome disassembly has been supported by the crystal structure of Mcm2, a subunit of the MCM2-7 complex, in association with the $(H3\text{-}H4)_2$ tetramer. This study showed that Mcm2 interacts with one H3-H4 molecule via its N-terminus (Richet et al., 2015; Huang et al., 2015).

Evicted parental nucleosomes are further separated into H2A-H2B dimers, H3-H4 dimers, and $(H3\text{-}H4)_2$ tetramer. The histone chaperone responsible for this remains unclear. These pre-existing building blocks are designated as the parental histones, while newly synthesized histones are provided at the same time, which need to be carefully differentiated from the parental histones in order to preserve the faithful inheritance of histone PTMs. In yeast models, a predominant marker for newly synthesized histones is found to be the acetylation on the lysine 56 of histone H3 (H3K56Ac) (Kuo et al., 1996; Masumoto et al., 2005). The acetylation of H3K56 is performed by the histone acetyltransferase Rtt109 when H3-H4 is in a complex with Asf1 (Han et al., 2007; Xhemalce et al., 2007). H3K56Ac is shown to promote sequential ubiquitylation of K121, K122 and K125 on histone H3 in budding yeast by Rtt101-MMS1, a modification that compromises the association between Asf1 and H3-H4 to facilitate the hand-off of H3-H4 from Asf1 to the downstream chaperones including Rtt106 and CAF-1 (Han et al., 2013).

Nucleosome assembly occurs as a stepwise process in which the $(H3\text{-}H4)_2$ tetramer is deposited before two H2A-H2B dimers (Hatakeyama et al., 2016; Smith and Stillman, 1991a). A long-lived question was about the stoichiometry of histone deposition during DNA replication. Because histone H3 and H4 form a stable tetramer under physiologically conditions (Baxevanis et al., 1991), it has been long believed that a parental nucleosome is disassembled into two H2A-H2B dimers and a $(H3\text{-}H4)_2$ tetramer, and the entire parental $(H3\text{-}H4)_2$ tetramer is then directly deposited onto nascent DNA strands behind the replication fork (Figure 3.4 a) (Jackson, 1988). The force generated by the unwinding of the parental DNA via the replicative helicase, and the accumulation of DNA supercoiling ahead of the replication fork are thought to both facilitate the eviction of the parental nucleosomes (Gruss et al., 1993; Hall et al., 2009; Ramsperger and Stahl, 1995). Recently, the conserved subunits of the DNA polymerase ε, Dpb3 and Dbp4 which can form a H2A-H2B like dimer that binds to dsDNA (Barrera-Oro et al., 2008; Li et al., 2000), have been proposed to be integral components of the chromatin remodeling complex CHRAC (CHRomatin Accessibility Complex) (Kukimoto et al., 2004) to participate in coupling nucleosome disruption and DNA synthesis at the replication fork (Figure 3.4 b). A recent study showed that mammalian POLE3 and POLE4, two subunits of the DNA polymerase Epsilon, have an intrinsic histone chaperone activity to promote tetramer formation and to maintain chromatin integrity at replication forks (Bellelli et al Mol Cell 2018). However, alternative models proposed that the parental $(H3\text{-}H4)_2$ tetramer is disrupted into two H3-H4 dimers resulting in a different segregation mechanism of parental histone. Indeed, recent protein crystallization studies showed that, Mcm2, a subunit of the MCM2-7 complex which is part of the replicative helicase, associates with a $(H3\text{-}H4)_2$ tetramer via two Mcm2 N-terminal histone-binding domains (HBDs) (Huang et al., 2015; Richet et al., 2015). The conformation of the Mcm2-$(H3\text{-}H4)_2$ complex leads to the masking of the DNA binding surface and the H2A-H2B docking site on H3-H4. Such interactions may prevent spurious octamer formation. In addition, a transient split of parental histone $(H3\text{-}H4)_2$ tetramer was also observed (Figure 3.4 c). It is reported that the Mcm2-$(H3\text{-}H4)_2$ complex can further interacts with the histone chaperone Asf1 (Anti-Silencing Factor 1) in a way that Asf1 blocks the H3 interface necessary for tetramer formation and therefore leads to the disruption of the $(H3\text{-}H4)_2$ tetramer into two H3-H4 dimers bound to Asf1 (Clément and Almouzni, 2015; Natsume et al., 2007; Richet et al., 2015). The association of Asf1 with a H3-H4 dimer contributes to histone recycling and histone deposition onto nascent strands. Therefore, both parental and newly synthetized H3-H4 could be concomitantly deposited onto newly replicated DNA. Such mechanism of recycling parental histones may facilitate the incorporation

of pre-existing histone marks to newly synthetized histones (Tagami et al., 2004). It cannot be excluded that these two alternative mechanisms of parental histone segregation are differently used during DNA replication or DNA repair or upon replication stress (Groth, 2009; Groth et al., 2007a). A recent study has analyzed the segregation of PTM between the lagging and leading strands in embryonic stem cells. Parental histones H3-H4 were found segregating to both strands with a weak leading strands bias in an MCM2-dependent manner (Petryk et al., 2018).

In the context of perturbed DNA replication by replication inhibitors such as Hydroxyurea (HU), that causes an uncoupling of replicative helicases from DNA polymerases, Asf1 associates with both parental and newly synthesized H3-H4 dimers that are differentiated by their PTMs. Asf1-(H3-H4) complexes are then employed to restore chromatin during replication recovery (Figure 3.4 d) (Jasencakova et al., 2010). Nonetheless, whether the deposition of parental histone H3-H4 during unperturbed DNA replication is via the direct transfer of an intact $(H3\text{-}H4)_2$ tetramer onto the DNA, or it goes through a temporary tetramer-to-dimer state of the parental $(H3\text{-}H4)_2$ tetramer, remains to be further determined.

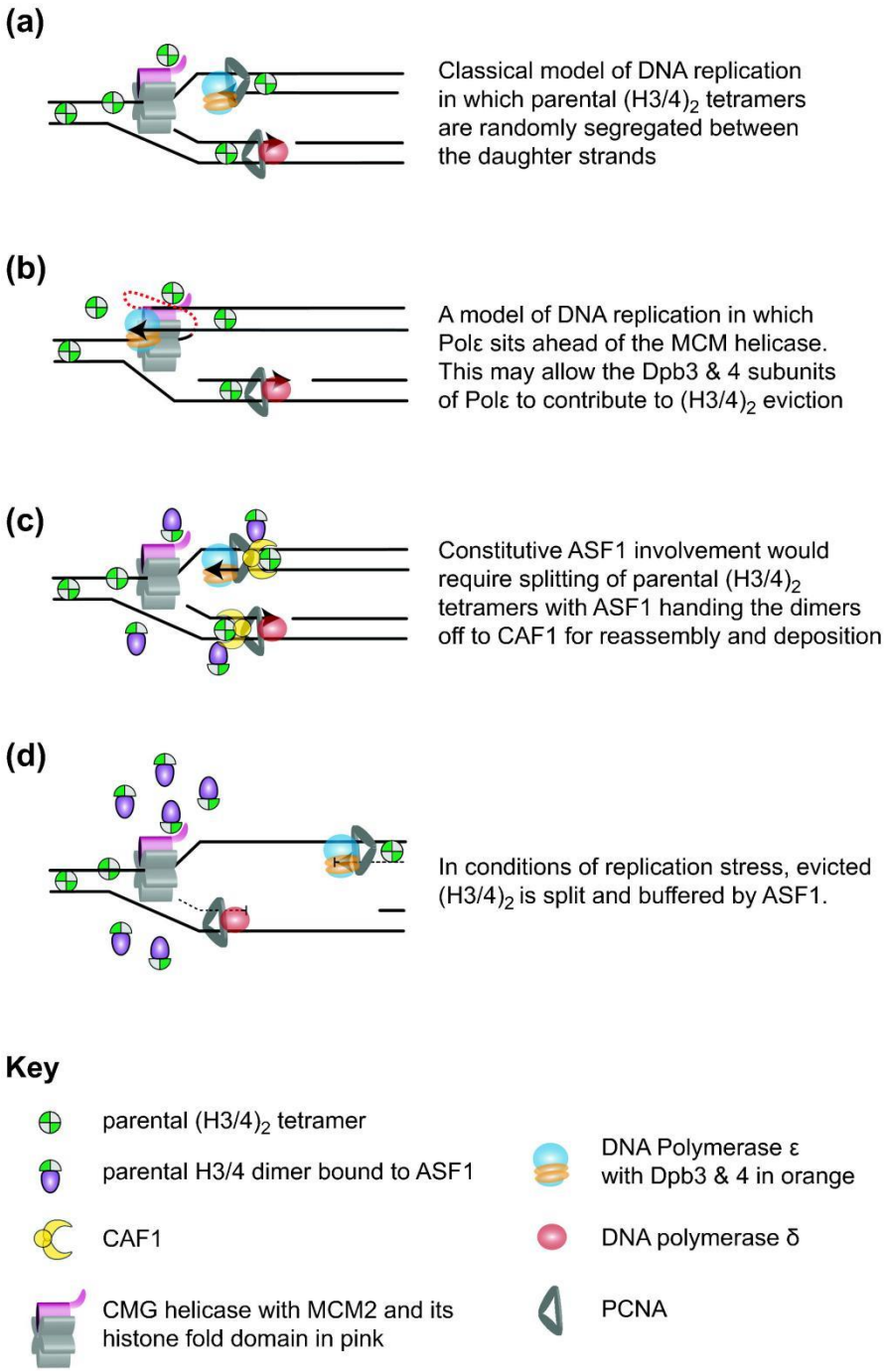

Figure 3.4. Models of parental histone H3 and H4 managements at the replication fork. (a) Deposition of the parental (H3-H4)$_2$ tetramer without split. A (H3-H4)$_2$ tetramer is bound by Mcm2 via the HBD domain located on the N-terminus of Mcm2 and then passed to nascent DNA strands. The histone chaperone in charge of depositing the (H3-H4)$_2$ tetramer remains unknown. (b) A suggested role for Polε in parental (H3-H4)$_2$ tetramer eviction ahead of the replication fork. (c) Deposition of parental (H3-H4)$_2$ tetramer with transient split. The binding of Asf1 causes the disruption of a (H3-H4)$_2$ tetramer into two H3-H4 dimers which are then handed off to CAF-1 for nucleosome assembly. (d) Displaced parental (H3-H4)$_2$ tetramers are split and buffered by Asf1 in the context of uncoupling of replicative helicases from DNA polymerases during replication stresses. Adapted from Šviković and Sale, 2011 (Šviković and Sale, 2017).

Furthermore, the participation of newly synthesized histones besides the parental histones has added more complexity to the mechanism of *de novo* nucleosome assembly at the replication fork. The process of the deposition of newly synthesized histones involves distinct factors capable of recognizing specific PTMs on the histones, and this will be further discussed in the rest of this chapter.

Histones are positively charged proteins and have intrinsic affinity for the negatively charged DNA. Without a histone chaperones to ensure the proper incorporation of histone into DNA, soluble histones might be engaged in non-specific histone-DNA aggregation formation. Histone chaperones are a class of highly conserved eukaryotic proteins that bind single or complexes histones to promote their deposition in a controlled manner onto DNA, without being part of the final product (Laskey et al., 1978; Polo et al., 2006a; Ray-Gallet et al., 2002a). Histone chaperones are negatively charged proteins necessary to escort histones to avoid promiscuous interactions and to assemble/disassemble chromatin. Since the elucidation of the histone chaperone function of nucleoplasmin by classical biochemical approaches in 1978 (Laskey et al., 1978), the members of histone chaperone family keep increasing. So far a variety of histone chaperones have been identified to function in different cellular processes and showing distinct affinities for histone and histone variants. According to their histone substrates, histone chaperones are classified into two main families: H2A-H2B chaperones and H3-H4 chaperones (Table 3.1) (Gurard-Levin et al., 2014; Ramirez-Parra and Gutierrez, 2007).

Nucleosome assembly behind the replication fork is carried out by the collaboration of multiple chromatin factors. As mentioned above, the process of replication-coupled nucleosome assembly is likely to include several mechanisms: the transfer of an intact parental $(H3\text{-}H4)_2$ tetramer, the deposition of parental H3-H4 dimers generated by splitting tetramers involving Asf1 binding, and the handling of newly synthesized histone H3 and H4. According to current knowledge, the deposition of an intact $(H3\text{-}H4)_2$ tetramer is poorly understood. Nonetheless, the histone H2A-H2B chaperone Nap1 (Nucleosome assembly protein 1) and the FACT (FAcilitate Chromatin Transcription) complex have been proposed as potential players in this scenario (Šviković and Sale, 2017). Nap1 is found to be present in a conformation with $(H3\text{-}H4)_2$ tetramer which can be used as a subnucleosome in chromatin assembly (Bowman et al., 2011). The FACT complex which chaperones both H2A-H2B and H3-H4 is demonstrated to associate with $(H3\text{-}H4)_2$ tetramer via its middle domain and its adjacent acidic AID segment on the Spt16 subunit in a crystal structure (Tsunaka et al., 2016). Furthermore, FACT also interacts with replisome

components including the replicative primase Pol α, the CMG (Cdc45–Mcm–GINS) helicase and RPA (Tan et al., 2006; VanDemark et al., 2006; Wittmeyer and Formosa, 1997). For the deposition of newly synthesized H3-H4, CAF-1 (Chromatin Assembly Factor 1) is found to be among the major player operating in a network of histone chaperones. Detailed description of CAF-1 will be given in section 3.3 and the mechanism of histone deposition by CAF-1 will be discussed in section 3.4.

Histone Chaperone	**Binding Partners**	**Functions**	**Conservation**
Asf1	H3–H4 dimer, HIRA, CAF-1, RFC, MCMs (via histones), Bdf1	Transcriptional regulation, replication, repair, transcriptional silencing, promotes histone acetylation, assembly of senescence associated heterochromatin foci (SAHF)	Asf1 (*S. cerevisiae*); Cia1 (*S. pombe*); ASF1a, ASF1b (*H. sapiens*)
Vps75	H3–H4, Rtt109	Transcriptional regulation, repair, telomere length maintenance, promotes histone acetylation	Vps75 (*S. cerevisiae*); Ccp1 (*S. pombe*)
Rtt106	H3–H4 CAF-1	Replication, transcriptional silencing, transcription repression	Rtt106 (*S. cerevisiae*); SPAC6G9.03c (*S. pombe*);
CAF-1 (heterotrimeric complex)	H3.1–H4, Rtt106, Asf1, HP1, PCNA, MBD1	Replication, repair, transcriptional silencing	Cac1/2/3 (*S. cerevisiae*); Pcf1/2/3 (*S. pombe*); p150/p61/p48 (*H. sapiens*)
HIRA	H3–H4, ASf1, Pax 3, Swi/Snf	DNA synthesis independent nucleosome assembly, transcriptional repression, transcriptional silencing, assembly of SAHF, sperm chromatin decondensation	HIR1/HIR2 (*S. cerevisiae*); Hip1, Sim2 (*S. pombe*); HIRA (*H. sapiens*)
MCM2	CENP-A–H4, H3.1–H4, H3.2–H4, H3.3–H4	Replication	Mcm2 (*S. cerevisiae*); Mcm2 (*S. pombe*); MCM2 (*H. sapiens*)
TONSL	H3–H4,MMS22L	Replication, recombination-dependent repair	TONSL (*H. sapiens*)

Histone Chaperone	Binding Partners	Functions	Conservation
FACT (heterodimeric complex)	H3–H4, H2A–H2B, RPA, MCMs	Replication, repair ,transcription, recombination	Spt16/Pob3 (*S. cerevisiae*, *S. pombe*); Spt16/SSRP (*H. sapiens*)

Table 3.1 Classification of histone H3-H4 chaperones. Adapted from Gurard-Levin et al.,2014, Hammond et al., 2017, an Das et al., 2010 (Das et al., 2010; Gurard-Levin et al., 2014; Hammond et al., 2017).

3.3. The chromatin assembly factor 1, CAF-1

The identification of CAF-1 dates back to 1986, when Stillman and colleagues noticed that 293T cell cytoplasmic extracts were capable of facilitating the replication of SV40 plasmid DNA, but no further mini-chromosome was formed until 293T cell nuclear extracts were added (Stillman, 1986). Such observation led to the following work by Stillman and Smith in which they purified a heterotrimeric complex containing p150, p60 and p48 from the nuclei of human cells. This complex exhibited the activity of DNA replication-coupled histone assembling, and hence was given the name CAF-1 (Chromatin Assembly Factor 1) (Smith and Stillman, 1989). Further studies confirmed that the three subunits of CAF-1 followed a 1:1:1 stoichiomerty when forming the complex and a novel pattern of lysine acetylation was identified on the histone H4 co-purified with the CAF-1 complex (Verreault et al., 1996). Since then, extensive studies on CAF-1 have been performed in various organisms leading to the realization of the high conservation of CAF-1 function, as well as its crucial role in nucleosome assembly during DNA replication and repair.

The large subunit of CAF-1

The large subunit of CAF-1 is named p150 (956 amino acids, also called CHAF1a) in human, p180 (1183 amino acids) in Drosophila, Cac1 (606 amino acids) in budding yeast and Pcf1 (544 amino acids) in fission yeast. The human p150 harbors several functional domains (Figure 3.5). The recombinant p150 was first produced by Kaufman et al. in 1995, by which they described three important domains of p150: the PEST box (residues 246-296, enriched in proline (P), glutamic acid (E), serine (S), threonine (T), and aspartic acid residues (D)), the KER domain (residues 311-445, mainly consists of lysine (K), glutamic acid (E), and arginine (R)), and the ED domain (residues 564-641, contains clusters of acidic residues glutamic acid (E) and aspartic acid (D)) (Kaufman et al., 1995). The PEST box is assumed to be a signal peptide for driving protein

degradation (Rogers et al., 1986). Indeed, p150 is proteolyzed in cell extracts. However, the deletion of the PEST box does not interfere with p150 protein function (Kaufman et al., 1995). The ED domain which is enriched in negatively charged residues and the highly acidic KER domain directly interact with newly synthesized acetylated histones; such interaction is important for the histone chaperone function of CAF-1 (Kaufman et al., 1995). The work carried out on the budding yeast Cac1 has shown that the ED domain together with a structured winged helix domain composes a minimal C-terminal region, which is sufficient for $(H3\text{-}H4)_2$ tetramerization (Liu et al., 2016).

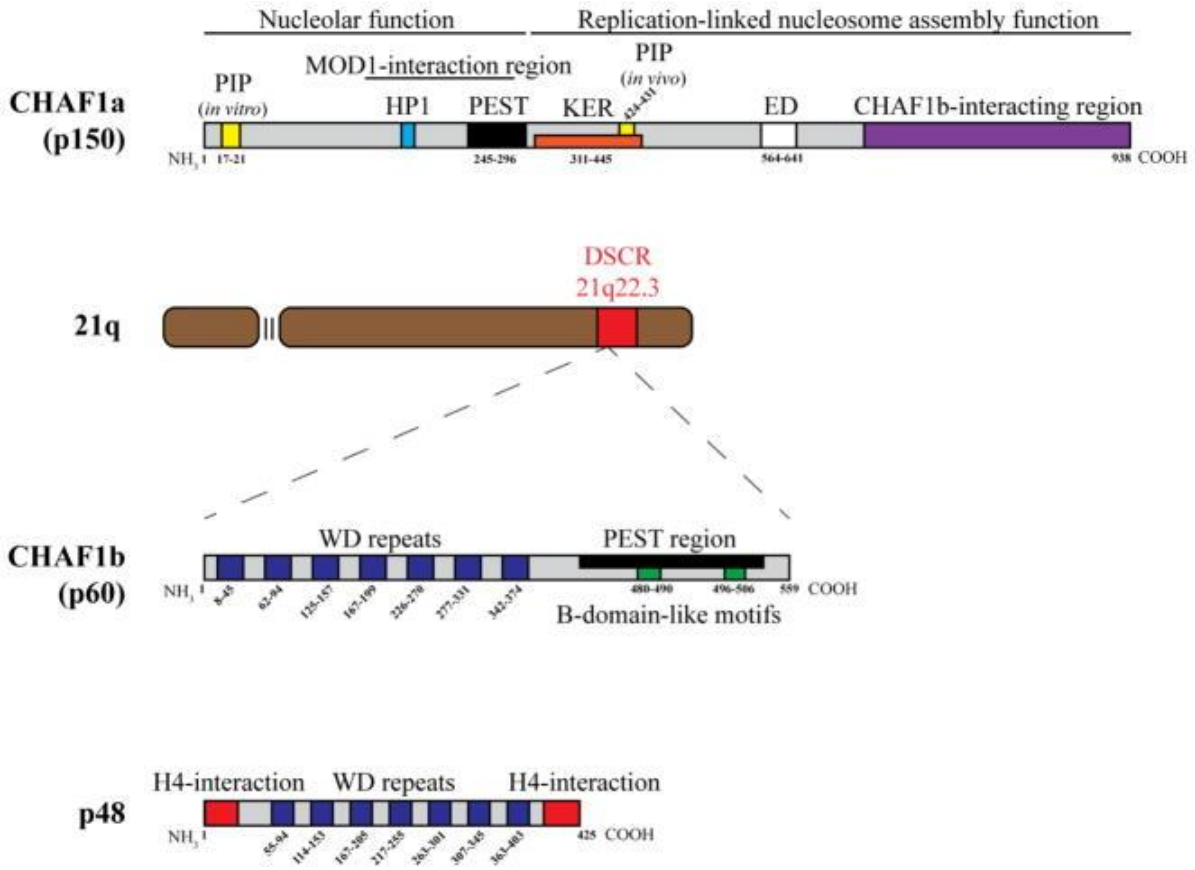

Figure 3.5. The three subunits of human CAF-1. Differently colored boxes on the protein diagram indicate domains of the subunits. The diagram of chromosome 21 shows that p60 is located within the DSCR (Down Syndrome Critical Region) of chromosome 21. Adapted from Volk and Crispino, 2015 (Volk and Crispino, 2015).

In mouse, a MIR domain (MOD1-Interacting Region, residues 176-327) was identified in p150. This domain interacts with the heterochromatin protein HP1α and is required for heterochromatin maintenance (Murzina et al., 1999). In fission yeast, although Pcf1 lacks the MIR domain, it has been shown that CAF-1 is involved in heterochromatin maintenance in a

replication-coupled manner by recruiting Swi1 (the HP1 homologue in fission yeast) to replicated heterochromatin in S phase (Dohke et al., 2008).

CAF-1 is targeted to site of DNA synthesis and this requires the large subunit. Evidences from multiple studies in different organisms demonstrate that the interaction between p150 and PCNA (Proliferating Cell Nuclear Antigen) via the PIP (PCNA Interacting Peptide) motif on p150 is crucial for targeting CAF-1 to replication factories (Ben-Shahar et al., 2009; Gérard et al., 2006a; Krawitz et al., 2002; Moggs et al., 2000; Pietrobon et al., 2014; Shibahara and Stillman, 1999; Xhemalce et al., 2007). PCNA is a homo-trimer ring that encircles the DNA and is the processivity factor for DNA polymerases. PCNA plays multiple roles in DNA synthesis-associated processes via its scaffolding function (Boehm et al., 2016). Protein-protein interaction with PCNA usually occurs through one or more PIP motifs (Hubscher et al., 1998; Maga and Hübscher, 2003; Wilkins, 2000). The canonical and minimal consensus of the PIP motif is defined by QXXhXXaa, wherein h represents residues with moderately hydrophobic side chains such as leucine, isoleucine, or methionine (L, I, M), a represents residues with highly hydrophobic, aromatic side chains such as phenylalanine and tyrosine (F, Y), while X is not specifically defined (Warbrick, 1998). Human p150 harbors two distinct PIP motifs: a canonical one located in the N-terminal part (PIP1, residues 25-29), and a less conserved motif in the middle of p150 (PIP2, residues 4254-428) (Ben-Shahar et al., 2009). Data from *in vitro* system show that PIP1 exhibits high affinity for PCNA in a way that the deletion of PIP1 completely abolishes the interaction between p150 and PCNA interaction. In contrast, PIP2 has a weak affinity for PCNA, and the deletion of PIP2 only slightly compromises the interaction between p150 and PCNA. Surprisingly, PIP2 is critical to target CAF-1 to replication factories *in vivo* and for *in vitro* replication-coupled chromatin assembly, whereas PIP1 appears dispensable (Ben-Shahar et al., 2009).

The PIP motif is also conserved in the large subunit of CAF-1 of yeast models (Figure 3.6). In budding yeast, mutations of the PIP motif impair the interaction with PCNA resulting *in vivo* in a slight defect in silencing telomeres in an Asf1-dependent manner and impair DNA replication-coupled histone deposition activity *in vitro* (Krawitz et al., 2002). In fission yeast, mutation of the PIP motif severely compromises PCNA/Pcf1 interaction as well as the targeting of Pcf1 to replication foci (Pietrobon et al., 2014).

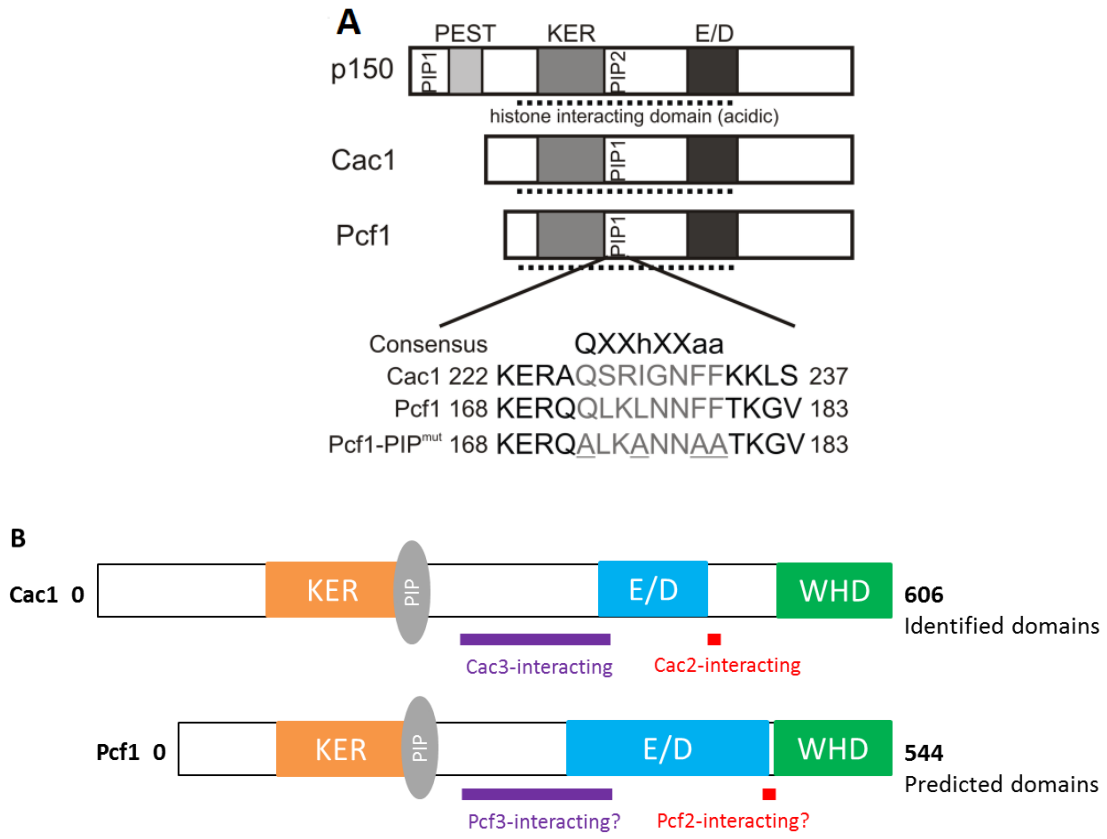

Figure 3.6. A. Diagram showing PIP motif, KER and ED domain in human p150, budding yeast Cac1, and fission yeast Pcf1. The human p150 possesses two PIP motifs, and a PEST box which is lacking in the yeast models. The dashed line indicates the acidic region involved in histone binding. Adapted from Pietrobon et al., 2014 (Pietrobon et al., 2014). B. Updated diagrams of the large CAF-1 subunit in yeast models. Upper panel: diagram of budding yeast Cac1 showing different functional domains. KER domain (in orange, residues 129–230) contains the DNA-binding coiled-coil (spanning the KER domain, residues 135-230, shown as the orange line above). At the end of the KER domain is the PIP box (in gray, residues 222-237) which mediates PCNA interaction. The acidic ED domain is located in the middle of Cac1 (in blue, residues 386-464), together with Cac2, it shapes the histone H3-H4 binding surface. The DNA-binding WHD is located at the C-terminus of Cac1 (in green, residues 520-606). The two left-right arrows in red represent Cac2-binding domains (residues 361-367 and 462-472). The two left-right arrows in purple represent Cac3-binding domains (residues 280-286 and 344-349). Lower panel: diagram of fission yeast Pcf1 showing different functional domains. These domains are predicted by sequence alignment. KER domain (in orange, residues 76–170) contains the DNA-binding coiled-coil (spanning the KER domain, residues 69-165, shown as the orange line above). At the end of the KER domain is the PIP box (in gray, residues 168-183) which mediates PCNA interaction. The acidic ED domain is located in the middle of Pcf1 (in blue, residues 296-396). The DNA-binding WHD is located at the C-terminus of Pcf1 (in green, residues 494 -544). The two left-right arrows in red represent Pcf2-binding domains (residues 418-421 and 490-499). The two left-right arrows in purple represent Pcf3-binding domains (residues 381-384 and 481-486).

Besides interaction with PCNA, a C-terminal DNA-binding winged helix domain (WHD) has been identified in the large subunit of CAF-1. This domain has been demonstrated to synergize with the PIP motifs to stabilize CAF-1 at replication factories (Mattiroli et al., 2017a; Zhang et al., 2016b). The WHD was also identified in the CAC-1 C-terminal part (residues 520–606) as a domain with a positively charged surface which binds to DNA but not PCNA. These residues were shown to be important for the cellular tolerance to DNA damaging agents. When this domain is mutated within the mouse p150, this resulted in a loss of co-localization between p150 and PCNA during S phase (Zhang et al., 2016b). Later works on Cac1 showed that WHD is sequestered within the acidic region of Cac1 when CAF-1 is free of cargo. The WHD is then unmasked when CAF-1 binds to a H3-H4 dimer, a change of conformation that is critical to the mechanism by which CAF-1 promotes histone deposition (Mattiroli et al., 2017a). Another exciting discovery came out at the same time from a work focusing on defining the important domains of CAF-1 to promote histone deposition *in vitro*. Sauer and collaborators reported the existence of a DNA-binding coiled-coil domain in the N-terminus of Cac1. This domain which is located within the first 230 amino acids containing the KER domain of Cac1, together with the C-terminal WHD, facilitates histone deposition by CAF-1 (Sauer et al., 2017). Indeed, in the work of Mattiroli and colleagues, a truncated Cac1 missing the first 233 amino acids in a CAF-1 complex (designated as tCAF-1) was demonstrated to be able to assemble histones *in vitro.* However, unlike the full-length CAF-1, tCAF-1 does not bind to DNA (Mattiroli et al., 2017a). This further supports that the N-terminus of Cac1 mediates DNA binding with CAF-1. More details on the mechanism by which CAF-1 promotes histone deposition will be given in the section 3.4. Based on the recent discoveries on the budding yeast large CAF-1 subunit, Cac1, an updated diagram of Cac1 was generated (Figure. 3.6 B upper panel), and the alignment of the fission yeast Pcf1 with predicted domains is shown below (Figure. 3.6 B lower panel).

The C-terminal domain (residues 620-937) of p150 has been reported to directly mediate *in vitro* interaction with p60. This interaction is resistant up to 0.5 M NaCl. The deletion of this C-terminal domain cripples the nucleosome assembly activity of CAF-1 (Kaufman et al., 1995). Interestingly, mutations of the WHD of Cac1 do not impact the interaction with Cac2 *in vitro* (Zhang et al., 2016b).

The C-terminus part of the large CAF-1 subunit also plays a role in the dimerization of two large CAF-1 subunits (Quivy et al., 2001). The work in Xenopus and human cells reveals that a region of 36 amino acids in the C-terminus of p150 is necessary for dimerizing two p150 molecules.

Moreover, the chromatin assembly activity of CAF-1 is abolished *in vitro* by deleting this region (Quivy et al., 2001). Such C-terminal domain involved in the dimerization of the large CAF-1 subunits has not been clearly defined in yeast models but a Cac1-dimer has been observed *in vitro* (Winkler et al., 2012).

Besides the PIP1 and MIR domain in the N-terminal part p150, a SIM (Sumoylation-Interacting Motif) motif consisting of residues 98-105 has been identified (Uwada et al., 2010). The interaction between human p150 and the chromatin modifier SUMO2/3, which is mediated by the SIM motif is likely to regulate the association of SUMO2/3 or SUMO2/3-modified proteins (or both) to the replication foci (Uwada et al., 2010). The SIM motif of p150 is also required for maintaining a normal level of proliferation antigen Ki-67, a fundamental component of the perichromosomal layer forming the sheath surrounding condensed chromosome during mitosis (Matheson and Kaufman, 2017).

The mid subunit of CAF-1

The mid subunit of CAF-1 is p60 (559 amino acids, also called CHAF1b) in human, p105 (747 amino acids) in Drosophila (sometimes exists as p75 due to the truncation of the C-terminus), Cac2 (468 amino acids) and Pcf2 (512 amino acids) in budding yeast and fission yeast, respectively. Compared to the large CAF-1 subunit, functional domains identified on the mid subunit are less diverse. The human p60 (Figure 3.5) can be dissected into three major parts: an N-terminal region containing seven tandem WD (tryptophan-aspartate) repeats, followed by two B-like motifs and a PEST box. The WD repeats are short motifs of approximately 40 residues which often terminate with a tryptophan-aspartate dipeptide. The protein domain containing WD repeats is thought to be folded into a beta-propeller serving as a protein platform without any catalytic activity (Smith et al., 1999). The budding yeast Cac2 is predicted to have five WD repeats spanning over the protein. The mutations of the residues 361-367 (partially involving the fifth WD repeat at the C-terminus) result in the loss of interaction with Cac1 without affecting the level of Cac2 expression (Mattiroli et al., 2017b). The human and budding yeast mid CAF-1 subunits are both reported to associate with Asf1 (Krawitz et al., 2002; Tagami et al., 2004; Malay et al., 2008). However, the human N-terminal WD repeats region alone exhibits no affinity for ASF1a *in vitro* (Tang et al., 2006). Indeed, it is the C-terminal B-like motifs of p60 that mediates the interaction with ASF1a. This interaction is proposed to regulate ASF1a-HIRA interaction *in vivo* by exclusively occupying ASF1a, which leads to distinct chromatin regulatory activities (Tang et al., 2006). Similar interactions between the C-terminal part of the CAF-1 mid

subunit with Asf1 have been also reported in other organisms such as fission yeast and Drosophila (Malay et al., 2008; Tyler et al., 2001). The PEST box has a role in protein degradation, especially when the expression of p150 is downregulated by shRNA (Ye et al., 2003).

Both p150 and p60 have been found to undergo phosphorylation (Smith and Stillman, 1991b). The kinases that phosphorylate p60 can be classified into two families: CDKs (Cyclin-Dependent kinases) and DNA-PK (DNA-dependent Protein Kinases). The phosphatase involved in the dephosphorylation of p60 is PPI (Protein Phosphatase 1) (Keller and Krude, 2000). The hyperphosphorylation of p60 has been shown to correlate with chromatin displacement and inactivation during mitosis, suggesting a role of phosphorylation events in regulating the nucleosome assembly activity of CAF-1 (Marheineke and Krude, 1998).

Intriguingly, overexpression of p60 has been identified in many tumor types. The loss of p60 has been implicated in causing some characteristics of the Down syndrome (reviewed in Tagami et al., 2004; Volk and Crispino, 2015). However, so far little is known about the contributions of p60 to human diseases.

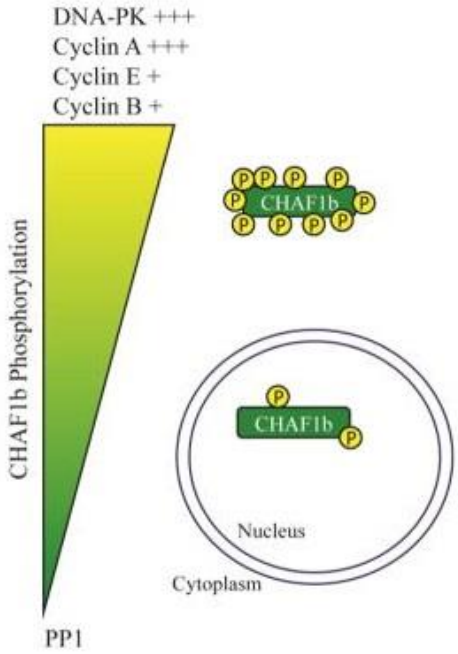

Figure 3.7. Schematic showing the phosphorylation of CHAF1b (p60). p60 is phosphorylated by several factors listed above, the number of the symbol '+' indicates relative phosphorylation strength of each factor. p60 is dephosphorylated by PP1 (Protein Phosphatase 1). Hyperphosphorylation of p60 is correlated with chromatin displacement and inactivation during mitosis. Adapted from Volk and Crispino, 2015 (Volk and Crispino, 2015).

The small subunit of CAF-1

The small subunit of CAF-1 is p48 (425 amino acids, also called RbAp48, Retinoblastoma-Associated Protein) in human, p55 (429 amino acids) in Drosophila, Cac3 (422 amino acids) in budding yeast and Pcf3 (408 amino acids) in fission yeast. Like human p60, p48 is also largely composed of seven WD repeats in addition to the histone H4 binding regions on both N- and C-terminus (Figure 3.5) (Zhang et al., 2013). The budding yeast Cac3 has six WD repeats, and two Cac1-interacting regions are found within the WD repeats based on cross-linking mass spectrometry approaches (XL-MS) (Kim et al., 2016). The same study also shows that Cac2 and Cac3 were both cross-linked to Cac1, while no cross-links were observed between Cac2 and Cac3. This indicates that Cac1 bridges Cac2 and Cac3 to form the full CAF-1 complex. This work led to the identification of key residues within Cac1 that mediate protein-protein interactions within the complex: the residues 361-367 and 462-472 mediate interactions with Cac2 and the interaction with Cac3 involves the 280–286 and 344–349 (Mattiroli et al., 2017b).

It has been shown that without being inside the CAF-1 complex, p48 alone binds to a H3–H4 dimer but not a $(H3–H4)_2$ tetramer *in vitro*. This binding leads to structural rearrangement of the H3-H4 dimer. Recombinant p48 also associates with Asf1 in the presence of H3-H4 dimers which probably serve as a bridge for the association (Zhang et al., 2013). Similarly, in budding yeast, Cac3 alone can bind to H3-H4, but the affinity is 50-fold weaker than that of a CAF-1 complex. Moreover, the absence of Cac3 has only minor impact on the ability of CAF-1 to bind H3-H4 (Mattiroli et al., 2017b). However, the removal of Cac2 leads to a 50-fold decreased in the affinity for H3-H4 binding, highlighting an important role of Cac2 in shaping the H3-H4 binding interface within the CAF-1 complex (Mattiroli et al., 2017b). Collectively these data indicate that, in both human and yeast models, the omission of any subunit of CAF-1 leads to the loss of integrity of CAF-1-H3-H4 complexes *in vivo* (Kaufman et al., 1997; Linger and Tyler, 2005; Pietrobon et al., 2014).

Only a small amount of the cellular p48 exists within the CAF-1 complex, while most p48 is found in macromolecules, such as the histone deacetylase HDAC1, the NuRD (Nucleosome Remodeling and Deacetylase) remodeling/deacetylase complex and the NURF (NUcleosome Remodeling Factor) remodeling complex (Kuzmichev et al., 2002; Marheineke and Krude, 1998; Martnez-Balbs et al., 1998; Taunton et al., 1996; Zhang et al., 1999).

3.4. Mechanisms of histone deposition by CAF-1

The mechanism by which CAF-1 promotes histone deposition coupled to DNA synthesis has been an interesting research topic for a long time. The difficulties to purify the complex or to produce recombinant proteins to reconstitute *in vitro* the CAF-1 complex in interaction with H3-H4 have prevented to address if CAF-1 promotes the deposition of a H3-H4 dimer or a $(H3\text{-}H4)_2$ tetramer. Recent studies have provided breakthrough in understanding how CAF-1 promotes histone deposition *in vitro* (Liu et al., 2016; Mattiroli et al., 2017a, 2017b; Sauer et al., 2017; Zhang et al., 2016b). Two works have put forward a model in which one CAF-1 complex binds a single H3-H4 dimer, allowing unmasking the C-terminal WHD domain and thus to bind DNA. Then, DNA-mediated dimerization of two CAF-1 complexes allows the $(H3\text{-}H4)_2$ tetramer formation and deposition onto DNA (Mattiroli et al., 2017a; Sauer et al., 2017). Importantly, the $(H3\text{-}H4)_2$ tetramerization is required to achieve its deposition onto DNA and then the release of H3-H4 from CAF-1. Indeed, a histone H3 mutant that destabilizes the H3-H3 interface impairs *in vitro* tetramer deposition (Sauer et al., 2017).

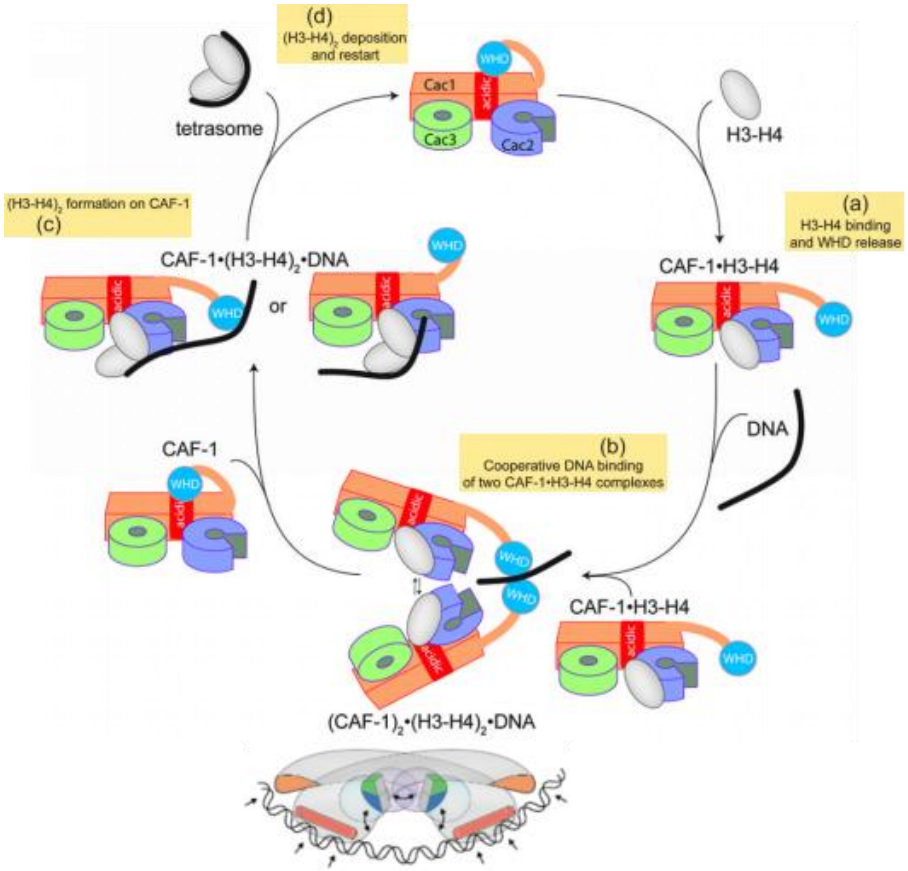

Figure 3.8. Model of the mechanism of histone deposition by CAF-1. (a) The WHD domain masked in the acidic region of Cac1 is released upon the binding of a H3-H4 dimer to the CAF-1 complex. (b) The binding of the WHD domain to the DNA, cooperates with a coiled-coil segment of high DNA-binding affinity brings two CAF-1-H3-H4

complexes to the proximity of the DNA. (c) A (H3-H4)2 tetramer is then formed within a CAF-1 complex. (d) The (H3–H4)2 tetramer is deposited onto the DNA, and the WHD domain is sequestered back to acidic region leading to its dissociation from DNA. Adapted from Sauer et al,, 2017 and Mattiroli et al., 2017 (Mattiroli et al., 2017a; Sauer et al., 2017).

It is thought that the CAF-1 complex is targeted to site of DNA synthesis via its interaction with PCNA. Recently, Zhang and colleagues have identified a DNA-binding domain in the C-terminal part of the budding yeast Cac1 (Zhang et al., 2016b). This domain displays a winged helix (WHD) in the crystal structure and contributes to a stronger interaction between PCNA and Cac1, suggesting that the coupling of Cac1 to the replication fork via PCNA-interaction is further stabilized by the DNA-binding function of the WHD domain (Zhang et al., 2016b).

An earlier study in *C. elegans* has demonstrated that impairing the H3-H3 interface to prevent $(H3\text{-}H4)_2$ tetramerization leads to an inhibition of CAF-1-mediated nucleosome assembly during replication, supporting that $(H3\text{-}H4)_2$ tetramer are the final substrate deposited onto DNA by CAF-1 (Nakano et al., 2011). In light of the discovery of the WHD domain, following *in vitro* studies of budding yeast CAF-1 have provided further evidence showing details of how a histone $(H3\text{-}H4)_2$ tertramer is formed and deposited. First, the fact that the binding of Cac1 to H3-H4 induces a conformational change reveals that Cac1 plays an important role in organizing the H3-H4 architecture within the complex (Liu et al., 2016). Second, using different recombinant Cac1 peptides, Mattiroli et al. have demonstrated that the WHD domain is masked by the Cac1 acidic domain in the absence of H3-H4, suggesting that the WHD domain is masked within the acidic domain by an inhibitory intramolecular interaction. Possibly, masking the WHD domain can result in the loss of DNA binding (Mattiroli et al., 2017a). This study further showed that the binding of a H3-H4 dimer promotes the release of the WHD domain from the acidic domain. The H3-H3 interaction is then sufficient to promote a dimerization of two CAF-1-(H3-H4) dimers and promote the formation and deposition of the $(H3\text{-}H4)_2$ tetramer (Mattiroli et al., 2017a). The work form Sauer and colleagues have provided more insights into the mechanism of CAF-1-mediated histone deposition. They have identified a second DNA-binding coiled-coil domain within Cac1, which together with the previously described WHD domain enables high DNA-binding affinity of CAF-1. Both domains would be necessary to promote a DNA-mediated dimerization of two CAF-1 complexes and allow $(H3\text{-}H4)_2$ tetramer formation and deposition onto DNA (Sauer et al., 2017). Although Cac1 alone is able to bind H3-H4, Cac2 is indispensable for productive histone binding, potentially by shaping the histone binding interface with Cac1 (Mattiroli et al., 2017b).

Intriguingly, RPA, a single stranded DNA binding protein involved in DNA replication and repair, has been reported to be engaged in replication-coupled histone deposition. The work of Liu et al. in budding yeast showed that RPA interacts with CAF-1 in a PCNA-independent manner, and as well as with histone H3-H4. Interestingly, a fraction of H3-H4 associated to RPA was found to harbor the histone mark H3K56Ac, the mark of newly synthesized histones and the preferential histones bound by CAF-1. Therefore, RPA may act as a binding platform for histone H3-H4 and CAF-1 to facilitate histone deposition during replication and repair (Liu et al., 2017).

Besides the key role in replication-dependent histone deposition, the function of CAF-1 in mediating chromatin assembly is also instrumental in response to DNA damage to restore chromatin coupled to DNA repair. The role of CAF-1 during DNA repair will be discussed in Chapter 4.

4. Chromatin dynamics during DNA repair

The dynamic nature of chromatin

Eukaryotic chromatin is highly compacted via multiple-leveled organization to allow it to fit into the nucleus. The three-dimensional organization of the genome also reflects the dynamic of the chromatin (Phair and Misteli, 2000; Woodcock and Ghosh, 2010). The genome is organized in a way that distinct functional territories are clustered along the chromatin via the contact between discrete chromosomal regions (Tarailo-Graovac and Chen, 2013). Metazoan chromosomes contain linear gene clusters that share common regulatory sequences, such as the structural units called "topologically associating domains" (TADs), and spatially clustered sequences that are found within the same transcription hotspots (Hu and Tee, 2017; Siersbfk et al., 2011; Smith et al., 2016). Chromatin dynamics impacts on nuclear processes such as gene regulation and DNA recombination via large-scale inter-/intra- chromosomal interactions. In support of this, many studies have presented microscopy evidences that capture stochastic or directional movements of fluorescently-tagged foci in living cells (Cho et al., 2014; Chuang et al., 2006; Hajjoul et al., 2013; Hauer et al., 2017; Herbert et al., 2017; Heun et al., 2001; Marshall et al., 1997; Miné-Hattab et al., 2017). Therefore, although chromatin fibers are highly organized and compartmentalized in the nucleus, they are also highly dynamics and flexible in response to various stresses.

The plasticity of chromatin is required for the accessibility to many DNA-associated machineries such as DNA replication, gene transcription and DNA repair. Chromatin dynamics relies on several mechanisms including nucleosome remodeling, post-translational modifications (PTMs) of histones tails, histone variants incorporation, non-histone DNA binding proteins and long non-coding RNAs (lncRNAs) (Tyagi et al., 2016).

Nucleosome remodeling is carried out by remodeling enzymes designated as chromatin remodelers (Strahl and Allis, 2000). These enzymes remodels the chromatin structure via three major actions: 1) the sliding of an entire histone octamer along the DNA (nucleosome sliding); 2) the alteration of the nucleosomal DNA conformation and 3) changing the composition of the nucleosome with histone variants (Rippe et al., 2007). Chromatin remodelers are classified into four main families: SWI/SNF (switch/sucrose-non-fermenting), ISWI (imitation switch), CHD (chromodomain-helicase-DNA binding) and INO80 (inositol requiring 80). In terms of function,

chromatin remodelers are categorized as readers, writers and erasers. The catalyzing activities of chromatin remodelers are executed by imprinting the PTMs on histone tails and changing the histone-DNA association within a nucleosome via ATP-dependent hydrolysis (Figure 4.1) (Clapier and Cairns, 2009). Each member of these families is involved in distinct cellular processes. Chromatin remodelers also serve as platforms mediating the interaction with lncRNAs to control gene transcription and post-transcriptional regulation (Han and Chang, 2015). Evidences start to emerge demonstrating the links between human diseases and the role of lncRNAs in regulating epigenetic state (De Majo and Calore, 2018; Tang et al., 2017).

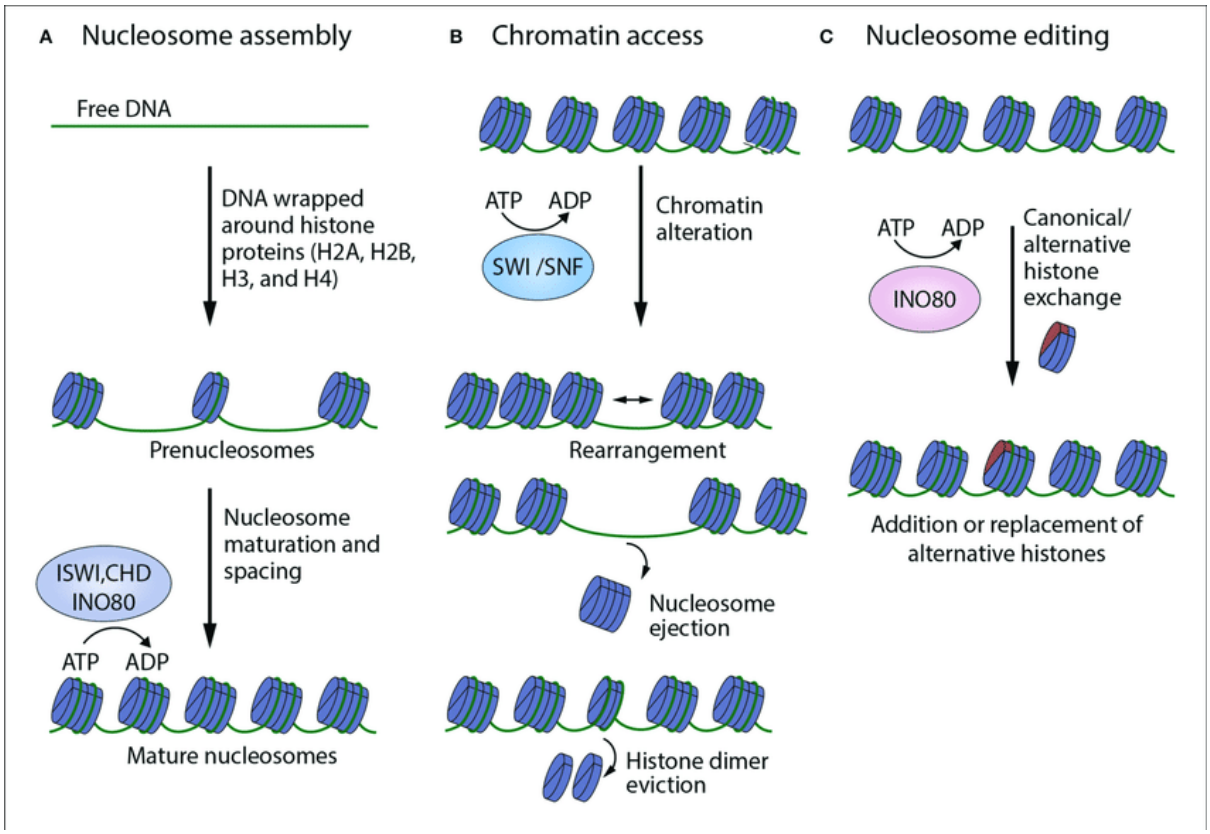

Figure 4.1. Illustration of actions of ATP-dependent chromatin remodelers. A. Members belonging to the ISWI, CHD and INO80 families are in charge of random distribution of newly formed nucleosomes onto the DNA and promote the maturation of nucleosomes by arranging them into regularly-spaced chromatin structures. B. Members mainly belong to the SWI/SNF family promote DNA accessibility by nucleosome sliding, nucleosome ejection or histone eviction. C. Members of the INO80 family aid the exchange of canonical into non-canonical histone variants (H2A.X for example) into the chromatin. Adapted from Clapier et al., 2017 (Clapier et al., 2017).

4.1. Chromatin and nucleosome dynamics in response to DNA damage

The cellular response to DNA damage is orchestrated by the DNA damage response (DDR) network that carries out the detection of DNA damage, signaling events such as the activation of cell cycle checkpoint and DNA repair (Ciccia and Elledge, 2010; Giglia-Mari et al., 2011). Given that DNA lesions can be generated at any stage of the cell cycle, the DDR needs to be active at any time of the cell cycle and any genomic location in order to maintain the integrity of genome as well as epigenome. Since DNA lesions occur at the nucleotide level, the repair mechanisms need to conquer the intrinsic packing of DNA, namely chromatin. To this end, the DDR network is elicited together with the dynamics of chromatin which includes 1) chromatin structure alterations, 2) the mobilization of nucleosome components and 3) various modifications on histone tails that affect the epigenetic landscape (Figure 4.2) (Dabin et al., 2016).

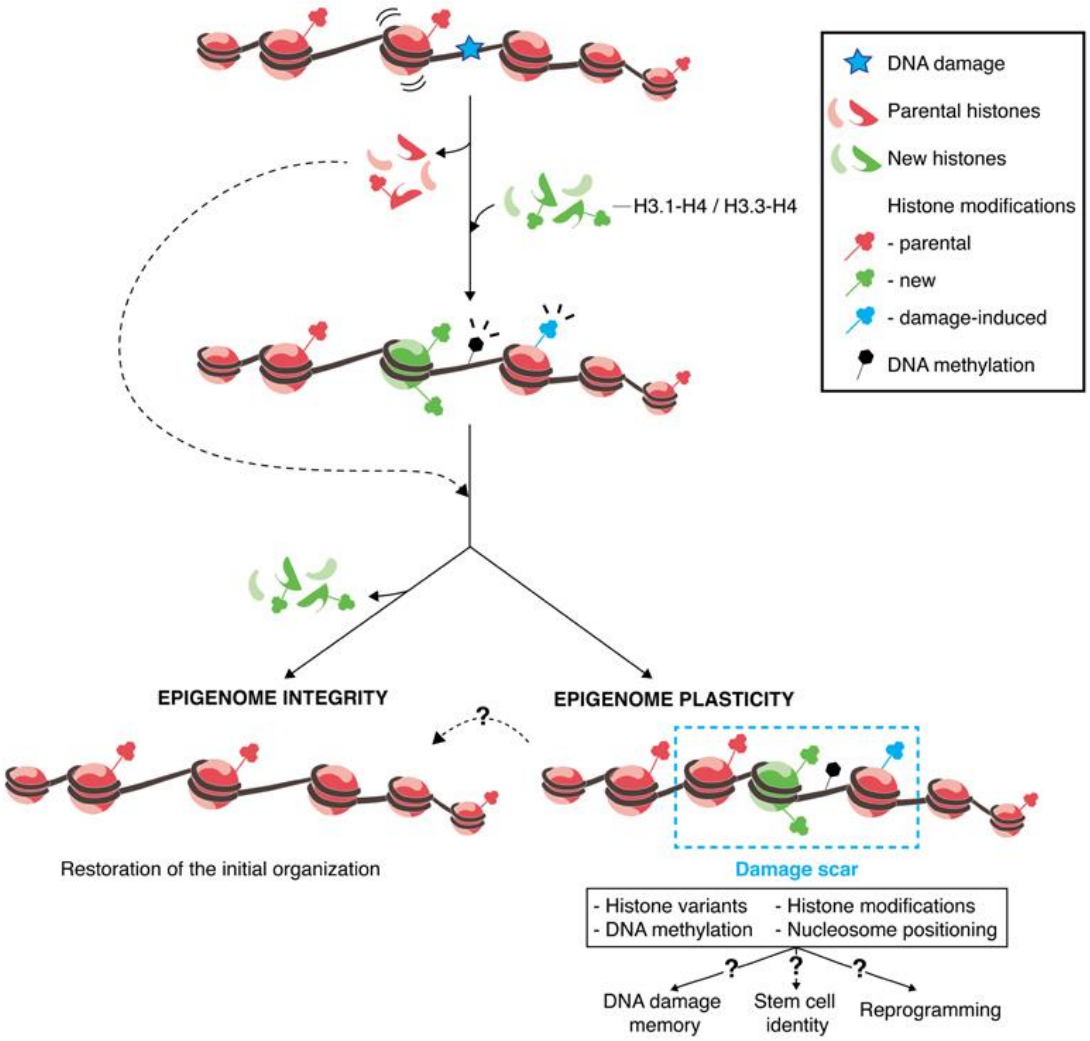

Figure 4.2. Chromatin dynamics in response to DNA damage in mammalian cell. DNA damage (indicated as the blue star) leads to sequential chromatin rearrangements, such as replacing the pre-existing parental histone (in

red) with histone variant (in green) containing new histone modifications, this leads to a loss of parental epigenetic information. DNA damage also brings in distinct modifications (indicated in blue) to the pre-existing histones and modifies the DNA (indicated in black). The local density of chromatin may be as well changed as a DNA damage-induced consequence. It remains to be further elucidated whether or not, and how the chromatin landscape is restored faithfully post DNA repair to maintain epigenetic integrity, as well as how the "damage scars" on the chromatin (dotted line box in blue) could impact on damage memory, stem cell identity or reprogramming. Adapted from Dabin et al., 2016 (Dabin et al., 2016).

Chromatin structure alterations

DNA damage not only alters locally the chromatin structure but may also lead to genome-wide changes of chromatin organization. Indeed, studies in budding yeast have shown that in the context of DNA repair by homologous recombination, a single DSB can lead to chromosome-wide structural change allowing the homology search by Rad51 which takes place all over the chromosome (Renkawitz et al., 2013). DSB can also induce large-scale spread of the phosphorylation of histone H2A (γ-H2A.X) depending on where it occurs (Lee et al., 2014; Shroff et al., 2004).

Chromatin structure can be influenced by the alterations of histone landscape after DNA damage. The decondensation of chromatin can be a consequence of the decrease of the density of core histones and linker histones. Notably, different types of DNA damage shape the histone landscape via distinct mechanisms. For example, UV-C irradiation in mammalian cells triggers large-scale ATP-dependent decrease of the density of core histones, and this process requires the NER pathway-related protein DDB2 (damaged DNA-binding protein 2) (Luijsterburg et al., 2012). By imaging living cells containing a photoactivatable version of GFP-tagged histone H2B, it has been shown that laser-induced DSBs lead to local chromatin decondensation in an H2A.X and ATM-independent manner (Kruhlak et al., 2006). A recent study has further investigated the underlying mechanism. Poly(ADP-ribose) polymerase 1 (PARP1) mediates the accumulation of poly(ADP-ribosyl)ation at the site of DNA damage resulting in the rapid decondensation of chromatin (Strickfaden et al., 2016). DNA damage also impacts on the density of chromatin via the degradation of core histones as well as histone eviction. Acetylation-mediated degradation of core histones upon DSB has been reported in mice cells (Qian et al., 2013). Multiple studies have revealed that histone eviction at DSBs plays an instrumental role in the binding of KAT5 (Lysine Acetyltransferase 5, the catalytic subunit of the NuA4 histone acetyltransferase complex) to H3K9me3 (trimethylation of histone 3 lysine 9) and therein facilitates the acetyltransferase activity of KAT5 (Berkovich et al., 2008; Goldstein et al., 2013; Kruhlak et al., 2006; Ziv et al.,

2006). This modification by KAT5 contributes to altering nucleosome-DNA interactions (Doyon et al., 2004).

Nucleosome eviction and sliding carried out by ATP-dependent chromatin remodelers largely contribute to the chromatin mobility in response to DNA damage. There are a large number of chromatin remodelers that have been identified to disrupt DNA-histone association by utilizing the energy of ATP hydrolysis, and consequentially, to facilitate the accessibility of DNA repair machinery to the sites of DNA damage. However, it still remains elusive whether chromatin remodeling occurs before or during DNA repair (Lans et al., 2012). The restoration of nucleosome occupancy post DNA repair is mainly orchestrated by the action of histone chaperones (Gurard-Levin et al., 2014). Histone chaperones involved in the restoration of chromatin after DNA repair are partially overlapping with those acting during DNA replication, including Asf1, CAF-1, Rtt106 and NAP1. The mechanisms of DNA repair-coupled histone restoration will be discussed in section 4.2.

Non-histone proteins such as HP1 (heterochromatin protein 1), PcG (Polycomb group) proteins and the high-mobility group (HMG) chromatin proteins are also active factors in bringing out chromatin dynamics in the DDR. For instance, HP1 is recruited to or released from DNA lesions to promote signaling events and repair of damaged DNA (Soria et al., 2012). Members of HMG are small highly charged proteins and are the second most abundant proteins found in association with chromatin besides the core histones (Bianchi and Agresti, 2005; Bustin and Reeves, 1996). They have been implicated in different DNA repair pathways by recognizing distorted DNA structure and altering chromatin architecture (Reeves, 2015).

Histone variants and the mobilization of nucleosome components

The variants of core histones play an instrumental role in chromatin dynamics in the DDR. Generally in mammalian cells, histone H2B and H4 have only few variants, whereas histone H2A and H3 have multiple variants (Buschbeck and Hake, 2017; Campos and Reinberg, 2009). In addition to the core histones, the linker histone H1 which binds between nucleosomes is also highly divergent. However, in unicellular eukaryotes like yeast, the versions of histone variants are very limited. In budding yeast there are only two variants: Htz1 (the counterpart of mammalian H2A.Z) and Cse4 (centromeric histone H3-like protein), for the core histone H2A and H3, respectively, and Hho1 for the linker histone H1 (Eriksson et al., 2012). In fission yeast there exist Pht1 (the counterpart of mammalian H2A.Z) for histone H2A and Cnp3 (the orthologue of

CENP-C) for histone H3, whereas the linker histone is lacked (Carr et al., 1994b; Holland et al., 2005).

Recent studies have shown that almost all histone variants are involved in DNA repair via different mechanisms (Chen and Jin, 2017). The incorporation of histone variants can lead to changes in nucleosome dynamics, signaling via specific PTMs carried by the histones variants and the recruitment of downstream DNA repair factors.

The mobilization of nucleosome components are mainly achieved by histone chaperones in concert with ATP-dependent chromatin remodelers (Clapier and Cairns, 2009). Distinct histone variants with their corresponding histone chaperones carry out different functions in the DDR. A well-known example is the conserved phosphorylation of H2A.X (γ-H2A.X) by DDR kinases to amplify DNA damage signaling (Rogakou et al., 1998; Yuan et al., 2010; (Downs et al., 2000). HJURP, a recently identified histone chaperone of histone H3 variant CENP-A, has an emerging role in the DDR via its association with HR intermediates *in vitro* and its DNA damage-induced expression, bridging a potential function of CENP-A in the DDR (Dunleavy et al., 2009; Foltz et al., 2009; Kato et al., 2007; Shuaib et al., 2010).

The coordination of histone variants, histone chaperones and chromatin remodelers contributes largely to prime the chromatin for the downstream DNA repair events (Gurard-Levin et al., 2014; Soria et al., 2012). After the rapid phosphorylation of histone H2A.X (γ-H2A.X) upon genotoxic stress, the signaling of DNA damage is amplified via the bidirectional spreading of γ-H2A.X in a region-dependent manner (Caron et al., 2012; Iacovoni et al., 2010; Kim et al., 2007; Yuan et al., 2010). Other modifications of H2A.X such as acetylation and ubiquitylation also contribute to the DDR by recruiting DDR factors and increase H2A.X mobility mainly mediated by the histone chaperone FACT (facilitates chromatin transcription) which replaces nucleosomal H2A.X with H2A (Heo et al., 2008; Ikura et al., 2007; Yuan et al., 2010). Notably, DNA damage also induces poly-ADP-ribosylation of the Spt16 subunit of the FACT complex, which in turn inhibits the exchange of H2A.X/H2A by FACT (Heo et al., 2008). Accompanied with parental histones eviction and nucleosome sliding from the damage site, γ-H2A.X creates a potential boundary on the chromatin for the DDR (Soria et al., 2012). Another variant of histone H2A, H2A.Z has a role in later stage of the DDR via the exchange with γ-H2A.X. Interestingly, there exists a balance between the composition of H2A.Z and H2A.X in an antagonistic manner, that the replacement of γ-H2A.X by H2A.Z mediated by SWR1 (Sick with Rat8 ts) promotes DSB resection (Kalocsay et al., 2009; Mizuguchi et al., 2004), whereas the chromatin remodeler INO80 counteracts this

action by facilitating the replacement of unacetylated H2A.Z by H2A.X to promote genome stability (Papamichos-Chronakis et al., 2011) (Figure 4.3 left). The deposition of the histone H3 variant, H3.1 mediated by the CAF-1 complex at the sites of DNA damage plays an important role in restoring chromatin organization and potentially in terminating DNA damage signaling (Kim and Haber, 2009; Polo et al., 2006b). In addition, the incorporation of other histone H3 variants including CENP-A and H3.3 are proposed to sustain the chromatin integrity based on studies from multiple model organisms (Anderson et al., 2009; Dunleavy et al., 2011; Ray-Gallet et al., 2011b; Schwartzentruber et al., 2012; Zeitlin et al., 2009) (Figure 4.3 right). More future work is required to provide clear evidence in elucidating the underlying mechanisms.

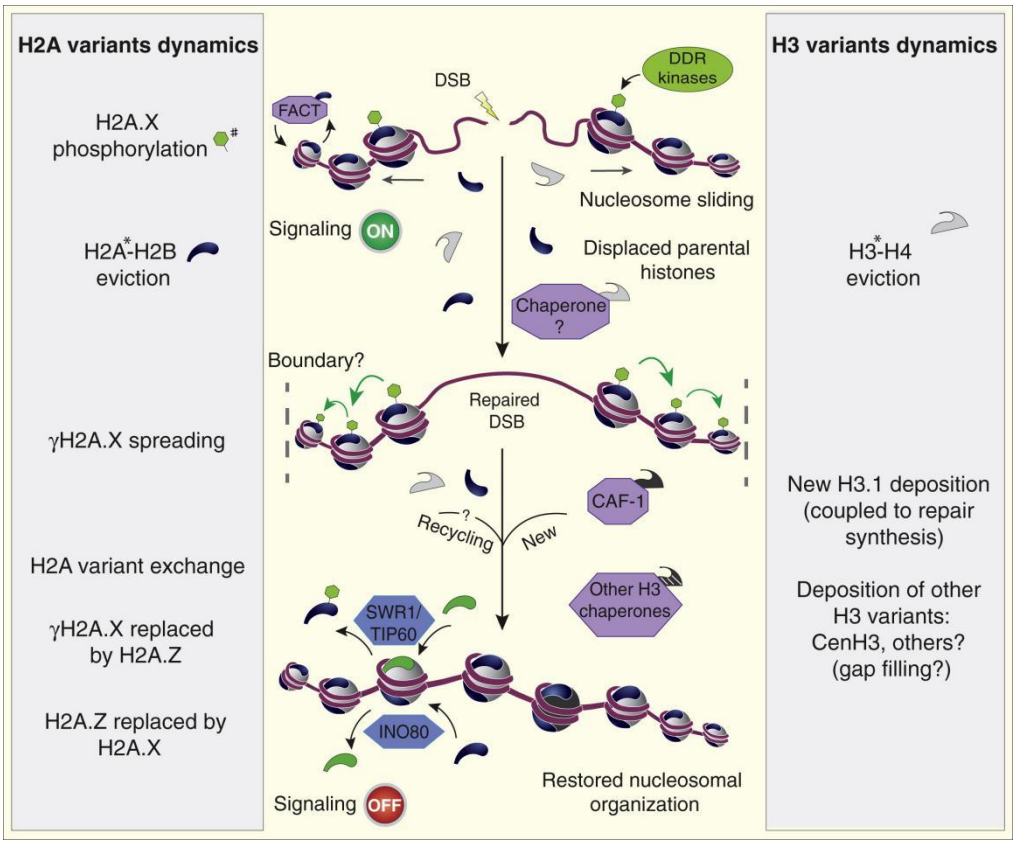

Figure 4.3. Dynamics of histone H2A and H3 variants upon DNA damage. Left: dynamics of histone H2A variants. H2A.X gets phosphorylated (γ-H2A.X) upon DNA damage and such modification is spread in a bidirectional manner to amplify DNA damage signaling. The propagation of γ-H2A.X might contribute to defining the chromatin region for the DDR. The functional importance of the exchange between H2A.X and H2A.Z remains to be further explored. Right: dynamics of histone H3 variants. The CAF-1 complex deposits H3.1 in a repair synthesis-coupled manner being an important action in chromatin restoration and possibly in turning off DNA damage signaling. The significance of the participation of other histone H3 variants in the DDR remains to be elucidated. Adapted from Soria et al., 2012 (Soria et al., 2012).

Post-translational modifications of histones

While the core of the nucleosome is very compact, the lysine-rich histone tails protruding from the nucleosome are highly flexible. They mediate inter-nucleosome contacts as well as serve as a platform for the binding of non-histone proteins. The N-terminal tails of histones H3 and H4 and the C-terminal tails of H2A and H2B are the carriers of diverse PTMs that confer flexibility to the nucleosomes (Figure 4.4) (Campos and Reinberg, 2009; Zentner and Henikoff, 2013). In addition, the C-terminal of the linker histone H1 also undergoes various PTMs. The outcomes of PTMs on the histone tails impact on the chromatin structure, which are realized via different mechanisms including 1) intrinsically affecting histone-histone or histone-DNA interactions leading to change of nucleosome stability, 2) extrinsically affecting long-range inter-nucleosome contacts leading to the alteration of higher chromatin organization, and 3) scaffolding effector molecules such as chromatin modifiers (Hauer and Gasser, 2017).

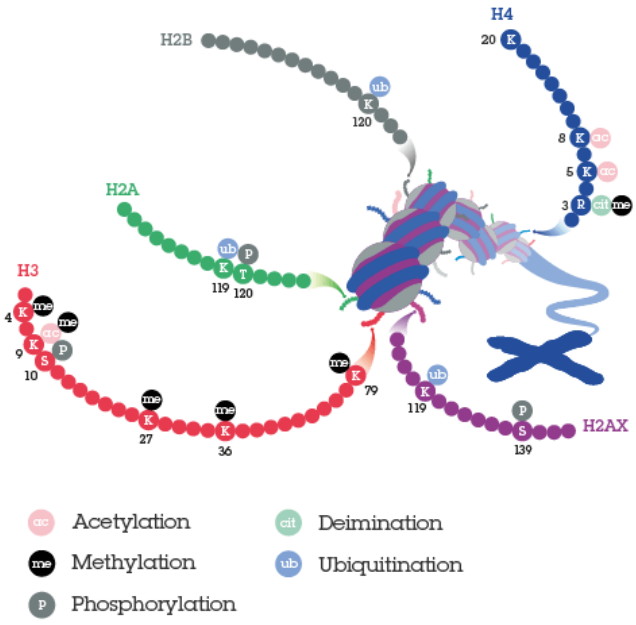

Figure 4.4. Common PTMs on histone tails in human cells. Adapted from web source (https://www.abcam.com/epigenetics/histone-modifications-a-guide).

Besides the most well-known histone modification involved in the DDR, the phosphorylation of H2A.X (γ-H2A.X) on serine 139, many other PTMs are also implicated in response to DNA damage. For example, hyperacetylated histone H4 (H4K16ac) accumulates at ionizing radiation-induced DSB sites and is implicated in recruiting downstream DNA repair factors acting in homologous recombination (Murr et al., 2006). Furthermore, it has been shown that the reduction of the H4K16ac level correlates with a defective DDR and DSB repair in response to

ionizing radiation (Sharma et al., 2010). The ubiquitynation of H2A and H2A.X at the DSB sites by the E3 ubiquitin-protein ligase RNF8 has been proposed to have a role in licensing DSB-flanking chromatin in a way that repair proteins are recruited near the DNA lesions (Mailand et al., 2007). In addition, RNF8 also targets linker histone H1 resulting in K63-ubiquitylated H1 which has a role in promoting the accumulation of repair factors at DSB-flanking chromatin (Thorslund et al., 2015).

The PTMs of histones are key epigenetic marks that regulate gene expression (Dong and Weng, 2013). In order to maintain the integrity of epigenome, it is important to restore the original PTMs to the histones after DNA lesions are repaired. However, this remains an open question and requires more future work.

4.2. The prime/access-repair/restore model

The highly organized structure of chromatin poses as a major obstacle for the accessibility of DNA repair machineries to the damaged sites. To facilitate DNA repair, orchestrated rearrangements of chromatin structure are carried out in response to genotoxic stresses. The molecular framework impacting on the dynamics of chromatin in the DDR has been firstly integrated in an “access-repair-restore” model (Smerdon 1991). This model mainly describes that the chromatin becomes more open in order to accommodate DNA repair factors followed by the restoration of chromatin after DNA lesions are repaired (Green and Almouzni, 2002; Groth et al., 2007b). However, accumulated studies have demonstrated that chromatin factors are not only acting to remodel the chromatin but that they are also active players in priming the chromatin for the repair events. Therein, after more than two decades since the first version of the access-repair-restore model, an updated model has been proposed, namely the prime-repair-restore model (Soria et al., 2012). Currently, based on reconsideration on the concomitance of chromatin restoration and early DNA damage detection, the “repair” and “restore” stages in the model have been revised as coupled to each other, leading to a more refined working model: the prime/access-repair/restore model (Polo and Almouzni, 2015).

Prime/access the chromatin upon DNA damage

The structure of chromatin hinders the access of DNA repair factors to DNA lesions. For instance, nucleosomes are known to represent a barrier to the NER mechanism at the synthesis step (Wang et al., 1991). The dynamics of intrinsic nucleosome components in response to DNA damage has been discussed above. Further effort is needed to alleviate the chromatin

constraints when DNA lesions occur within the highly compact heterochromatin area (Lemaître and Soutoglou, 2014). Importantly, besides the function in maintaining the heterochromatin compaction, a role in promoting the DDR for certain heterochromatin proteins have emerged recently (Soria et al., 2012). This brings out the concept that changing the chromatin structure upon genotoxic stresses is rather an action of priming the chromatin for the downstream repair events. Indeed, the major component of heterochromatin, heterochromatin Protein 1 (HP1) and its binding factor KAP-1 (KRAB-associated protein 1) are recruited to the sites of DSBs where they facilitate DNA repair (Ayoub et al., 2008; Baldeyron et al., 2011; Chiolo et al., 2011; Ziv et al., 2006). The function of HP1 in the context of heterochromatin requires direct binding of HP1 to the histone mark H3K9me3 (Maison and Almouzni, 2004). However, the rapid and transient recruitment of HP1 to the sites of DNA damage does not require the presence of H3K9me (Baldeyron et al., 2011; Luijsterburg et al., 2009). Furthermore, the interaction between HP1 and p150, the large subunit of mammalian CAF-1 complex is involved in the accumulation of HP1 to the DNA lesions (Baldeyron et al., 2011). The collective consequences of targeting HP1 to the sites of DNA damage has been channeled to the subsequent recruitment of DDR factor 53BP1 and BRCA1 as well as the HR factor Rad51, therein supporting an active role of HP1 in promoting DNA repair in the DDR (Figure 4.5) (Baldeyron et al., 2011).

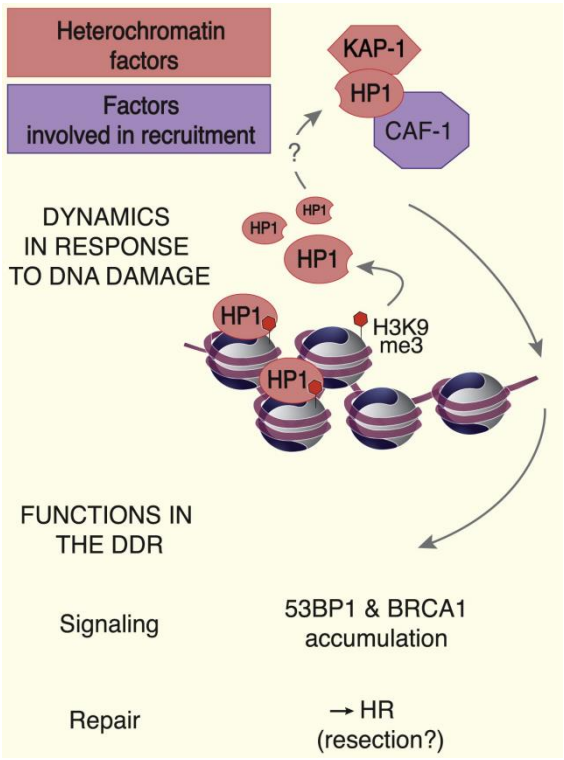

Figure 4.5. An active role of HP1 in the DDR in mammalian cells. The heterochromaitin protein HP1 and its binding factor KAP-1 are recruited to sites of DNA damage via the interaction of HP1-CAF-1. This promotes the

accumulation of DDR factor and facilitates DNA damage signaling. Modified from Soria et al., 2012 (Soria et al., 2012).

Repair DNA lesions and restore chromatin

Several studies have provided both *in vitro* and *in vivo* data supporting that DNA repair and chromatin assembly are integrated as a concerted process (Polo and Almouzni, 2015). *In vitro* analyses on adducts-containing DNA templates incubated with cell-free extracts from different model organisms have demonstrated that damaged DNA undergoing the NER repair pathway is the preferred substrate for nucleosome assembly which occurs concomitantly with DNA repair synthesis (Gaillard et al., 1996, 1997; Gérard et al., 2006b). Furthermore, the newly assembled nucleosomes are spread from the repair site in a bidirectional manner (Gaillard et al., 1996, 1997). *In vivo* studies on UV-irradiated human cells have revealed the temporal relations between DNA repair and histone dynamics carried out by their corresponding chaperones (Adam et al., 2013; Dinant et al., 2013; Green and Almouzni, 2003; Martini et al., 1998; Polo et al., 2006b). Among these histone chaperones, the FACT complex participates in facilitating the exchange of histone H2A-H2B at sites of UV-induced DNA lesions, , and such action is proposed to allow efficient recruitment of downstream factors involved in the TC-NER pathway (Dinant et al., 2013). The HIRA (histone chaperone histone regulator A) complex deposits newly synthesized histone H3.3 to UV-induced DNA lesions upon the detection of DNA damage before the repair events (Adam et al., 2013). Whereas the CAF-1 complex deposits newly synthesized histone H3.1 after the repair of UV-induced DNA lesions (Green and Almouzni, 2003; Martini et al., 1998; Polo et al., 2006b). In the next section, a focus on the role of CAF-1 in DNA repair including its histone chaperone function will be given.

Taking into consideration the active roles of chromatin components in the early stage of the DDR and their role in restoring chromatin at sites of DNA repair, a simplified illustration of the prime/access-repair/restore model is presented in Figure 4.6. Noteworthy that one major view to be refined on this current model is how faithful the restoration of the epigenetic landscape is after the DDR (Polo and Almouzni, 2015).

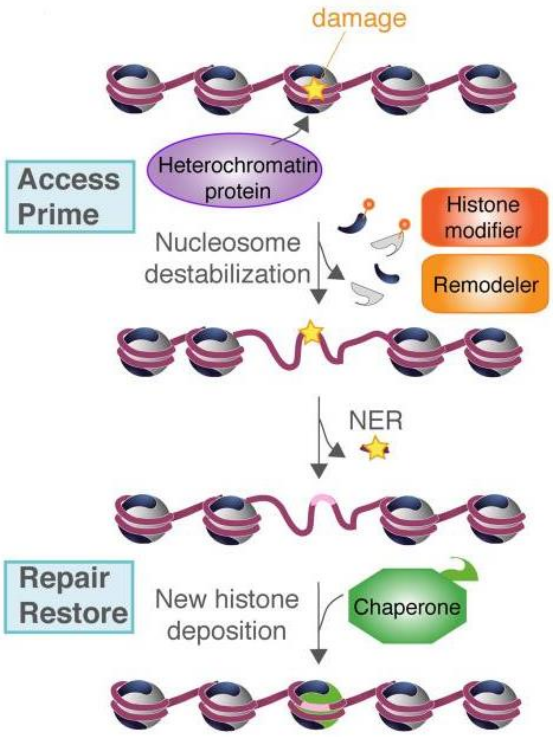

Figure 4.6. The current prime/access-repair/restore model. Upon DNA damage, multiple proteins acting on the chromatin to prime for the sequential DNA repair events which are coupled by the restoration of chromatin. Adapted from Polo and Almouzni, 2015 (Polo and Almouzni, 2015).

4.3. Roles of CAF-1 during DNA repair

Besides the previously discussed role of CAF-1 in DNA replication-coupled histone deposition, CAF-1 is also an active player in chromatin restoration in the DDR network. Moreover, studies have further put forward the role of CAF-1 in promoting DNA repair events beyond its histone chaperone function (Baldeyron et al., 2011). This section will be dedicated to the activities of CAF-1 in the context of DNA repair.

Role of CAF-1 in nucleotide excision repair (NER) pathway

The highly conserved NER pathway removes a wide range of DNA lesions that do not alter DNA structure, such as UV-C-induced photoproducts as well as chemical-induced DNA adducts. CAF-1, together with its partner histone chaperone Asf1 which donates histone substrates to CAF-1, contribute to the chromatin reassembling over the site repaired by NER (Gaillard et al., 1996; Mello et al., 2002). The coupling of CAF-1 to the DNA repair-synthesis is mediated by the interaction between the large CAF-1 subunit and PCNA (Moggs et al., 2000).

Besides CAF-1, other histone chaperones are also recruited to UV-C-induced damaged chromatin including HIRA and FACT (Adam et al., 2013; Dinant et al., 2013; Green and Almouzni, 2003; Martini et al., 1998). Importantly, although both CAF-1 and HIRA are chaperoning the variants of histone H3, histone deposition mediated by them occurs at different stages during the NER. The deposition of newly synthesized histone H3.3 by HIRA is coupled to the damage detection step after UV-C-irradiation, while the newly synthesized histone H3.1, and possibly H3.2 as well, are deposited by CAF-1 at the later DNA repair-synthesis step (Figure 4.7) (Adam et al., 2013; Latreille et al., 2014; Polo et al., 2006b). However, at least in human cells it seems that histone deposition coupled to NER is not required for the process of DNA repair *per se*, as demonstrated by the fact that the knockdown of CAF-1 does not inhibit the NER (Adam et al., 2013; Polo et al., 2006b).

The action of CAF-1 at repair sites is synergized with Asf1 (Mello et al., 2002). Remarkably, although Asf1 is shown to promote repair-coupled nucleosome assembly with CAF-1, a recruitment of Asf1 to sites of DNA damage is not observed *in vitro* and Asf1 alone does not exhibit nucleosome assembly activity (Mello et al., 2002). Given that the repair-coupled CAF-1-dependent histone deposition is also mediated by PCNA and requires Asf1 (Green and Almouzni, 2003; Moggs et al., 2000), this process is thought to resemble the replication-coupled chromatin assembly counterpart (Ransom et al., 2010).

Collectively to support the role of CAF-1 during NER, evidences from different model organisms have demonstrated that the deletion of any CAF-1 subunit-encoding gene elevates the sensitivity to UV irradiation (Endo et al., 2006a; Game and Kaufman, 1999; Kaufman et al., 1997; Kim and Haber, 2009; Kirik et al., 2006).

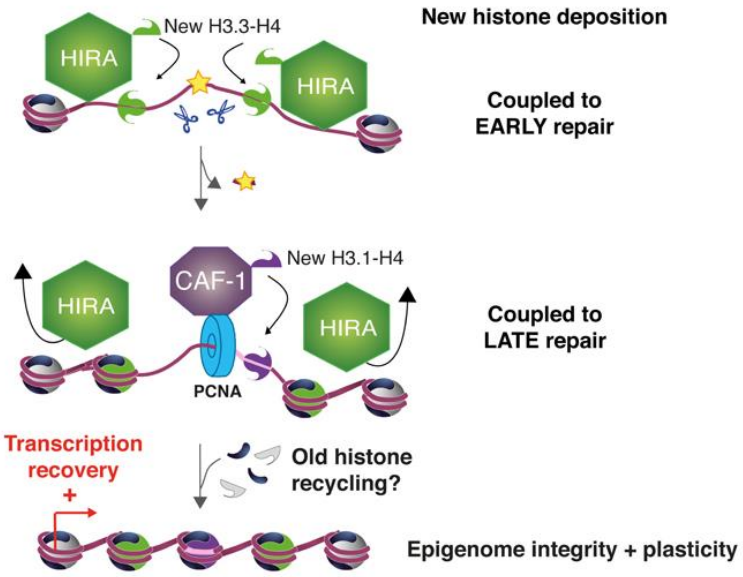

Figure 4.7. Chromatin assembly during the NER pathway. The action of the NER machinery is accompanied with chromatin restoration. Histone chaperone CAF-1 and HIRA are the major delivers of histone H3 variants in reassembling nucleosomes at sites of DNA damage. Histone H3.3 deposited by HIRA at the early stage of the NER is required for transcription recovery after the removal of DNA lesions. CAF-1 is targeted to the repaired site at the later stage of the NER via PCNA-interacting. Modified from Solo and Almouzni, 2016, (Polo and Almouzni, 2015).

Role of CAF-1 in base excision repair (BER) pathway

Compared to the NER pathway, the BER pathway serves for removing base-leveled small DNA lesions. The short-patch BER leads to the fixation of a single nucleotide and the long-patch BER repairs at least two nucleotides (Robertson et al., 2009). Unlike during the other DNA repair pathways which require nucleosome reassembly little is known on whether histone deposition or nucleosome remodeling occurs during the BER. *In vitro* studies suggest that BER steps involving Flap Endonuclease 1 (FEN1) and DNA ligase I could take place on nucleosomal substrates and might not require chromatin remodeling (Chafin et al., 2000; Huggins et al., 2002). Thus, it is likely that BER does not require chromatin disassembly/assembly. However, whether this is true still remains to be further confirmed (Linger and Tyler, 2007). Nonetheless, it has been shown that CAF-1 and PCNA are recruited to damaged DNA undergoing BER (Nabatiyan et al., 2006), raising the possibility that chromatin assembly is associated with the BER. Interestingly, a regulatory role in the BER pathway for the large CAF-1 subunit p150 has been reported in human cells recently (Yang et al., 2016). *In vivo* data by immunoprecipitation have demonstrated that p150 and its partner chaperone ASF1a are found in a complex with

chromatin bound NEIL1 (Nei like DNA glycosylase 1), a DNA glycosylase acting in the BER. Both histone chaperones transiently dissociate from NEIL1 upon oxidative base damage. This study proposes that the release of p150 from the BER complex allows the BER pathway to repair DNA lesions, which is further supported by the fact that p150 inhibits DNA glycosylases activity *in vitro* (Yang et al., 2016). Thus, these data put forward a concept in which the large CAF-1 subunit regulates the timing of BER by sequestering the BER complexes in unstressed cells and releasing them to remove DNA lesions when DNA damage is induced by oxidative stress (Yang et al., 2016).

Role of CAF-1 in DNA mismatch repair (MMR) pathway

The major function of the MMR pathway is to repair mis-incorporated dNTP during DNA replication and recombination (Li, 2008b), hence it is critical for suppressing mutations. However, the chromatin context for the MMR pathway remains a long-term unclear issue. Recently, a study using the cell-free Xenopus egg extracts has shown that nucleosomes are excluded from a >1 kb region flanking a mismatched site in a MutSα- (the heterodimer for recognizing base-base mismatches, containing the subunit Msh2 and Msh6) dependent manner (Terui et al., 2018). The same study also found that the budding yeast chromatin remodeler FUN30 counteracts chromatin assembly by CAF-1, suggesting a positive role of FUN30 in priming the chromatin for the MMR mechanism and raises a negative role of CAF-1 before the MMR takes place (Terui et al., 2018).

The work using reconstituted human systems has shown that the presence of MutSα inhibits CAF-1- and ASF1a-dependent $(H3\text{-}H4)_2$ tetramer deposition onto the mismatching site as well as onto the -40 bp DNA on the right side of the mismatching site, but does not affect histone deposition onto the -450 bp DNA on the left side of the mismatching site, revealing that MutSα prevents the CAF-1- and ASF1a-dependent $(H3\text{-}H4)_2$ tetramer deposition onto mismatch-containing DNA only before the lesions are removed (Blanko et al., 2016; Kadyrova et al., 2013). Nonetheless, the wrapping of mismatch-containing DNA strand around a nucleosome by CAF-1 can be critical as well. As shown by the work of Kadyrova and colleagues, CAF-1-dependent nucleosome assembly of irreparable mismatch-containing DNA contributes to cell survival to DNA-methylating agents (Kadyrova et al., 2011, 2016).

Collectively, the crosstalk between CAF-1 and MutSα is likely to promote the MMR pathway on the chromatin (Blanko et al., 2016; Kadyrova et al., 2011; Schopf et al., 2012). Importantly, the

CAF-1 subunit p150 interacts with MutSα. The interaction is enhanced by DNA damage and may affect the affinity of CAF-1 for histone-binding, indicating the importance of such interaction in the CAF-1-MutSα interplay (Schopf et al., 2012).

Role of CAF-1 in DNA double strand break (DSB) repair

Efficient and accurate repair of DNA double strand breaks (DSBs) is key for maintaining genome integrity. The criticality of chromatin disassembly and reassembly during DSB repair is demonstrated by increased cellular sensitivity to DSB-inducing agents when mutations are introduced into histone chaperones including CAF-1 and Asf1, and multiple ATP-dependent chromatin remodelers (Linger and Tyler, 2007).

CAF-1 is implicated in both DSB repair pathways: homologous recombination (HR) and non-homologous end-joining (NHEJ). *In vivo* co-localization of CAF-1 and the NHEJ protein XRCC4 (X-Ray Repair Cross Complementing 4) has been observed in tissue culture (Nabatiyan et al., 2006). Additional inactivation of CAF-1 further sensitizes HR-deficient budding yeast cells (deleted for *RAD51*) to DNA damage (Linger and Tyler, 2005). However, the impacts of CAF-1 on these two pathways seem to be rather distinct. In budding yeast, the lack of CAF-1 and Asf1 leads to hypersensitivity to DSBs-inducing agents such as MMS (methyl methane sulfonate) and CPT (camptothecin), indicating that DSB repair is compromised (Lewis et al., 2005). Furthermore, this study also demonstrated that the defect in NHEJ in the absence of CAF-1- is rather an indirect consequence via the de-repressing of the silent mating type loci (Lewis et al., 2005). The role of CAF-1 in HR is rather direct. The knockout of p180, the large CAF-1 subunit in Drosophila, results in an increased sensitivity to γ-irradiation as well as a 2.5-fold reduction in the efficiency of gap repair by HR (Song et al., 2007). *In vivo* data have demonstrated that the knockdown of CAF-1 leads to reduced recruitment of Rad51 to DNA repair foci after Bleomycin treatment (Huang et al., 2018). The expression levels of some HR factors, including Rad51 and BRAC1, are significantly increased when FAS1 is mutated (the large subunit of the plant CAF-1). The deletion of either FAS1 or FAS2 (the mid subunit of the plant CAF-1) leads to increased frequency of somatic recombination events, as reported in *Arabidopsis thaliana* (Endo et al., 2006b; Varas et al., 2017). Given that the histone deposition function of CAF-1 is linked to DNA synthesis and that NHEJ is associated with limited DNA synthesis, it could somehow explain the less significant role of CAF-1 in NHEJ. Nonetheless, nucleosome assembly by CAF-1 could still take part in NHEJ as a consequence of chromatin disassembly priming for the NHEJ mechanism (Linger and Tyler, 2007). This concept is supported by the DNA damage-stimulated interaction between PCNA and

NHEJ protein Ku70/80 (Balajee and Geard, 2001). Intriguingly, the large CAF-1 subunit also associates with Ku70/80 directly. This interaction has been proposed to mediate nucleosome assembly without long stretches of DNA synthesis (Hoek et al., 2011). Indeed, Li and Tyler have shown that the introduction of DSBs in mammalian cells leads to a rapid disruption of only about 8 nucleosomes flanking the damaged site, which is thought to efficiently recruit the NHEJ machinery. Importantly, CAF-1 has a major role in nucleosome assembly after the action of the NHEJ machinery, since incomplete knockdown of CAF-1 leads to almost complete block in chromatin assembly, and the function of CAF-1 in this scenario is likely to be independent of DNA synthesis (Figure 4.8) (Li and Tyler, 2016).

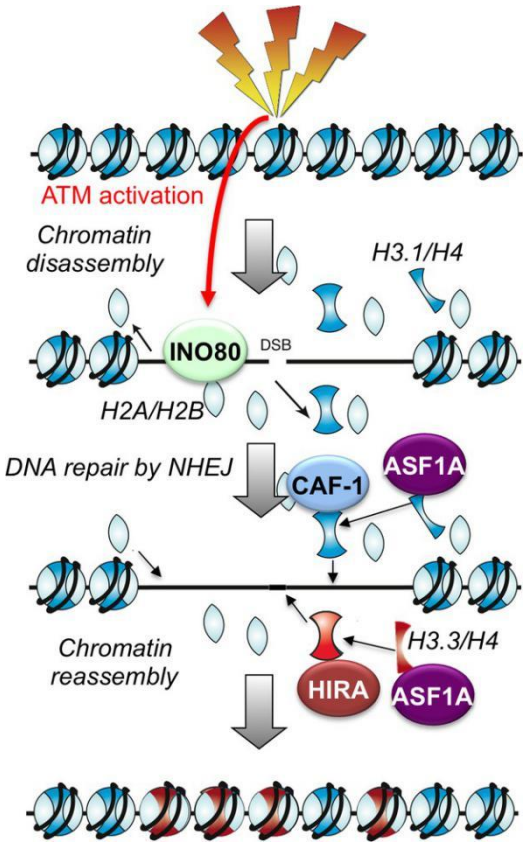

Figure 4.8. Chromatin disassembly and reassembly during the NHEJ pathway. The introduction of DSB leads to small-scale nucleosome removal which is promoted by ATM and the chromatin remodeler INO80. After DSB repair events, histone chaperones HIRA, ASF1a and CAF-1 mediate chromatin reassembly to the repaired site. Adapted from Li and Tyler, 2016 (Li and Tyler, 2016).

More studies have addressed the role of CAF-1 in DSB repair by HR. In mammalian cells the large CAF-1 subunit p150 is recruited to DNA lesions caused by laser irradiation where it promotes DSBs resection. Such recruitment of CAF-1 to sites of DNA damage is also important for recruiting the heterochromatin factor HP1 as well as the HR factor Rad51 (Baldeyron et al.,

2011). Importantly, both HP1 and its interacting partner KAP-1 are found in a complex with CAF-1. The depletion of p150 but not p60 (the mid subunit of CAF-1) impairs the accumulation of both HP1 and KAP-1 at the sites of DNA damage, implying an individual role of p150 outside the chromatin assembly function (Baldeyron et al., 2011).

Physical interactions between CAF-1 and HR factors have been identified. (Jiao et al., 2004, 2007; Pietrobon et al., 2014). In mammalian cells, p150 has been reported to directly interact with two RecQ helicases: BLM (Bloom syndrome protein) and WRN (Werner syndrome protein). p150 has been found to co-localize with both helicases after DNA damage and replication stress (Jiao et al., 2004, 2007). BLM has been found to impede CAF-1-mediated chromatin assembly , and the interaction of WRN-p150 is proposed to be required for recruiting CAF-1 to the sites of DNA damage during DNA synthesis (Jiao et al., 2007). In fission yeast, CAF-1 has been reported to act at the DNA synthesis step of recombination-dependent replication (RDR) and protect D-loop from disassembly by Rqh1, the fission yeast orthologue of the RecQ helicase BLM. Importantly, this study has also identified the physical interaction between Pcf1, the large CAF-1 subunit in fission yeast and Rqh1 (Pietrobon et al., 2014).

The role of CAF-1 during meiotic DSB repair has been studied. The meiotic DSBs are programmed events spread along chromosomes to promote homologous recombination genetic diversity. A study on *Coprinus cinereus* has reported a direct interaction between CAF-1 and the meiosis-specific recombinase Lim15/Dmc1 and suggests that chromatin assembly by CAF-1 is coupled to meiotic recombination via the interaction with PCNA (Ishii et al., 2008). A recent study on budding yeast shows that CAF-1 and HIRA are both targeted to meiotic DSBs. However, the absence of these histone chaperones has no impact on meiotic recombination (Brachet et al., 2015).

Different roles of CAF-1 have branched out from different stages of DNA repair, and they involve the histone deposition activity of CAF-1 as well as the distinct function of CAF-1 subunits. It will be as well important that more future studies are carried out to elucidate the underlying mechanisms for the individual role of each CAF-1 subunit in the DDR.

5. Fission yeast as a model organism

The term "*schizo*" in the scientific name of fission yeast, *Schizosaccharomyces pombe*, means "split" or "fission". The additional "*pombe*" means "beer" in Swahili language, due to that fission yeast was originally isolated from East African beer in 1893 by Linder. The history of fission yeast as a model organism in molecular and genetic research dates back to 1946, when the founder of fission yeast genetics, Urs Leopold started analyzing fission yeast for the first time for his PhD thesis. Since then, fission yeast started to be used for molecular cell biology research which has generated a large number of publications to date. Remarkably, the research on cell cycle control which was largely attributed to the work in fission yeast by Paul Nurse was recognized with a Nobel Prize in Physiology or Medicine in 2001. So far the studies by using fission yeast have provided tremendous knowledge in the fundamental mechanisms of many cellular processes such as DNA replication, cell cycle control, and DNA repair, only to name a few (Fantes and Hoffman, 2016).

Fission yeasts are cylindrical-shaped with hemispherical-ended unicellular organisms. The cells measure about 3.5 µm in diameter and 8-15 µm in length during exponential growth in rich medium. The newborn fission yeasts are about 8 µm in length, and their size expands mainly in length throughout the cell cycle. Thus the length of the cells can be used to estimate the cell age, and when it reaches about 15 µm, the cells undergo a closed mitosis without breaking down the nuclear envelope (Figure 5.1). After the division of the nucleus, a septum is formed medially and is then cleaved to generate two daughter cells in a symmetric manner (Hoffman et al., 2015).

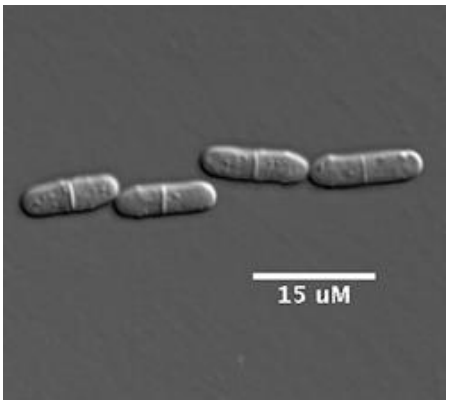

Figure 5.1. Fission yeast cells with septa formed in the middle. Adapted from Hoffman et al.,2015 (Hoffman et al., 2015).

Under vegetative growth condition, fission yeast is haploid with a transient diploid stage when it undergoes mating in response to nutrient starvation. The formation of a diploid zygote is followed by meiosis rapidly giving birth to four haploid spores (Egel and Egel-Mitani, 1974). Although diploids of fission yeast are unstable, they can be recovered by interrupting the mating process under laboratory conditions (Forsburg and Rhind, 2006).

The genome of fission yeast is rather small. The number of protein-coding genes contained in the fission yeast genome is 4824, which is the smallest number of protein-coding genes found in eukaryotes so far. The whole genome is about 13.8 Mb. It consists of three relatively large chromosomes: chromosome I of 5.7Mb, chromosome II of 4.6Mb, and chromosome III of 3.5Mb (Wood et al., 2002).

The mitotic cell cycle of fission yeast resembles that of higher eukaryotes. However, it has peculiar features: 1) the distribution of each phase, and 2) the different timing for karyokinesis and cytokinesis. Under vegetative growth, fission yeast spends almost 70% of its cell cycle in G2 phase. G2 cells are uni-nuclear and can be easily recognized by their short length as well as the absence of septum. Whereas G1 phase is very short and difficult to detect, mitosis (M phase) is followed almost immediately by S phase (Figure 5.2). The nuclear division in fission yeast is finished by the end of mitosis, while the formation of septum occurs in G1 phase followed by cytoplasmic segregation and DNA replication in S phase (Figure 5.2).

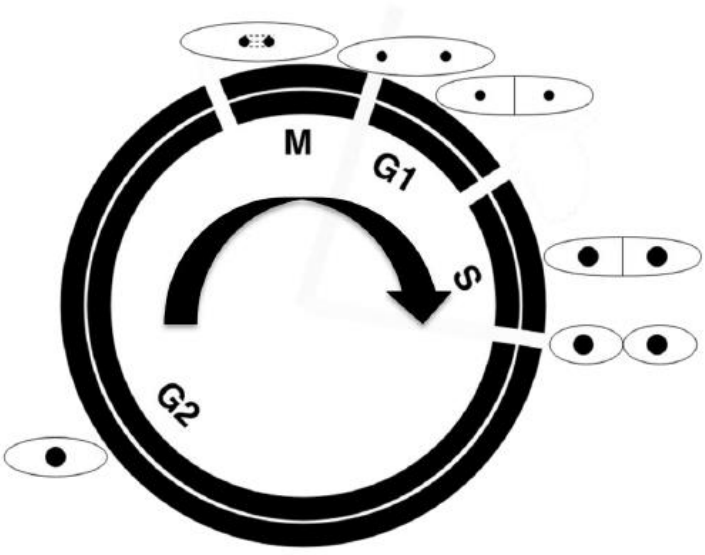

Figure 5.2. Schematic of the cell cycle of fission yeast.

There are many merits of fission yeast making it a great model organism for genetic research. Such as that the chromatin organization of fission yeast reassembles that of higher eukaryotes and it possesses conserved heterochromatin assembly mechanism (Mizuguchi et al., 2015). The replication of fission yeast genome starts at multiple origins in a bidirectional manner. Importantly, fission yeast is the sixth eukaryotic model organism to have its genome fully sequenced (Yanagida, 2002). Furthermore, fission yeast has a short cell cycle of 3 hours when growing under standard condition and is non-pathogenic, making its handling relatively convenient under lab conditions.

5.1. Objectives

A previous report has identified a physical and direct interaction between the large subunit of mammalian CAF-1, p150, and the RecQ helicase BLM both *in vivo* and *in vitro* (Jiao et al., 2004). BLM and p150 were found co-localized *in vivo* within discrete nuclear foci in response to DNA damage and replication stress. Moreover, BLM was found to inhibit CAF-1 mediated chromatin assembly coupled to DNA repair. In fission yeast, the lab has previously reported a novel role for CAF-1 in recombination-dependent replication (RDR) (Pietrobon et al., 2014). Fission yeast CAF-1 was found acting at the DNA synthesis step of RDR to protect the D-loop from disassembly by the RecQ helicase Rqh1, the fission yeast orthologue of BLM. The lab has proposed that the likelihood of chromosomal instability at the site of arrested forks results from antagonistic activities of CAF-1 and Rqh1 in processing recombination intermediates: Rqh1 favors the disassembly of the D-loop and CAF-1 counteracts this activity. Interestingly, an *in vivo* interaction between Rqh1 and Pcf1 was also identified, showing that physical and functional interactions between CAF-1 and RecQ helicases are evolutionarily conserved.

The working model summarizing the previous observations is present in Figure 5.3 (Pietrobon et al., 2014). However, several questions remain to address: 1) what is the role of the physical interaction between CAF-1 and Rqh1 in maintaining genome stability in response to replication stress, 2) How CAF-1 associates with RDR sites, 3) Is the chromatin assembly function of CAF-1 necessary to promote RDR.

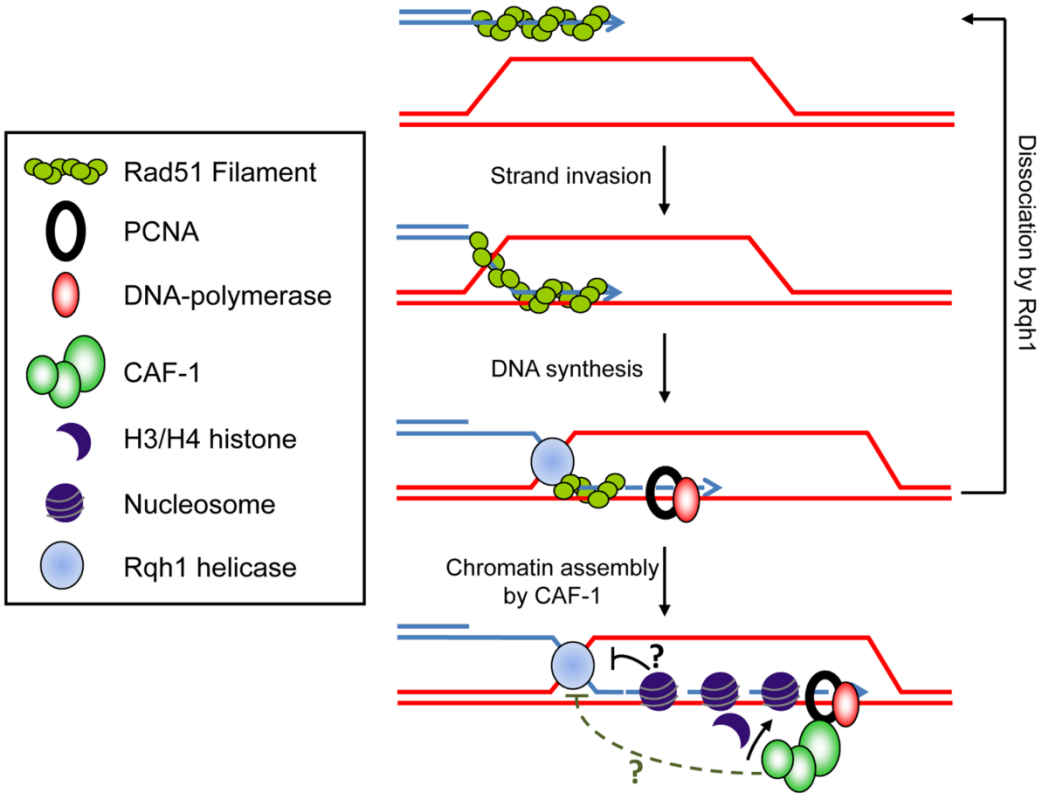

Figure 5.3. Working model of D-loop stabilization by CAF-1 at the DNA synthesis step of recombination-dependent replication (RDR). CAF-1 might prevent the disassembly of the D-loop by promoting histone deposition coupled to DNA synthesis during RDR. Newly synthesized DNA on the D-loop is assembled into chromatin and can counteract the D-loop disassembling activity of Rqh1 (black line). Alternatively, CAF-1 is targeted on the D-loop via its interaction with PCNA and counteracts the activity of Rqh1 directly or indirectly (dashed green line). However, the targeting of CAF-1 to the d-loop might also be mediated via its interaction with HR factors. Adapted from Pietrobon et al., 2014 (Pietrobon et al., 2014).

During my PhD, I have contributed to answering these three questions. I combined *in vivo* and *in vitro* approaches to characterize the physical interaction between CAF-1 and Rqh1. I have developed an *in vivo* chromatin binding assay to explore the association of CAF-1 to chromatin in response to DNA damage. The assay was also employed to address the role of HR factors in CAF-1 association to the chromatin.

Results

1. Characterization of the physical interaction between the RecQ helicase Rqh1 and CAF-1

To address the role of CAF-1 in the DNA damage response (DDR), fission yeast strains defective for CAF-1 have been previously constructed in the lab by Dr. Stefania Francesconi (UMR 3525, Institut Pasteur). Strains deleted for genes encoding each subunit of CAF-1 were generated: *pcf1-d, pcf2-d* or *pcf3-d*. Unlike *asf1*, the gene encoding the essential histone H3-H4 chaperone Asf1 (Tanae et al., 2012), strains deleted for each CAF-1 subunits were found to be viable (Dohke et al., 2008; Pietrobon et al., 2014).

In light of the evolutionarily conserved and physical interactions between CAF-1 and RecQ helicases ((Jiao et al., 2004; Pietrobon et al., 2014), my objective was to define the cellular function of the physical interaction between Pcf1 and Rqh1 *in vivo*, with the aim to identify loss-of-interaction mutants. Therefore, I have first better characterized the *in vivo* interactions between CAF-1 and Rqh1 in fission yeast.

1.1. The Pcf1 and Pcf2 subunits interact with Rqh1 independently of each other

As a first approach, I have tested if Rqh1 interacts only with Pcf1 or also with the other two subunits of CAF-1, Pcf2 and Pcf3. I have constructed strains expressing a myc-tagged version of Rqh1 (Rqh1-myc) in combination with YFP or GFP-tagged version of Pcf1 or Pcf2 (Pcf1-YFP, Pcf2-GFP and Pcf1-GFP being a gift from Dr. Tatsuki Kunoh, (Kunoh & Habu, 2014)), or a FLAG-tagged version of Pcf2 (Pcf2-FLAG), or a HA-tagged version of Pcf3 (Pcf3-HA). A strain expressing both Pcf1-GFP and Pcf2-FLAG was also generated. The viability of the tagged strains was evaluated by drop test (Figure 1-4).

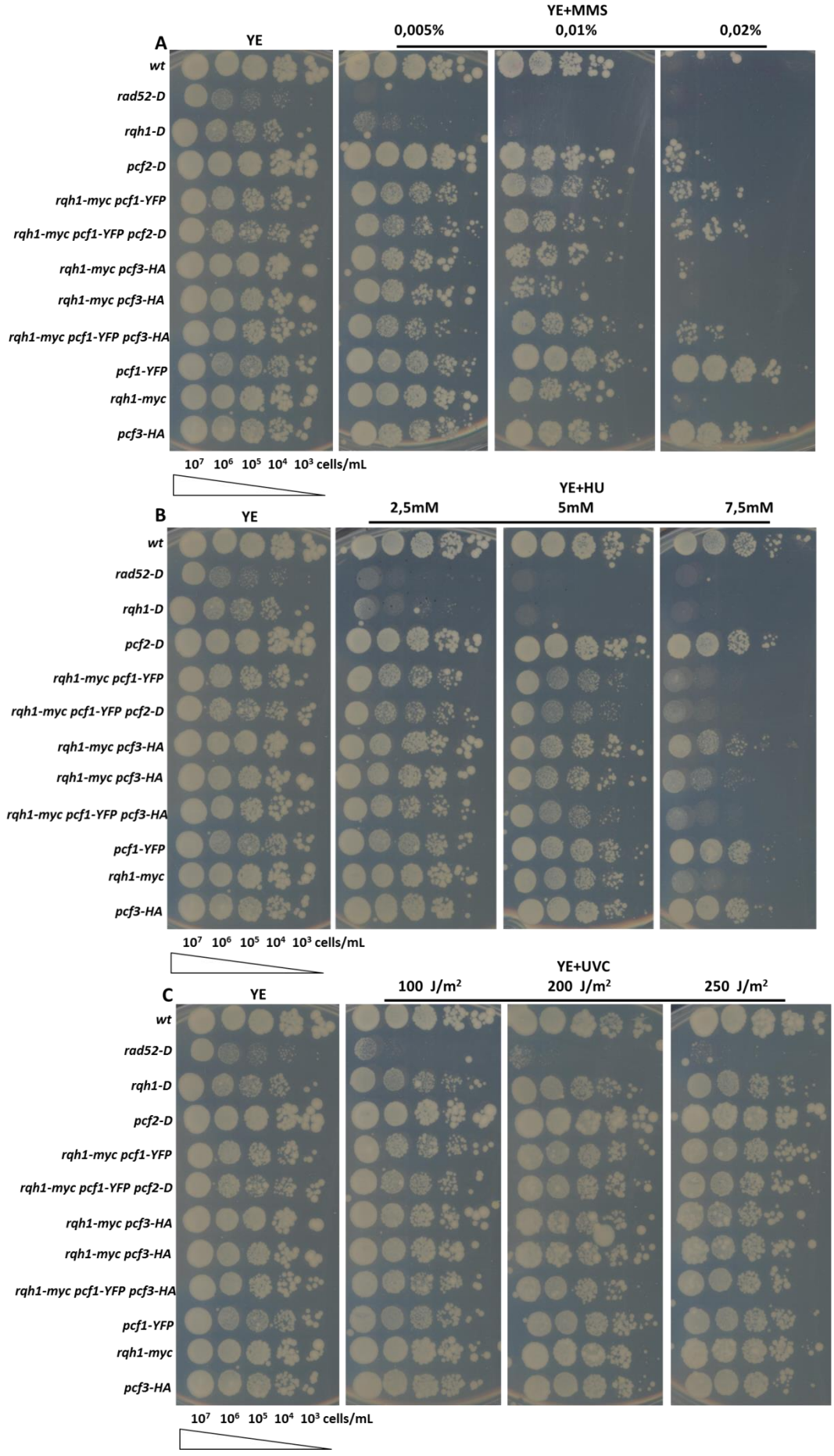
A
YE
YE+MMS
0,005%
0,01%
0,02%
wt
rad52-D
rqh1-D
pcf2-D
rqh1-myc pcf1-YFP
rqh1-myc pcf1-YFP pcf2-D
rqh1-myc pcf3-HA
rqh1-myc pcf3-HA
rqh1-myc pcf1-YFP pcf3-HA
pcf1-YFP
rqh1-myc
pcf3-HA
10⁷ 10⁶ 10⁵ 10⁴ 10³ cells/mL
B
YE
YE+HU
2,5mM
5mM
7,5mM
wt
rad52-D
rqh1-D
pcf2-D
rqh1-myc pcf1-YFP
rqh1-myc pcf1-YFP pcf2-D
rqh1-myc pcf3-HA
rqh1-myc pcf3-HA
rqh1-myc pcf1-YFP pcf3-HA
pcf1-YFP
rqh1-myc
pcf3-HA
10⁷ 10⁶ 10⁵ 10⁴ 10³ cells/mL
C
YE
YE+UVC
100 J/m²
200 J/m²
250 J/m²
wt
rad52-D
rqh1-D
pcf2-D
rqh1-myc pcf1-YFP
rqh1-myc pcf1-YFP pcf2-D
rqh1-myc pcf3-HA
rqh1-myc pcf3-HA
rqh1-myc pcf1-YFP pcf3-HA
pcf1-YFP
rqh1-myc
pcf3-HA
10⁷ 10⁶ 10⁵ 10⁴ 10³ cells/mL

Figure 1. Sensitivity of fission yeast strains to different DNA damaging and replication blocking agents. A. YE plates with different concentrations of MMS. B. YE plates with different concentrations of HU. C. YE plates exposed to different doses of UV-C. *2 clones of *rqh1-myc pcf3-HA* were tested in this drop test. YE plates were used as a control. The strain deleted for *rad52* served as a control for the quality of the plates, because of its hypersensitivity to DNA damaging and replication blocking agents.

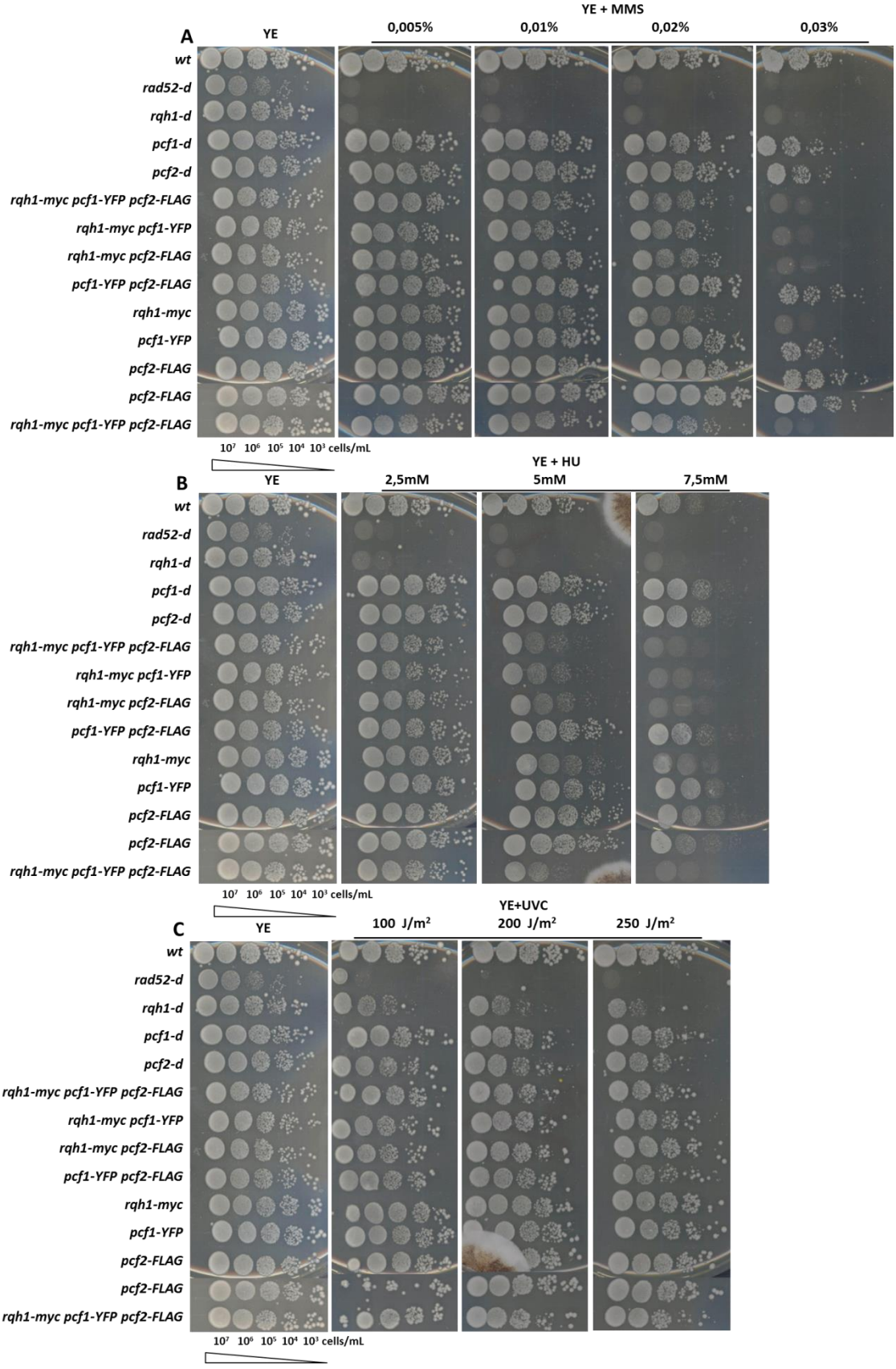
A
YE
YE + MMS
0,005%
0,01%
0,02%
0,03%
wt
rad52-d
rqh1-d
pcf1-d
pcf2-d
rqh1-myc pcf1-YFP pcf2-FLAG
rqh1-myc pcf1-YFP
rqh1-myc pcf2-FLAG
pcf1-YFP pcf2-FLAG
rqh1-myc
pcf1-YFP
pcf2-FLAG
pcf2-FLAG
rqh1-myc pcf1-YFP pcf2-FLAG
10⁷ 10⁶ 10⁵ 10⁴ 10³ cells/mL
B
YE
YE + HU
2,5mM
5mM
7,5mM
wt
rad52-d
rqh1-d
pcf1-d
pcf2-d
rqh1-myc pcf1-YFP pcf2-FLAG
rqh1-myc pcf1-YFP
rqh1-myc pcf2-FLAG
pcf1-YFP pcf2-FLAG
rqh1-myc
pcf1-YFP
pcf2-FLAG
pcf2-FLAG
rqh1-myc pcf1-YFP pcf2-FLAG
10⁷ 10⁶ 10⁵ 10⁴ 10³ cells/mL
C
YE
YE+UVC
100 J/m²
200 J/m²
250 J/m²
wt
rad52-d
rqh1-d
pcf1-d
pcf2-d
rqh1-myc pcf1-YFP pcf2-FLAG
rqh1-myc pcf1-YFP
rqh1-myc pcf2-FLAG
pcf1-YFP pcf2-FLAG
rqh1-myc
pcf1-YFP
pcf2-FLAG
pcf2-FLAG
rqh1-myc pcf1-YFP pcf2-FLAG
10⁷ 10⁶ 10⁵ 10⁴ 10³ cells/mL

Figure 2. Sensitivity of fission yeast strains to different DNA damaging and replication blocking agents. A. YE plates with different concentrations of MMS. B. YE plates with different concentrations of HU. C. YE plates exposed to different doses of UV-C. *2 clones of *pcf2-FLAG* and *rqh1-myc pcf1-YFP pcf2-FLAG* were tested in this drop test. YE plates were used as a control. The strain deleted for *rad52* served as a control for the quality of the plates, because of its hypersensitivity to DNA damaging and replication blocking agents.

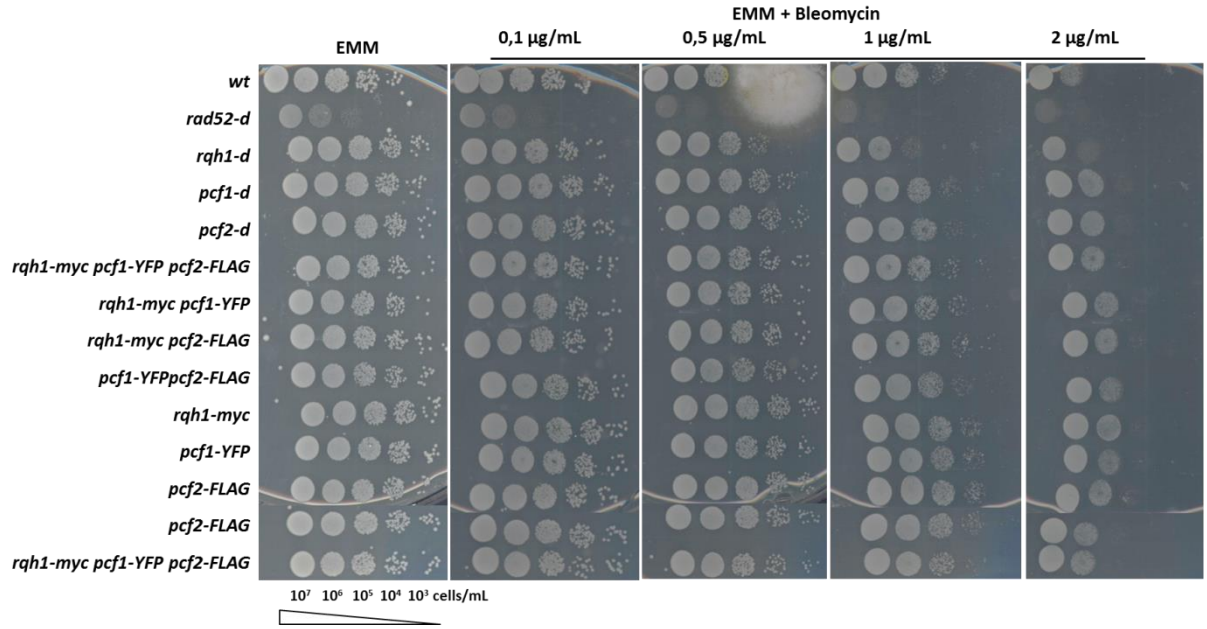

Figure 3. Sensitivity of fission yeast strains to DNA damaging agent Bleomycin. EMM plates with different concentrations of Bleomycin. *2 clones of *pcf2-FLAG* and *rqh1-myc pcf1-YFP pcf2-FLAG* were tested in this drop test. EMM plate was used as a control. The strain deleted for *rad52* served as a control for the quality of the plates, because of its hypersensitivity to DNA damaging agents.

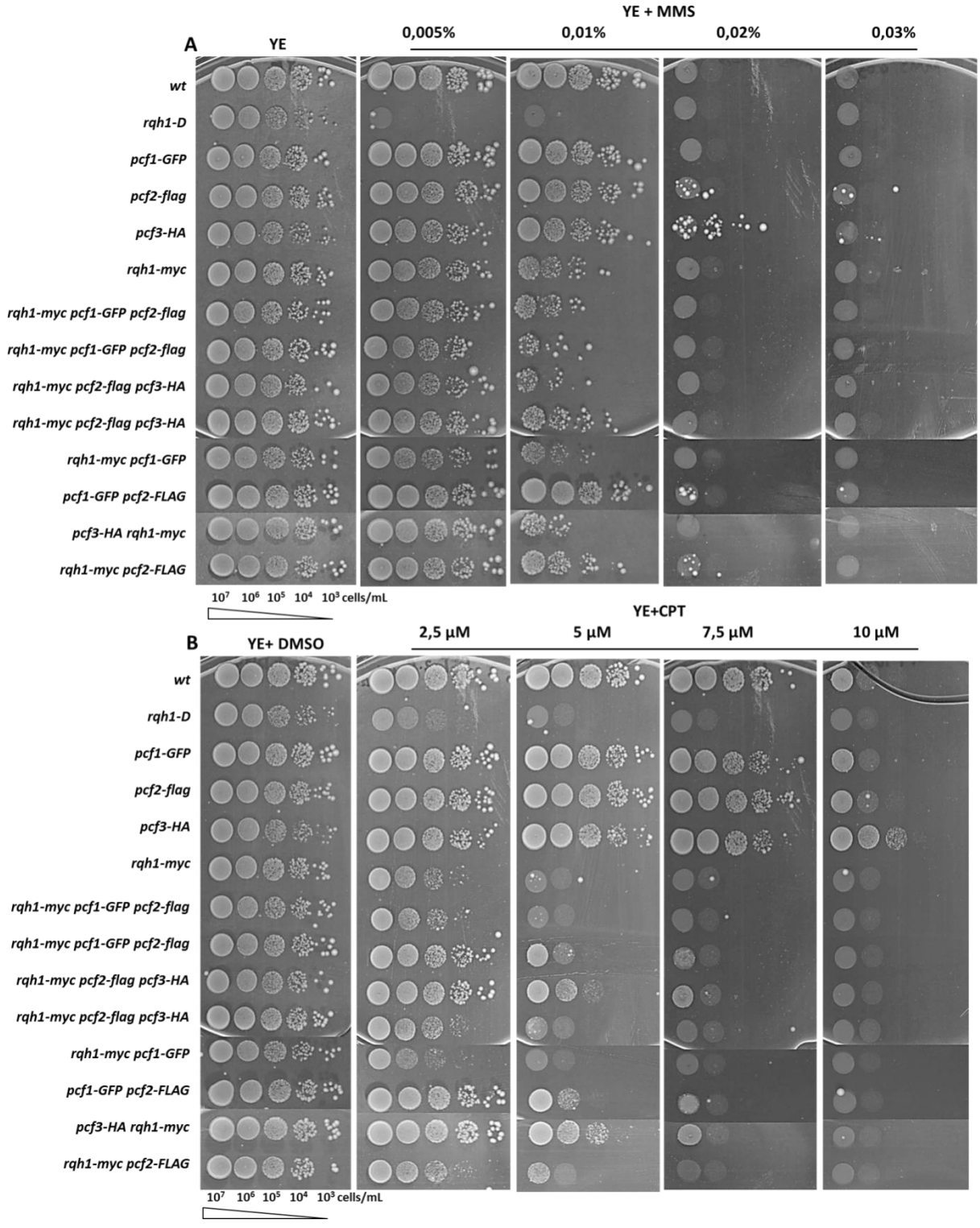

Figure 4. Sensitivity of fission yeast strains to different DNA damaging and replication blocking agents. A. YE plates with different concentrations of MMS. B. YE plates with different concentrations of CPT. *2 clones of *rqh1-myc pcf1-GFP pcf2-FLAG* and *rqh1-myc pcf2-FLAG pcf3-HA* were tested in this drop test. YE and YE+DMSO plates were used as a control.

The function of the C-terminally tagged version of Pcf1, Pcf1-YFP and Pcf1-GFP, was also evaluated by synthetic lethality assays with *hip1-d* (*hip1* encodes one of the subunits of the fission yeast HIRA homologue, the Hir complex) (Figure 5). Indeed, it has been previously reported that *pcf1-d* is co-lethal with *hip1-d* (work from a previous lab member Violena Pietrobon). The results showed that the YFP- and GFP-tagged Pcf1 appeared to be partially functional as 9 out of 20 *pcf1-YFP hip1-d* spores were viable and 7 out of 15 *pcf1-GFP hip1-d* spores were viable, respectively (Figure 5, middle and right panel).

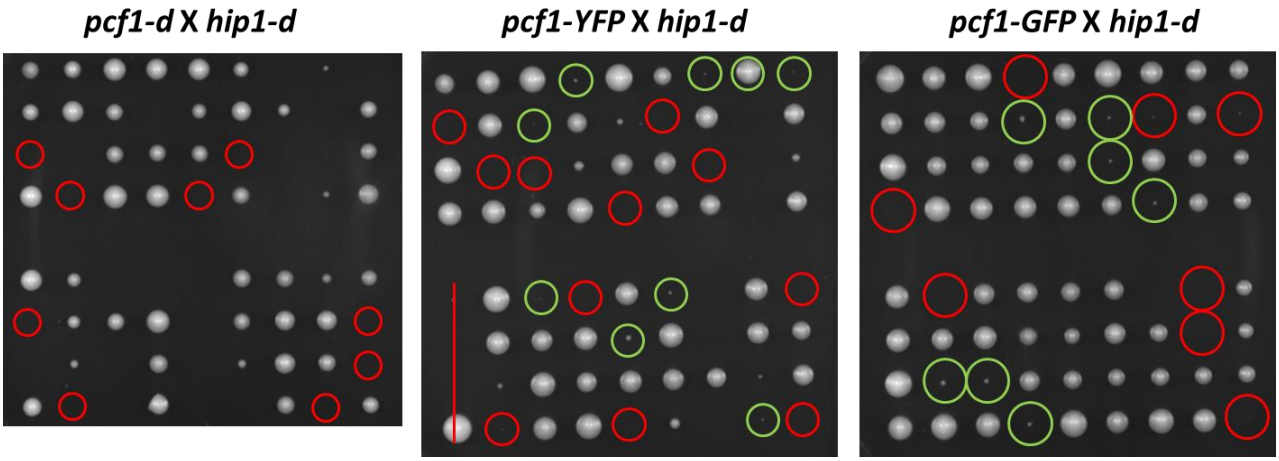

Figure 5. Synthetic lethality between *tagged pcf1* and *hip1-d*. Left panel: tetrads from the cross between *pcf1-d* and *hip1-d* strains are represented. Red circles indicate *pcf1-d hip1-d* spores that were unviable. 68 spores from 17 tetrads were analyzed. Middle panel: tetrads from the cross between *pcf1-YFP* and *hip1-d* strains are represented. Red circles indicate *pcf1-YFP hip1-d* spores that were unviable. Green circles indicate *pcf1-YFP hip1-d* spores that were viable. 68 spores from 17 tetrads were analyzed. The red line indicates the tetrad that was not analyzed. Right panel: tetrads from the cross between *pcf1-GFP* and *hip1-d* strains are represented. Red circles indicate *pcf1-GFP hip1-d* spores that were unviable. Green circles indicate *pcf1-GFP hip1-d* spores that were viable. 72 spores from 18 tetrads were analyzed.

These results suggest that the tagging of CAF-1 subunits does not sensitize cells to DNA damage, while the tagging of Rqh1 yields mild sensitivity to high dose of DNA damaging agents. However, the fusion with YFP- or GFP- tag leads to a partial loss of function of Pcf1. Nonetheless, these strains were later utilized in co-immunoprecipitation (co-IP) experiments and GST-pulldown approaches to reveal *in vivo* and *in vitro* interactions between Rqh1 and CAF-1 subunits, but not to perform genetics analysis. Of note, all interactions were tested in the presence of Benzonase to digest DNA and RNA and to avoid the detection of protein-protein interactions bridged by nucleic acids.

First, a co-IP experiment was performed to confirm that the tagging of CAF-1 subunits does not interfere with their interactions within the CAF-1 complex. This co-IP showed that Pcf1-GFP binds to Pcf2-FLAG and PCNA (Figure 6A). Further co-IP experiments showed that Pcf1-YFP and Pcf2-FLAG bound to PCNA and Histone H3 (Figure 6B and D), showing that the tagged versions of Pcf1 and Pcf2, even if partially functional, are able to mediate physical interactions within the CAF-1-PCNA-H3 complex. Next, I have reproduced the interaction between Pcf1 and Rqh1 by the IP of Pcf1-YFP (Figure 6B). This interaction has been previously reported by the lab (Pietrobon et al., 2014). The reversed co-IP, the IP of Rqh1-myc, has confirmed the interaction between Rqh1 and Pcf1 (Figure 6C).

The interaction between Pcf2 and Rqh1 was analyzed by co-IP (Figure 6D and E). The IP of Pcf2-FLAG showed that Rqh1 physically interacted with Pcf2, and the presence of PCNA and histone H3 was also observed in the IP fraction (Figure 6D). Moreover, the IP of Rqh1-myc showed that Rqh1 binds to Pcf2 but also to Histone H3 and PCNA (Figure 6E). Thus, the data revealed an *in vivo* physical interaction between Pcf2 and Rqh1. To my knowledge, this is the first time that the interaction between Rqh1 and the mid subunit of CAF-1 was observed.

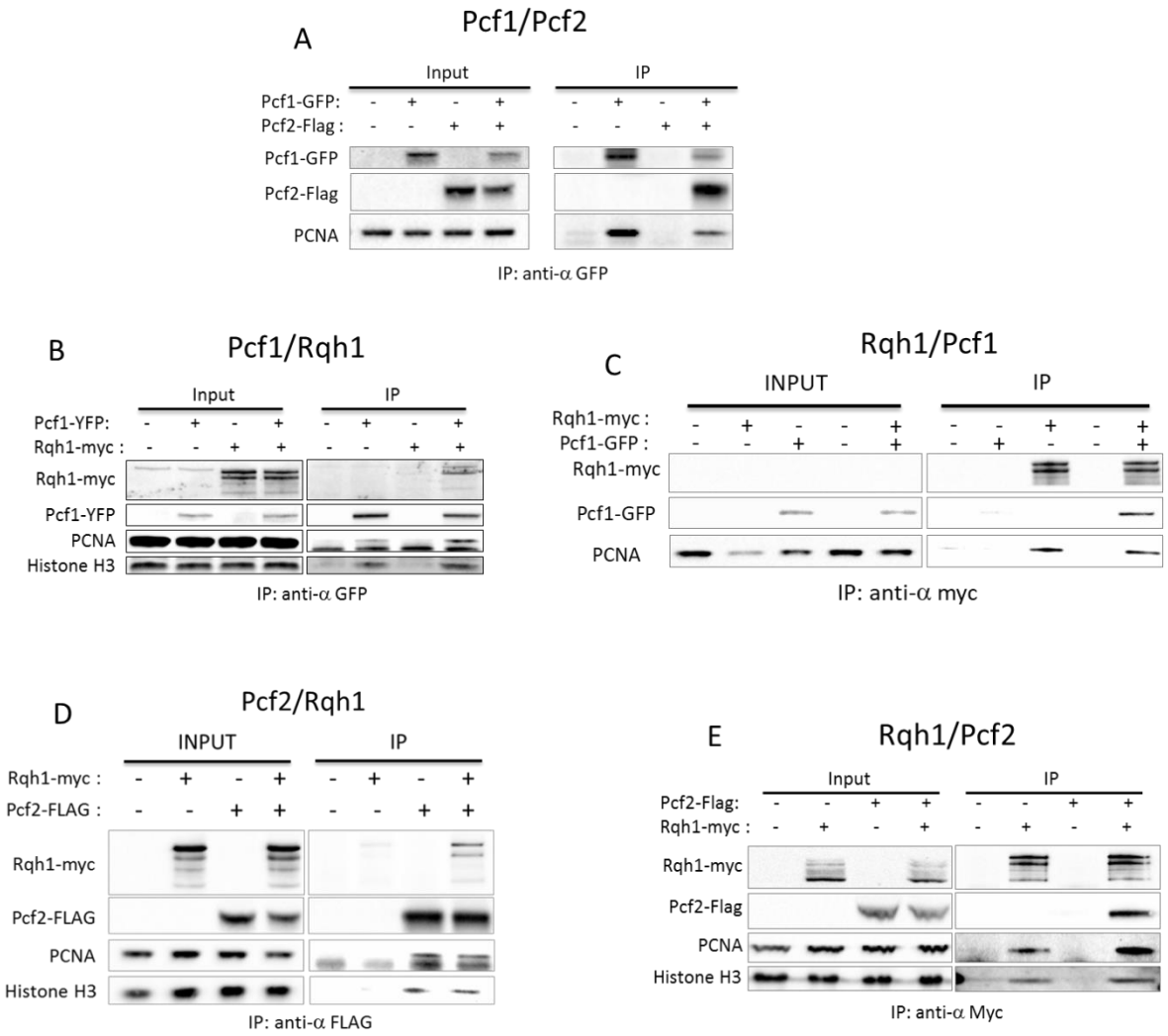

Figure 6. Pcf1 and Pcf2 both physically interact with Rqh1 *in vivo*. A. Immuno-precipitation (IP) of Pcf1-GFP. B. IP of Pcf1-YFP. C. IP of Rqh1-myc. *the amount of Rqh1-myc in the input was too low to be detected by the antibody. D. IP of Pcf2-FLAG. E. IP of Rqh1-myc. The co-IP experiments were performed by using antibodies against the tag of the protein. IP refers to the immunoprecipitation fraction. Proteins detected by Western Blot are indicated in the figure, as well as the expressed epitope tagged proteins.

An attempt to probe for Pcf3 and Rqh1 interaction was made using a strain expressing Pcf3-HA and Rqh1-myc (data not shown). However, due to technical issues, I could not yet provide conclusive data showing unambiguous interaction between Pcf3 and Rqh1. This question will be addressed in the future using a different tag for Pcf3, such as the GFP-tag. Since co-IP approaches cannot differentiate if the protein-protein interaction is direct or indirect, it is possible that the Pcf2-Rqh1 interaction is bridged by Pcf1 within the CAF-1 complex. To address this question, I have deleted the *pcf2* gene and the *pcf1* gene in a strain expressing Rqh1-myc

Pcf1-YFP and in a strain expressing Rqh1-myc Pcf2-FLAG, respectively. The IP of Pcf1-GFP from *pcf2-d* cells showed that Pcf1-Rqh1 interaction was not abolished when Pcf2 was absent (Figure 7A), indicating that Pcf1-Rqh1 interaction does not require the presence of Pcf2. Surprisingly, the IP of Pcf2-FLAG (Figure 7B) or Rqh1-myc (Figure 7C) from cells deleted for *pcf1* showed that Pcf2-Rqh1 interaction was still observed in the absence of Pcf1, indicating that the interaction between Pcf2 and Rqh1 is not bridged by Pcf1. Furthermore, these data indicate that the integrity of the CAF-1 complex is not required to allow Rqh1 interacting with either Pcf1 or Pcf2.

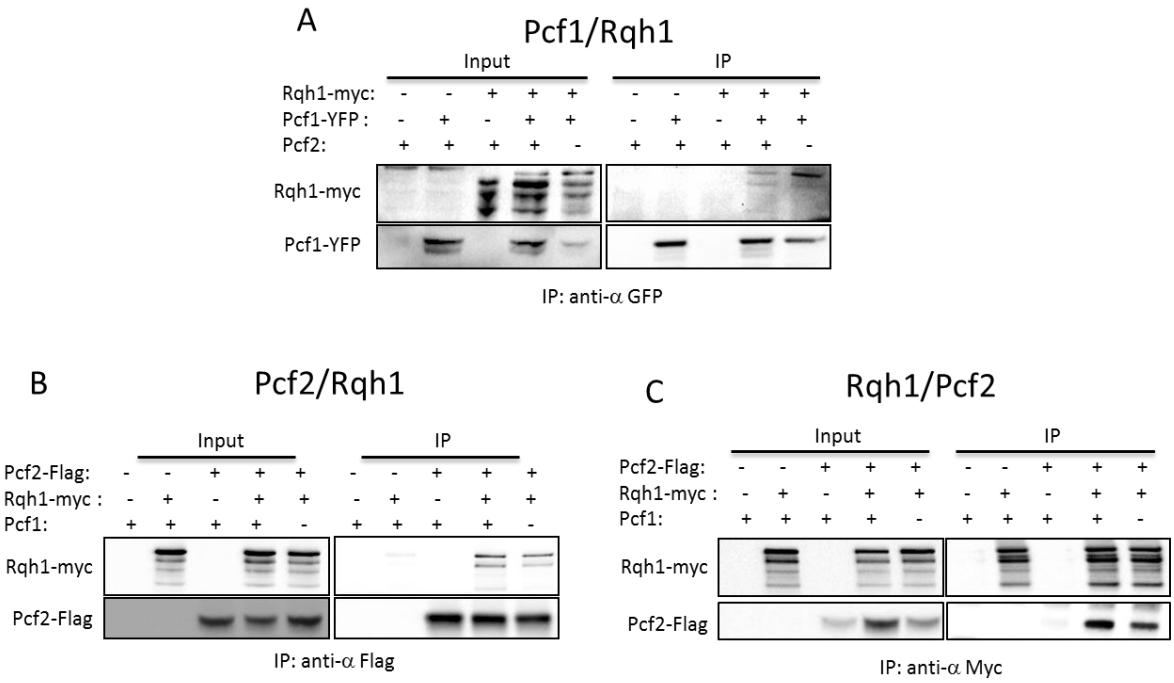

Figure 7. Pcf1 and Pcf2 physically interact with Rqh1 independently of each other. A. IP of Pcf1-YFP showing that Pcf1 interacts with Rqh1 independently of Pcf2. B. and C. IP of Pcf2-FLAG and IP of Rqh1-myc, respectively showing that Pcf2 interacts with Rqh1 independently of Pcf1. The co-IP experiments were performed by using antibodies against the tag of the protein. IP refers to the immunoprecipitation fraction. Proteins detected by immuno-blot are indicated in the figure, as well as the expressed epitope tagged proteins.

To verify the interactions between Pcf1 and Rqh1 and with the aim to map the interaction domains, I have developed an *in vitro* GST-pulldown assay. To this end, I have purified recombinant GST-tagged Pcf1 from *E. coli* system using the plasmids kindly sent by Dr. Françoise Ochsenbein (CEA, Saclay, FR).

In the production of recombinant Pcf1, due to that the recombinant Pcf1 was undergoing a lot of degradation during the protein expression and purification, I have tried different strategies to improve the quality of recombinant Pcf1. I have tried to optimize the protein yield by expressing

the plasmids in different *E. coli* strains, manipulating the culturing conditions including different *E. coli* growth media as well as the culturing time and trying different buffers for pelleting and lysing *E. coli* (data not shown). After experimenting in multiple conditions, I found that compared to my construct of recombinant Pcf1 (Pcf1-GST, constructed in pGEX6p1), the construct of recombinant Pcf1 kindly given by Dr. Françoise Ochsenbein (Pcf1-his-GST, constructed in pETM30) expressed in the *E. coli* strain BL21 gold cultured in 2xyt media for 3 hours resulted in the best quality of recombinant Pcf1 after the purification (a typical Western Blot is shown in Figure 8, sample from indicated condition was loaded in lane 7). The purification from this condition yielded a more prominent band of recombinant Pcf1 as well as less protein degradation, thus hereafter I used the recombinant Pcf1 purified in this condition for my GST-pulldown assays.

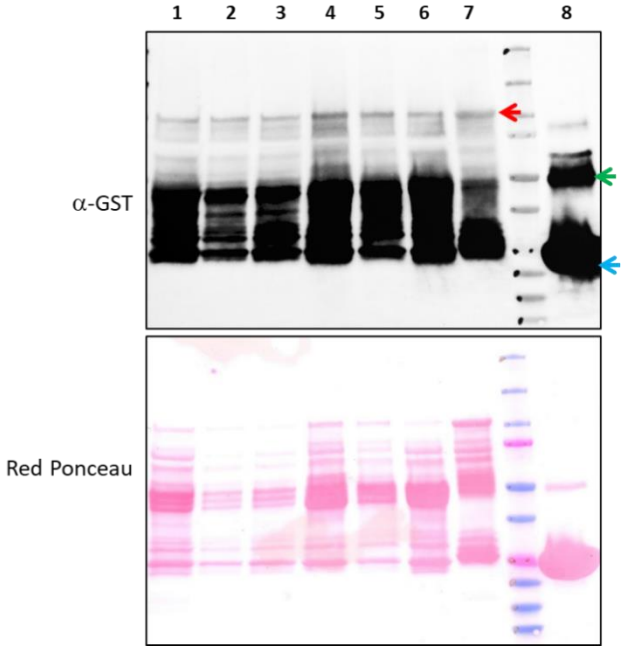

Figure 8. The purification of recombinant Pcf1 in different conditions. Equal amount of GSH-beads bound by purified proteins were loaded in each lane. The number of each lane indicates the condition for protein production. 1, 2 and 3: Pcf1-GST constructed in pGEX6p1 expressed in the *E. coli* strains BL21, BL21 star and Rosetta2, respectively, cultured in LB media overnight. 4: Pcf1-GST constructed in pGEX6p1 expressed in the *E. coli* strain BL21 cultured in LB media for 3 hours. 5 and 6: Pcf1-GST constructed in pGEX6p1 expressed in the *E. coli* strain BL21 cultured overnight in 2xyt and TB media, respectively. 7: Pcf1-his-GST constructed in pETM30 expressed in the *E. coli* strain BL21 gold cultured in 2xyt media for 3 hours. 8: GST-tag alone purified from the *E. coli* strain BL21 expressing pGEX6p1 cultured in LB media overnight. The red arrow indicates the band corresponding to recombinant Pcf1. The blue arrow indicates the band corresponding to GST-tag and the green arrow indicates dimerized GST-tags.

To validate the conditions of the Pcf1-GST pulldown assay, I first probed for the interaction of Pcf1 with Pcf2, Pcf3, Rqh1, PCNA and Histone H3 and H4 using proteins extract from a *wild type* (*wt*) strain and from a *pcf2-FLAG pcf3-HA rqh1-myc* strain (Figure 9A). The washing conditions (to wash the recombinant protein bound-GSH-beads) were done in an EB buffer (50mM HEPES High salt, 50mM KOAc pH7.5, 5mM EGTA, 1% Triton X-100, 1mM PMSF, and Complete Protease Inhibitor EDTA-Free Tablet (Roche, 04 693 159 001)) at 150 mM NaCl. As expected, the GST-pulldown experiment showed that recombinant Pcf1 was able to interact with Rqh1, Pcf2, PCNA as well as with histone H3 and H4. The interaction with Pcf3 was more difficult to interpret because of an unspecific band migrating just near Pcf3-HA (Figure 9A).

Next, I have tested the stringency of these interactions by increasing the salt concentration of the washing buffer (ranging from 150 mM to 700 mM NaCl) (Figure 9B). All the observed interactions in the previous assay were resistant to 700mM NaCl-added EB buffer, indicating that these interactions are resistant to stringent salt conditions. Therefore, most of the subsequent GST pulldown assays were done at 700 mM NaCl during the washing steps. To further strengthen the specificity of the GST-pulldown assays, I have tested the interaction with an exogenous protein. Protein extracts from fission yeast expressing an exogenous protein, LacI-GFP, were used to incubate with recombinant Pcf1 in a GST-pulldown assay (Figure 9C). Recombinant Pcf1 was found to interact with endogenous PCNA and histone H3 and H4 but not with LacI-GFP. These observations have further confirmed that the interactions observed in the GST-pulldown assays are indeed specific.

Therefore, I have employed this GST-pulldown assay to confirm that Pcf1 interacts with Rqh1 independently of Pcf2. Protein extracts from *rqh1-myc pcf2-d* cells were incubated with recombinant Pcf1. Pcf1 was able to interact with Rqh1 independently of Pcf2 *in vitro* (Figure 9D), supporting our *in vivo* data from the co-IP experiment (Figure 7A).

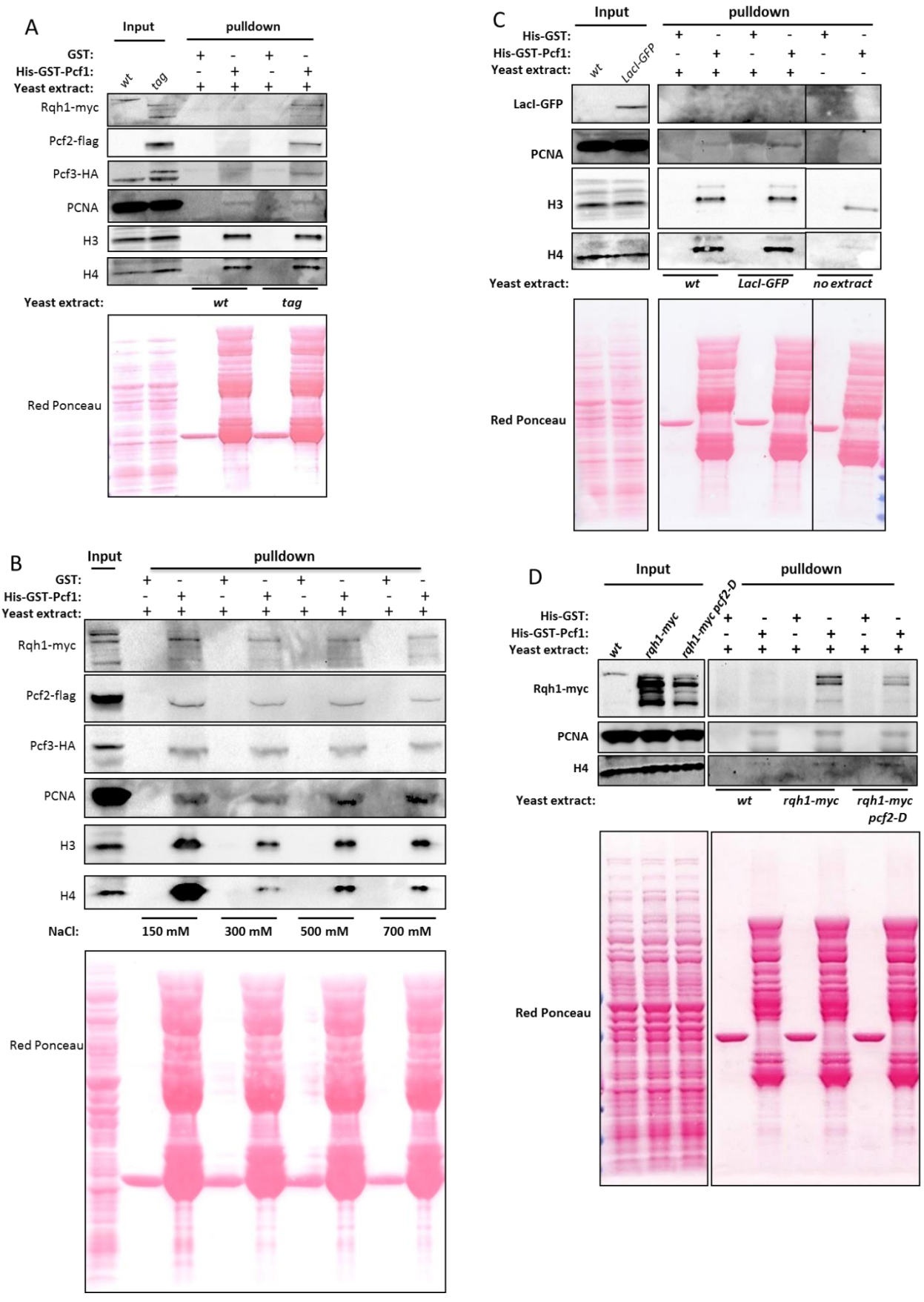
A
Input
pulldown
GST:
His-GST-Pcf1:
Yeast extract:
wt
tag
Rqh1-myc
Pcf2-flag
Pcf3-HA
PCNA
H3
H4
Yeast extract:
wt
tag
Red Ponceau
B
Input
pulldown
GST:
His-GST-Pcf1:
Yeast extract:
Rqh1-myc
Pcf2-flag
Pcf3-HA
PCNA
H3
H4
NaCl:
150 mM
300 mM
500 mM
700 mM
Red Ponceau
C
Input
pulldown
His-GST:
His-GST-Pcf1:
Yeast extract:
wt
LacI-GFP
LacI-GFP
PCNA
H3
H4
Yeast extract:
wt
LacI-GFP
no extract
Red Ponceau
D
Input
pulldown
His-GST:
His-GST-Pcf1:
Yeast extract:
wt
rqh1-myc
rqh1-myc pcf2-D
Rqh1-myc
PCNA
H4
Yeast extract:
wt
rqh1-myc
rqh1-myc pcf2-D
Red Ponceau

Figure 9. Verification of GST-pulldown assay. A. GST-pulldown assay using recombinant Pcf1 showing *in vitro* interactions between recombinant Pcf1 and Rqh1, Pcf2, Pcf3, PCNA and histone H3 and H4. This assay was performed using EB buffer at 150 mM NaCl during the washing steps. B. GST-pulldown assay using recombinant Pcf1 showing that the interactions between Pcf1 and Rqh1, Pcf2, Pcf3, PCNA, and histone H3 and H4 are resistant to 700 mM NaCl. *The weak signals in the lane corresponding to 300 mM NaCl washing conditions were a consequence of a part of the sample accidentally leaked out from the well before it migrated inside the gel. C. GST-pulldown assay using recombinant Pcf1 showing that recombinant Pcf1 does not interact with the exogenous protein LacI-GFP. *The faint bands appeared in the control samples without yeast extract are non-specific bands recognized by the antibodies. 700 mM NaCl was added to the buffer during the washing steps. D. GST-pulldown assay using recombinant Pcf1 showing that Pcf1-Rqh1 interaction is independent of Pcf2 *in vitro*. The bands of histone H4 were faint in the pulldown fraction because of reusing the antibody multiple times. 700 mM NaCl was added to the buffer in the washing step.

Altogether, these data indicate that Rqh1 not only interacts with Pcf1, but also with Pcf2. More importantly, Rqh1 interacts with Pcf1 independently of Pcf2 and Rqh1 interacts with Pcf2 independently of Pcf1. First, the integrity of the CAF-1 complex is not necessary for these interactions to occur. Second, Rqh1 is likely to interact with CAF-1 via multiple protein contacts, which questions about the feasibility and the relevance to define a loss-of-interaction mutant of Rqh1.

1.2. Rqh1 interacts with histone H3 and PCNA and these interactions are bridged by Pcf2 and Pcf1

When Rqh1 was immuno-precipitated, PCNA and histone H3 were found interacting with Rqh1 (Figure 6E and 10A). Given that Rqh1 interacts with two subunits of CAF-1, Pcf1 and Pcf2, and that PCNA interacts with CAF-1 via the PIP-box on Pcf1 (Pietrobon et al 2014), as well as that CAF-1 interacts with Histone H3, I have questioned the possibility that Rqh1-PCNA and Rqh1-Histone H3 interactions were bridged by CAF-1. To address this question, a co-IP experiment was performed by IP Rqh1-myc from cells lacking Pcf1, Pcf2, or expressing a form of Pcf1 mutated in the PIP-box (*pip-mut*). In the absence of either Pcf1 or Pcf2, the amount of PCNA and histone H3 observed in the IP fraction was reduced compared to *wild type* cells (Figure 10B). Similar observation was made when Pcf1-pip-mut was expressed (Figure 10B). These data indicate that the interactions of Rqh1 with PCNA and histone H3 are bridged by Pcf1 and Pcf2 and thus are likely bridged by the CAF-1 complex.

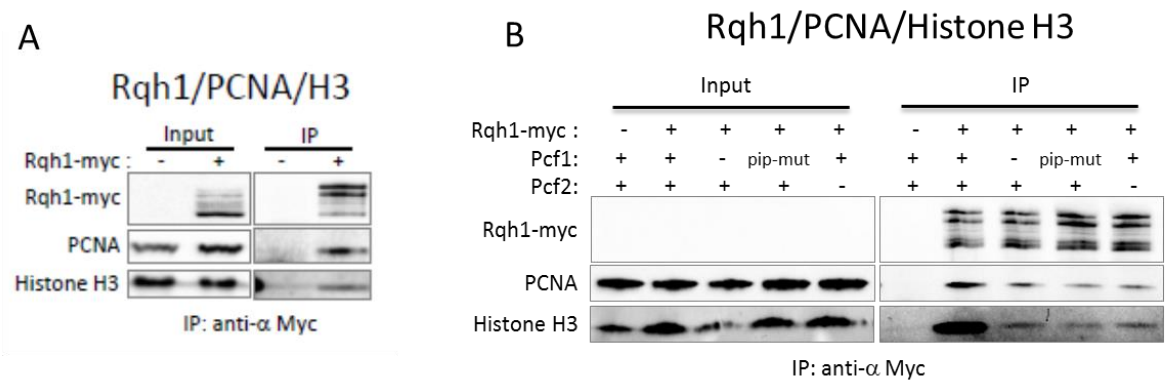

Figure 10. The interactions of Rqh1 with histone H3 and PCNA are mediated by Pcf1 and Pcf2. A. IP of Rqh1-myc showing that Rqh1 interacts with PCNA and histone H3. B. IP of Rqh1-myc from *pcf1-d, pcf1-pip-mut* and *pcf2-d* cells, respectively. The co-IP experiments were performed using antibodies against the tag of the protein. IP refers to the immunoprecipitation fraction. Proteins detected by immuno-blot are indicated in the figure, as well as the expressed epitope tagged proteins.

1.3. DNA damage stimulates Pcf1-Rqh1 interactions

To further characterize the physical interactions between Rqh1 and CAF-1 and the role of this interaction in response to DNA damage, I have tested how DNA damages modulate those interactions. To this end, I have employed MMS (Methyl Methane Sulfonate), an alkylated agent that induces damaged replication fork, and Bleomycin, a double strand break (DSB)-inducing agent. The IP of Pcf1-YFP from cells treated with MMS and Bleomycin showed that there was more Rqh1 interacting with Pcf1 in the IP fraction compared to the untreated sample. (Figure 11A and B), suggesting that Pcf1-Rqh1 interaction is stimulated by DNA damage. The IP of Pcf2-FLAG from cells treated with MMS showed that the amount of Rqh1 interacting with Pcf2 in the IP fraction stayed the same with or without treatment, suggesting that Pcf2-Rqh1 interaction is not affected by DNA damage (Figure 11C). The reverse co-IP, the IP of Rqh1-myc revealed the same result that DNA damage did not stimulate Pcf2-Rqh1 interaction (Figure 11D).

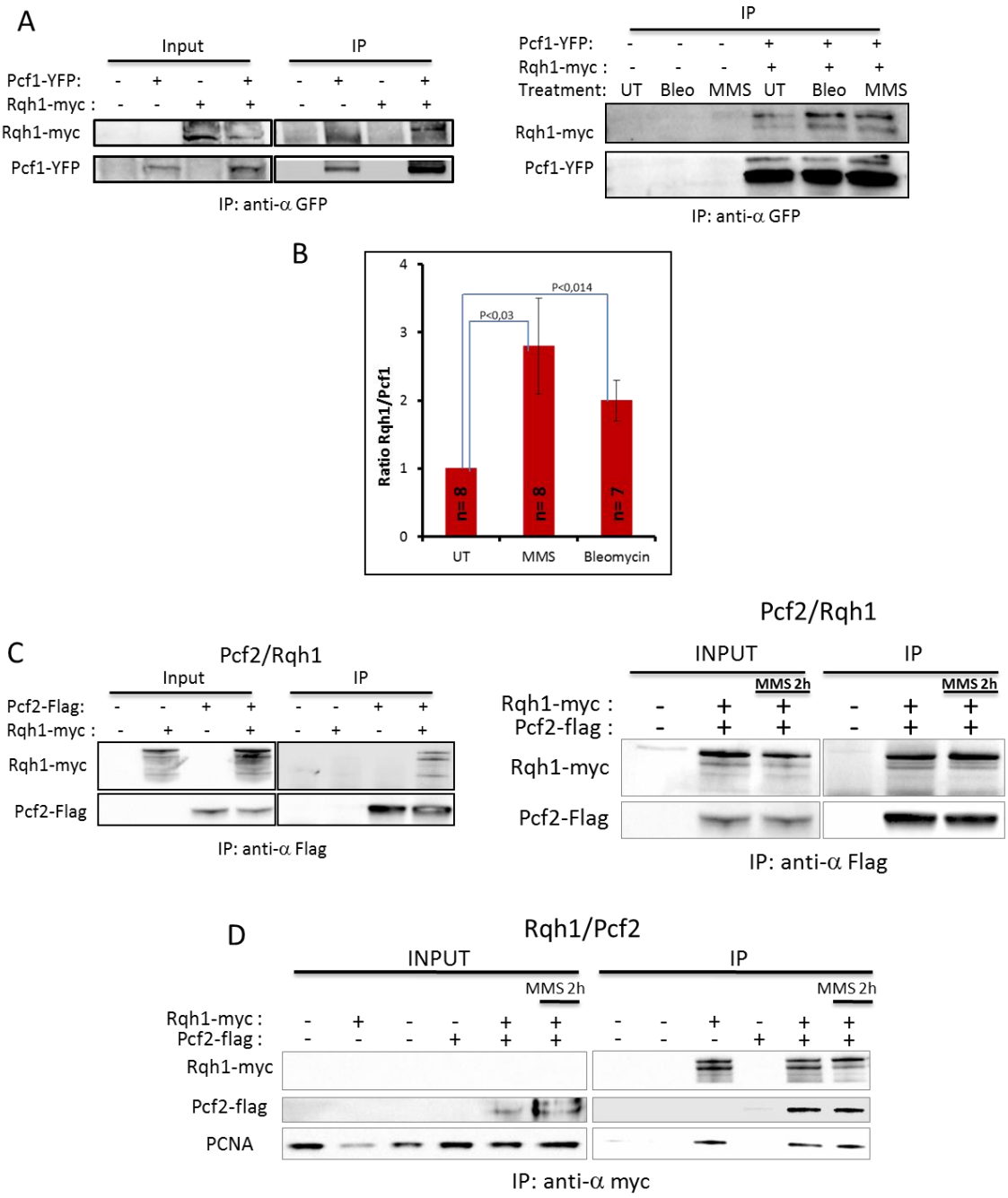

Figure 11. DNA damage stimulates Pcf1-Rqh1 interaction *in vivo*. A. Left panel: IP of Pcf1-YFP showing that Pcf1 physically interacts with Rqh1. Right panel: IP of Pcf1-YFP showing that Pcf1-Rqh1 interaction is stimulated by the indicated DNA damaging agents. The treatment was performed by culturing cells in media containing 0.03% of MMS for 2h or 10 mU/mL of Bleomycin for 2h, respectively. B. Quantification of more than three biological replicates of the experiment showed on the right panel A. The quantification is expressed by the ratio of the band intensity of Rqh1 divided by the band intensity of Pcf1. Error bars are standard error of the mean (SEM). Statistical analysis was performed by using Student's t-test. C. Left panel: IP of Pcf2-FLAG showing that Pcf2 physically interacts with Rqh1. Right panel: IP of Pcf2-FLAG showing that Pcf2-Rqh1 interaction is not stimulated by the indicated DNA damaging agents. D. IP of Rqh1-myc showing that Pcf2-Rqh1 interaction is not

stimulated by the indicated DNA damaging agents. *The input was absent because the concentration of proteins was not enough to be detected by Western Blot. The treatment was performed by culturing cells in media containing 0.03% of MMS for 2h. The co-IP experiments were performed using antibodies against the tag of the protein. IP refers to the immunoprecipitation fraction. Proteins detected by immuno-blot are indicated in the figure, as well as the expressed epitope tagged proteins.

To further confirm that DNA damages stimulate interactions between Rqh1 and Pcf1, I have employed the GST-pulldown approach. Equal amount of recombinant Pcf1 was incubated with the same amount of protein extract from MMS-treated cells. The data was quantified as a ratio of Rqh1-myc signal from the pulldown (PD) fraction by the amount of Rqh1-myc found in the input. The data showed that the Pcf1-Rqh1 interaction was stimulated by two to three-fold as soon as 1 hour of MMS treatment (Figure 12A and B). Similar observations were obtained when cells were treated with Bleomycin (Figure 12C and D). Interestingly, none of these DNA-damaging agents were found to modulate the interactions of Pcf1 with either PCNA or Histone H3. Based on these results, a GST-pulldown was performed using *pcf2-FLAG pcf3-HA rqh1-myc* cells treated with MMS treatment for 3 hours or untreated (Figure 12E and F). The Pcf1-Rqh1 interaction was stimulated by MMS, but not the interactions of recombinant Pcf1 with Pcf2, Pcf3, PCNA and histone H3, suggesting that DNA damage, and in particular replication stress, modulate Pcf1-Rqh1 interaction but not the CAF-1-Rqh1 interactions.

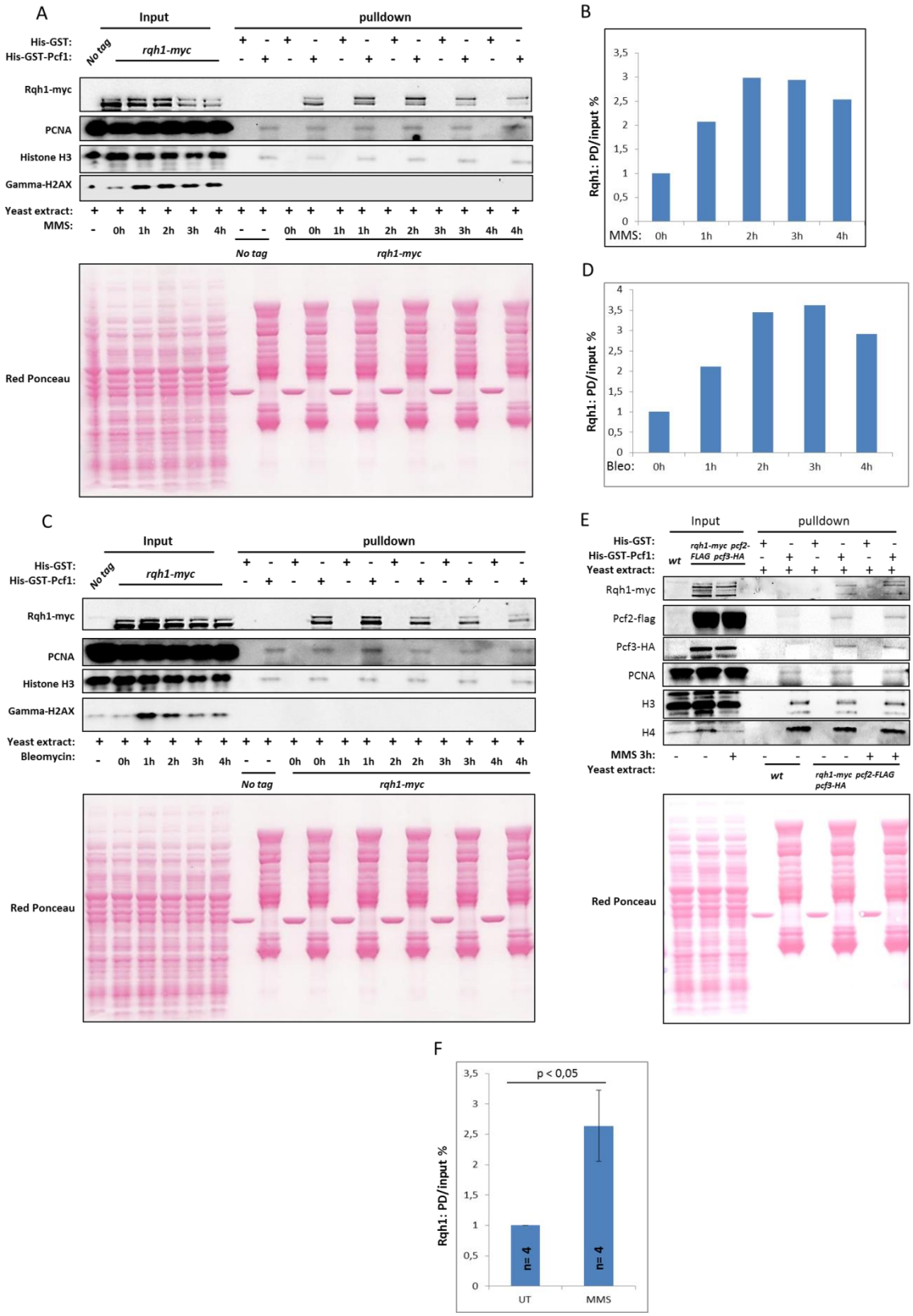

Figure 12. DNA damage stimulates Pcf1-Rqh1 interaction *in vitro*. A, C and E. GST-pulldown assays using recombinant Pcf1 showing that Pcf1-Rqh1 interaction is stimulated by indicated DNA damaging agents. 700 mM NaCl was added to the buffer during the washing steps. The treatment was performed by culturing cells in

media containing 0.03% of MMS or 10 mU/mL of Bleomycin for indicated hours. Gamma-H2AX was probed as an indicator of the effect of DNA damaging treatment. B, D and F. Quantification of data from GST-pulldown assays represented by panel A, C and E, respectively. The quantification is expressed by the ratio of the band intensity of Rqh1 in the pulldown (PD) fraction divided by the band intensity of Rqh1 in the input. *Panel B shows the mean values from two biological replicates. The error bar in panel C is standard error of mean (SEM). Statistical analysis was performed by using Student's t-test.

During the experiments, I have noticed that the pattern of the Rqh1 bands that were pull-downed upon MMS treatment was different from the pattern from untreated cells. In the MMS time course, the intensity of the upper band was getting much stronger compared to the lower band which was getting weaker (Figure 12A). In the Bleomycin time course, the intensity change for both upper and lower bands were following a similar dynamics (Figure 12C). Rqh1 has been reported to undergo SUMOylation, and this modification is enhanced by MMS treatment (Rog et al., 2009; Watts et al., 2007). Intriguingly, Pcf1 harbors two potential SIMs domains (SUMO Interacting Motif) (Figure 13A). Therefore, I have hypothesized that the upper band of Rqh1 could correspond to the SUMOylated form of Rqh1 and that this post translational modification could serve to modulate Pcf1-Rqh1 interaction. To address this hypothesis, a GST-pulldown assay was performed using cells expressing a mutated allele of *rqh1* that impairs SUMOylation (designated as *rqh1-SM-myc*, the strain being a kind gift from Dr. Julia Cooper (Rog et al., 2009)) with or without MMS treatment (Figure 13A and B). However, I found that the pattern of the Rqh1 bands after MMS from the *rqh1-SM-myc* cells was similar to that of the *rqh1-myc* cells, and the intensity of the upper band of Rqh1 remained the same between the mutants and *wild type* cells in all conditions (Figure 13B), suggesting that the upper band is unlikely to correspond to SUMOylated Rqh1.

Nonetheless, our GST-pulldown data do not exclude the possibility that MMS-induced SUMOylation of Rqh1 is involved in Rqh1-Pcf1 interaction, and it would be informative to explore this if a more specific anti-SUMO antibody for fission yeast could be obtained.

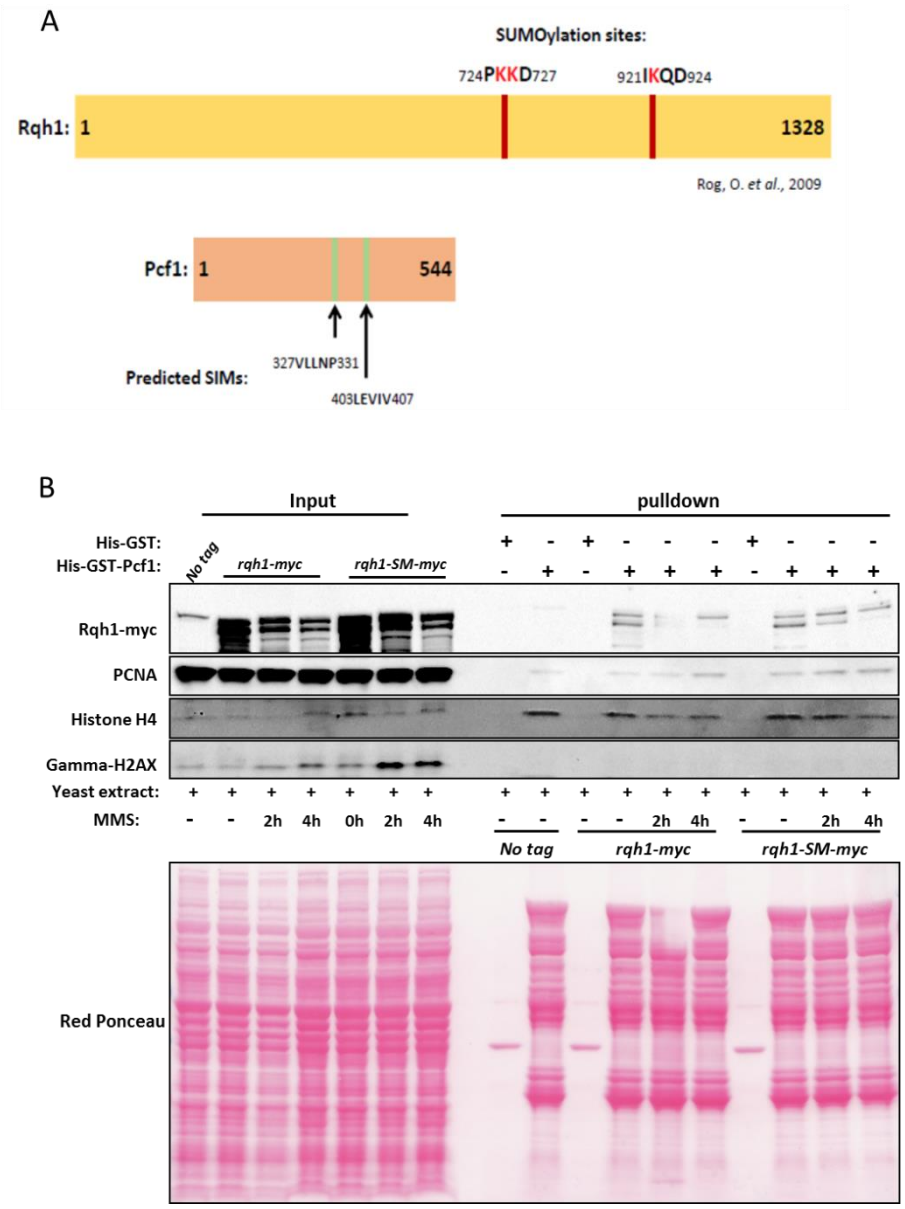

Figure 13. Investigation of the role of SUMOylated Rqh1 in Rqh1-Pcf1 interaction in response to MMS. A. Upper panel: diagram showing the SUMOylation sites on Rqh1. Lower panel: diagram showing predicted SIMs on Pcf1 (prediction by K. Kramarz by using open online prediction resource GPS-SUMO). B. GST-pulldown assay using recombinant Pcf1 and protein extracts from indicated strains. The bands of histone H4 were faint in the input fraction is a consequence of reusing the antibody multiple times. 700 mM NaCl was added to the buffer during the washing steps. *there was a transfer issue during the Western Blot as shown by the red ponceau staining and resulted in a small missing part in the Rqh1 bands.

Altogether, the data obtained so far indicate that DNA damage, induced by MMS and Bleomycin, stimulates the interactions between Rqh1 and Pcf1, but not with Pcf2. The tentative to involve SUMOlyation events in this stimulation has been inconclusive.

1.4. Domain mapping of Pcf1

In light of a previous publication showing that human BLM interacts with p150 directly via the ED domain (Jiao et al., 2004), I have tried to map the Pcf1 domain that promotes interaction with Rqh1 with the aim to generate a loss-of-interaction mutant of *pcf1*. Such a mutant, unable to interact with Rqh1, would be very useful in studying the role of physical interactions between Rqh1 and Pcf1 *in vivo*. The strategy for achieving this goal was first to verify whether Pcf1 directly interacts with Rqh1. Unfortunately, a yeast two-hybrid strategy has been unsuccessful as Rqh1 and Pcf1 were found auto-activating the reporter system. Therefore, a GST-pulldown approach was employed with the expectation to identify the Pcf1 domain required for interacting with Rqh1. In collaboration with Dr. Françoise Ochsenbein, Pcf1 was fragmented into several parts (Figure 14A) that were predicted to have distinct functions. GST-tagged Pcf1 fragments were purified from *E. coli* system (Figure 14B). Since Pcf2 is able to interact with Rqh1, the experiment was performed by incubating recombinant Pc1 fragments with protein extracts from both *rqh1-myc* and *rqh1-myc pcf2-d* cells to avoid any Pcf2-mediated interaction (Figure 14C). The data showed that the fragment 2 (F2), which contains the large ED domain, demonstrated a high affinity for Rqh1 as well as for PCNA and histone H3, which was similar to the full-length Pcf1 (FL). Similar interactions were observed from the *pcf2-d* samples indicating that Pcf2 is not mediating these interactions.

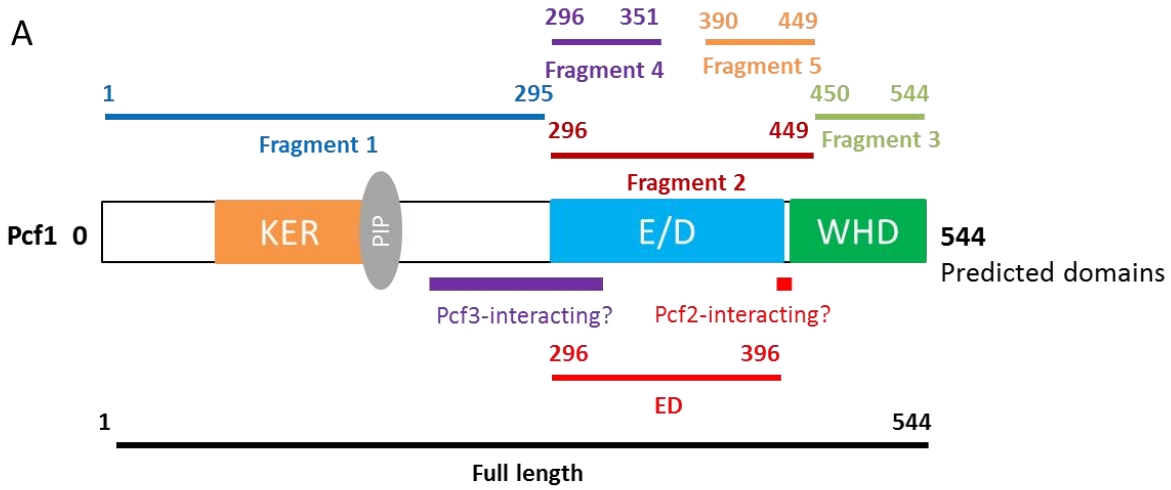
A
296
351
390
449
Fragment 4
Fragment 5
1
295
450
544
296
449
Fragment 1
Fragment 3
Fragment 2
Pcf1 0
KER
PIP
E/D
WHD
544
Predicted domains
Pcf3-interacting?
Pcf2-interacting?
296
396
ED
1
544
Full length

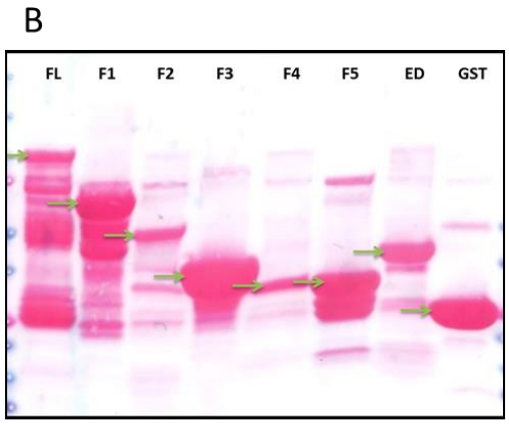
B
FL
F1
F2
F3
F4
F5
ED
GST

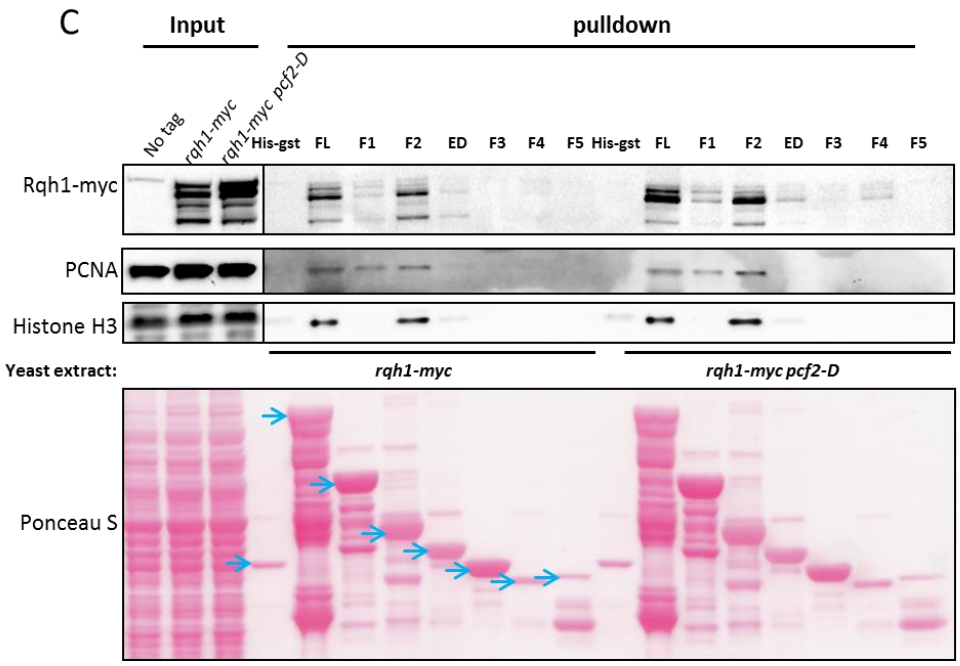
C
Input
pulldown
No tag
rqh1-myc
rqh1-myc pcf2-D
His-gst
FL
F1
F2
ED
F3
F4
F5
Rqh1-myc
PCNA
Histone H3
Yeast extract:
rqh1-myc
rqh1-myc pcf2-D
Ponceau S

Figure 14. Domain mapping of Pcf1. A. Diagram showing fragmentation of Pcf1 based on predicted functional domains. Fragment 1 contains the KER domain which interacts with histones, and the PIP-box which mediates the direct interaction with PCNA. Fragment 2 covers the predicted ED domain, and it is sub-divided into two short domains, fragment 4 and fragment 5. A shorter ED domain is indicated in red and has been used in the GST-pulldown assay. Fragment 3 covers the C-terminus of Pcf1 and might harbor the WHD domain that has been recently characterized in budding yeast. B. Red ponceau showing purified recombinant Pcf1 and its fragments. The corresponding bands are indicated by green arrows. C. GST-pulldown assay using recombinant Pcf1 fragments showing that fragment 2 containing the ED domain demonstrates a high affinity for Rqh1 as well as for PCNA and histone H3. 700 mM NaCl was added to the buffer in the washing steps. The blue arrows indicate the corresponding bands to each recombinant fragment of Pcf1. The amount of GSH-beads bound by the recombinant fragments used in each sample was calculated in a way that the same molecular number of each fragment was applied to each sample with equal amount of cell extracts.

It was encouraging to observe that the ED domain has high affinity for Rqh1, as observed in mammalian cells. Nonetheless, the ability of the ED domain to pulldown PCNA was unexpected. However, the ED domain is a highly acidic domain and might mediate nonspecific interactions.

In order to find an alternative approach to probe for direct interactions between Pcf1 and Rqh1, we decided to generate recombinant Pcf1 and Rqh1 in baculovirus expression system from the Recombinant protein platform of the Institut Curie. If this approach succeeded, we could then test if these two recombinant proteins directly interact. I have constructed the expression plasmids and sent them to the platform for protein production. The plasmids were successfully transfected and expressed (data not shown). However, when trying to purify the proteins in large scale, an unexpected protein degradation problem occurred and led to insufficient protein yielding. The platform has further tried to perform a double purification but failed. Therefore, without further evidences of direct interactions between Rqh1 and Pcf1, this research path was difficult to conduct further with the final aim to identify loss-of-interaction mutants.

2. Characterization of CAF-1 association to chromatin upon replication stress

CAF-1 promotes chromatin restoration during DNA repair and replication (Gaillard et al., 1996; Polo et al., 2006a; Smith and Stillman, 1989; Tyler et al., 1999). In the scenario of replication fork-restart by the recombination-dependent replication (RDR) pathway, CAF-1 has been shown to promote RDR via its ability to interact with PCNA and via histone deposition (Pietrobon et al., 2014, Hardy et al., publication in preparation, see annexe 1). To place CAF-1 within the network of proteins involved in DNA repair in response to replication stress, there is a need for an assay that could give the information on the dynamics of the binding of CAF-1 to chromatin and the genetic dependency of this association to chromatin. To this end, the team has first started with performing chromatin fraction assays. However, CAF-1 is a scarce complex (500-900 molecules/cells) (Carpy et al., 2014) and is thus difficult to be detected in the total fraction. Furthermore, it was technically difficult to generate good-quality chromatin fractions when working in recombination defective genetics backgrounds. Therefore, an alternative approach was required. I have developed an *in vivo* chromatin binding assay based on the method described by Kearsay et al. (Kearsey et al., 2005). This assay allows to monitor and to quantify the genome-wide association of CAF-1 to chromatin in response to various genotoxic agents.

2.1. Development of an *in vivo* chromatin binding assay

According to the data obtained from chromatin fraction assay (generated by Julien Hardy in the team), Pcf1 was found more associated to the chromatin after 2 hours of 0.03% MMS treatment (an alkylating agent resulting in damaged replication forks), but not after Bleomycin treatment (a double strand break-inducing drug) or after HU treatment (an inhibitor of the ribonucleotide reductase that results in stalled replication forks) (Figure 15A). Furthermore, the amount of Pcf1 in the chromatin fraction kept increasing up to 4 h after MMS treatment and this association to chromatin was concomitant with PCNA binding to chromatin (Figure 15B).

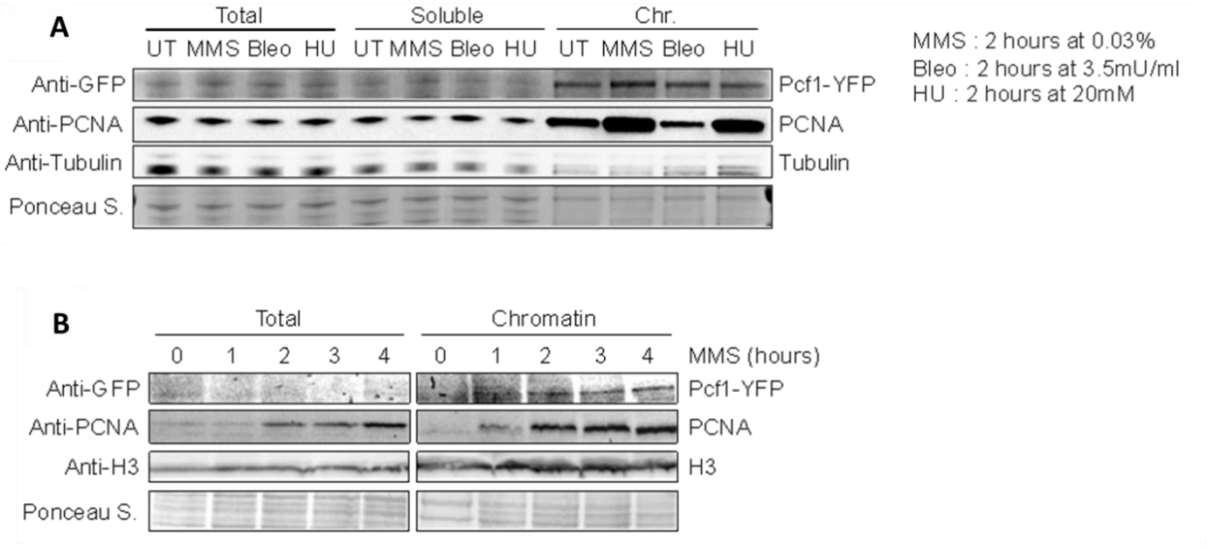

Figure 15. MMS treatment stimulates the association of Pcf1 to the chromatin A. Chromatin fraction assay showing chromatin-associated Pcf1-YFP in indicated conditions. B. Chromatin fraction assay showing the kinetics of chromatin-associated Pcf1-YFP in response to 0.03% MMS.

Based on these observations, I chose 3 hours of MMS treatment to first optimize the chromatin binding assay using a strain expressing the fusion protein Pcf1-GFP (Kunoh and Habu, 2014). The assay was carried out by following the previously described protocol (see in the **Materials and methods chapter**) (Kearsey et al., 2005). This protocol is based on the detection of nuclear fluorescence signal after partial digestion of the cell wall followed by the removal of the soluble fraction using triton extraction or not. The results showed that without triton extraction (thereafter, samples without triton extraction will be referred to as -T), both MMS-treated and untreated cells harbored comparable levels of nuclear Pcf1-GFP signals (Figure 16). In the same experiment, I have also included an untagged strain which served as a negative control showing very low level of GFP signal in any condition, indicating that the positive signals observed from the *pcf1-GFP* cells are indeed reflecting Pcf1-GFP. Upon triton extraction (thereafter samples with triton extraction will be referred to as +T) which removes the soluble protein fraction to reveal the protein fraction associated to the chromatin, the nuclear Pcf1-GFP signal from untreated cells was largely decreased (by nearly 9 fold) compared to the -T counterparts. These data indicate that a major part of Pcf1 pool is soluble and only a minor fraction is chromatin-associated in untreated cells. Upon MMS treatment, the nuclear Pcf1-GFP signal was unaffected in -T condition and was reduced by ~ 4.4 fold by triton extraction. Compared to untreated cells, the chromatin-bound fraction of Pcf1 was found increased by ~ 2 fold (Figure 16 and 17B).

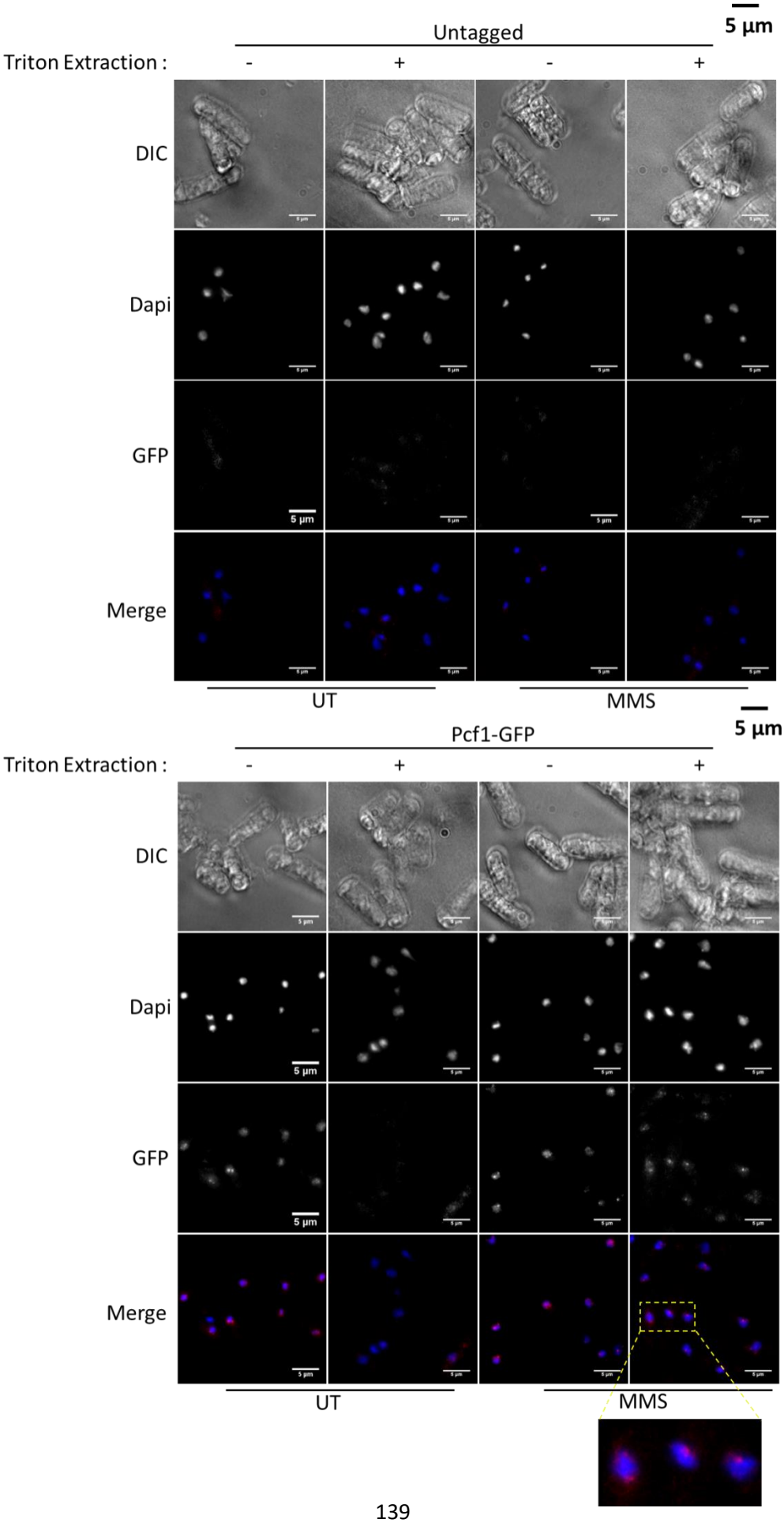
5 µm
Untagged
Triton Extraction :
-
+
-
+
DIC
Dapi
GFP
Merge
5 µm
UT
MMS
5 µm
Pcf1-GFP
Triton Extraction :
-
+
-
+
DIC
Dapi
GFP
Merge
5 µm
UT
MMS

Figure 16. Representation of *in vivo* chromatin binding assay performed on cells expressing Pcf1-GFP or not (untagged). The scale bar in black on top of each figure is the same as the scale bar in each microscopy image. Cells were treated with 0.03% MMS for 3 hours. Untagged cells were included as negative control.

The average nuclear Pcf1-GFP signal from this chromatin binding assay was analyzed as described in the **Materials and Methods chapter**, and plotted in arbitrary unit (a.u.) normalized to nucleus area and cytoplasmic signal (Figure 17A and B). The scatter plots of +T samples clearly showed that MMS treatment led to twice more chromatin-bound Pcf1-GFP compared to untreated cells, showing that damaged replication forks promote Pcf1 association to chromatin.

In addition, I have quantified the percentage of cells showing Pcf1-GFP staining after triton extraction. This analysis showed that in untreated condition only about 15% of the cells contain nuclear Pcf1-GFP foci, while MMS treatment resulted in more than 75% of the cells containing nuclear Pcf1-GFP foci (Figure 17C).

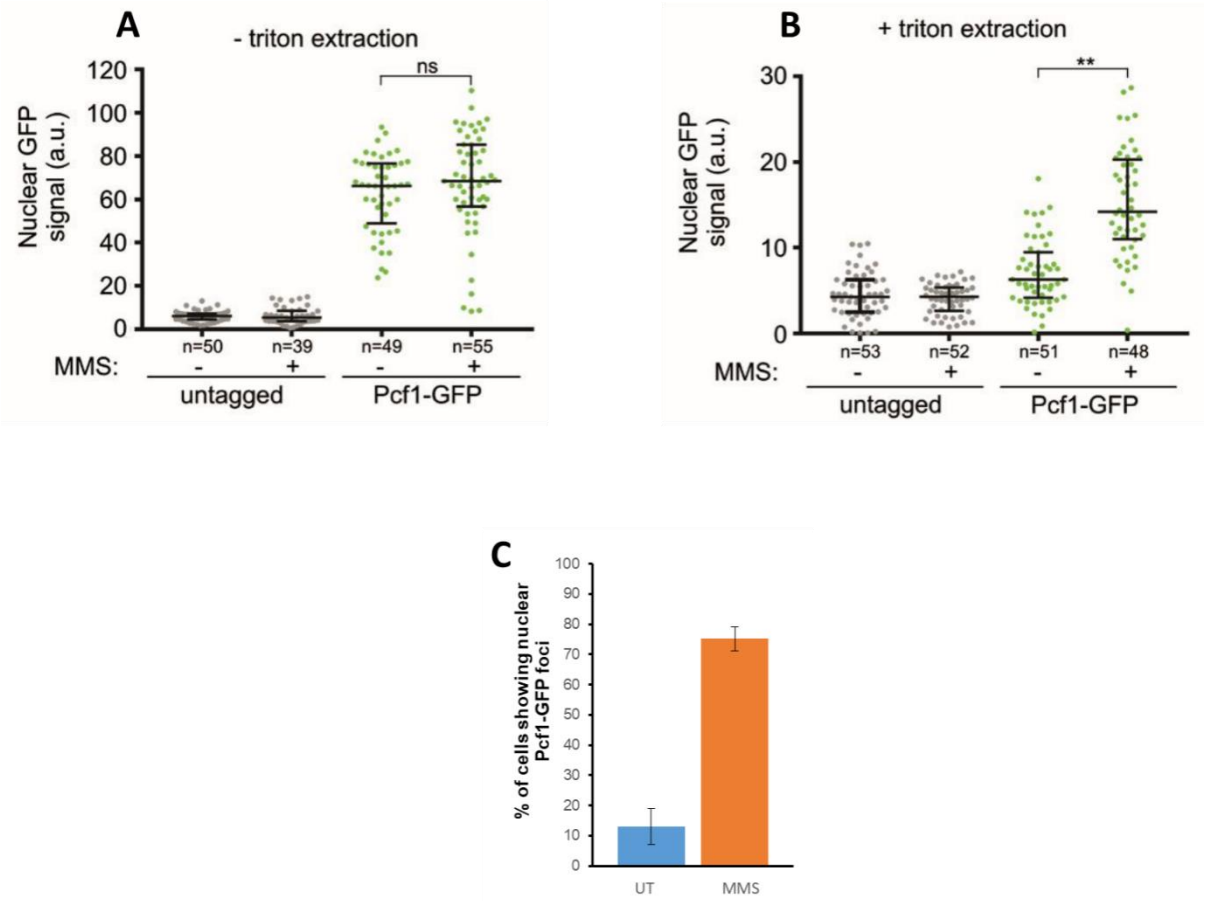

Figure 17. The *in vivo* chromatin binding assay reveals the chromatin-bound Pcf1 fraction which increases after MMS treatment. A. and B. Quantification of nuclear GFP signal in arbitrary unit (a.u.) normalized to nucleus area and cytoplasmic signal. Quantification bars indicate the median and interquartile, n indicates the

number of cell analyzed. Statistical analysis was performed by using Mann & Whitney U test. ** indicates p<0.0001. C. Quantification of % of cells showing nuclear Pcf1-GFP foci after triton extraction in indicated conditions. Values are means of two independent experiments ± standard deviation (SD). More than 50 cells were analyzed for each condition in each experiment.

This experiment has been reproduced in the same condition for more than 3 times resulting in consistent observations. Therefore, I have successfully developed an assay to monitor and quantify Pcf1 association to the chromatin after the removal of soluble fraction by triton extraction.

2.2. Pcf1 and Pcf2 associate to chromatin upon replication stress but not Pcf3

After setting up the *in vivo* chromatin binding assay for Pcf1-GFP, I have investigated whether the two other subunits of CAF-1, Pcf2 and Pcf3 also associate to chromatin upon replication stress. To this end, I have constructed strains expressing Pcf2-GFP or Pcf3-GFP. Like for *pcf1-GFP* strain, the function of GFP-tagged Pcf2 was also evaluated by synthetic lethality assay with *hip1-d* (Figure 18). Genetics analysis showed that the deletion of *pcf2*, but not pcf2-GFP, is synthetic lethal with the deletion of *hip1*, indicating that the fusion protein Pcf2-GFP is functional. The synthetic lethality assay will also be performed on cells expressing Pcf3-GFP in the future.

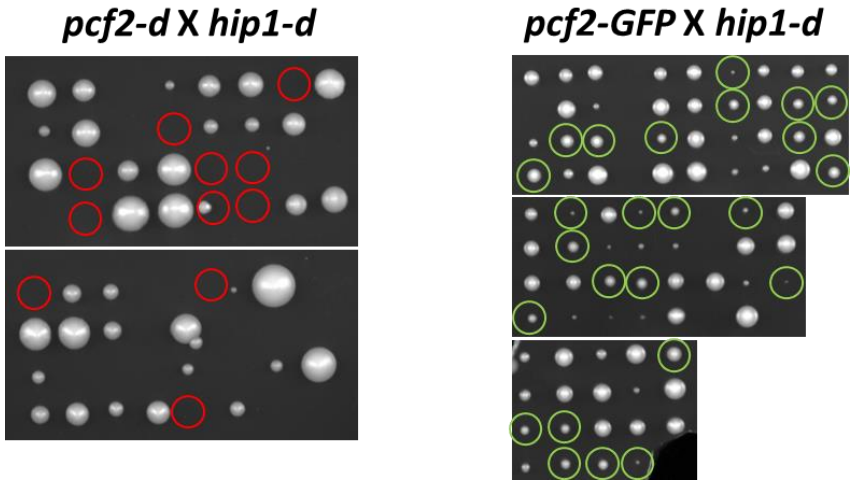

Figure 18. Synthetic lethality between *pcf2* or *pcf2-GFP* and *hip1-d*. Left panel: tetrads from the cross between *pcf2-d* and *hip1-d* strains are represented. Red circles indicate *pcf2-d hip1-d* spores that were unviable. 64 spores from 16 tetrads were analyzed. Right panel: tetrads from the cross between *pcf2-GFP* and *hip1-d* strains are represented. Green circles indicate *pcf2-GFP hip1-d* spores that were viable. 88 spores from 22 tetrads were analyzed.

The strains expressing either Pcf2-GFP or Pcf3-GFP were subjected to the *in vivo* chromatin binding assay, in the same conditions, in untreated conditions or after 3 hours of MMS

treatment (Figure 20). The results of this assay showed that the three CAF-1 subunits behave differently. In contrast to Pcf1-GFP (Figure 19), the total Pcf2-GFP nuclear signal was found increased after MMS treatment (Figure 20A and 21A). As reported for Pcf1-GFP, the chromatin-bound fraction of Pcf2-GFP was increased by nearly two fold after MMS treatment (Figure 20A, 21B and C). Another behavior was found for Pc3-GFP. The total nuclear signal was increased after MMS treatment but none of this staining was resistant to triton extraction (Figure 20B, 21A and B). Thus, in contrast to Pcf1-GFP and Pcf2-GFP, MMS treatment did not promote the association of Pcf3 to the chromatin (Figure 21C). Triton extraction revealed that Pcf1 and Pcf2 were bound to the chromatin in response to 3 hours of MMS treatment, while there was no Pcf3 fraction associated to the chromatin in the same conditions (Figure 21B). Finally, the fold enrichment of chromatin-bound signal was calculated and plotted in the column chart (Figure 21C) which demonstrated that 3 hours of MMS treatment induces about two fold enrichment of chromatin-associated Pcf1 and Pcf2, while barely no enrichment for Pcf3. These data reveal that the three subunits of CAF-1 exhibit distinct properties regarding their ability to associate to chromatin in response to MMS.

Interestingly, the total GFP signal of Pcf2 and Pcf3, but not Pcf1, is increased after MMS treatment (Figure 21A). The explanation of this observation could be that MMS treatment stimulates the expression of Pcf2 and Pcf3, or affect protein folding of the tagged proteins. A future TCA extraction should be performed on these strains with or without MMS treatment to test whether MMS treatment stimulates the expression of each CAF-1 subunit.

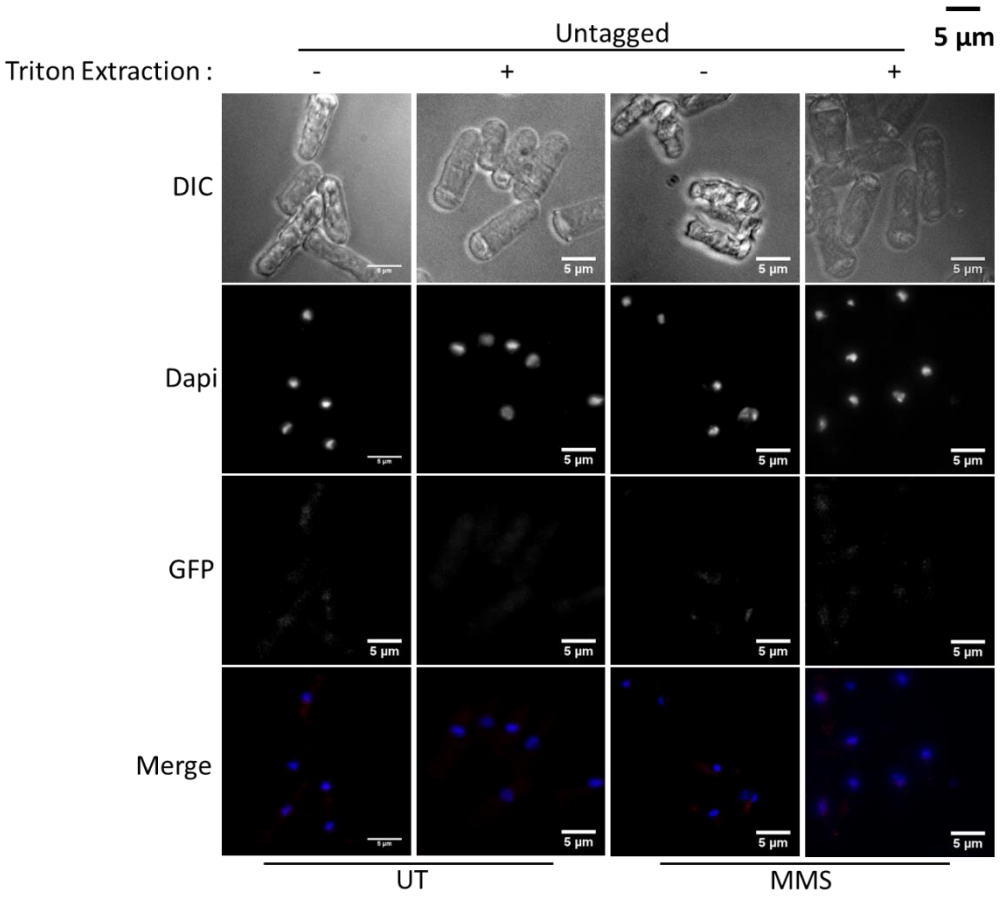
Untagged
5 µm
Triton Extraction :
-
+
-
+
DIC
Dapi
GFP
Merge
5 µm
UT
MMS

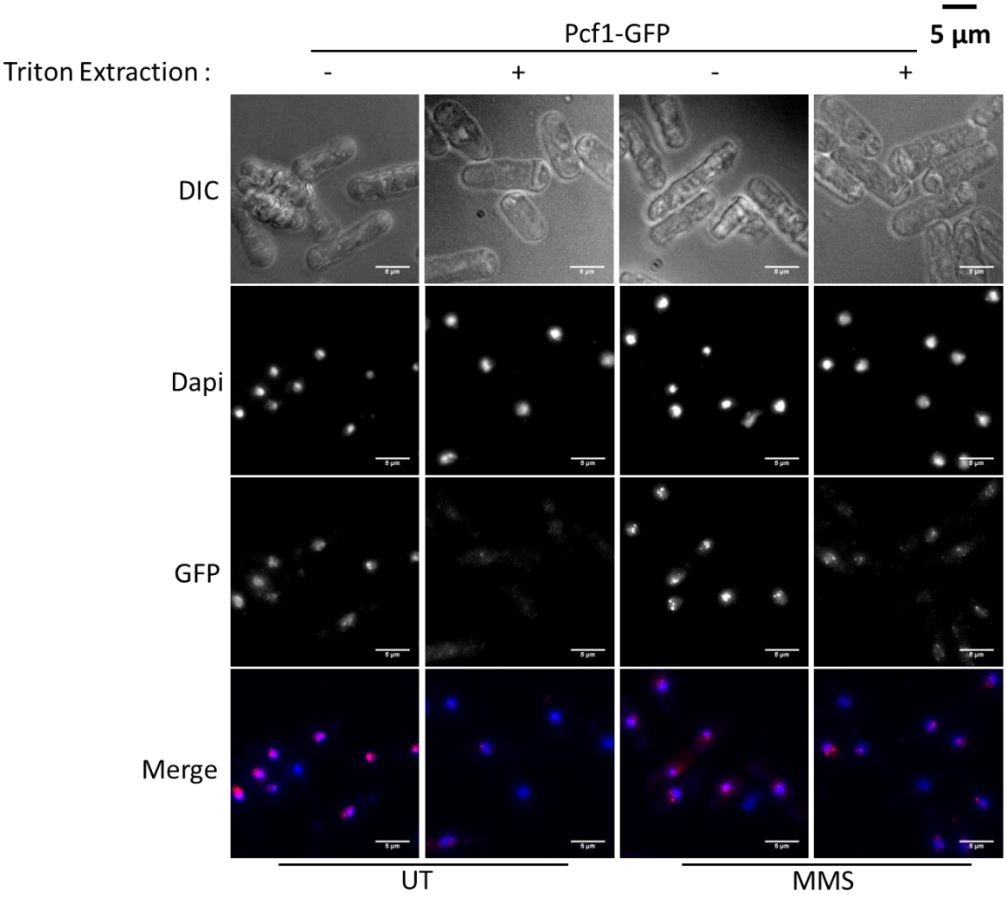
Pcf1-GFP
5 µm
Triton Extraction :
-
+
-
+
DIC
Dapi
GFP
Merge
UT
MMS

Figure 19. Representation of *in vivo* chromatin binding assay performed on cells expressing Pcf1-GFP or not (untagged). The scale bar in black on top of each figure is the same as the scale bar in each microscopy image. Cells were treated with 0.03% MMS for 3 hours. Untagged cells were included as negative control.

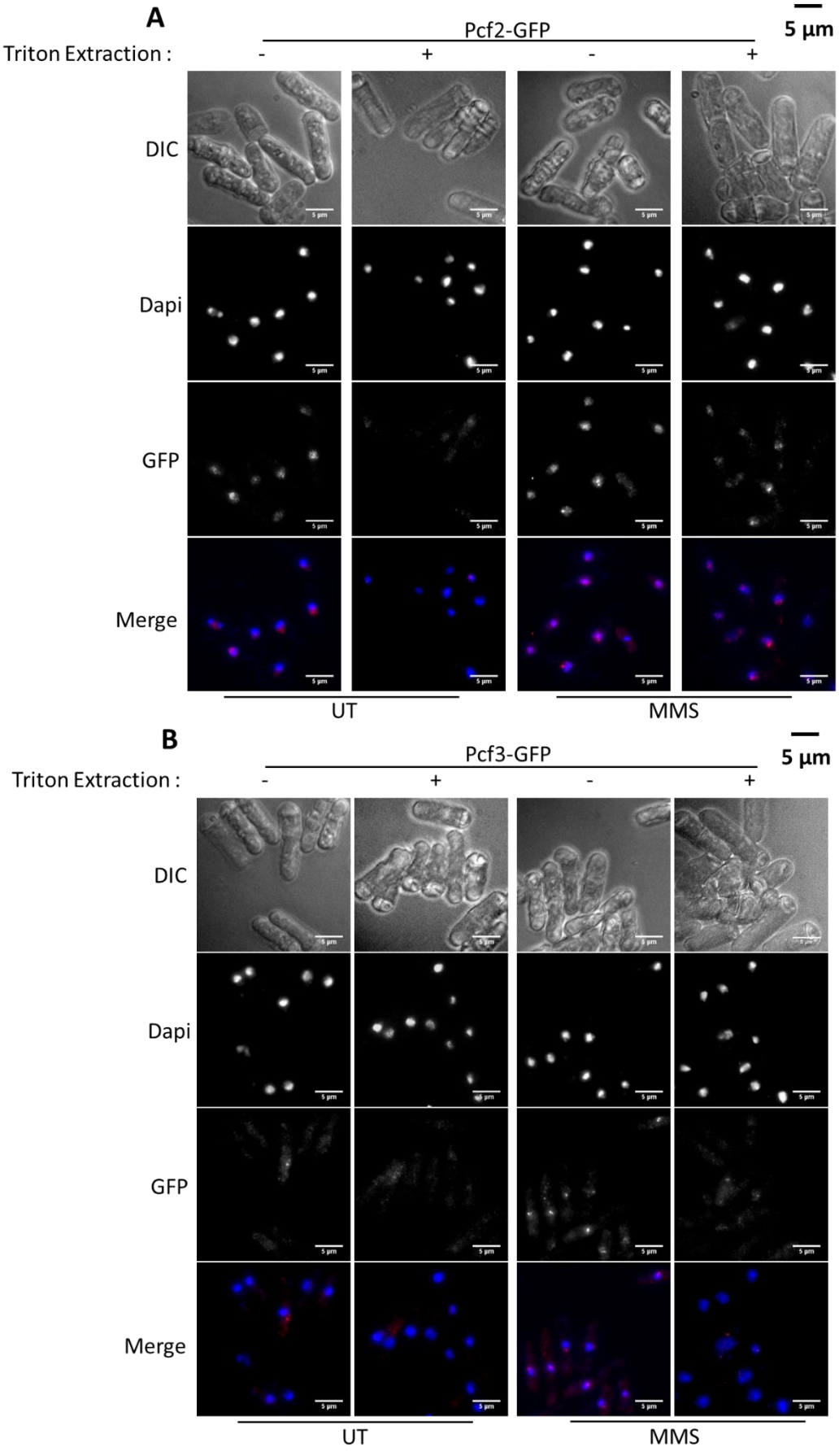
A
Pcf2-GFP
5 µm
Triton Extraction :
-
+
-
+
DIC
Dapi
GFP
Merge
UT
MMS
B
Pcf3-GFP
5 µm
Triton Extraction :
-
+
-
+
DIC
Dapi
GFP
Merge
UT
MMS

Figure 20. Representation of *in vivo* chromatin binding assay performed on cells expressing Pcf2-GFP or Pcf3-GFP. A. Chromatin binding assay performed on cells expressing Pcf2-GFP. B. Chromatin binding assay performed on cells expressing Pcf3-GFP. The scale bar in black on top of each figure is the same as the scale bar in each microscopy image. Cells were treated with 0.03% MMS for 3 hours.

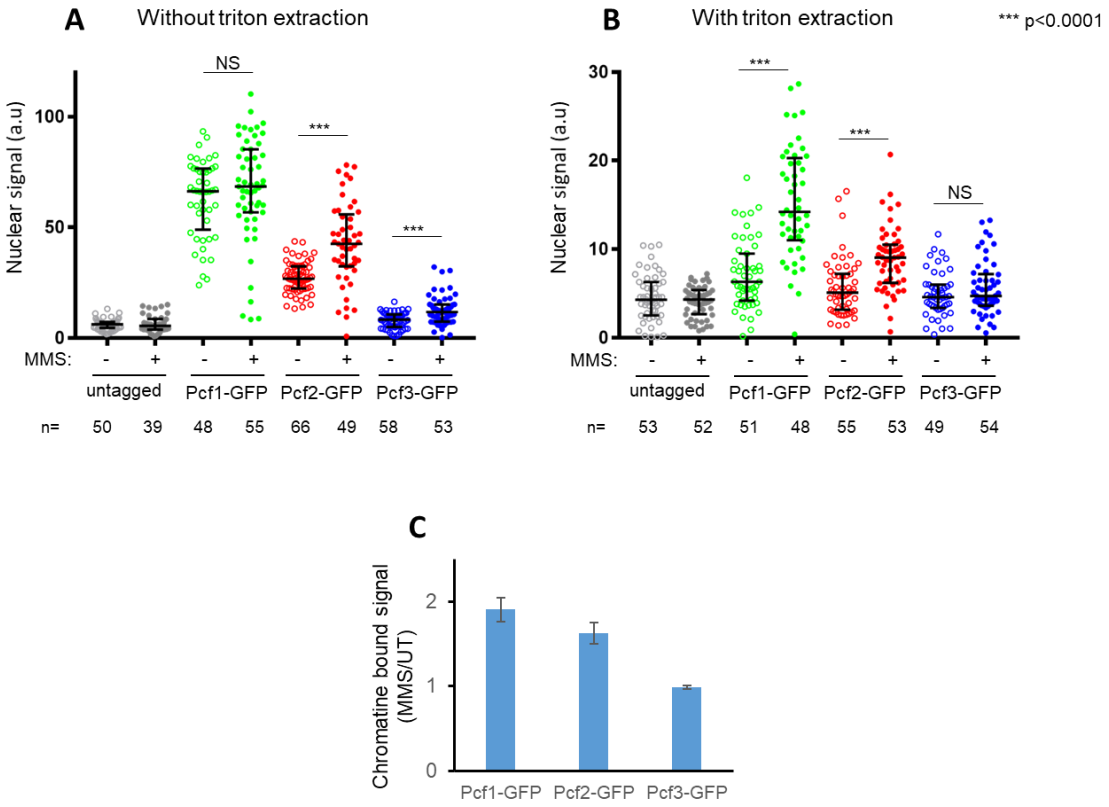

Figure 21. Pcf1 and Pcf2 associate with chromatin upon replication stress but not Pcf3. A and B. Quantification of nuclear GFP signal in arbitrary unit (a.u.) normalized to nucleus area and cytoplasmic signal. Quantification bars indicate the median and interquartile, n indicates the number of cell analyzed. Statistical analysis was performed by using Mann & Whitney U test. C. Fold enrichment of GFP nuclear staining associated to the chromatin upon MMS treatment in indicated strains. Values are means of three independent experiments ± standard deviation (SD).

2.3. Kinetics of Pcf1 and Pcf2 association to chromatin upon MMS treatment

The data obtained so far indicate that the 3 subunits of CAF-1 exhibit different properties regarding their association to the chromatin, in response to 3 hours of MMS treatment. In order to confirm these data, I have performed time course experiments to address the kinetics of chromatin association for each CAF-1 subunits (Figure 22, 23 and 24). The chromatin-bound fraction of Pcf1-GFP was found to increase significantly from 1 hour to 4 hours of MMS treatment, with a peak of nearly two-fold enrichment between 2-3 hours (Figure 22 and 25A). The amount of chromatin-associated Pcf2-GFP was found significantly increased from 2 to 4

hours of MMS treatment, with a peak of enrichment between 3 to 4 hours (Figure 23 and 25B). In contrast, the chromatin-bound fraction of Pcf3 was found unaffected throughout the time course (Figure 24 and 25C). The fold-change in the chromatin-bound fraction of the three CAF-1 subunits during the time course showed that, upon MMS treatment, the amount of chromatin-associated Pcf1 reached a peak between 2 h and 3 h, the amount of chromatin-associated Pcf2 reached a peak about 1 h later than Pcf1, whereas no enrichment of chromatin-associated Pcf3 was observed (Figure 25D).

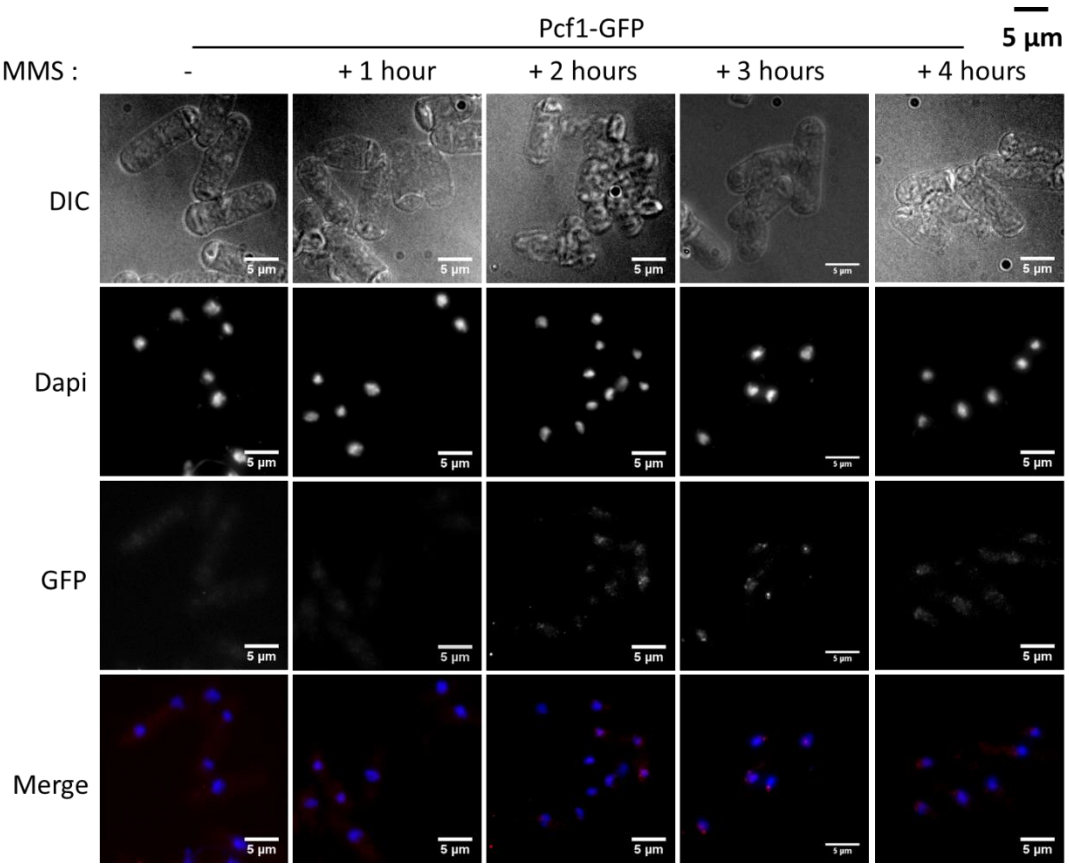

Figure 22. Representation of the kinetics of chromatin associated Pcf1-GFP in response to MMS treatment. Cells were treated with 0.03% MMS for indicated time. The scale bar in black on top of each figure is the same as the scale bar in each microscopy image.

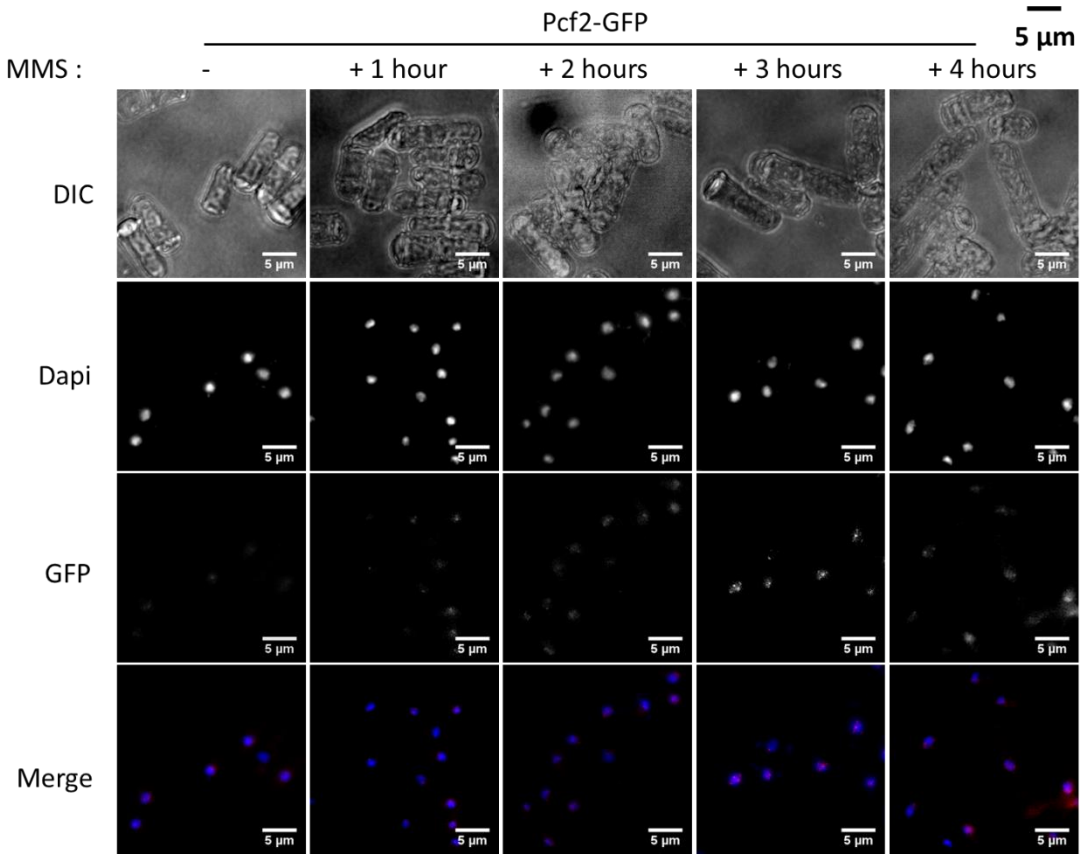

Figure 23. Representation of the kinetics of chromatin associated Pcf2-GFP in response to MMS. Cells were treated with 0.03% MMS for indicated time. The scale bar in black on top of each figure is the same as the scale bar in each microscopy image.

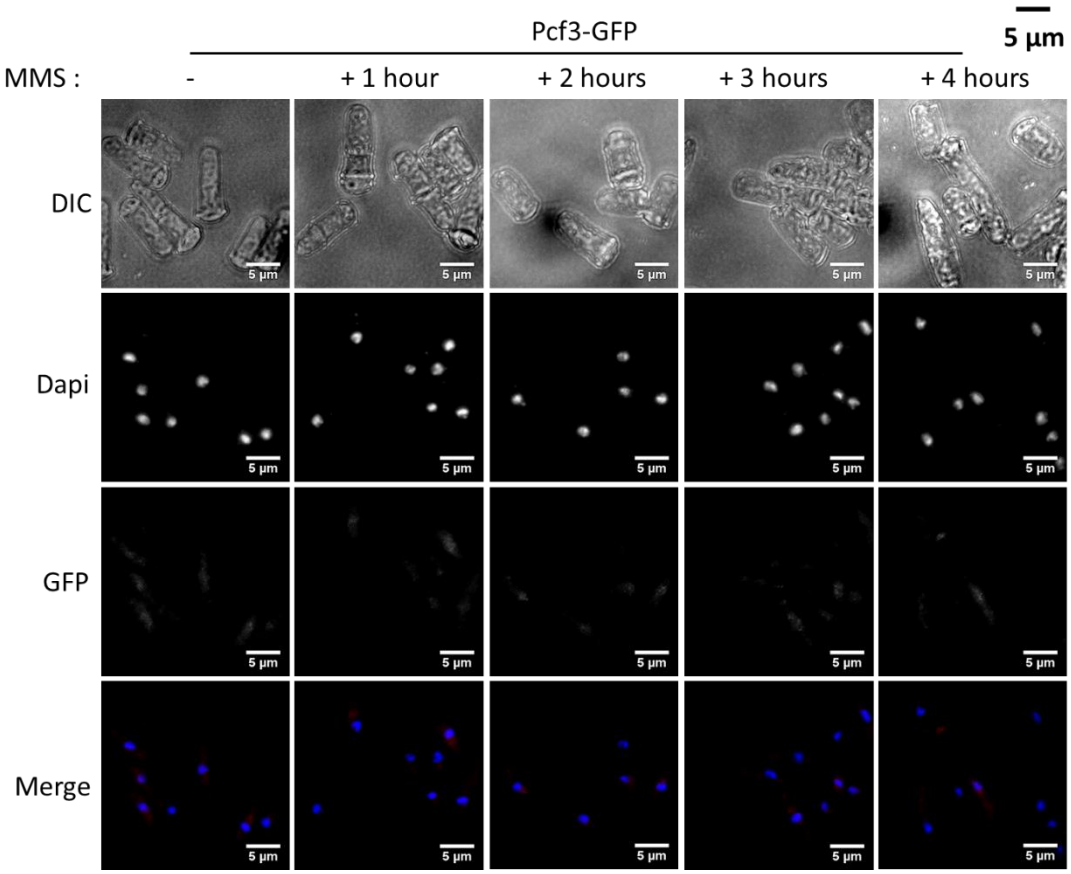

Figure 24. Representation of the kinetics of chromatin associated Pcf3-GFP in response to MMS. Cells were treated with 0.03% MMS for indicated time. The scale bar in black on top of each figure is the same as the scale bar in each microscopy image.

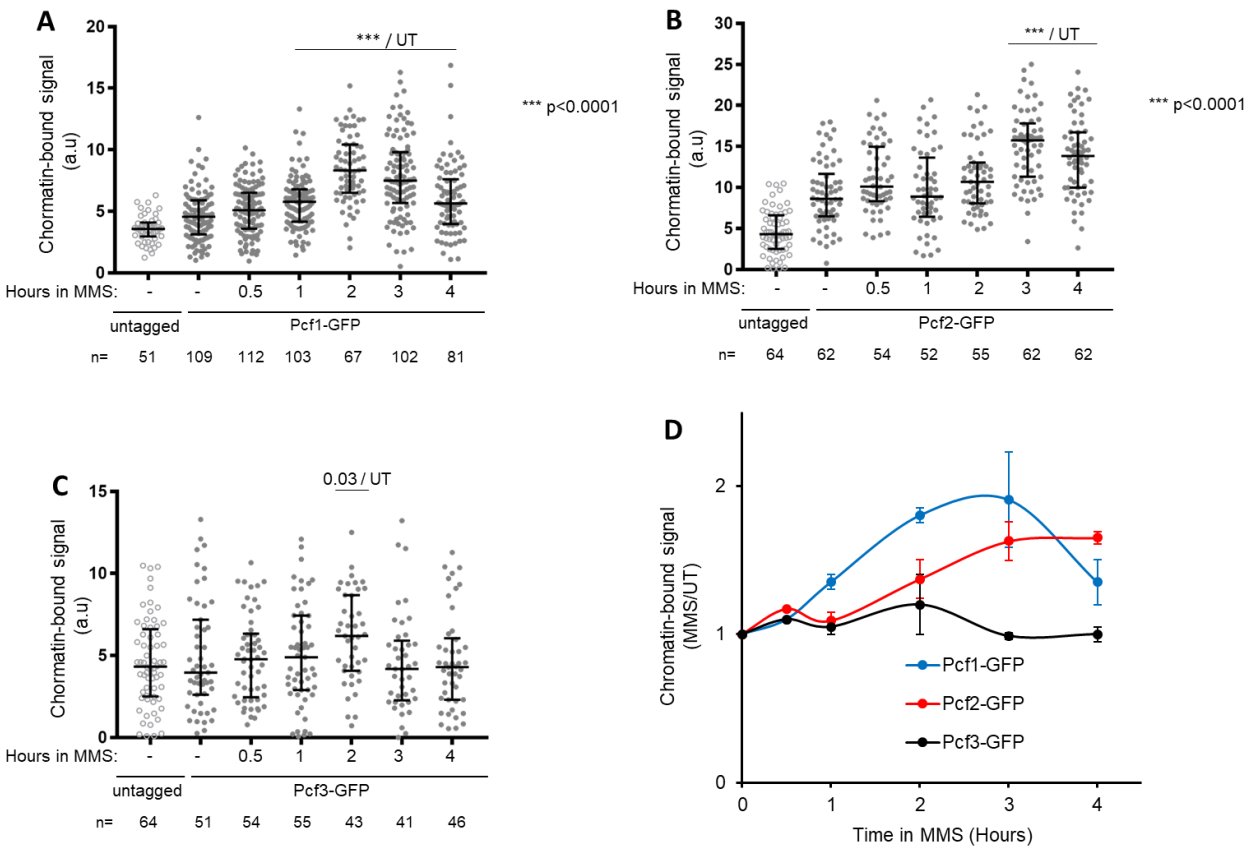

Figure 25. Pcf1 and Pcf2, but not Pcf3, associate to chromatin upon MMS treatment. A, B and C. Quantification of the chromatin-associated GFP signal in arbitrary unit (a.u.) normalized to nucleus area and cytoplasmic signal in indicated strains and conditions. Quantification bars indicate the median and interquartile, n indicates the number of cell analyzed. Statistical analysis was performed by using Mann & Whitney U test. D. Fold enrichment of chromatin-bound GFP staining upon MMS treatment in indicated strains. Values are means of more than two independent experiments ± standard deviation (SD).

Altogether, these data further confirm that the 3 subunits of CAF-1 behave differently in response to MMS treatment with Pcf1 and Pcf2 being associated to chromatin, but not Pcf3. The data also reveal that the association to the chromatin of Pcf1 and Pcf2 follows distinct kinetics, with Pcf1 being chromatin-bound earlier than Pcf2. The underlying mechanisms of such discrepancy were further explored by asking the inter-dependency of Pcf1 and Pcf2 association to chromatin.

Thus, I conclude that replication stress induced by MMS leads to the association of two CAF-1 subunits, Pcf1 and Pcf2, to the chromatin. Notably, in contrast to Pcf1 and Pcf2, the small CAF-1 subunit Pcf3 is not associated to the chromatin after MMS treatment.

2.4. Pcf1 does not associate to chromatin in response to double strand break induction

Then, I asked if the association of CAF-1 to the chromatin can be stimulated by other type of DNA damage than MMS. I have employed Bleomycin, a double strand break-inducing agent and tested if Bleomycin treatment induces Pcf1-GFP association to chromatin using the *in vivo* chromatin binding assay. Similar to the treatment of 0.03% MMS, DNA damage was induced by the treatment of 10mU/mL Bleomycin, as revealed by the level of phospho-H2A (the equivalent of mammalian Gamma-H2AX) detected by Western Blot (Figure 26D). In -T samples, 3 hours of Bleomycin treatment slightly stimulated (by around 1.15 fold) the total nuclear Pcf1-GFP signal (Figure 26 A and B). In contrast to MMS treatment, no increase in the chromatin-bound fraction was observed in response to Bleomycin whatever the time of the treatment (Figure 26 A and B). The scatter plots of a Bleomycin time course clearly demonstrated that there was no enrichment of chromatin-bound Pcf1 after Bleomycin treatment (Figure 26B). A comparison of the enrichment in chromatin-bound Pcf1-GFP from Bleomycin-treated cells and MMS-treated cells was displayed in a line chart (Figure 26C).

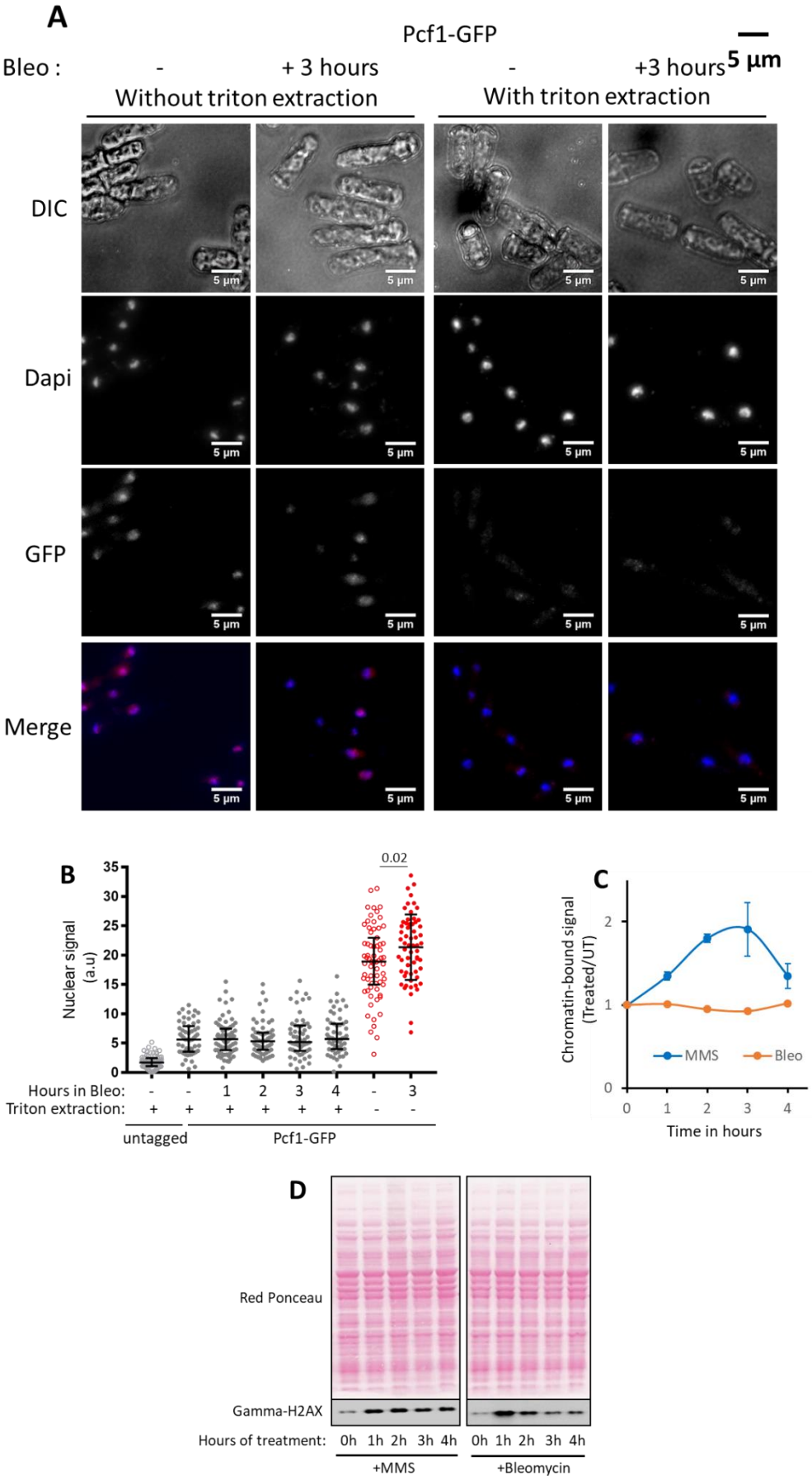
A
Pcf1-GFP
5 µm
Bleo :
-
+ 3 hours
-
+3 hours
Without triton extraction
With triton extraction
DIC
Dapi
GFP
Merge
B
0.02
Nuclear signal (a.u)
Hours in Bleo:
Triton extraction:
untagged
Pcf1-GFP
C
Chromatin-bound signal (Treated/UT)
MMS
Bleo
Time in hours
D
Red Ponceau
Gamma-H2AX
Hours of treatment:
0h 1h 2h 3h 4h
+MMS
+Bleomycin

Figure 26. Global DSBs do not stimulate Pcf1 binding to chromatin. A. Representation of chromatin binding assay performed on cells expressing Pcf1-GFP. Cells were treated with 10mU/mL Bleomycin for 1, 2, 3 and 4 hours. B. Quantification of nuclear Pcf1-GFP signal in arbitrary unit (a.u.) normalized to nucleus area and cytoplasmic signal. Quantification bars indicate the median and interquartile, n indicates the number of cell analyzed. Statistical analysis was performed by using Mann & Whitney U test. C. Fold enrichment of Pcf1-GFP nuclear staining in MMS- and Bleomycin-treated cells, respectively. Values for MMS-treated cells are means of three independent experiments ± standard deviation (SD). D. DNA damage induced by MMS treatment and Bleomycin treatment after indicated time is indicated by the level of phosphor-H2A, an equivalent of the mammalian gamma-H2AX.

Therefore, these data indicate that MMS treatment that induces damaged replication forks, and thus replication stress, promotes CAF-1 association to chromatin, but not double strand breaks.

2.5. MMS-induced chromatin-binding of Pcf1 does not require Pcf2 whereas MMS-induced chromatin-binding of Pcf2 requires Pcf1

Pcf1 interacts with Pcf2 within the CAF-1 complex, and Pcf1 associates to damaged chromatin before Pcf2. Therefore, it is intriguing to speculate that the chromatin-associated Pcf1 might serve as a scaffold for the subsequent binding of Pcf2. To test this, I have addressed the role of Pcf2 in Pcf1 association to chromatin, and *vice et versa*, in both untreated and MMS-treated conditions. The result of -T samples showed that the total Pcf1-GFP nuclear signal was decreased in the absence of Pcf2 (*i.e.* in *pcf2* deleted cells, *pcf2-d*) in untreated conditions (Figure 27 and 28A). Nonetheless, the chromatin-bound fraction (+T) of Pcf1-GFP was only slightly reduced in *pcf2-d* cells (Figure 27 and 28B). To quantify these data, the level of chromatin-bound Pcf1-GFP in *pcf2-d* cells was normalized to *wild type* level (100 %) in untreated conditions: the chromatin-bound Pcf1-GFP fraction was reduced by only 20 % in the absence of Pcf2 (Figure 28C).

In response to MMS treatment, the chromatin-bound fraction of Pcf1-GFP increased both in *wild type* and in *pcf2-d* cells. To quantify these data, the level of MMS-induced chromatin-bound Pcf1-GFP in *pcf2-d* cells was normalized to the *wild type* level upon MMS treatment (Figure 28C). The chromatin-bound Pcf1-GFP fraction is enriched by nearly two fold in *wild type* strain (Figure 21C) and this two-fold enrichment is normalized to 100%. This analysis showed that MMS treatment stimulated better the association of Pcf1 to the chromatin in the absence of Pcf2 than in *wild type* cells. Therefore, these data indicate that Pcf1 is able to associate to the chromatin without Pcf2, even in response to damaged replication forks and that Pcf2 might play a regulatory role in fine-tuning the amount of Pcf1 associated to the chromatin.

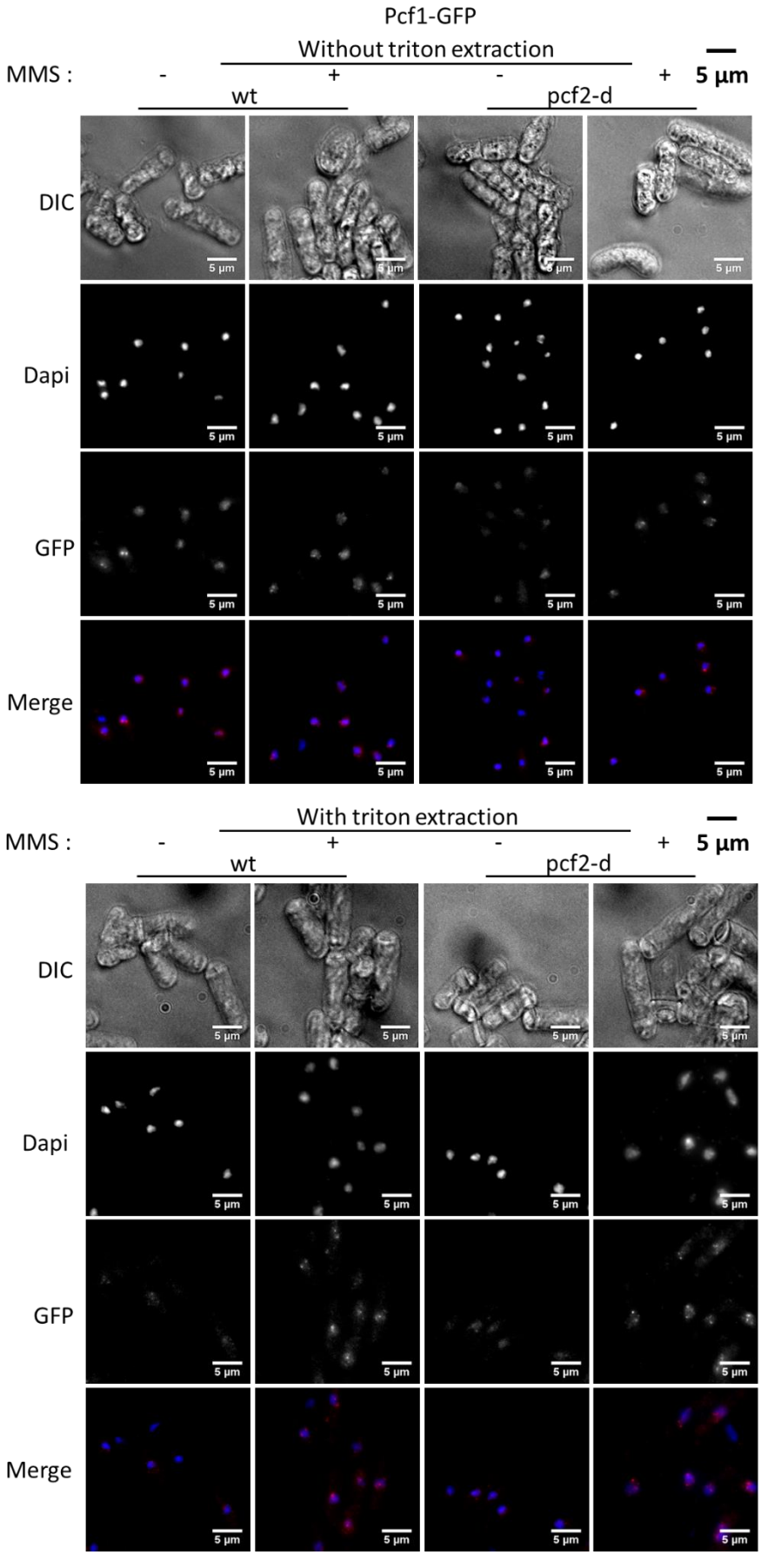
Pcf1-GFP
Without triton extraction
MMS :
-
+
-
+
5 µm
wt
pcf2-d
DIC
Dapi
GFP
Merge
5 µm
With triton extraction
MMS :
-
+
-
+
5 µm
wt
pcf2-d
DIC
Dapi
GFP
Merge
5 µm

Figure 27. Representation of chromatin binding assay performed in cells expressing Pcf1-GFP in indicated strains. The scale bar in black on top of each figure is the same as the scale bar in each microscopy image. Cells were treated with 0.03% MMS for 3 hours.

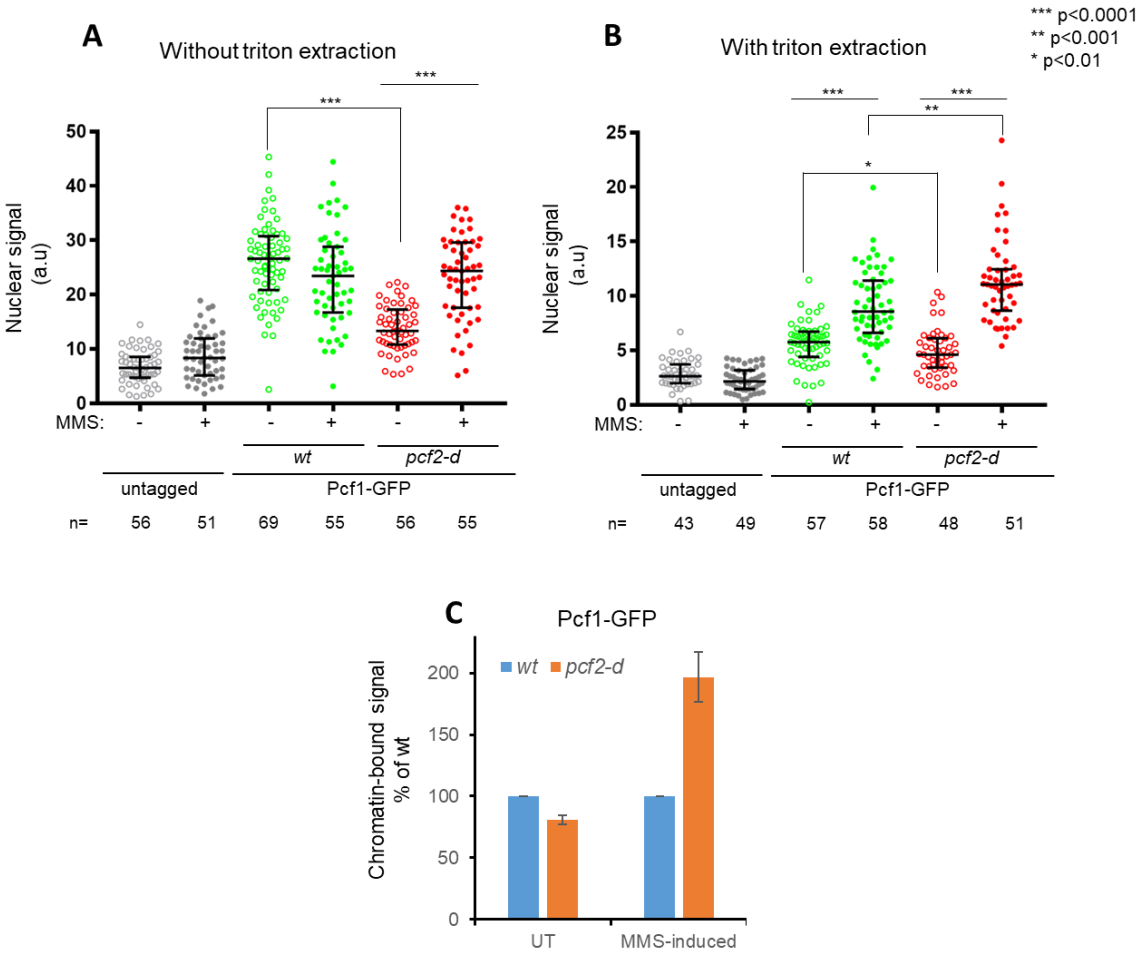

Figure 28. Pcf1 associates to chromatin independently of Pcf2 in both untreated and MMS-treated conditions. A and B. Quantification of nuclear Pcf1-GFP signal in arbitrary unit (a.u.) normalized to nucleus area and cytoplasmic signal. Quantification bars indicate the median and interquartile, n indicates the number of cell analyzed. Statistical analysis was performed by using Mann & Whitney U test. C. Histograms showing % of chromatin-bound signal of Pcf1-GFP normalized to *wild type* level in both untreated (UT) and MMS-induced conditions. Values are medians of at least two independent experiments ± standard deviation (SD). For example, the values for **UT *pcf2-d*** on the chart represent the % of chromatin-bound Pcf1 relative to *wild type* level which is normalized to 100%. The values for **MMS-induced *pcf2-d*** represents the % of MMS-induced chromatin-bound Pcf1 relative to the level observed in *wild type* cells upon MMS treatment and that is normalized to 100 %.

Then, I have asked if the association of Pcf2 to the chromatin depends on Pcf1 (Figure 29A). The result showed that the association of Pcf2-GFP to the chromatin was decreased by only ~ 20 % in untreated conditions in the absence of Pcf1 (*i.e.* in *pcf1* deleted cells, *pcf1-d*). Interestingly, the

absence of Pcf1 severely decreased the chromatin-bound fraction of Pcf2 in response to MMS treatment (Figure 29B). These data indicate that Pcf2 can associate to the chromatin independently of Pcf1 in unchallenged conditions, but Pcf1 becomes indispensable to stable association of Pcf2 to the chromatin upon MMS. Pcf1 might be required for stabilizing chromatin-associated form of Pcf2. The binding of Pcf1 to the chromatin is likely to be a prerequisite for the subsequent binding of Pcf2 to the chromatin upon replication stress. Altogether, these data establish that DNA damage impacts on the mechanisms of CAF-1 association to the chromatin and that these mechanisms are different in stressed *versus* undressed conditions.

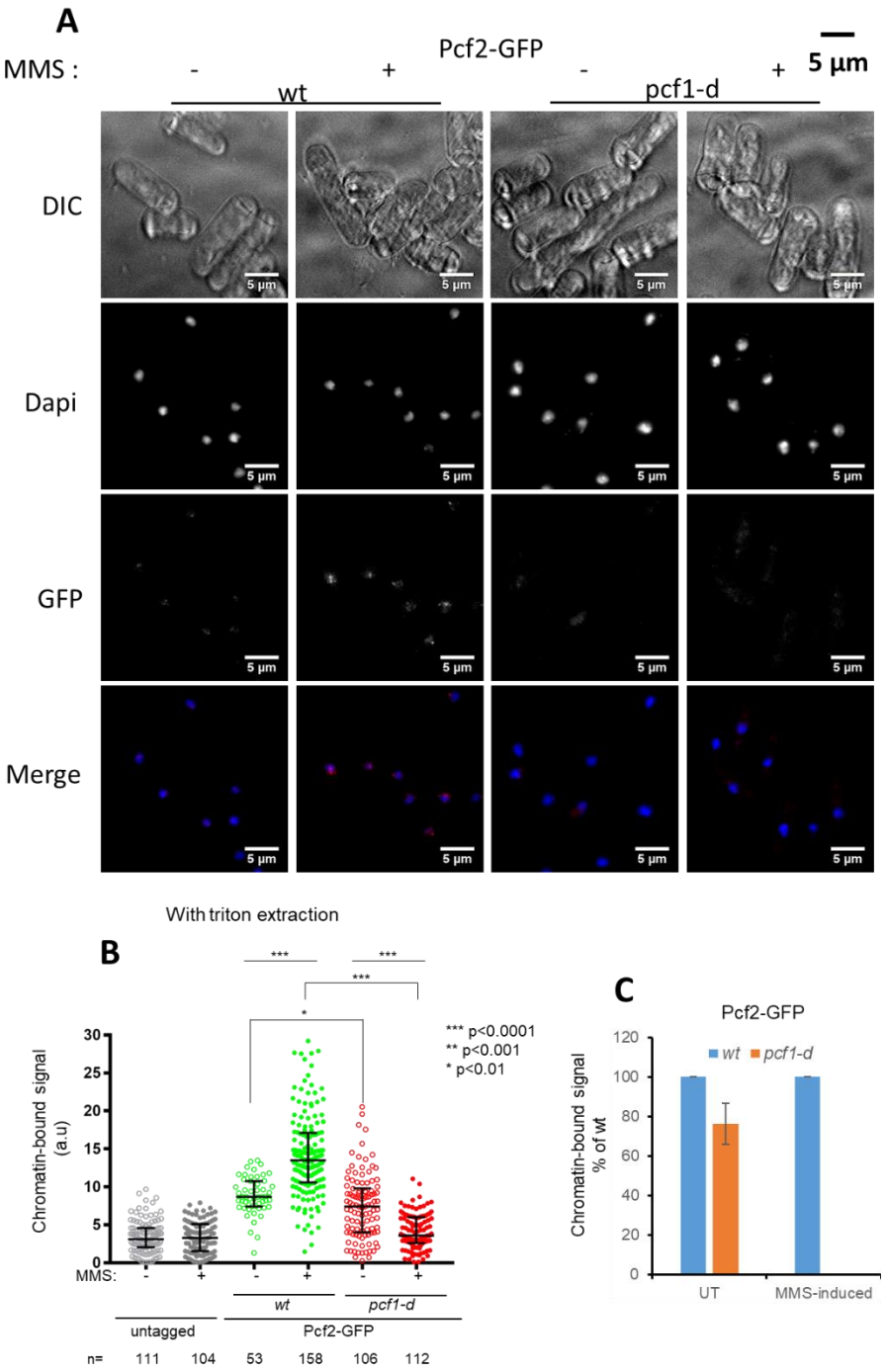

Figure 29. The association of Pcf2 to the chromatin is dependent on Pcf1 in response to MMS treatment. A. Representation of chromatin binding assay performed in cells expressing Pcf2-GFP in indicated strains. Cells were treated with 0.03% MMS for 3 hours. B. Quantification of chromatin-bound Pcf2-GFP signal in arbitrary unit (a.u.) normalized to nucleus area and cytoplasmic signal. Quantification bars indicate the median and interquartile, n indicates the number of cell analyzed. Statistical analysis was performed by using Mann & Whitney U test. C. Histograms showing % of chromatin-bound signal of Pcf2-GFP normalized to *wild type* level

in both untreated (UT) and MMS-induced conditions, as explained on Figure 28. Values are medians of at least two independent experiments ± standard deviation (SD).

Thus, Pcf1 associates to damaged chromatin independently of Pcf2. In contrast, the association of Pcf2 to damaged chromatin is dependent on Pcf1. Our data suggest that CAF-1 subunits could be recruited to the chromatin hierarchically.

2.6. Pcf1 association to chromatin is partially Rad3-dependent in response to MMS treatment

So far I have shown that Pcf1 associates to the chromatin upon replication stress, and I wanted to know if this chromatin-association is regulated by the DNA damage checkpoint pathway. To address this question, I have deleted the *rad3* gene that encodes the fission yeast homologue of the checkpoint kinase ATR. I have observed that Pcf1-GFP slightly increased the sensitivity of cells deleted for *rad3* (*rad3-d*) to MMS (Figure 30A), suggesting that the fusion protein might not be fully functional when combined with checkpoint defective strains. A chromatin binding assay was performed on *rad3-d* cells treated with MMS for 3 hours or not (Figure 30B). The results showed that the chromatin-bound fraction of Pcf1-GFP was unaffected in untreated cells. Although, MMS treatment stimulated the chromatin-bound fraction of Pcf1-GFP in both *wild type* and *rad3-d* cells, the enrichment was less pronounced in *rad3-d* cells than the one observed in *wild type* cells (Figure 30B and C). The quantification of the data showed that Pcf1-GFP was 40% less enriched in the chromatin faction in the absence of Rad3, compared to checkpoint proficient cells (Figure 30D). Thus, Pcf1 is able to associate to damaged chromatin in the absence of the checkpoint protein Rad3 that fine-tunes Pcf1 association to damaged chromatin.

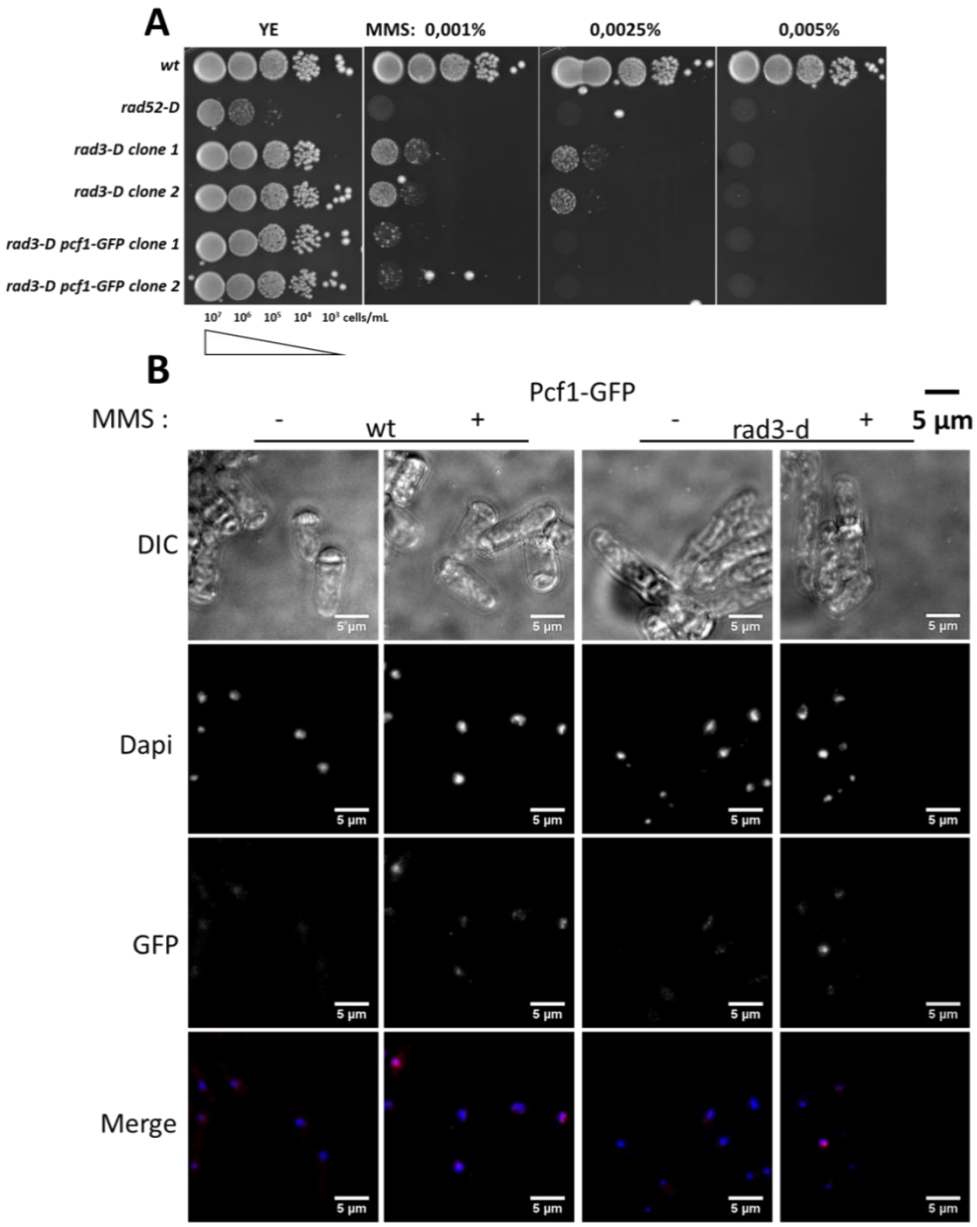
A
YE
MMS: 0,001%
0,0025%
0,005%
wt
rad52-D
rad3-D clone 1
rad3-D clone 2
rad3-D pcf1-GFP clone 1
rad3-D pcf1-GFP clone 2
10⁷ 10⁶ 10⁵ 10⁴ 10³ cells/mL
B
Pcf1-GFP
MMS :
wt
rad3-d
5 µm
DIC
Dapi
GFP
Merge
C
Chromatin-bound signal (a.u)
*** p<0.0001
** p<0.001
* p<0.01
MMS:
wt
rad3-d
untagged
Pcf1-GFP
n= 65 55 49 53 73 81
D
Chromatin-bound signal % of wt
wt
rad3-d
UT
MMS-induced

Figure 30. Pcf1 association to chromatin is partially Rad3-dependent in response to MMS treatment. A. Drop test of 10-fold serial dilutions of indicated cells s in indicated conditions. YE plate was used as a control. The strain deleted for *rad52* served as a control for the quality of the plates, because of its hypersensitivity to DNA damaging and replication-blocking agents. B. Representation of chromatin binding assay performed in indicated cells and conditions. Cells were treated with 0.03% MMS for 3 hours. C. Quantification of chromatin-bound Pcf1-GFP signal in arbitrary unit (a.u.) normalized to nucleus area and cytoplasmic signal. Quantification bars indicate the median and interquartile, n indicates the number of cell analyzed. Statistical analysis was performed by using Mann & Whitney U test. D. Histograms showing % of chromatin-bound signal of Pcf1-GFP normalized to *wild type* level in both untreated (UT) and MMS-induced conditions, as explained on figure 28. Values are medians of at least two independent experiments ± standard deviation (SD).

Rad3 impacts the association of Pcf1 to damaged chromatin. However, the deletion of *rad3* does not completely abolishes Pcf1 binding to chromatin upon replication stress, suggesting that the key determinant of Pcf1 binding to damaged chromatin might be other proteins which function upstream or independently of the DNA replication checkpoint pathway. In the next chapter, I will present results on the identification of HR factors that are crucial for CAF-1 association to the chromatin upon replication stress.

I have planned to support the data from chromatin binding assays with PALM (photo-activated localization microscopy) microscopy (Etheridge et al., 2014) in collaboration with the lab of Tony Carr in University of Sussex, UK. PALM microscopy offers the possibility to analyze the mobile *versus* immobilized fractions of proteins under various conditions. This technic would allow monitoring the chromatin-associated fraction of Pcf1 and Pcf2, without using enzyme to digest the cell wall and triton extraction. I have constructed several strains expressing special versions of tagged Pcf1 specifically for PALM (Pcf1-mEos3 and Pcf1-Dendra2). However, all these strains were later found to be co-lethal with *hip1-d*, indicating that the fusion with these specific tags for PALM leads to dysfunction of Pcf1 (Figure 31). Thus, unfortunately I could not apply these strains to PALM to reinforce my data.

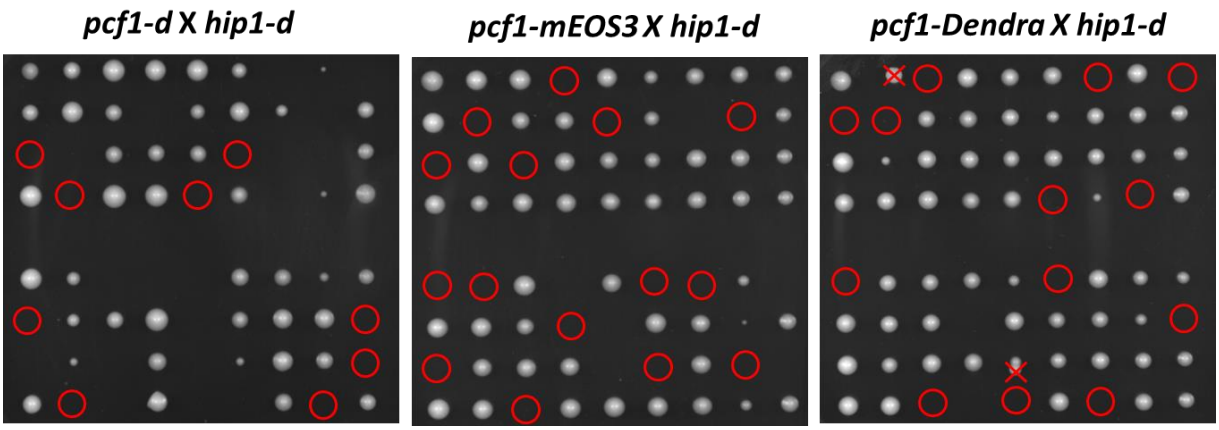

Figure 31. Synthetic lethality between tagged *pcf1* and *hip1-d*. Left panel: tetrads from the cross between *pcf1-d* and *hip1-d* strains are represented. Red circles indicate *pcf1-d hip1-d* spores that were unviable. 68 spores from 17 tetrads were analyzed. Middle panel: tetrads from the cross between *pcf1-mEOS3* and *hip1-d* strains are represented. Red circles indicate *pcf1-mEOS3 hip1-d* spores that were unviable. 72 spores from 18 tetrads were analyzed. The red line indicates the tetrad that was not analyzed. Right panel: tetrads from the cross between *pcf1-Dendra* and *hip1-d* strains are represented. Red circles indicate *pcf1-Dendra hip1-d* spores that were unviable. Red crosses indicate contaminations that mimic fission yeast colonies. 72 spores from 18 tetrads were analyzed.

3. A functional homologous recombination pathway is required for CAF-1 association to chromatin upon replication stress

So far my data suggest that CAF-1 is associated to the chromatin in response to replication stress, and the subunits of CAF-1 could bind damaged chromatin hierarchically. The large subunit of CAF-1, Pcf1, is associated to damaged chromatin first and this is necessary for the subsequent association of the mid CAF-1 subunit, Pcf2. In light of the previous finding that CAF-1 protects the D-loop from disassembly by the RecQ helicase Rqh1 during the DNA synthesis step of recombination-dependent replication (RDR) (Pietrobon et al., 2014), it is possible that factors acting in the HR pathway play a role in regulating the association of CAF-1 to the chromatin upon replication stress. In this chapter, I have investigated whether HR factors are necessary for the association of CAF-1 subunits to chromatin in response to MMS treatment.

3.1. The role of Rqh1

Previous works from our lab have reported that CAF-1 is required to complete RDR and promotes Rad51-dependent template switches at the replication fork by counteracting the anti-recombinase activity of Rqh1 which disassembles the D-loop (Pietrobon et al., 2014, Hardy et al., publication in preparation). The physical interaction between CAF-1 and Rqh1 has been revealed both *in vivo* and *in vitro*. Therefore, I have questioned the role of Rqh1 in the association of CAF-1 to the chromatin. To address this, I have constructed strains deleted for *rqh1* in combination with *pcf1-GFP* or *pcf2-GFP* to which I have applied the *in vivo* chromatin binding assay in both treated and untreated conditions. In untreated cells, the chromatin-bound fraction for Pcf1-GFP was found slightly increased in *rqh1-d* cells compared to *wild type* (Figure 32A, B and E) whereas the chromatin-bound fraction for Pcf2-GFP was not altered (Figure 32C, D and E). The chromatin-bound fraction for Pcf1-GFP and Pcf2-GFP were found increased both in *wild type* and *rqh1-d* cells, after 3 hours of MMS treatment (Figure 32A and C). The quantification of chromatin-bound signal of Pcf1-GFP further revealed that the deletion of *rqh1* led to slightly increased chromatin-bound Pcf1 in untreated condition, whereas the absence of *rqh1* remarkably reduced the amount of MMS-induced chromatin-bound Pcf1 to about 60% of that in MMS-treated *wild type* cells (Figure 32E). Interestingly, the chromatin-bound fraction of Pcf2-GFP was not significantly affected in the absence of Rqh1 in both treated and untreated conditions, indicating that the association of Pcf1 and Pcf2 to the chromatin upon replication stress is likely under distinct regulations.

These data indicate that Rqh1 is partially required for the association of Pcf1, but not Pcf2, to the chromatin upon replication stress. However, how Rqh1 affects Pcf1 binding to damaged chromatin remains elusive. Possibly, a direct or indirect interaction between Rqh1 and Pcf1 may play a role. Alternatively, the role of Rqh1 in shaping the molecular structure of HR intermediates that accommodate CAF-1 activity may be involved.

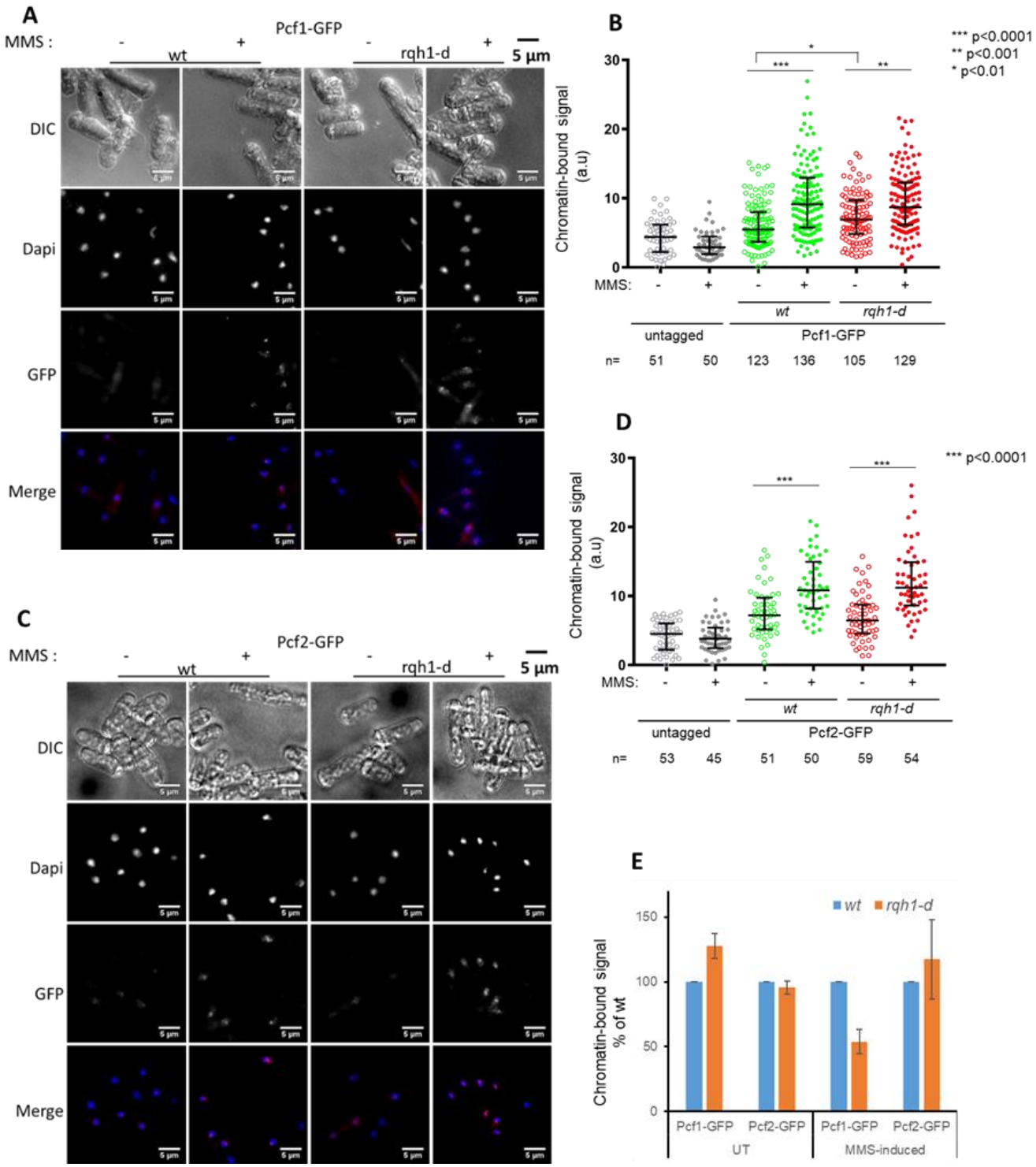

Figure 32. Rqh1 is partially required for Pcf1, but not Pcf2, binding to chromatin in response to MMS treatment. A and C. Representation of *in vivo* chromatin binding assays performed in *pcf1-GFP rqh1-d* cells and *pcf2-GFP rqh1-d* cells, respectively. Cells were treated with 0.03% MMS for 3 hours. The scale bar in black on top of each figure is the same as the scale bar in each microscopy image. B and D. Quantification of the chromatin-associated nuclear GFP signal in arbitrary unit (a.u.) normalized to nucleus area and cytoplasmic signal. Quantification bars indicate the median and interquartile, n indicates the number of cell analyzed. Statistical analysis was performed by using Mann & Whitney U test. E. Histograms showing % of chromatin-bound signal of Pcf1-GFP and Pcf2-GFP, normalized to *wild type* level in both untreated (UT) and MMS-induced conditions, as explained on figure 28. Values are medians of at least two independent experiments ± standard deviation (SD).

SUMOylation of Rqh1 has been speculated earlier in this study to facilitate Pcf1-Rqh1 interaction after MMS treatment, and I failed to provide evidence to verify whether this is true. An attempt has been made to perform chromatin binding assay on *pcf1-GFP pmt3-d* cells (Pmt3 being the Small Ubiquitin-like protein MOdifier SUMO in fission yeast, Tanaka et al., 1999). However, due to the sick growth of this strain, the Pcf1-GFP signal was too weak to be detected and could not be analyzed. Nonetheless, the chromatin binding assay data in *rqh1-d* cells demonstrated that Rqh1 partially impacts the association of Pcf1 to chromatin without addressing the involvement of the SUMOylation of Rqh1.

Thus my data demonstrate that Rqh1 is partially required for the binding of Pcf1 to damaged chromatin, but not for Pcf2. Together with my previous conclusion that Pcf1 associates to chromatin independently of Pcf2 but not *vice et versa*, it supports that replication stress-induced association of Pcf1 and Pcf2 to the chromatin is regulated differently.

3.2. A requirement for HR factors

The role of HR factors in the association of CAF-1 to the chromatin has been investigated. I have constructed strains deleted for *ssb3* (Ssb3 being the small subunit of the trimeric single stranded DNA binding protein RPA in fission yeast), or *rad52* (DNA recombination protein Rad52, the main loader of Rad51), or *rad51* (recombinase Rad51) or *rad54* (DNA translocase Rad54), combined with either *pcf1-GFP* or *pcf2-GFP*. I have applied the *in vivo* chromatin binding assay to these strains in both treated and untreated conditions.

Physical interactions between histone H3-H4 and RPA have been identified and proposed to mediate DNA replication-coupled chromatin assembly (Liu et al., 2017). I therefore questioned if RPA could be instrumental in CAF-1 association to chromatin. The chromatin-bound fraction of

Pcf1-GFP was enriched in *ssb3-d* cells compared to *wild type* cells in untreated conditions (Figure 33A, B and E), which was not the case for Pcf2-GFP (Figure 33C, D and E). In response to MMS, the chromatin-bound fraction for both Pcf1 and Pcf2 were found increased in response to MMS treatment (Figure 33A, B, C and D). The quantification of the data indicated that Pcf1 was marginally less associated to damaged chromatin in the absence of Ssb3, whereas Pcf2 was better enriched in the chromatin fraction in the absence of Ssb3, compared to *wild type* cells (Figure 33E). Based on these data, I concluded that CAF-1 association to damaged chromatin is not defective in the absence of RPA, but that RPA may play a role in releasing Pcf2 from the chromatin in response to MMS.

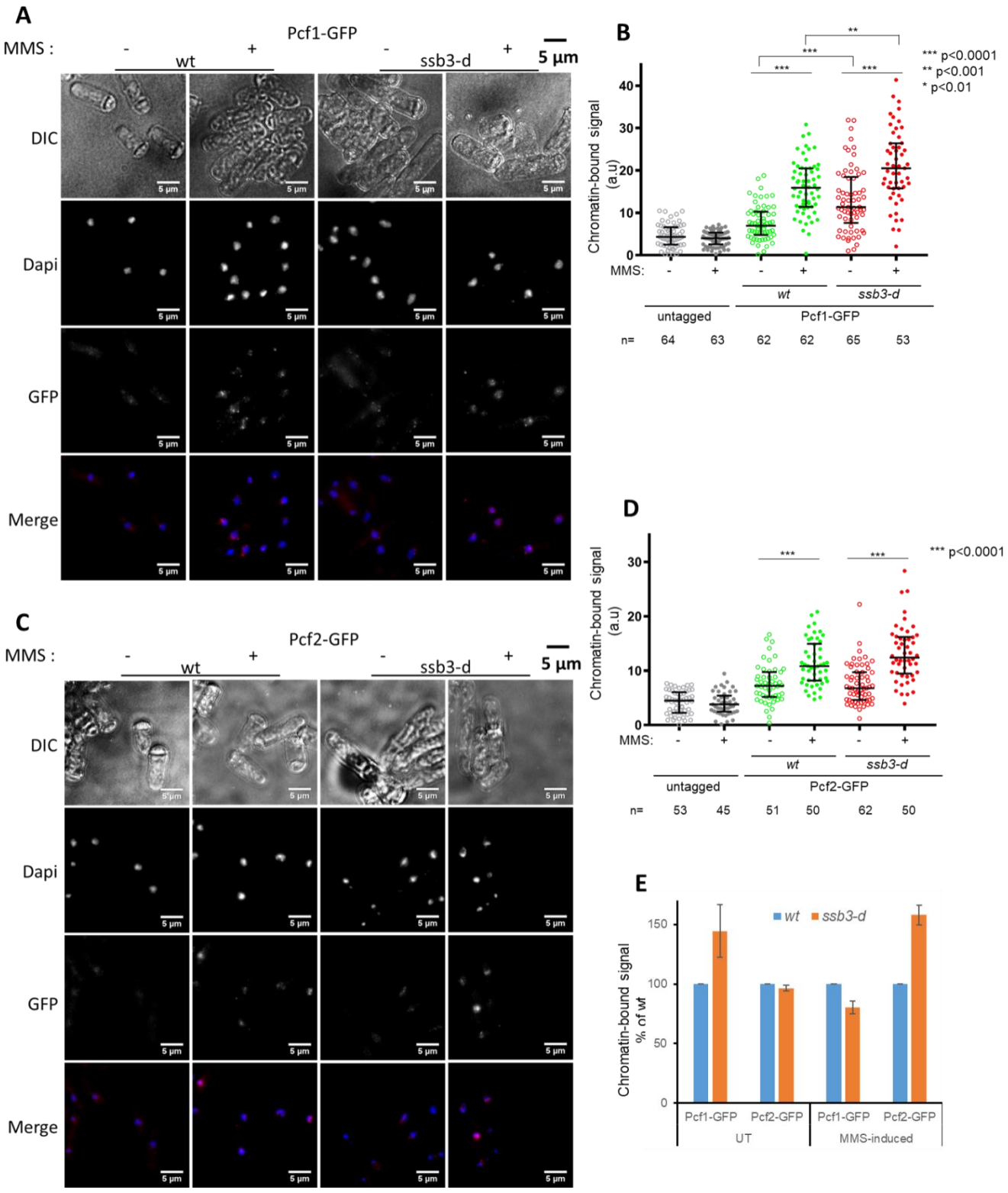

Figure 33. CAF-1 association to damaged chromatin is not defective in the absence of Ssb3. A and C. Representation of *in vivo* chromatin binding assays performed in *pcf1-GFP ssb3-d* cells and *pcf2-GFP ssb3-d* cells, respectively. Cells were treated with 0.03% MMS for 3 hours. The scale bar in black on top of each figure is the same as the scale bar in each microscopy image. B and D. Quantification of the chromatin-associated nuclear GFP signal in arbitrary unit (a.u.) normalized to nucleus area and cytoplasmic signal. Quantification bars

indicate the median and interquartile, n indicates the number of cell analyzed. Statistical analysis was performed by using Mann & Whitney U test. E. Histograms showing % of chromatin-bound signal of Pcf1-GFP and Pcf2-GFP, normalized to *wild type* level in both untreated (UT) and MMS-induced conditions, as explained on figure 28. Values are medians of at least two independent experiments ± standard deviation (SD).

The team has shown that the binding of Pcf1 to the site of recombination-dependent replication requires the HR factor Rad52 (Hardy et al., publication in preparation). I therefore tested the requirement of Rad52 to CAF-1 association to the chromatin at the genome-wide level. In untreated conditions, both Pcf1 and Pcf2 were more associated to the chromatin in *rad52-d* cells, compared to *wild type* cells (Figure 34A, B, C and D). Although MMS treatment stimulated the association of Pcf1 and Pcf2 to the chromatin in *wild type* cells, no increase was observed in the absence of Rad52 (Figure 34E). These data indicate that Rad52 is not required for CAF-1 binding to the chromatin in untreated cells but it becomes pivotal in response to MMS treatment. These data reveal distinct modes of CAF-1 association to chromatin in untreated versus replication stress conditions.

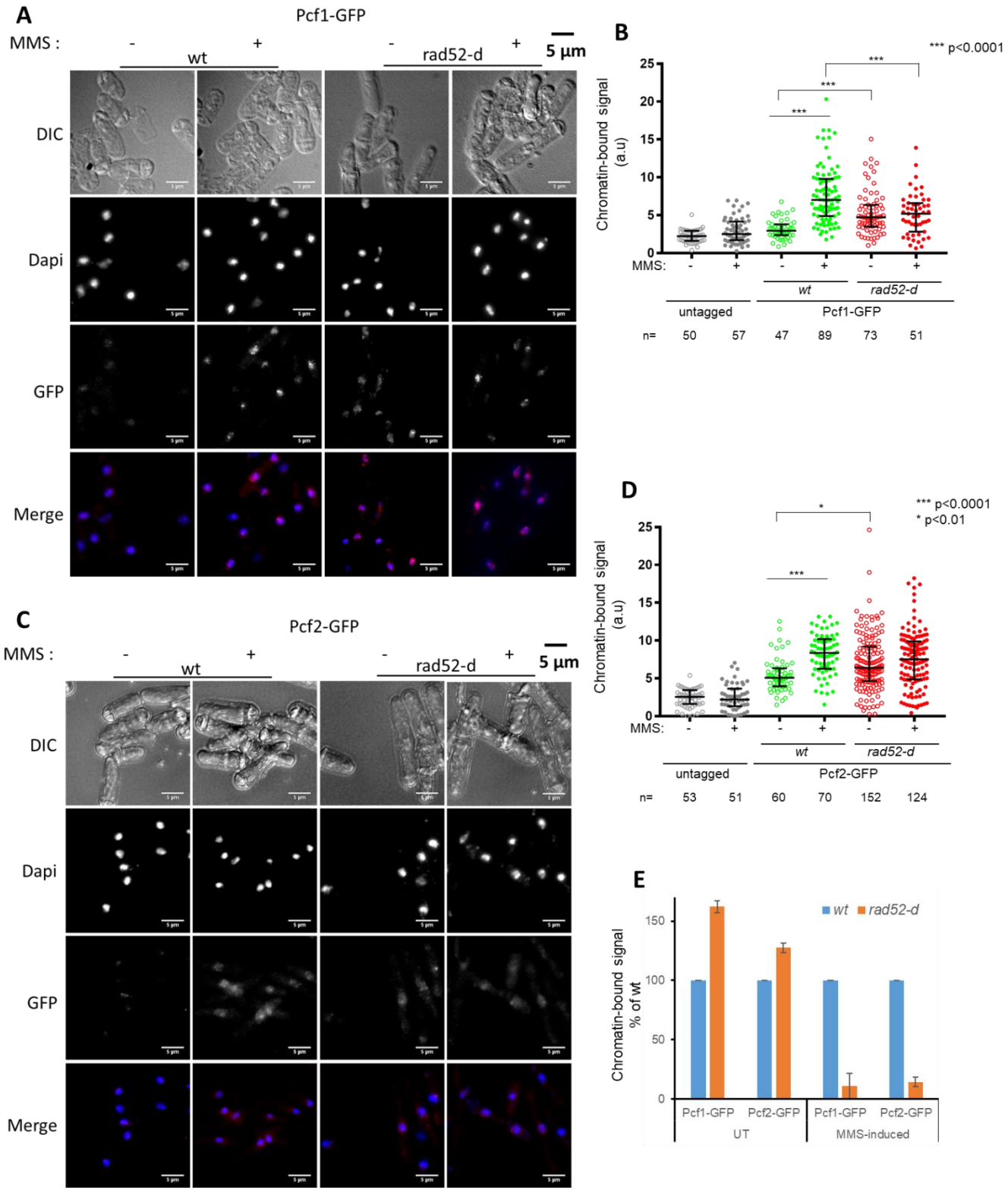

Figure 34. CAF-1 association to damaged chromatin requires Rad52. A and C. Representation of *in vivo* chromatin binding assays performed in *pcf1-GFP rad52-d* cells and *pcf2-GFP rad52-d* cells, respectively. Cells were treated with 0.03% MMS for 3 hours. The scale bar in black on top of each figure is the same as the scale bar in each microscopy image. B and D. Quantification of the chromatin-associated nuclear GFP signal in arbitrary unit (a.u.) normalized to nucleus area and cytoplasmic signal. Quantification bars indicate the median

and interquartile, n indicates the number of cell analyzed. Statistical analysis was performed by using Mann & Whitney U test. E. Histograms showing % of chromatin-bound signal of Pcf1-GFP and Pcf2-GFP, normalized to *wild type* level in both untreated (UT) and MMS-induced conditions, as explained on figure 28. Values are medians of at least two independent experiments ± standard deviation (SD).

Rad52 is the main loader of the recombinase Rad51. I therefore tested if the role of Rad52 in promoting CAF-1 association to chromatin in response to MMS is linked to the loading of the recombinase Rad51. In untreated conditions, the chromatin-bound signal for both Pcf1-GFP and Pcf2-GFP were slightly higher in *rad51-d* cells compared to *wild type* (Figure 35A, B, C and D). In response to 3 hours of MMS treatment, the chromatin-bound signal for both Pcf1-GFP and Pcf2-GFP increased compared to untreated cells in *wild type* and *rad51-d* cells (Figure 35A, B, C and D). When analyzing the level of enrichment induced by MMS in *rad51-d* cells compared to *wild type* (normalized to 100 %), the MMS-induced chromatin-bound signal for Pcf1-GFP and Pcf2-GFP was reduced by 2 fold in the absence of Rad51 (Figure 35E). Therefore, I concluded that Rad51 partially affects the association of CAF-1 to the chromatin in response to 3 hours of MMS treatment. To strengthen these data, I have analyzed the kinetics of CAF-1 association to damaged chromatin in the absence of Rad51 by performing chromatin binding assays on *pcf1-GFP rad51-d* and *pcf2-GFP rad51-d* cells following a time course upon MMS treatment. The results showed that Pcf1-GFP and Pcf2-GFP association to damaged chromatin in the absence of Rad51 followed similar kinetics as observed in *wild type* cells, but this chromatin-enrichment was reduced by ~ 2 fold at any time point analyzed (Figure 36). These data further support that CAF-1 association to chromatin upon replication stress is partially dependent on the recombinase Rad51.

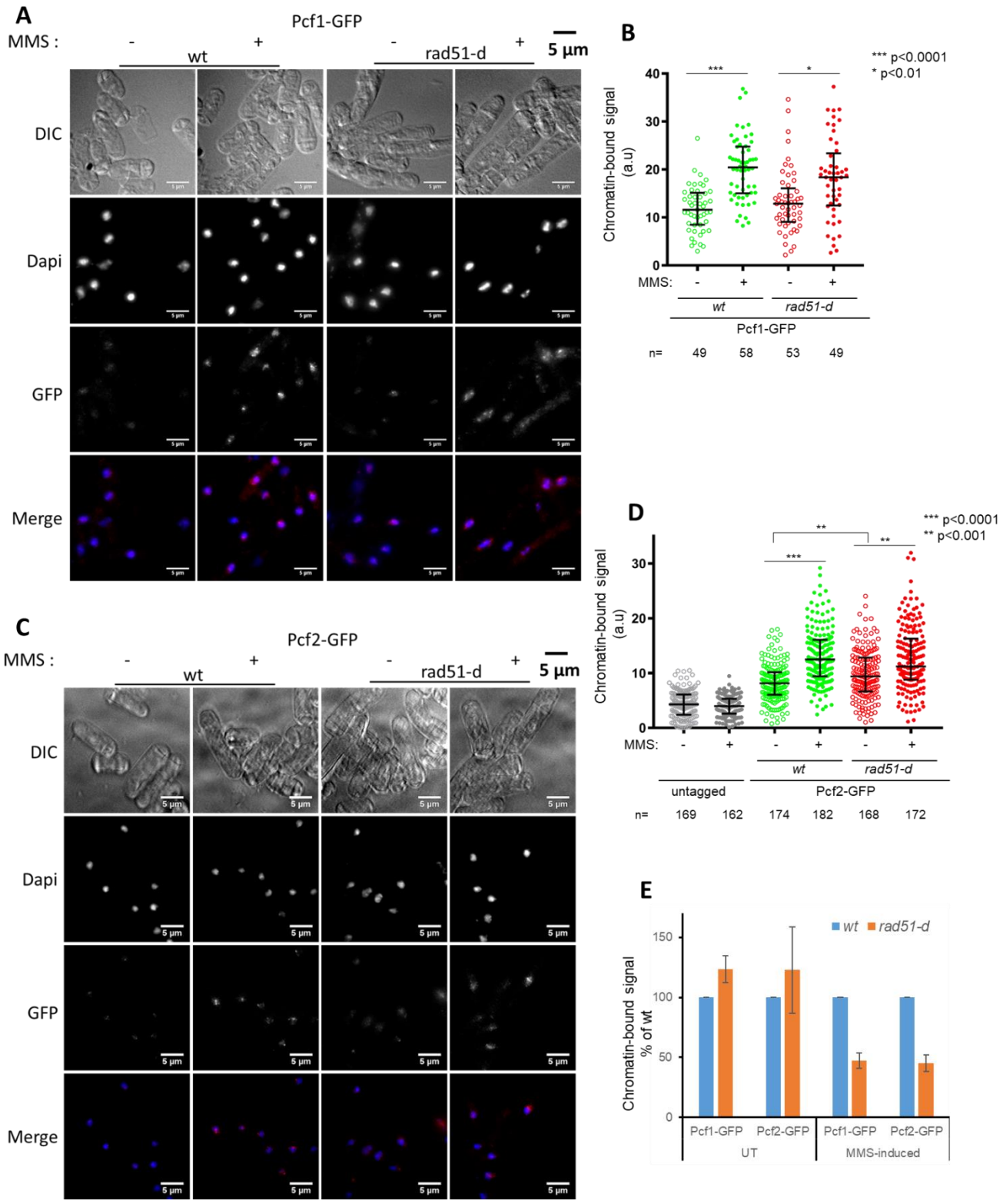

Figure 35. CAF-1 association to the chromatin upon replication stress is partially dependent on Rad51. A and C. Representation of *in vivo* chromatin binding assays performed in *pcf1-GFP rad51-d* cells and *pcf2-GFP rad51-d* cells, respectively. Cells were treated with 0.03% MMS for 3 hours. The scale bar in black on top of each figure is the same as the scale bar in each microscopy image. B and D. Quantification of the chromatin-associated nuclear GFP signal in arbitrary unit (a.u.) normalized to nucleus area and cytoplasmic signal.

Quantification bars indicate the median and interquartile, n indicates the number of cell analyzed. Statistical analysis was performed by using Mann & Whitney U test. E. Histograms showing % of chromatin-bound signal of Pcf1-GFP and Pcf2-GFP, normalized to *wild type* level in both untreated (UT) and MMS-induced conditions, as explained on figure 28. Values are medians of at least two independent experiments ± standard deviation (SD).

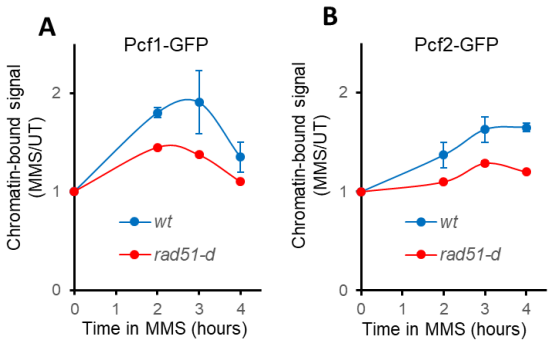

Figure 36. Rad51 partially impacts the association of CAF-1 to chromatin in response to MMS treatment. Fold enrichment of chromatin-bound GFP staining upon MMS treatment in indicated strains for indicated time. Values ± standard deviation (SD) are means of at least two independent experiments.

Finally, I have asked if the translocase Rad54 is required to CAF-1 association to chromatin in response to replication stress. The data showed that the chromatin-bound signal for Pcf1-GFP was increased in *rad54-d* cells compared to *wild type* in untreated conditions (Figure 37A and B). However, in response to 3 hours of MMS treatment, no increase in the chromatin-bound signal was observed in *rad54-d* cells, in contrast to *wild type* cells (Figure 37C). These data establish that Pcf1 association to chromatin upon replication stress requires Rad54.

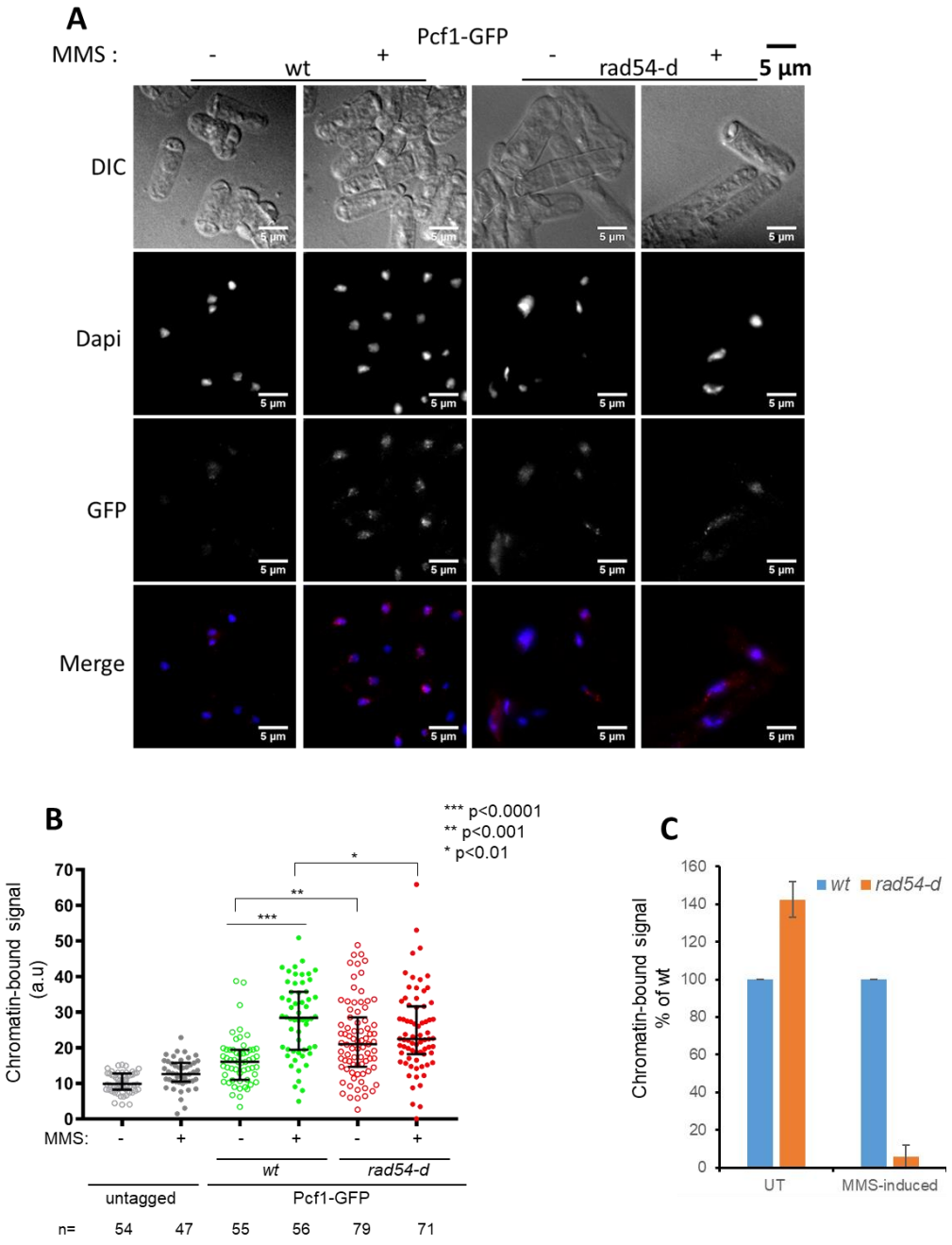

Figure 37. Pcf1 association to damaged chromatin requires Rad54. A. Representation of *in vivo* chromatin binding assays performed in *pcf1-GFP rad54-d* cells, respectively. Cells were treated with 0.03% MMS for 3 hours. The scale bar in black on top of each figure is the same as the scale bar in each microscopy image. B. Quantification of the chromatin-associated nuclear GFP signal in arbitrary unit (a.u.) normalized to nucleus area and cytoplasmic signal. Quantification bars indicate the median and interquartile, n indicates the number of cell analyzed. Statistical analysis was performed by using Mann & Whitney U test. C. Histograms showing % of chromatin-bound signal of Pcf1-GFP, normalized to *wild type* level in both untreated (UT) and MMS-induced conditions, as explained on figure 28. Values are medians of at least two independent experiments ± standard deviation (SD).

In conclusion, in the absence of HR factors (Rad52, Rad51 or Rad54), CAF-1 has the tendency to be more associated to chromatin in unchallenged conditions. This could reflect the fact that DNA replication is perturbed in the absence of a functional HR pathway, with more replication origins being activated and thus ongoing forks. This would suggest that the HR pathway is not required to CAF-1 mediated DNA replication-coupled chromatin assembly. In contrast, a functional HR pathway is required for sustaining the binding of CAF-1 to the chromatin in response to MMS treatment and thus replication stress.

In agreement with Rad52 being necessary to target Pcf1 to sites of recombination-dependent replication (data generated by Julien Hardy in the team, Hardy et al., publication in preparation, see annex 1), chromatin binding assays data from this study show that the association of CAF-1 to damaged chromatin requires Rad52. Therefore, my data have revealed important roles for HR factors in the association of CAF-1 to the chromatin upon replication stress. Rad52 and Rad54 are essential for the association of CAF-1 to the chromatin in response to damaged replication forks, whereas Rad51 plays a partial role in this scenario. Considering that CAF-1 stabilizes the D-loop and promotes Rad51-dependent template switches by preventing D-loop disassembly by the helicase Rqh1 (Pietrobon et al., 2014), together with my data, it suggests that Rad51 and Rqh1 might collectively sustain a certain molecular conformation of the RDR intermediate that is required for the action of CAF-1.

3.3. Physical interactions between CAF-1 and HR factors

Rqh1 physically interacts with Pcf1 and Pcf2 (see Chapter 1 of the results, (Pietrobon et al., 2014)) and CAF-1 association to damaged chromatin partially requires Rqh1. Rad52, Rad54 and Rad51 are also necessary for optimal binding of CAF-1 to damaged chromatin. Therefore, I have investigated if these HR factors physically interact with CAF-1 using both *in vivo* and *in vitro* approaches.

GST-pulldown assay using recombinant Pcf1 revealed that two subunits of RPA, Ssb3 and Rad11 both interacted with Pcf1 (Figure 38A). However, these interactions were not stimulated by MMS treatment, which is in agreement with the data from the IP of Pcf1-GFP showing that Pcf1-Ssb3 interaction was not stimulated upon MMS treatment *in vivo* (Figure 38A and B).

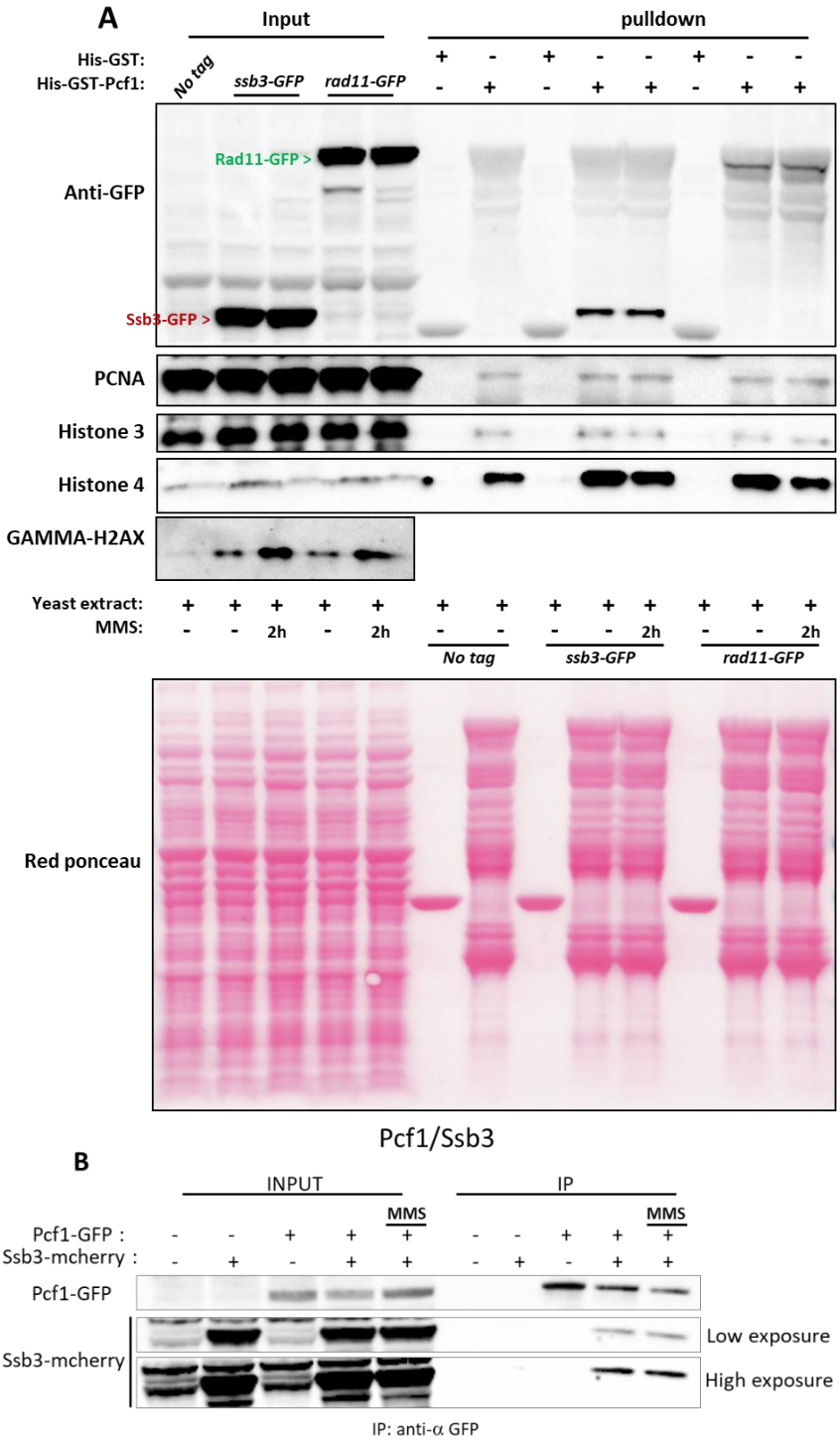

Figure 38. Pcf1 physically interacts with two subunits of RPA. A. GST-pulldown assay using recombinant Pcf1 showing Pcf1-Ssb3 and Pcf1-Rad11 interactions. 700 mM NaCl was added to the buffer during the washing steps. The MMS treatment was performed by culturing cells in media containing 0.03% of MMS for 2 hours. Gamma-H2AX was probed as an indicator of the effect of DNA damaging treatment. B. IP of Pcf1-GFP showing that Pcf1 interacts with Ssb3. The MMS treatment was performed by culturing cells in media containing 0.03% of MMS for 3 hours. The co-IP experiment was performed using antibodies against the tag of the protein.

I have also tried to examine the interaction between Pcf1 and Rad51 or Rad52 by GST-pulldown assays using recombinant Pcf1. However, I could not observe clear bands corresponding to Rad51 or Rad52 either with or without MMS treatment (data not shown). Nonetheless, IP of Pcf1-GFP clearly demonstrated that Pcf1-Rad51 and Pcf1-Rad52 interactions were stimulated by MMS treatment (Figure 39A and C). Importantly, the fact that these interactions were only observed *in vivo* but not *in vitro* indicates that potential post-translational modifications of Pcf1 might be critical for mediating these interactions.

It has been reported that in human and budding yeast, RAD51 directly interacts with BLM/Sgs1 (homologues of Rqh1) (Campos-Doerfler et al., 2018; Wu et al., 2001). Furthermore, the co-IP results also showed that Pcf1-Rad51 interaction occurred independently of Rqh1 (Figure 39B), excluding the possibility of Rqh1 mediating this interaction. IP of Pcf1-GFP also revealed that Pcf1 interacted with Rad54 and the interaction was stimulated by MMS (Figure 39D).

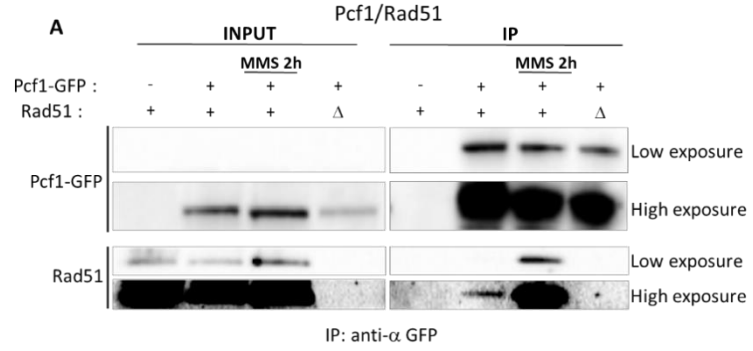

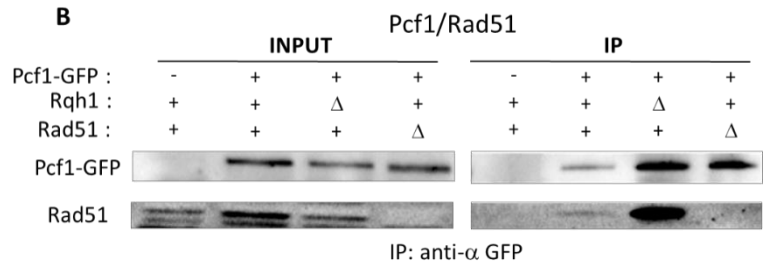

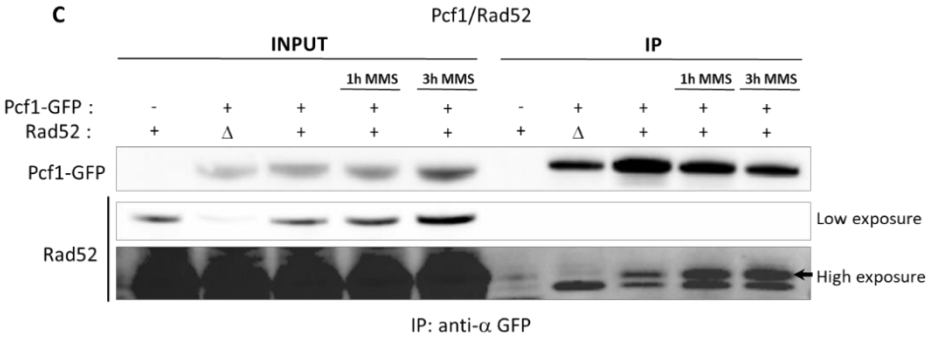

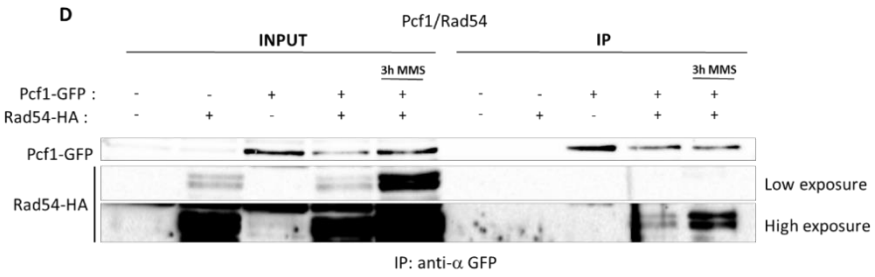

Figure 39. Interactions between Pcf1 and HR factors are stimulated by MMS. A. IP of Pcf1-GFP that Pcf1 interacts with Rad51. The MMS treatment was performed by culturing cells in media containing 0.03% of MMS for 3 hours. The co-IP experiment was performed using antibodies against the tag of the protein. B. IP of Pcf1-GFP showing that Pcf1 interacts with Rad51 in the absence of Rqh1. The co-IP experiment was performed using antibodies against the tag of the protein. C. IP of Pcf1-GFP showing that Pcf1 interacts with Rad52. The MMS treatment was performed by culturing cells in media containing 0.03% of MMS for indicated hours. The co-IP experiment was performed using antibodies against the tag of the protein. The bands corresponding to Rad52 in the IP fraction are indicated by the black arrow. D. IP of Pcf1-GFP showing that Pcf1 interacts with Rad54. The MMS treatment was performed by culturing cells in media containing 0.03% of MMS for 3 hours. The co-IP experiment was performed using antibodies against the tag of the protein.

Interactions between Pcf2 and HR factors were examined by co-IP. IP of Pcf2-GFP showed that Rad51 and Rad52 both interacted with Pcf2. MMS treatment only stimulated Pcf2-Rad52 interactions, but no noticeable stimulation was observed for Pcf2-Rad51 interactions (Figure 40A and B).

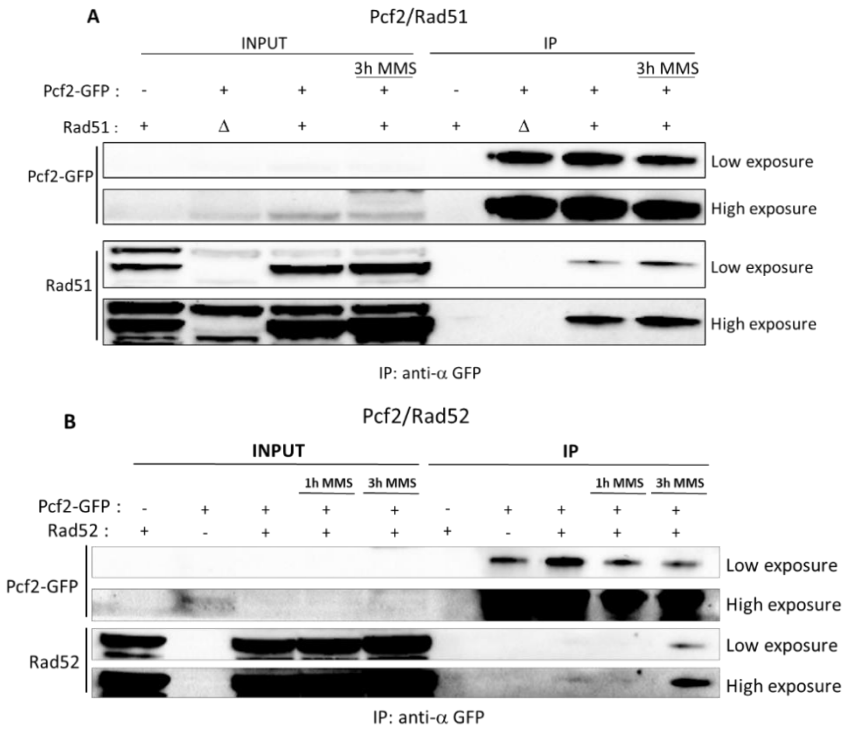

Figure 40. Interactions between Pcf2 and HR factors. A. IP of Pcf2-GFP that Pcf2 interacts with Rad51. The MMS treatment was performed by culturing cells in media containing 0.03% of MMS for 3 hours. The co-IP experiment was performed using antibodies against the tag of the protein. B. IP of Pcf2-GFP showing that Pcf2 interacts with Rad52. The MMS treatment was performed by culturing cells in media containing 0.03% of MMS for indicated hours. The co-IP experiment was performed using antibodies against the tag of the protein. The level of Pcf2-FLAG in the input fraction was too low to be detected by the antibody.

Taking together the data of the chromatin binding assays and the interactions between CAF-1 and HR factors, it is likely that these interactions are playing regulatory roles in the association of CAF-1 to the chromatin in response to replication stress. These observations demonstrate the requirement of a functional HR pathway for CAF-1 association to chromatin upon replication stress.

4. Histone deposition plays an active role in Recombination-dependent replication

Manuscript see annex 1

Data in this chapter are the object of Julien Hardy's project which I also participated in. Results are presented in the form of a manuscript entitled "Histone deposition promotes recombination-dependent replication at arrested forks", to which I signed as a second author. For this study, I performed *in vivo* chromatin fraction assays (Figure 7 c and d) and chromatin fraction assays (Figure S6 a).

Discussion and Perspectives

In this study, I have investigated the physical interactions between the RecQ helicase Rqh1 and the CAF-1 complex in fission yeast. The data obtained from this work have allowed a better characterized of the interactions between Rqh1 and CAF-1 subunits in response to replication stress. By developing an *in vivo* chromatin binding assay, I was able to ask the kinetics of the association of the different CAF-1 subunits to damaged chromatin. The roles of HR factors in the association of CAF-1 to damaged chromatin have been examined. My results put forward a working model in which a functional HR pathway is needed to promote CAF-1 association to chromatin upon replication stress.

1. Rqh1 physically interacts with two CAF-1 subunits, Pcf1 and Pcf2

Using co-IP and GST-pulldown approaches, the previously reported physical Rqh1-Pcf1 interaction has been reproduced both *in vivo* and *in vitro* (Pietrobon et al., 2014). I have shown that this interaction is stimulated by DNA damage. I have also shown that Rqh1 interacts with the mid CAF-1 subunit, Pcf2, which is, to my knowledge, revealed for the first time. Interestingly, in contrast to Pcf1, the interaction between Pcf2 and Rqh1 is not stimulated by DNA damage. So far I could not generate convincing data to clarify if Rqh1 interacts with Pcf3. Importantly, my data have demonstrated that Pcf1 and Pcf2 interact with Rqh1 independently of each other.

Based on these observations, some intriguing points have been revealed and should be further explored and clarified, especially the architecture of the protein complex containing Rqh1 and CAF-1 subunits, in the context of unchallenged cellular environment as well as upon DNA damage:

1) Does Rqh1 mainly interact with the full CAF-1 complex or with CAF-1 subunits individually, or both types of interaction exist in unchallenged cellular environment?

2) How does DNA damage modulate the dynamics of these protein complexes?

3) What are the functional consequences of DNA damage-induced modulation of Rqh1-CAF-1 interactions?

Overall, PCNA and histone H3-H4 should also be placed in the model, as I have observed that Rqh1 interacts with PCNA and histone H3 in a CAF-1-dependent manner.

To further address these questions, it would be important to re-test the interaction between Rqh1 and Pcf3. To date, our co-IP data were still elusive to conclude if Rqh1 interacts with Pcf3, mainly because of technical issues when using cells expressing Pcf3-HA. One solution could be

performing co-IP experiments on cells expressing Pcf3-GFP. Likewise, the potential interaction between Pcf3 and Rqh1 should also be examined in the presence of MMS.

To study the architecture of protein complex containing Rqh1 and CAF-1 subunits, size exclusion chromatography could be performed to distinguish if Rqh1 interacts with the full CAF-1 complex, or with individual CAF-1 subunits, or both.

It is noteworthy that the fusion with YFP- or GFP- tag leads to a partial loss of function of Pcf1, but not for GFP-fused Pcf2, as revealed by synthetic lethality assays with *hip1-d*, a gene encoding one of the subunits of the Hir complex (the fission yeast homologue of the HIRA complex). The HIRA complex is a histone H3-H4 chaperone that assembles nucleosomes independently of DNA synthesis. Its role has been found in gene transcription and gene silencing (Van Der Heijden et al., 2007; Loppin et al., 2005; Ray-Gallet et al., 2002b; Sherwood et al., 1993; Tagami et al., 2004). The fission yeast Hir complex consists of three subunits: the large subunit Hip3, the mid subunit Hip1 and the small subunit Slm9. Deficiency in the Hir complex in fission yeast leads to cell cycle delay, sensitivity to DNA damaging agents, increased rates of chromosome loss, de-repression of core histone genes expression outside of S-phase and results in a decreased transcriptional silencing in the outer centromere repeats (Anderson et al., 2010; Greenall et al., 2006; Kanoh and Russell, 2000; Pidoux et al., 2004). The genes encoding the HIR subunits in budding yeast regulate histone gene expression. The combination of mutations in genes encoding the HIR complex proteins and the genes encoding the CAF-1 complex subunits leads to increased sensitivity to DNA-damaging agents and a synergistic decrease in gene silencing at both mating type and telomeric loci (Kaufman et al., 1998; Sutton et al., 2001). It is possible that the synthetic lethality of *pcf1-d* and *hip1-d* as well as *pcf2-d* and *hip1-d* could be a consequence of unregulated histone pool during the cell cycle via the selective transcription of core histone genes, which is maintained redundantly by CAF-1 and Hir. It would also be important to test the synthetic lethality of *pcf3-d* and *hip1-d* and further examine the functionality of Pcf3-GFP.

Before performing the synthetic lethality assay with *hip1-d* to test the functionality of tagged versions of Pcf1, the Pcf1-YFP strain has been used for microscopy and it demonstrated co-localization of Pcf1-YFP and PCNA foci in S-phase cells (published data from the lab, data not shown, Pietrobon et al., 2014). This suggests that the fusion of Pcf1 with the YFP-tag is unlikely to interfere with the ability of Pcf1 to interact with PCNA. Therefore, we did not further question the functionality of Pcf1-YFP. However, when the synthetic lethality assays were performed on *pcf1-YFP* and *pcf1-GFP* with *hip1-d*, I noticed that Pcf1-YFP and Pcf1-GFP are both partially

functional. Nonetheless, the co-IP experiments in this study have shown that Pcf1-GFP interacts with PCNA, Pcf2 and histone H3. Thus, Pcf1-YFP or Pcf1-GFP fusion proteins are properly targeted to replication foci, form complexes with PCNA and histone H3, but for reasons that remain to be identified, are not fully functional.

2. The ED domain on Pcf1 alone interacts with Rqh1

The previous work from the lab has proposed that CAF-1 and Rqh1 have antagonistic activities in the resolution of D-loops intermediates during recombination-dependent replication (RDR). The physical interaction between CAF-1 and Rqh1 has been speculated to have a role in this scenario (Pietrobon et al., 2014).

It has been reported in human cells that BLM and p150 co-localized *in vivo* within discrete nuclear foci in response to DNA damage and replication stress. Also, BLM was found to inhibit CAF-1-mediated chromatin assembly coupled to DNA repair *in vitro*. Moreover, the ED (glutamic acid (E) and aspartic acid (D)) domain of the large CAF-1 subunit p150 mediates direct interaction between p150 and BLM (Jiao et al., 2004). In light of this, it urged us to test if Rqh1 and Pcf1 directly interact in fission yeast. Unfortunately, several issues have hindered this research path. First, the yeast two-hybrid strategy has been unsuccessful due to the fact that Rqh1 and Pcf1 auto-activate the reporter. Second, the production of recombinant Pcf1 and Rqh1 via the baculovirus expression system was difficult because of a protein degradation issue. To conquer such difficulties, techniques such as rabbit reticulocyte lysate *in vitro* translation and Fluorescence resonance energy transfer (FRET) microscopy could be tried.

The original aim of my PhD project was to identify the domain of Pcf1 that mediates the hypothesized direct interaction with Rqh1, to then generate a *pcf1* mutant unable to interact with Rqh1. Such mutant was thought to be instrumental for studying the role of CAF-1-Rqh1 interaction in maintaining genome stability in response to replication stress. However, with the updated results from this work, it is likely that the generation of a loss-of-interaction *pcf1* mutant would be very challenging since Rqh1 interacts not only with Pcf1 but also with Pcf2. So far, data from this study could exclude that the Pcf2-Rqh1 interaction is bridged by Pcf1. Hence, it gives rise to another interesting question to be addressed: how does Rqh1 interacts with Pcf2, directly or indirectly? Intriguingly, the interaction between BLM and p60 (mid subunit of human CAF-1) has also been revealed by co-IP (data from the lab, data not shown). Altogether, these observations highlight the functional importance of the interactions between BLM/Rqh1 and the mid CAF-1 subunit, which implies: 1) these interactions are evolutionarily conserved; 2) the

rather complex interaction between BLM/Rqh1 and CAF-1 could reflect important roles of CAF-1 in the context of genome stability. Indeed, down-regulation of CAF-1 decreases the rate of sister chromatid exchange (SCE) in BS cells (derived from Bloom syndrome patients, these cells carry mutated BLM) (data from the lab, data not shown).

As expected, the data obtained from GST-pulldown assays in this study have shown that the fragment covering the predicted ED domain (fragment 2, F2) in Pcf1 exhibits a high affinity for Rqh1 in a Pcf2-independent manner. This is an encouraging observation as it resembles the observation made in mammalian cells. However, none of the two sub-fragments of fragment 2, fragment 4 (F4) and fragment 5 (F5), showed an affinity for Rqh1. This could be a consequence of losing essential protein folding. Such possibility could be tested by including both fragment 4 and fragment 5 in the same sample of a GST-pulldown assay to test if the presence of these two fragments would lead to any affinity for Rqh1. The fragment 2 has also demonstrated a high affinity for histone H3, which is consistent with the reports from budding yeast (Liu et al., 2016; Mattiroli et al., 2017a, 2017b; Sauer et al., 2017). Nonetheless, my data are still not sufficient to define if the interaction between the ED domain and Rqh1 is direct or indirect. Notably, an unexpected observation for the fragment 2 is that it also interacts with PCNA, while the PCNA-interacting motif, the PIP-box, is located outside the ED domain. One explanation could be that the ED domain is highly acidic and mediates nonspecific interactions. In addition, due to the high content of aspartic acid and glutamic acid repeats, the ED domain exhibits strong negative charge distribution and it might be involved in DNA/RNA mimicry (Chou and Wang, 2015). Since PCNA contacts DNA via a surface created by several positively charged residues (De March et al., 2017; McNally et al., 2010), the affinity of the ED domain for PCNA could be a consequence of the mimicry of DNA.

By GST-pulldown assay, I have also tested a shorter ED fragment which contains exactly the predicted ED domain in Pcf1 (fragment ED). The difference between fragment 2 and fragment ED is that fragment 2 contains 53 more residues at the C-terminus part of the predicted ED domain. However, in contrast to fragment 2, fragment ED did not demonstrate any affinity for Rqh1, PCNA or histone H3. A potential explanation for such observation could be that the ED domain in Pcf1 is not well defined and difficult to predict. The additional 53 amino acids could be essential in assisting proper folding of the ED domain to carry out its function.

According to the studies on Cac1, the large subunit of budding yeast CAF-1, the domain interacting with the mid CAF-1 subunit, Cac2, is located right after the ED domain (Kim et al.,

2016; Mattiroli et al., 2017b). The binding of Cac2 to Cac1, together with the ED domain of Cac1, shape an interface that is essential for productive histone H3-H4 interaction (Mattiroli et al., 2017b). However, my data showed that the affinity of fragment 2 (which could potentially contain the Pcf2-interacting domain) for histone H3 did not obviously change when Pcf2 was absent. This questions if the mechanism for productive histone binding is different in fission yeast. As mentioned in Chapter 3 of the introduction (section 3.3, Figure 3.6), it was difficult to predict the Pcf2-interacting domain in Pcf1 based on protein sequence alignment. In order to gain the information on potential position of Pcf2-interacting domain in Pcf1, a GST-pulldown assay could be performed with fragment 2 and fragment ED to test if these fragments exhibit affinity for Pcf2. Since the predicted Pcf2-interacting domain in Pcf1 is located at the C-terminus part of the fragment ED, it could be expected that the fragment 2, but not the fragment ED, interacts with Pcf2 (section 3.3, Figure 3.6).

As expected, the N-terminal fragment 1 that covers the PIP-box showed an affinity for PCNA. Furthermore, fragment 1 might also contain a large part of Pcf3-interacting domain which was also difficult to predict based on sequence alignment. Therefore, the affinity of fragment 1 for Pcf3 could be tested *in vitro*. This experiment could coarsely indicate the location of Pcf3-interacting region in Pcf1. The conserved KER domain in the large CAF-1 subunit has been suggested to form coiled-coil binding to long DNA fragment (40 bp) and to contribute to histone deposition (Sauer et al., 2017). Since the fragment 1 covers the predicted KER domain, it could be used in a DNA electrophoretic mobility shift assay (EMSA) for testing its affinity for DNA.

Fragment 3 (F3) of Pcf1 did not show any affinity for the proteins that were tested in the GST-pulldown assay (PCNA, Histone, Rqh1). Fragment 3 might potentially cover the WHD which has been recently studied in budding yeast and crystallized (Figure 6.1A) (Liu et al., 2016; Mattiroli et al., 2017a; Zhang et al., 2016b). The WHD binds to 10 - 16 bp DNA to promote the association of two histone H3-H4-carrying CAF-1 complexes and then to promote tetramer formation of histone $(H3\text{-}H4)_2$. The WHD also contributes to the association of CAF-1 to replication forks together with CAF-1-PCNA interaction (Liu et al., 2016; Mattiroli et al., 2017a; Zhang et al., 2016b). Therefore, defining the WHD of Pcf1 will be very instrumental for studying the role of CAF-1 in fork restart in fission yeast. However, due to that the WHD is highly structured, more evidence is required to better predict the WHD in Pcf1. With fragment 3, an EMSA assay could also be carried out to test its ability for DNA binding.

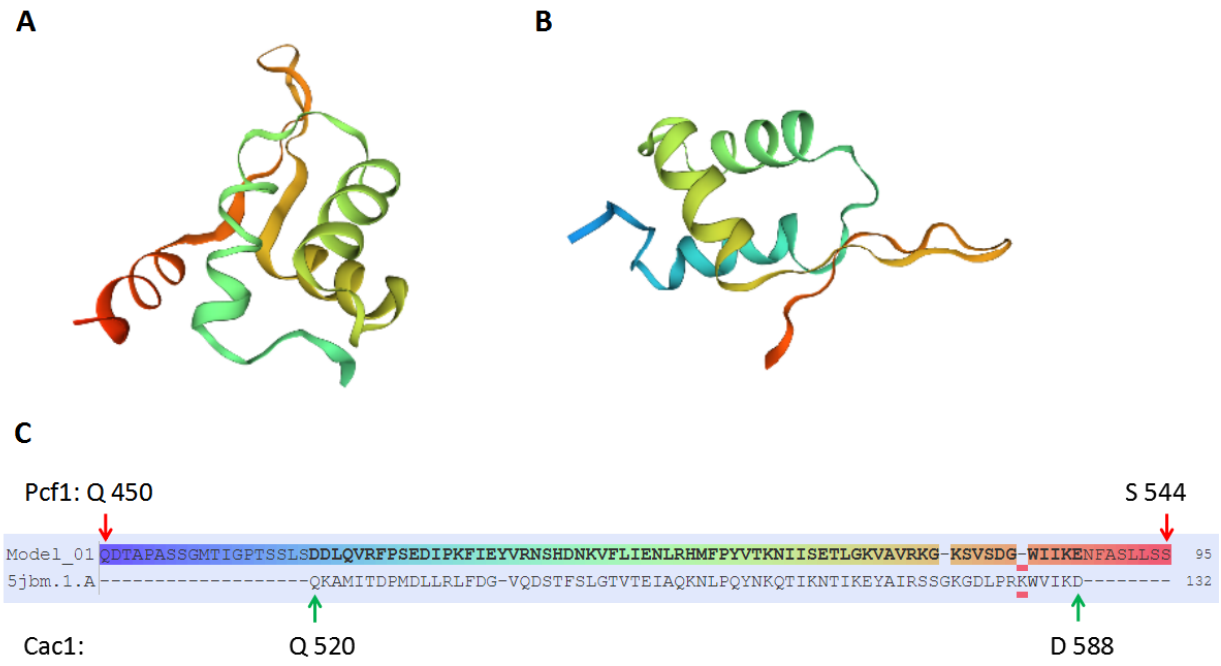

Figure 6.1 3D structure of the WHD on Pcf1 built by SWISS-MODEL. A. The crystal structure of the WHD on budding yeast Cac1 (residues 520–600) at a resolution of 2.9 Å (PDB ID 5JBM). B. The predicted 3D structure of the WHD on fission yeast Pcf1 (residues 450-544). The modelling was performed by SWISS-MODEL by using the WHD of Cac1 as the template. C. Alignment of the amino acid sequence of Pcf1 and Cac1. The color code of the amino acids in the Pcf1 sequence corresponds to the colored regions in the 3D structure shown in panel B. The indicated range of residues on Cac1 (Q520-D588) is covered by the predicted model shown in panel B.

3. The association of CAF-1 subunits to damaged chromatin is regulated differently

Using the *in vivo* chromatin binding assay, I have shown that Pcf1 and Pcf2, but not Pcf3, are associated to chromatin upon replication stress. Kinetics experiments revealed that the maximal association of Pcf1 to chromatin occurs between two and three hours upon MMS treatment, while it is three to four hours for Pcf2. These data rather suggest a complex hierarchy of interactions between CAF-1 subunits to damaged chromatin and imply that CAF-1 subunits might function independently of the histone chaperone function. Indeed, it has been proposed that in human cells, the large CAF-1 subunit, p150, is involved in the early step of DNA repair by HR. After the DNA repair event, the function of p150 could be switched to the histone chaperone function together with the other CAF-1 subunits (Baldeyron et al., 2011).

Furthermore, chromatin binding assays revealed that the association of Pcf2 to the chromatin upon replication stress requires Pcf1 but not *vice et versa*. Pietrobon et al. have reported that the interaction between Pcf2 and PCNA is mediated by Pcf1 (supporting data from (Pietrobon et

al., 2014), data not shown here). Therefore, it is possible that Pcf1 association to damaged chromatin requires the interaction with PCNA to then scaffold the association of Pcf2 to the chromatin.

In the context of nucleosome assembly during DNA replication, the association of the large CAF-1 subunit to the sites of DNA synthesis is via the contact with PCNA (Ben-Shahar et al., 2009; Moggs et al., 2000; Shibahara and Stillman, 1999). The recruitment of PCNA to the sites of DSBs is rather rapid as it occurs 2 min after laser irradiation (Hashiguchi et al., 2007; Mortusewicz and Leonhardt, 2007). In budding yeast, a 40 min time gap is observed between the invasion of Rad51-nucleoprotein filament and the extension of the D-loop by DNA synthesis. This delay might reflect the time required to assemble a competent replication machinery involving PCNA (Hicks et al., 2011). Therefore, it is tempting to speculate that the Pcf1-PCNA interaction promotes Pcf1 to associate to the chromatin upon replication stress. Such hypothesis could be tested by performing a chromatin binding assay on cells expressing a version of Pcf1-GFP carrying mutated PIP-box (*pcf1-pip-mut-GFP*) to see if Pcf1-PCNA interaction is instrumental in Pcf1 binding to damaged chromatin.

In light of the recent studies on the WHD of the large CAF-1 subunit showing that the binding of the WHD to DNA facilitates the association of CAF-1 to replication forks (Liu et al., 2016; Mattiroli et al., 2017a; Zhang et al., 2016b), it would be intriguing to ask if the WHD plays a role in the association of Pcf1 to the chromatin upon replication stress. Therefore, a mutant of Pcf1 missing the WHD needs to be generated. Using SWISS-MODEL, I have performed a preliminary modeling of the C-terminal part of Pcf1 (residues 450-544) using the crystal structure of the WHD of budding yeast Cac1 (residues 520–600) as the template (Figure 6.1) (Liu et al., 2016). The canonical WHD has a winged helix-turn-helix (HTH) structure where the "wings" (also referred to as “loops”) are small beta-sheets (Harami et al., 2013). The structure of the WHD in Cac1 contains four alpha-helices (Figure 6.1A), and the predicted structure of the C-terminus of Pcf1 contains three alpha-helices which resembles a canonical WHD (Figure 6.1A and B). A truncated version of Pcf1 missing this C-terminal part could be generated for testing the requirement of the WHD in the association of Pcf1 to the chromatin upon replication stress. Nonetheless, the WHD of Pcf1 still requires to be precisely defined.

4. Impacts of HR factors on the association of CAF-1 subunits to the chromatin upon replication stress.

The data obtained from chromatin binding assays put forward a scenario in which a functional HR pathway is pivotal for the association of CAF-1 to the chromatin upon replication stress. Moreover, the HR factors involved in RDR impact the association of the different CAF-1 subunits to chromatin through distinct mechanisms.

The absence of Rad52 leads to the abolishment of MMS-induced chromatin-association of Pcf1 and Pcf2, and the absence of Rad54 leads to the abolishment of MMS-induced chromatin-association of Pcf1 (Figure 6.2A and B). Rad52 and Rad54 are both involved in the early steps of RDR to promote and stabilize the Rad51-nucleoprotein filament formation (Seong et al., 2008; Solinger et al., 2002; Sugiyama and Kowalczykowski, 2002). However, the explanation for Rad54 in this scenario is rather elusive and would require further investigation. Indeed, many of the activities of Rad54 are also found downstream the formation of Rad51-nuceloprotein filament. These activities of Rad54 include an important role during the homology search by stimulating Rad51 DNA strand exchange activity (Mazin et al., 2003; Mazina and Mazin, 2004; Petukhova et al., 1998; Sigurdsson et al., 2002), promoting chromatin remodeling (Alexeev et al., 2003), displacing Rad51 from dsDNA (Li et al., 2007), and promoting branch migration of HR intermediates (Bugreev et al., 2006, 2007b; Mazina et al., 2007; Rossi and Mazin, 2008). The absence of Rad54 might lead to an alteration of the D-loop structure, in a way that D-loop would less permissive to CAF-1 association. Rad52 is the main loader of Rad51 and it displaces RPA from ssDNA to facilitate the loading of Rad51 (Benson et al., 1998; New et al., 1998; Shinohara and Ogawa, 1998; Sung, 1997a). My data showed that the absence of RPA, or at least the absence of Ssb3, does not affect the association of CAF-1 to damaged chromatin (Figure 6.2 A and B), indicating that the association of CAF-1 to damaged chromatin likely occurs independently of RPA displacement. Moreover, using a site-specific fork stalling assay, the team showed that Rad52 binds to arrested forks when CAF-1 is absent (Pietrobon et al., 2014), but Pcf1 binding to arrested forks and restarted DNA synthesis requires Rad52 (data generated in our team by Julien Hardy, see article in preparation in annex 1). Altogether, the data indicate that CAF-1 association to damaged chromatin and RDR events occurs downstream from Rad52.

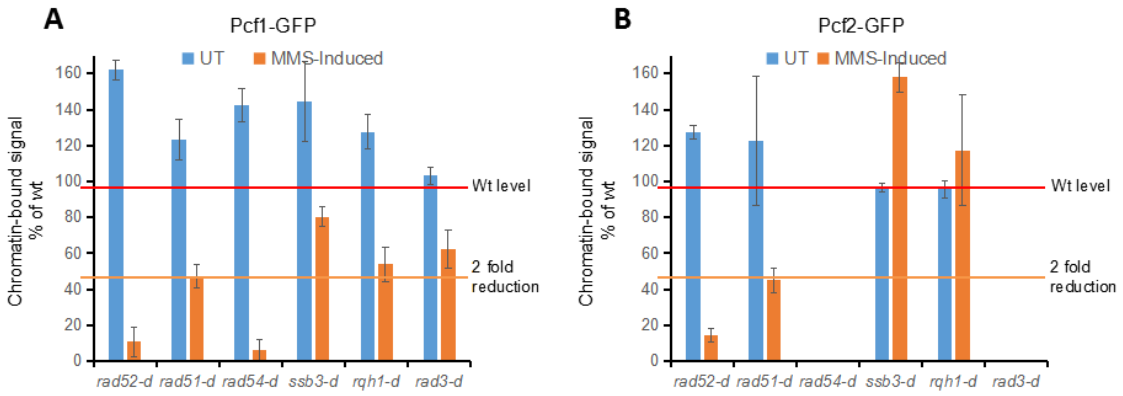

Figure 6.2 Impacts of HR factors on the association of CAF-1 to the chromatin upon replication stress. A and B. Histograms showing % of chromatin-bound signal of Pcf1-GFP and Pcf2-GFP, respectively, normalized to *wild type* level in both untreated (UT) and MMS-induced conditions (*wild type* level is indicated by the red line at 100%), as explained on Figure 28. The orange line indicates 2-fold of reduction of chromatin-bound GFP signal. Values are medians of at least two independent experiments ±SD. *These two charts summarize the data previously presented in chapter 2 and chapter 3 of the Results.

Notably, the absence of Rad51 or Rqh1 both resulted in about 2-fold reduction of MMS-induced chromatin-bound Pcf1 (Figure 6.2A), indicating that Rad51 and Rqh1 both have a partial role in the association of CAF-1 to the chromatin upon replication stress. Rqh1 is reported to act during early steps of HR by dismantling the Rad51-nucleoprotein filament or by dissolving the D-loop intermediates (Aylon et al., 2003; Fabre et al., 2002; Ira et al., 2003; Lambert et al., 2010; Oh et al., 2007; Robert et al., 2006). In fission yeast, Rqh1 regulates Rad51-dependent recombination at the RTS1 replication fork barrier limiting the likelihood of rearrangements without affecting the efficiency of fork restart (Lambert et al., 2010). This effect was attributed to the function of Rqh1 in processing the D-loop (Doe et al., 2002; Stewart et al., 1997). Mutations in *rqh1* demonstrate hypersensitivity to agents affecting DNA replication including UV-irradiation, MMS and CPT (Boddy et al., 2000; Stewart et al., 1997). In the absence of *rqh1*, the D-loop could be more stabilized, and the reduced amount of chromatin-bound Pcf1 upon replication stress could reflect a more continuously processed histone deposition event. Given the interplay between Rqh1 and Rad51, one hypothesis is that the activities of Rad51 and Rqh1 are essential for maintaining a certain molecular conformation of the recombination intermediate during RDR that is required for the function of CAF-1. In support of this hypothesis, the work from Julien Hardy in the team has proposed that CAF-1-mediated histone deposition would occur onto the extended D-loop in the later steps of RDR (Hardy et al., publication in preparation). This

hypothesis will be further tested by assaying the chromatin-bound Pcf1 after MMS in a double mutant deleted for both *rad51* and *rqh1*.

Interestingly, the deletion of *rad51* results in similar reduction of chromatin-bound fraction for both Pcf1 and Pcf2 upon replication stress, while the deletion of *rqh1* only led to the reduction of chromatin-bound Pcf1 (Figure 6.2A and B). These data indicate that the binding of Pcf1 and Pcf2 to damaged chromatin is differently controlled by distinct HR factors. My data suggest that Pcf1 is likely to scaffold the association of Pcf2 to damaged chromatin. Therefore, it is interesting to note that the absence of either Rad51 or Rqh1 results in a similar reduction in MMS-induced chromatin binding of Pcf1 whereas Pcf2 association to damaged chromatin was only affected by the absence of Rad51. This raises question about the hierarchical order by which Rqh1 and Rad51 act to promote CAF-1 association to damaged chromatin. Previous publication showed that CAF-1 stabilizes the D-loop formed in a Rad51-dependent manner by counteracting D-loop disassembly by Rqh1 (Pietrobon et al., 2014). Hence, it is likely that the function of Rad51 in CAF-1-chromatin association is prior to that of Rqh1. My data showed that the absence of Rqh1 did not affect chromatin-bound Pcf2 upon replication stress, even though chromatin-bound Pcf1 was significantly reduced, suggesting that there might be other factors promoting Pcf2-chromatin association. Given that this study has revealed the physical interaction between Pcf2 and Rqh1, it is intriguing to speculate that this interaction might impact on regulating the association of CAF-1 to the chromatin. To address this question, further characterization of the interaction between Pcf2 and Rqh1 will be necessary. Especially considering that the interaction between BLM and p60 is also conserved in human cells (data from the lab, data not shown), a better characterization of Pcf2-Rqh1 interaction will be important to reveal its conserved cellular functions.

The observation that the interactions between Pcf1 and the HR factors Rad51 and Rad52 only occurred *in vivo* but not *in vitro* leads to the speculation that potential post-translational modifications (PTMs) of Pcf1 could be critical in mediating these interactions. So far, no PTM of Pcf1 has been reported in fission yeast. Nonetheless, several phosphorylation sites have been characterized on budding yeast Cac1 (Albuquerque et al., 2008; Holt et al., 2009; Jeffery et al., 2015; Swaney et al., 2013). Furthermore, among these sites, the phosphorylation of serine 94 and serine 515 on Cac1 have been proposed to be involved in the regulation of the recruitment of CAF-1 to chromatin in early S phase but not in regulating the association of CAF-1 with PCNA

(Jeffery et al., 2015). It would be interesting to also address the potential PTMs of Pcf1 in the interactions with HR factors as well as in the association of Pcf1 to the chromatin.

To reinforce my data, it would be more convincing to visualize the co-localization of CAF-1 and HR factors upon replication stress by microscopy. To this end, I have made an effort to 1) visualize the co-localization of Pcf1 and Rad51 after fixing MMS-treated cells, and 2) perform chromosome spread on MMS-treated cells followed by immunofluorescence (IF) microscopy. The first approach was not successful due to a fixation issue. The preliminary data of chromatin spread was encouraging, and it will be further optimized in the future.

Rqh1 partially impacts the association of Pcf1 to the chromatin upon replication stress. However, evidences are lacking for placing the interaction between Rqh1 and Pcf1 in this scenario. I have attempted with no success to examine whether the SUMOylation of Rqh1 is involved in modulating Rqh1-Pcf1 interaction after DNA damage by GST-pulldown assay. If this hypothesis is true, one could expect that the MMS-induced chromatin-bound Pcf1 would be reduced in cells deficient for Rqh1 SUMOylation. To achieve this, a *pcf1-GFP rqh1-SM* strain (a strain carrying mutated allele of *rqh1* that impairs SUMOylation (Rog et al., 2009)) should be generated and then subjected to the chromatin binding assay to ask if the SUMOylation of Rqh1 plays a role in the association of Pcf1 to the chromatin upon replication stress.

Recent studies have provided valuable data on the architecture of the CAF-1 complex as well as insights into the mechanisms of histone deposition by CAF-1 (reviewed by Sauer et al., 2018). CAF-1 as a histone chaperone contributes to maintaining genome stability. Deficiency in CAF-1 impairs replication-coupled chromatin assembly and leads to the instability of advancing forks which require the processing by the HR machinery (Clemente-Ruiz and Prado, 2009; Clemente-Ruiz et al., 2011; Endo et al., 2006a; Myung et al., 2003). However, the interplay between DNA repair events upon replication stress and chromatin restoration remains elusive. In this study, the crosstalk of CAF-1 and the HR factors during the RDR has been investigated. My data have revealed a rather dynamic role of each CAF-1 subunit in the RDR network and indicate that the association of CAF-1 to the chromatin is achieved by complex regulatory mechanisms consisting of multiple HR factors. In light of previous studies reporting the role CAF-1 in stabilizing the D-loop during RDR (Pietrobon et al., 2014; Hardy et al., publication in preparation), work from this study has added details on the regulatory mechanism of CAF-1 in this context. The different behaviors of each CAF-1 subunit in association to damaged chromatin also raise the necessity to study the significance of such discrepancy. Furthermore, high expression of CAF-1 has been

reported to associate to various cancer types, while replication stress is a major cause of genome instability and is a mark of cancer cells (Gaillard et al., 2015; Polo et al., 2010). Therefore, deciphering the role of CAF-1 in the RDR network could also provide potential clinical value.

Methods and Materials

1. Media and conditions for fission yeast growth

The rich medium, Yeast Extract (YE), and the minimal medium, Edinburgh Minimum Media L-Glutamate (EMM-G) were used for growing fission yeast cells. The growth media were supplemented with amino acids and bases listed below, unless noted otherwise.

Amino acids and bases: adenine hydrochloride hemihydrate (TCI A0150), L-leucine (Sigma Aldrich L8000), uracil (Sigma Aldrich U0750), L-histidine monohydrochloride monohydrate (Sigma Aldrich H8125), and L-arginine monohydrochloride (Sigma Aldrich A5131). All the supplements were prepared in stock solutions at a final concentration of 1.25%. The stock solutions were diluted 100-fold in the media to reach the working concentration. The pH of uracil stock solution was adjusted to 12.5, and the solution was stored at 4°C protected from light.

The YE media was supplemented with 2% of glucose (diluted from the 20% stock solution). For solid media, the YE and the EMM-G media were supplemented with 2% of agar. Antibiotics were added to the solid media in order to perform phenotype selection. The antibiotics used in this study are listed below.

Antibiotics: G418 (Invivogen, used for Kanamycin/Kan-resistant strains), nourseothricin (Werner Bioagents, used for ClonNat/Nat-resistant strains), and hygromycin (Invitrogen, used for Hygromycin/Hyg-resistant strains). All these antibiotics were applied to the media at a final concentration of 200 mg/L. The agar plates containing antibiotics were stored at 4°C.

Unless noted otherwise, cells were grown at 30°C. The liquid cultures were realized in the incubator at 30°C with 180 rpm agitation.

2. Fission yeast strains

Fission yeast strains used in this study were listed in **Table. strain**. Strains were constructed by classical genetic crossing and transformation (Bähler et al., 1998; Hentges et al., 2005; Moreno et al., 1991).

3. Genetic crossing

Two strains of opposite mating types were mixed in sterile water and then spotted onto a sporulation plate (SPA). The SPA plate was incubated at 25°C for 2-3 days for the cells to sporulate. The sporulation status was checked under a light microscope. Spores in a tetrad were separated by dissection using a micromanipulator (Singer), or random spore analysis. To perform

random spore analysis, a mixture of parental cells and tetrads was inoculated into a glusulase (NEE-154) solution at 100 U/mL for 3-5 days. The solution was then spread onto a fresh agar plate. Since the spores but not the cells are resistant to glusulase treatment, the spores will survive and grow on the agar plate.

The agar plates containing isolated spores were incubated at 30°C for several days (the time may vary depending on the genotype of the spores) until visible colonies appeared. The cells of desired genotype were then selected and inoculated into 50% YE-glycerol for long-term storage at -80°C.

4. Genetic transformation

Genetic transformation is an efficient technique to modify the genome of fission yeast at a specific locus. This technique utilizes PCR amplified DNA cassettes containing the sequence to be integrated into the genome and flanking homologous sequences to the gene to be modified. To generate such cassettes, primers consisting of two parts were designed: the first part was a 100 bp complementary sequence to the flanking region of the gene to be modified, and the second part is a 20 bp complementary sequence to the flanking region of a certain sequence (depending on the purpose of gene modification, this can be the sequence encoding an antibiotic marker or a fluorescent tag conjugated with an antibiotic marker) on the plasmid template. For gene replacement by a kanamycin, nourseothrycin or hygromycin marker, the template plasmids for PCR were pFA6a-kanMX6, pFA6a-natMX6 or pFA6a-hphMX6, respectively (Bähler et al., 1998; Hentges et al., 2005). The DNA cassettes were then transformed into fission yeast by using the method described by Bähler et al., 1998. The protocol of transformation used in the study is described below.

1) 2×10^8 log phase cells were collected by spinning down at 1200 x g for 4 min. 2) Wash the cell pellet once with equal volume of sterile water. Spin down at 1200 x g for 4 min. 3) Resuspend the cell pellet in 1 mL of sterile water. Transfer to an Eppendorf tube. Spin down at 17000 x g for 1 min. 4) Wash the cell pellet once with 1 mL of LiAc/TE (lithium acetate and tris-EDTA). Spin down at 17000 x g for 1 min. 5) Resuspend the cell pellet in 100 µL of LiAc/TE for per transformation. 6) Mix 100 µL of the concentrated cells with 2 µL of 10 mg/mL sheared herring testes DNA (Invitrogen) and 1 µg of purified transforming DNA. Incubate at room temperature for 10 min. 7) Mix gently with 260 µL of 40% PEG/LiAc/TE (Polyethylene glycol prepared in 1× LiAc/TE) and incubate for 30-60 min at 25°C. This step could be increased up to 2 h for better transformation efficiency. 8) Add 43 µL of DMSO and heat shock the cell suspension for 5 min at

42°C in water bath. Spin down at 17000 x g for 1 min. 9) Resuspend the cells in 50% EMM with essential supplements (15 mL H2O + 15 mL EMM). Incubate the cells on the roller at room temperature overnight. 10) Plate out the overnight culture to five YE agar plates following a serial dilution (ranging from 50 µL to 250 µL). 11) Incubate at 30°C for a few days until the colonies are visible. 12) Pick the colonies and inoculate them onto a fresh YE agar plate and incubate at 30°C until the cells grow into visible patches. 13) Replica-plate the cells onto selective plates and incubate at 30°C. 14) Streak out the colonies that are growing on the selective plate onto another fresh selective plate as for double-check. The colonies obtained are further checked by colony PCR to confirm fragment integration.

5. Colony PCR

Colony PCR allows a rapid check that can be directly performed on the cells without the requirement of DNA extraction. To perform the colony PCR, a tipful cells were inoculated into a PCR tube containing 20 µL of prepared PCR mix. The composition of the PCR mix is: 250 µM of dNTPs, OneTaq Standard Reaction buffer 1x (#B90225 NEB), 0.5 µM of forward and reverse primers, respectively, and 25 U/mL of OneTaq polymerase (#M0481L NEB).

6. Serial dilution assay (drop test)

The sensitivity of cells to different environmental genotoxic agents was characterized by the serial dilution assay which is also known as drop test.

Genotoxic agents used for drop tests in this study are hydroxyurea (HU, Sigma), camptothecin (CPT, Sigma), methyl methane sulfonate (MMS, Sigma), and Bleomycin (Bellon). UV-C irradiation generated by the Stratalinker (Stratagene) was also used to induce DNA damage to certain tested strains.

To perform a drop test, log phase cells were diluted in sterile water to different concentrations (ranging from $1x10^7$ to $1x10^3$ cells/mL, ten-fold difference between each two concentrations, five concentrations in total). Agar plates were prepared with implemented genotoxic drugs. 10 µL of cells at each concentration was dropped onto the agar plate, and the plates were incubated at 30°C. The drugs and their doses used in this study are listed in the table below.

Drug	**Stock solution**	**Final concentration applied in the agar plate**
MMS	100%	0.001%-0.03%

Bleomycin	2 mg/mL	0.1 µg/mL, 0.5 µg/mL, 1 µg/mL, 2 µg/mL,
CPT	10 mM in DMSO	2.5 µM, 5 µM, 7.5 µM, 10 µM
HU	1.2 M in water	2.5 mM, 5 mM, 7.5 mM, 10 mM
UV-C		100 J/m2, 200 J/m2, 250 J/m2

7. TCA protein extraction (total cellular protein extract)

TCA (Trichloroacetic acid) is widely used for the extraction of macromolecules including proteins, DNA and RNA. To perform TCA extraction, $1x10^8$ log phase cells in liquid culture were collected and their growth was stopped by 0.1% sodium azide. The cells were then pelleted at 4°C by spinning at 4000 rpm for 5 min. The cell pellet was suspended in 1 mL stop buffer (50 mM NaF, 10 mM NaN_3 in PBS 1X) and transferred to a special tube for the Precellys24 homogenizer (Bertin instruments). The cells were washed again with 1 mL stop buffer by spinning at 13000 rpm for 1 min at 4°C. The stop buffer was removed and the pellet was resuspended in 1 mL 20% TCA. Remove TCA and pellet the cells by spinning at 13000 rpm for 1 min at 4°C. The cell pellet was resuspended in 200 µL 20% TCA and glass beads were added in order to mechanically break down the cell walls by the homogenizer (at 6000 rpm, 3 rounds of 30 sec on with one minute interval between each two rounds, performed in the cold room). After the breakage, 400 µL 5% TCA was added directly to the lysate and the lysate was retrieved by isolating the glass beads. Spin down the lysate at 13000 rpm for 5 min at 4°C and keep only the pellet at the bottom of the tube. Resuspend the pellet in 200 µL TCA buffer (for preparing 10 mL: 5 mL of 2x SDS loading buffer, 2 mL Tris-HCl 1M pH 8 and 3 mL of sterile water). The samples were boiled at 95°C for 5 min to denature the proteins before forwarding to the Western Blot, otherwise the samples was snap frozen in liquid nitrogen and stored at -20°C.

8. Co-immuniprecipitation (Co-IP)

Co-IP is a technique used to characterize the interaction among proteins. The interpretation of co-IP results shows if certain proteins are in the same macromolecular complex. In this study, co-IP was employed to explore *in vivo* protein interactions in fission yeast cells. Due to the limit of antibodies for fission yeast, most of the proteins studied here were tagged with an epitope-tag (Pcf1 tagged with YFP- or GFP-tag, Pcf2 tagged with FLAG-tag, Pcf3 tagged with HA-tag and Rqh1

tagged with myc-tag). Co-IP was then performed by using an antibody against the epitope-tag, or using µMACS epitop-tagged protein isolation kits (Miltenyi Biotec).

For performing co-IP with an antibody against the epitope-tag, $5x10^8$ log phase cells were harvested and their growth was stopped with 0.1% sodium azide. The cells were then washed in 50 mL cold water and resuspended in 400 µL of EB buffer (50mM HEPES High salt, 50mM KOAc pH7.5, 5mM EGTA, 1% Triton X-100, 1mM PMSF, and Complete Protease Inhibitor EDTA-Free Tablet (Roche, 04 693 159 001)). Cell lysis was performed with a Precellys24 homogenizer (Bertin instruments) (at 6000 rpm, 3 rounds of 30 sec on with one minute interval between each two rounds, performed in the cold room). The cell lysate was then treated with 250 mU/µL of Benzonase (Novagen, NOVG 70664-3) for 30 min. After enzyme treatment, the cell lysate was spun down at 1300 rpm for 25 min at 4°C in order to retrieve the supernatant. The supernatant was recovered and an aliquot of 50 µL was saved as the INPUT control. To 300µl of the supernatant, antibodies against the epitope-tag of the protein of interest were added and incubated on a wheel for 1.5 hours at 4°C. Then, 20 µL of PBS-prewashed Dynabeads protein-G (Life Technologies, 10004D) were added to the lysate and then incubated at 4°C overnight. Alternatively, lysates were incubated overnight with 20 µL of antibody-coupled magnetic beads (anti-MYC from Life Technologies, 88842 or anti-HA from Life Technologies, 88836). After the overnight incubation, spin down the magnetic beads and take an aliquot of 50 µL of the surpernatant as UNBOUND control, then wash the beads three times in 1 mL EB Buffer on a wheel for 10 min at 4°C. Lastly, resuspend the beads in 30 µL Laemmli buffer and boil at 95°C for 5 min (IP fraction).

For performing co-IP using µMACS epitop-tagged protein isolation kits, the protein lysate was prepared in the same way as described above, except that RIPA buffer (Tris-HCl pH7,5 50mM, EDTA pH8 5mM, NaCl 150mM, Triton X-100 1%, $MgCl_2$ 1mM, NEM 10mM, β-glycerophosphate 60mM, PMSF 1mM, and Complete Protease Inhibitor EDTA-Free Tablet (Roche, 04 693 159 001)) was used instead of EB buffer. The immunopricipitation of the cell lysate was performed by following the protocol provided by the manufacturer.

Western Blot: Samples were loaded and migrated in an acrylamide 4-12% gradient gel (NuPAGE® Gels). The proteins were then blotted by semi-try transfer onto the nitrocellulose membrane (Amersham Biosciences) and stained with Ponceau to check the loading. Antibodies used for Western Blot in this study are listed in **Table. antibody**. The signals of proteins were developed by ECL-Plus kit (Amersham Biosciences).

9. Chromatin fraction assay

Chromatin fraction assay was used to characterize certain protein levels in the cytoplasm and nucleus. To perform the assay, harvest $5x10^8$ log phase cells and stop the growth with 0.1% Sodium Azide. Pellet the cells by spinning at 4000 rpm for 5 min, and all steps from then on should be carried out at 4°C. Wash the pellet once with 25 mL STOP buffer (0.9% Sodium Chloride, 1 mM Sodium Azide, 50 mM Sodium Fluoride, 10 mM EDTA), then once with 25 mL water, and finally once with 10 mL 1.2M sorbitol, by resuspending the cells in the solution followed by centrifugation at 4000 rpm for 5 min at 4°C. The washed cell pellet was then resuspended in 1 mL CB1 (50 mM Sodium Citrate, 40mM EDTA, 1.2M Sorbitol), with additional 250 µL of CB1 + 10 mg lysing enzyme (L2265 Sigma) + 100 µg of zymolyase 20T (Amsbio, 120491-1) + 2.5 µl β-MercaptoEthanol to obtain spheroplasts. The enzyme digestion was realized by incubating the mixture in 30°C water bath for 30 min to 1 hour until 90% cells were digested. Add 1.25 mL of ice-cold 1.2M sorbitol to the lysate and then spin down at 2000 rpm for 8 min. Discard supernatant, and wash the pellet (spheroplasts) twice with 1.2 mL of 1.2M sorbitol by centrifuging at 2000 rpm for 8 min. Discard the supernatant and keep pellet. Resuspend the pellet in 240 µL of lysis buffer (50mM potassium acetate, 2mM $MgCl_2$, 20mM HEPES pH7.9, 1% Triton X-100, 1mM PMSF, 60mM β-glycerophosphate, 0.2mM Na_3VO_4, 1µg/ml AEBSF and Complete Protease Inhibitor EDTA-Free Tablet (Roche, 04 693 159 001). After lysis, extracts were subsequently fractionated into soluble and pellet fractions by centrifugation. The insoluble chromatin-enriched pellet fraction was washed twice with the lysis buffer without 1 % Triton X-100 and digested with 100 Units of DNase I HC (ThermoScientific, EN0523) on ice for 15 min followed by 15min at RT. The DNase I-digested chromatin-enriched fraction was centrifuged for 5 min at 16000 g. Supernatant was designated as the chromatin fraction. Samples corresponding to total soluble and chromatin fractions were migrated and transferred on nitrocellulose membrane (Amersham Biosciences). Antibodies used for reviewing proteins of interest are listed in **Table. antibody**. The signals of proteins were developed by ECL-Plus kit (Amersham Biosciences).

10. GST-pulldown assay

GST-pulldown assay was employed in this study to explore the interactions between recombinant Pcf1 or Pcf1 fragments and proteins from cellular extract.

Recombinant protein purification: *E. coli* cells (BL21 gold) transformed with expression plasmids (pGEX6p1) were cultured at 37°C with 160 rpm agitation until OD600 reached 0.7-0.8, then 0.5

M IPTG was added to induce overnight protein expression. The cells were harvested by centrifugation at 6760 g for 15 min at 4°C. The cell pellet was washed once with lysis buffer (50 mM Tris-HCL pH 8.0, 500 mM NaCl, 1 mM EDTA, 5% Glycerol, 1% Triton X-100, 1 mM DTT, Complete Protease Inhibitor EDTA-Free Tablet (Roche, 04 693 159 001), adjust the pH of the buffer to 8.2), and then snap frozen in liquid nitrogen before being stored at -80°C. Cells were lysed by a disruptor (Constant Systems Ltd, 2k bar, only once) in ice-cold lysis buffer (4 mL lysis buffer for 1.5 g cells), and the lysate was clarified by spinning at 20000 rpm at 4°C for 30 min, the supernatant was recovered. Then lysis buffer-washed 50% GSH-beads (Agarose Bead Technologies ABT) were added to the supernatant and incubated on a wheel at 4°C for 1.5 h in order to bind the GST-tagged proteins. After the binding, the beads were isolated and washed four times by the incubation with 1.5 mL lysis buffer on a wheel followed by spinning at 500 g for 5 min at 4°C. After all washes, estimate the volume of the beads, then add v/v of storage buffer (50 mM Tris-HCl pH 8.0, 500 mM NaCl, DTT 1mM, 45% glycerol) to the beads in order to obtain 50% GST-protein-matrix. Aliquots of 100 µL were made and stored at -20°C.

GST-pulldown reaction: Cell lysates of fission yeast were collected as described for co-IP. 200 µL of cell lysates were incubated with 20 µL of 50% GST-protein-matrix (beads) on a wheel at 4°C for 2.5 h. After the incubation, the beads were washed four times by generally resuspending in 1 mL high-salt EB buffer (700 mM NaCl) followed by spinning at 500g for 5 min at 4°C (no on-wheel incubation required). 20 µL of 2x Laemmli buffer was added to the washed beads and boiled at 95°C for 10 min. The samples were then stored at -20°C or forwarded to the Western Blot.

11. *In vivo* chromatin binding assay

Chromatin binding assay was performed to visualize the association of proteins of interest to the chromatin in response to DNA damage. The assay was performed based on the method previously described by Kearsay et al. (Kearsey et al., 2005) with some modification.

To perform the assay, $1.5x10^8$ log phase cells were harvested with 0.1% sodium azide and washed in 1.8 mL ice-cold EMM sorbitol buffer (1.2M sorbitol, 15mM KH phallate, 15mM Na_2HPO_4, 90mM NH_4Cl, pH7). Cells were spheroplasted in 500 µL EMM sorbitol buffer containing 10mM DTT and 2mg of zymolyase 20T (Amsbio, 120491-1) by incubating at 32°C for 10-20 minutes with gentle inversion every 5 min until 95% of the cells were digested. After the digestion, the spheroplasts (cell pellet) were washed twice with 2 mL ice-cold EMM sorbitol buffer and once with 2 mL ice-cold extraction buffer (20 mM PIPES-KOH pH 6.8, 0.4M sorbitol, 150mM KAc, 2mM MgAc). Cells were then resuspended in protease inhibitor-added (Roche, 04

693 159 001) extraction buffer with or without 1% triton. The samples without triton served as "-Triton CONTROL" and were kept on ice, while the samples with triton (+Triton) were incubated at 20°C for 5 min with gentle inversion every minute, in order to permeablize the membrane. Finally, cells were pelleted then incubated in 2 mL ice-cold methanol for 6 min before being stocked in 1 mL cold acetone at -20°C.

Slides preparation for microscopy: Take out the acetone-fixed samples from -20°C and resuspend the cells well by inverting the tubes gently. 100 µL of the sample was pelleted by spinning at 4000 rpm for 1 min at 4°C. Acetone was removed and the cells were resuspended in 100 µL 0.1 µg/mL hoechst (prepared in sterile water) to have nuclei stained. Mount 2 µL of the cells onto 1.4% EMM-agar covered slide. Dry the slide under the safehood and then cover it with an ethanol-cleaned cover slip.

Image acquisition: A 3D decovelution microscope equipped with an oil immersion 100X objective (provided by PICT-IBiSA Orsay Imaging facility of Institut Curie) was used for performing microscopy on chromatin binding assay samples. Image acquisition was performed with MetaMorph software (Molecular Devices). Signals from three channels: white field, DAPI and FITC were captured in z-stacks.

Image analysis: The images were analyzed by quantifying the average nuclear Pcf1-GFP signal using ImageJ/Fiji software. To analyze, a z-project was first made based on the z-stack obtained from DAPI or FITC channel. According to the signal from the z-project of DAPI channel, the area of nuclear staining was selected by using the "freehand selection tool"; the size of the area was measured (S) and the selected nuclear staining area was saved (mask). The mask was then applied to the z-project of FITC channel to measure the fluorescence intensity of Pcf1-GFP signal (FI); the mask was next dragged to cytoplasmic area of the same cell to measure the background fluorescence intensity (BG). To calculate the average nuclear Pcf1-GFP signal, the formula: (FI-BG)/S was used. At least 50 cells were analyzed for each sample. Quantification and statistical analysis were made using Graphpad Prism software.

Table. strain. List of strains used in this study

Strain	*Genotype*	*Notes*
VP003	*h+ pcf1::Kan, ura4-D18, leu1-32, ade6 M-216*	*Francesconi*
VP005	*h+ pcf2::Kan, ura4-D18, leu1-32, ade6 M-216*	*Francesconi*
VP007	*h+ pcf3::Kan, ura4-D18, leu1-32, ade6 M-216*	*Francesconi*
VP394	*h- smt0, ade6-704, leu1-32, ura4-D18, pcf1:YFP-Kan*	*Pietrobon*

SL80	*h+ rqh1::kan ade6-704 leu1-32 ura4D18*	*Lambert*
JH69	*h- pcf1-GFP*	*T. Kunoh*
VP520	*h- pcf1-YFP:Kan rqh1-Myc:Kan ade6-704, leu1-32, ura4-D12*	*Pietrobon*
SL75	*h- ade6-704, leu1-32, ura4-D18*	*Lambert*
SL76	*h+ ade6-704, leu1-32, ura4-D18*	*Lambert*
SL782	*h+ rqh1-myc :kan ade6-704, leu1-32, ura4-D18*	*Lambert*
DD 001	*h+ pcf2-myc (4.5 rep)-kanR rqh1-HA :kanR ura4-D18 leu1-32*	*Dingli DAI*
DD 004	*h+ pcf1-YFP:kanR rqh1-myc:kanR pcf2::ura4+ ade6-704 leu1-32 ura4-D18*	*Dingli DAI*
DD 006	*h- pcf1-YFP:kanR rqh1-myc:kanR pcf2::ura4+ ade6-704 leu1-32 ura4-D18*	*Dingli DAI*
DD 007	*h- pcf1-YFP:kanR rqh1-myc:kanR pcf2::ura4+ ade6-704 leu1-32 ura4-D18*	*Dingli DAI*
DD 011	*h- rqh1-myc:kanR ade6-704 leu1-32 ura4-D18*	*Dingli DAI*
DD 013	*h- pcf 3-HA:kanR rqh1-myc :kanR ade6-704 leu1-32 ura4-D18*	*Dingli DAI*
DD 021	*h+ pcf1-YFP:kanR pcf2-myc:kanR rqh1-HA:kanR leu1-32 ura4-D18*	*Dingli DAI*
DD 024	*h- rqh1-myc:kanR pcf1-YFP ade6-704 leu1-32 ura4-D18*	*Dingli DAI*
DD 025	*h- rqh1-myc:kanR pcf1-YFP pcf3-HA ade6-704 leu1-32 ura4-D18*	*Dingli DAI*
DD 030	*h+ pcf2-5FLAG:hphMX6 leu1-32 ade6-704 ura4-D18*	*Dingli DAI*
DD 031	*rqh1-myc:kanR pcf1-YFP:kanR pcf2-5FLAG:hphMX6 leu1-32 ade6-704 ura4-D18*	*Dingli DAI*
DD 037	*pcf1-YFP:kanR pcf2-5FLAG:hphMX6 leu1-32 ade6-704 ura4-D18*	*Dingli DAI*
DD 038	*h+ rqh1-myc:kanR pcf2-5FLAG:hphMX6 leu1-32 ade6-704 ura4-D18*	*Dingli DAI*
DD 040	*h+ pcf2-5FLAG:hphMX6 leu1-32 ade6-704 ura4-D18*	*Dingli DAI*
DD 042	*h+ pcf2-3HA:kanMX6 leu1-32 ade6-704 ura4-D18*	*Dingli DAI*
DD 046	*rqh1-myc:kanR pcf1-YFP:kanR pcf2-3HA:kanMX6 leu1-32 ade6-704 ura4-D18*	*Dingli DAI*
DD 047	*pcf1-YFP:kanR pcf2-3HA:kanMX6 leu1-32 ade6-704 ura4-D18*	*Dingli DAI*
DD 048	*rqh1-myc:kanR pcf1-YFP:kanR pcf2-3HA:kanMX6 leu1-32 ade6-704 ura4-D18*	*Dingli DAI*
DD 050	*rqh1-myc:kanR pcf1-YFP:kanR pcf2-3HA:kanMX6 leu1-32 ade6-704 ura4-D18*	*Dingli DAI*
DD 053	*rqh1-myc:kanR pcf2-3HA:kanMX6 leu1-32 ade6-704 ura4-D18*	*Dingli DAI*
DD 056	*pcf1-YFP:kanR pcf2-3HA:kanMX6 leu1-32 ade6-704 ura4-D18*	*Dingli DAI*
DD 059	*h- pcf1::kanR rqh1-myc:kanR ade6-704 leu1-32 ura4-D18*	*Dingli DAI*
DD 060	*h+ pcf1::kanR rqh1-myc:kanR ade6-704 leu1-32 ura4-D18*	*Dingli DAI*
DD 061	*pcf1::kanR rqh1-myc:kanR pcf2-FLAG:hphMX6 ade6-704 leu1-32 ura4-D18*	*Dingli DAI*
DD 063	*pcf1::kanR rqh1-myc:kanR pcf3-HA ade6-704 leu1-32 ura4-D18*	*Dingli DAI*
DD 067	*h+ rqh1-myc:kanR pcf1-GFP pcf2-5FLAG:hphMX6 ura4-D18*	*Dingli DAI*
DD 069	*h+ rqh1-myc:kanR pcf1-GFP ura4-D18*	*Dingli DAI*
DD 071	*rqh1-myc:kanR pcf1-GFP pcf2-5FLAG:hphMX6*	*Dingli DAI*
DD072	*h- rqh1-myc:kanR pcf2-FLAG:hphMX6 pcf3-HA:kanR leu1-32 ade6-704 ura4-D18*	*Dingli DAI*
DD074	*h- pcf2-5FLAG:hphMX6 leu1-32 ade6-704 ura4-D18*	*Dingli DAI*
DD076	*h+ rqh1-myc:kanR pcf2::ura4+ ade6-704 leu1-32 ura4-D18*	*Dingli DAI*
DD079	*h- pcf2-5FLAG:hphMX6 rqh1::kanR leu1-32 ade6-704 ura4-D18*	*Dingli DAI*
DD082	*h+ pcf1::kanR pcf2-5FLAG:hphMX6 leu1-32 ade6-704 ura4-D18*	*Dingli DAI*
DD086	*h+ rad51::kanR pcf2-5FLAG:hphMX6 leu1-32 ade6-704 ura4-D18*	*Dingli DAI*
DD087	*h+ rad51::kanR pcf2-5FLAG:hphMX6 leu1-32 ade6-704 ura4-D18*	*Dingli DAI*
DD090	*pcf1::kanR pcf2::ura4+ rqh1-myc:kanR ade6-704 leu1-32 ura4-D18*	*Dingli DAI*
DD091	*pcf1-GFP pcf2::kanR ura4-D18*	*Dingli DAI*
DD095	*h- pcf1-mcherry:kanR leu1-32 ade6-704 ura4-D18*	*Dingli DAI*

DD096	*h+ pcf1-mcherry:kanR leu1-32 ade6-704 ura4-D18*	*Dingli DAI*
DD097	*h+ pcf1-mcherry:kanR leu1-32 ade6-704 ura4-D18*	*Dingli DAI*
DD098	*h+ pcf1-mcherry:kanR leu1-32 ade6-704 ura4-D18*	*Dingli DAI*
DD099	*pcf1-pipboxmut :yfp -kanR rqh1-myc :kanR ade6-704 leu1-32 ura4-D18*	*Dingli DAI*
DD101	*pcf1-GFP rad51::kanR leu1-32 ura4-D18*	*Dingli DAI*
DD102	*pcf1-GFP rqh1::kanR ura4-D18*	*Dingli DAI*
DD106	*pcf1-GFP rad52::kanR ade6-704*	*Dingli DAI*
DD109	*h- rqh1-SM his3-D1 leu1-32 ura4-D18 ade6-210*	*Lab Julia Cooper*
DD110	*h- rqh1-8Gly-13xmyc::kanMX his3-D1 leu1-32 ura4-D18 ade6-210*	*Lab Julia Cooper*
DD111	*h- rqh1-SM-8Gly-13xmyc::kanMX taz::hygMX his3-D1 leu1-32 ura4-D18 ade6-210*	*Lab Julia Cooper*
DD112	*h+ pcf1-GFP rqh1::kanR pcf2::kanR ura4-D18*	*Dingli DAI*
DD113	*rqh1-SM-8Gly-13xmyc::kanMX his3-D1 leu1-32 ura4-D18 ade6-704*	*Dingli DAI*
DD115	*pcf1-GFP rad54::natR ade6-704 ura4-D18*	*Dingli DAI*
DD117	*pcf2-5FLAG:hphMX6 pcf3-HA:kanR leu1-32 ade6-704 ura4-D18*	*Dingli DAI*
DD119	*pcf1-GFP rad51::kanR*	*Dingli DAI*
DD120	*h- pcf1-pip-mut-GFP-natR leu1-32 ade6-704 ura4-D18*	*Dingli DAI*
DD121	*h+ pcf1-GFP-natR leu1-32 ade6-704 ura4-D18*	*Dingli DAI*
DD122	*h+ pcf2-GFP-natR leu1-32 ade6-704 ura4-D18*	*Dingli DAI*
DD123	*h+ pcf3-GFP-natR leu1-32 ade6-704 ura4-D18*	*Dingli DAI*
DD120A	*h- pcf1-pip-mut-GFP-natR leu1-32 ade6-704 ura4-D18*	*Dingli DAI*
DD121A	*h+ pcf1-GFP-natR leu1-32 ade6-704 ura4-D18*	*Dingli DAI*
DD122A	*h+ pcf2-GFP-natR leu1-32 ade6-704 ura4-D18*	*Dingli DAI*
DD123A	*h+ pcf3-GFP-natR leu1-32 ade6-704 ura4-D18*	*Dingli DAI*
DD126	*h+ ssb3::kanMX4 leu1-32 ura4-D18*	*Paul Russell*
DD133	*pcf1-GFP ssb3::kanMX6 ura4-D18*	*Dingli DAI*
DD135	*h- pcf2-GFP-natR leu1-32 ade6-704 ura4-D18*	*Dingli DAI*
DD136	*rad51::kanR pcf2-GFP-natR leu1-32 ade6-704 ura4-D18*	*Dingli DAI*
DD154	*pcf2-GFP-natR pcf1::kanR leu1-32 ade6-704 ura4-D18*	*Dingli DAI*
DD156	*pcf2-GFP-natR rad52::kanR leu1-32 ade6-704 ura4-D18*	*Dingli DAI*
DD158	*pcf2-GFP-natR rqh1::kanR leu1-32 ade6-704 ura4-D18*	*Dingli DAI*
DD160	*pcf2-GFP-natR ssb3::kanMX4 leu1-32 ura4-D18*	*Dingli DAI*
DD162	*h+ rad3::hph leu1-32 ura4-D18 ade6-704*	*Dingli DAI*
DD163	*rad3::hph leu1-32 ura4-D18 ade6-704*	*Dingli DAI*
DD165	*h- pcf1-GFP rad3::hph ura4-D18*	*Dingli DAI*
DD166	*pcf1-GFP rad3::hph*	*Dingli DAI*

Table. primer. Primers used in this study

Primer	*Sequence*
Pcf1-FL-F	*CCCGGATCCATGAATAGTGAAAGTGTTGATTC*
Pcf1-FL-R	*CCCGAATTCTTAAGAGGATAAAAGGGATGCA*
Pcf1-1-295-R	*CCCGAATTCTAAACAAGATAAAATTTCTTGAGG*

Pcf1-296-449 F	*CCCGGATCCTCACAGATTCCTATTAAATTCATT*
Pcf1-296-449R	*CCCGAATTCAGAAGCCCATAAATCCTCTTTA*
Pcf1-450-544 F	*CCCGGATCCCAAGATACTGCTCCAGCGTC*
Pcf1-296-351 R	*CCCGAATTCATCAGCTACCCATTCTGCTTC*
Pcf1-390-449 F	*CCCGGATCCAGTGTCAATGCTTCTAATACC*
For Bam pcf1	*GTACTTGAAATCCAGCAAGTA*
Rev Eco pcf1	*TCAGAGGTTTTCACCGTCATC*
For middle pcf1	*CTGAATGAGTTTGAGAAAGAGTT*
Fw-FLAG-tagging	*CTACTACAACACTAATTCCCAGAAAAGTTGAATCTTCAAAAGTATCAAAGAAGCGTATTGCACCTACC CCCGTTTATCCACGGATCCCCGGGGGAGGTGG*
Fw-in-pcf2	*CAAGACAATACGGCTGGGGG*
Re-in-kan	*CGGGCTTCCCATACAATCGA*
Fw-in-kan	*GCAGTTTCATTTGATGCTCGATG*
Re-after-pcf2	*GTTATGTGTAAGAGGGTTCCTCAATACG*
Re-in-hph	*CTGCATCAGGTCGGAGACGC*
Fw-in-hph	*CCGTGGTTGGCTTGTATGGA*
Fw-in-pcf2-seq	*CTGTAATTACCTTTGAACCTGG*
Re-after-STOP-seq	*GCTTATATCTAAGCAAATTACCG*
Fw-in-pcf3	*GAGGCACAATGTATTGCTTCGG*
Re-after-STOP	*AGCCCTGCAACATACCCATC*
Fw-in-rqh1	*GAAGAAGTGGATGGTCAACGG*
Re-after-STOP	*CGCACATGTACAATAAACGAACC*
Fw-643-in-pcf1	*GCATCAGATGTCCCTTTCCA*
Rev-165-after-pcf1	*GACAAAGCTTACAATTAAGGGCC*
Fw-391-in-kan	*CAGCGATCGCGTATTTCGTC*
Rqh1-FL-F	*CCCCCATGGGAATGACAGTAACGAAAACAAA*
Rqh1-FL-R	*CCCGGATCCTTAACGATAATTTTGCTTAACC*
Fw-SalI-PCF1	*AAAGTCGACTAAATAGTGAAAGTGTTGATTCAG*
Rev-NotI-PCF1	*AAGCGGCCGCTTAAGAGGATAAAAGGGATGC*
Fw-SalI-RQH1	*GGGGTCGACATGTGGAGCCATCCACAGTTTGAAAAGACAGTAACGAAAACAAACCTT*
Rev-NotI-RQH1	*AAGCGGCCGCTTAACGATAATTTTGCTTAACC*

Table. antibody. Antibodies used in this study

Antibody	*Antigen*	*Origin*	*Dilution*	*Supplier*
Primary	*GFP*	*mouse*	*1/1000*	*Roche 11814460001*
	GFP	*rabbit*	*1/1000*	*Thermo scientific a-11122*
	MYC	*Mouse*	*1/1000*	*Santa Cruz sc-40*
	MYC	*rabbit*	*1/500*	*Santa Cruz sc-789*
	FLAG	*mouse*	*1/1000*	*Sigma F1804*
	FLAG	*mouse*	*1/1000*	*Sigma F3165*
	HA	*mouse*	*1/1000*	*Santa Cruz sc-57592*
	HA	*Rat*	*1/1000*	*Roche 11867423001*
	Histone H3	*rabbit*	*1/2000*	*Abcam ab1791*
	Histone H4	*rabbit*	*1/50000*	*Millipore 05-858*

	H2AX	*rabbit*	*1/10000*	*Upstate 07-745*
	PCNA	*mouse*	*1/500*	*Santa Cruz sc-56*
	GST	*mouse*	*1/1000*	*Santa Cruz sc-138*
	HIS	*mouse*	*1/1000*	*Proteintech 66005-1-lg*
	Rad51	*rabbit*	*1/500*	*Santa Cruz sc-8349*
	Rad52	*rabbit*	*1/5000*	*Abcam ab63800*
	Tubulin	*Rat*	*1/5000*	*Abcam ab6160*
Secondary	*Anti-mouse*	*goat*	*1/1000*	*115-035-003*
	Anti-rabbit	*goat*	*1/1000*	*Jackson Immune Research 111-035-144*
	Anti-rat	*Chicken*	*1/1000*	*Santa Cruz sc-2964*

References

Adam, S., Polo, S., and Almouzni, G. (2013). 426.Transcription recovery after DNA damage requires chromatin priming by the H3. 3 histone chaperone HIRA. Cell.

Adams, M.D., McVey, M., and Sekelsky, J.J. (2003). 153. Drosophila BLM in double-strand break repair by synthesis-dependent strand annealing. Science (80-.).

Aguilera, A., and García-Muse, T. (2012). 30. R Loops: From Transcription Byproducts to Threats to Genome Stability. Mol. Cell.

Ahmad, K., and Henikoff, S. (2002). The histone variant H3.3 marks active chromatin by replication-independent nucleosome assembly. Mol. Cell.

Ait Saada, A., Teixeira-Silva, A., Iraqui, I., Costes, A., Hardy, J., Paoletti, G., Fréon, K., and Lambert, S.A.E. (2017). 525. Unprotected Replication Forks Are Converted into Mitotic Sister Chromatid Bridges. Mol. Cell.

Alabert, C., Bianco, J.N., and Pasero, P. (2009). 159. Differential regulation of homologous recombination at DNA breaks and replication forks by the Mrc1 branch of the S-phase checkpoint. EMBO J.

Albuquerque, C.P., Smolka, M.B., Payne, S.H., Bafna, V., Eng, J., and Zhou, H. (2008). 583. A Multidimensional Chromatography Technology for In-depth Phosphoproteome Analysis. Mol. Cell. Proteomics.

Alexeev, A., Mazin, A., and Kowalczykowski, S.C. (2003). Rad54 protein possesses chromatin-remodeling activity stimulated by the Rad51-ssDNA nucleoprotein filament. Nat. Struct. Biol.

Allan, J., Hartman, P.G., Crane-robinson, C., and Aviles, F.X. (1980). 202. The structure of histone H1 and its location in chromatin. Nature.

Allan, J., Mitchell, T., Harborne, N., Bohm, L., and Crane-Robinson, C. (1986). 201. Roles of H1 domains in determining higher order chromatin structure and H1 location. J. Mol. Biol.

Anand, R.P., Lovett, S.T., and Haber, J.E. (2013). 97. Break-induced DNA replication. Cold Spring Harb. Perspect. Biol.

Anderson, H.E., Wardle, J., Korkut, S. V., Murton, H.E., Lopez-Maury, L., Bahler, J., and Whitehall, S.K. (2009). 409. The Fission Yeast HIRA Histone Chaperone Is Required for Promoter Silencing and the Suppression of Cryptic Antisense Transcripts. Mol. Cell. Biol.

Anderson, H.E., Kagansky, A., Wardle, J., Rappsilber, J., Allshire, R.C., and Whitehall, S.K. (2010). 576. Silencing mediated by the Schizosaccharomyces pombe HIRA complex is dependent upon the Hpc2-like protein, Hip4. PLoS One.

Andrews, A.J., and Luger, K. (2011). 198. Nucleosome Structure(s) and Stability: Variations on a Theme. Annu. Rev. Biophys.

Antony, E., Tomko, E.J., Xiao, Q., Krejci, L., Lohman, T.M., and Ellenberger, T. (2009). 522. Srs2 Disassembles Rad51 Filaments by a Protein-Protein Interaction Triggering ATP Turnover and Dissociation of Rad51 from DNA. Mol. Cell.

Arents, G., and Moudrianakis, E.N. (1995). 208. The histone fold: a ubiquitous architectural motif utilized in DNA compaction and protein dimerization. Proc. Natl. Acad. Sci.

Arents, G., Burlingame, R.W., Wang, B.C., Love, W.E., and Moudrianakis, E.N. (1991). 207. The nucleosomal core histone octamer at 3.1 A resolution: a tripartite protein assembly and a left-handed superhelix. Proc. Natl. Acad. Sci.

Arora, H., Chacon, A.H., Choudhary, S., Mcleod, M.P., Meshkov, L., Nouri, K., and Izakovic, J. (2014). 538. Bloom syndrome. Int. J. Dermatol.

Ashton, T.M., Mankouri, H.W., Heidenblut, A., McHugh, P.J., and Hickson, I.D. (2011). 560. Pathways for Holliday Junction Processing during Homologous Recombination in Saccharomyces cerevisiae. Mol. Cell. Biol.

van Attikum, H., and Gasser, S.M. (2005). ATP-dependent chromatin remodeling and DNA double-strand break repair. Cell Cycle.

Aylon, Y., Liefshitz, B., Bitan-Banin, G., and Kupiec, M. (2003). Molecular dissection of mitotic recombination in the yeast Saccharomyces cerevisiae. Mol. Cell. Biol.

Ayoub, N., Jeyasekharan, A.D., Bernal, J.A., and Venkitaraman, A.R. (2008). 415. HP1-β mobilization promotes chromatin changes that initiate the DNA damage response. Nature.

Bachrati, C.Z., Borts, R.H., and Hickson, I.D. (2006). 152. Mobile D-loops are a preferred substrate for the Bloom's syndrome helicase. Nucleic Acids Res.

Bähler, J., Wu, J.Q., Longtine, M.S., Shah, N.G., McKenzie, A., Steever, A.B., Wach, A., Philippsen, P., and Pringle, J.R. (1998). 306. Heterologous modules for efficient and versatile PCR-based gene targeting in Schizosaccharomyces pombe. Yeast.

Balajee, A.S., and Geard, C.R. (2001). 448. chromatin-bound PCNA complex formation triggered by DNA damage occurs independent of the ATM gene product in human cells. Nucleic Acids Res.

Baldeyron, C., Soria, G., Roche, D., Cook, A.J.L., and Almouzni, G. (2011). 417. HP1α recruitment to DNA damage by p150CAF-1 promotes homologous recombination repair. J. Cell Biol.

Barrera-Oro, J., Liu, T.Y., Gorden, E., Kucherlapati, R., Shao, C., and Tischfield, J.A. (2008). 345. Role of the mismatch repair gene, Msh6, in suppressing genome instability and radiation-induced mutations. Mutat. Res. - Fundam. Mol. Mech. Mutagen.

Basu, A.K., Pande, P., and Bose, A. (2017). 317. Translesion synthesis of 2-deoxyguanosine lesions by eukaryotic DNA polymerases. Chem. Res. Toxicol.

Baudat, F., Imai, Y., and De Massy, B. (2013). 566. Meiotic recombination in mammals: Localization and regulation. Nat. Rev. Genet.

Baxevanis, A.D., Godfrey, J.E., and Moudrianakis, E.N. (1991). 228. Associative Behavior of the Histone (H3-H4)2Tetramer: Dependence on Ionic Environment. Biochemistry.

Bebenek, K., Garcia-Biaz, M., Patishall, S.M., and Kunkel, T.A. (2005). 67. Biochemical properties of Saccharomyces cerevisiae DNA polymerase IV. J. Biol. Chem.

Ben-Shahar, T.R., Castillo, A.G., Osborne, M.J., Borden, K.L.B., Kornblatt, J., and Verreault, A. (2009). 256. Two Fundamentally Distinct PCNA Interaction Peptides Contribute to Chromatin Assembly Factor 1 Function. Mol. Cell. Biol.

Bennett, C.B., Lewis, A.L., Baldwin, K.K., and Resnick, M.A. (1993). 333. Lethality induced by a single site-specific double-strand break in a dispensable yeast plasmid. Proc. Natl. Acad. Sci.

Benson, F.E., Baumann, P., and West, S.C. (1998). Synergistic actions of Rad51 and Rad52 in recombination and DNA repair. Nature.

Berkovich, E., Monnat, R.J., and Kastan, M.B. (2008). 377. Assessment of protein dynamics and DNA repair following generation of DNA double-strand breaks at defined genomic sites. Nat. Protoc.

Bernstein, K.A., Reid, R.J.D., Sunjevaric, I., Demuth, K., Burgess, R.C., and Rothstein, R. (2011). 509. The Shu complex, which contains Rad51 paralogues, promotes DNA repair through inhibition of the Srs2 anti-recombinase. Mol. Biol. Cell.

Bhargava, R., Onyango, D.O., and Stark, J.M. (2016). 84. Regulation of Single-Strand Annealing and its

Role in Genome Maintenance. Trends Genet.

Bianchi, M.E., and Agresti, A. (2005). 380. HMG proteins: Dynamic players in gene regulation and differentiation. Curr. Opin. Genet. Dev.

Bianco, P.R., Tracy, R.B., and Kowalczykowski, S.C. (1998). 174. DNA strand exchange proteins: a biochemical and physical comparison. Front. Biosci.

Billon, P., and Côté, J. (2012). Precise deposition of histone H2A.Z in chromatin for genome expression and maintenance. Biochim. Biophys. Acta - Gene Regul. Mech.

Binz, S.K., Sheehan, A.M., and Wold, M.S. (2004). 127. Replication Protein A phosphorylation and the cellular response to DNA damage. DNA Repair (Amst).

Black, B.E., Foliz, D.R., Chakravarthy, S., Luger, K., Woods, V.L., and Cleveland, D.W. (2004). 536? Structural determinants for generating centromeric chromatin. Nature.

Blanko, E.R., Kadyrova, L.Y., and Kadyrov, F.A. (2016). 435. DNA mismatch repair interacts with CAF-1- and ASF1A-H3-H4-dependent histone (H3-H4)2tetramer deposition. J. Biol. Chem.

Blanpain, C., Mohrin, M., Sotiropoulou, P.A., and Passegué, E. (2011). 32. DNA-damage response in tissue-specific and cancer stem cells. Cell Stem Cell.

Boddy, M.N., Lopez-Girona, A., Shanahan, P., Interthal, H., Heyer, W.D., and Russell, P. (2000). Damage tolerance protein Mus81 associates with the FHA1 domain of checkpoint kinase Cds1. Mol. Cell. Biol.

Boddy, M.N., Gaillard, P.H.L., McDonald, W.H., Shanahan, P., Yates, J.R., and Russell, P. (2001). 501. Mus81-Eme1 are essential components of a Holliday junction resolvase. Cell.

Boehm, E.M., Gildenberg, M.S., and Washington, M.T. (2016). 260. The Many Roles of PCNA in Eukaryotic DNA Replication. In Enzymes, p.

Boiteux, S., and Guillet, M. (2004). 13. Abasic sites in DNA: Repair and biological consequences in Saccharomyces cerevisiae. DNA Repair (Amst).

Bosco, G., and Haber, J.E. (1998). 482. Chromosome break-induced DNA replication leads to nonreciprocal translocations and telomere capture. Genetics.

Bowman, A., Ward, R., Wiechens, N., Singh, V., El-Mkami, H., Norman, D.G., and Owen-Hughes, T. (2011). 247. The Histone Chaperones Nap1 and Vps75 Bind Histones H3 and H4 in a Tetrameric Conformation. Mol. Cell.

Brachet, E., Béneut, C., Serrentino, M.E., and Borde, V. (2015). 449. The CAF-1 and Hir histone chaperones associate with sites of meiotic double-strand breaks in budding yeast. PLoS One.

Branzei, D., Sollier, J., Liberi, G., Zhao, X., Maeda, D., Seki, M., Enomoto, T., Ohta, K., and Foiani, M. (2006). 559. Ubc9- and Mms21-Mediated Sumoylation Counteracts Recombinogenic Events at Damaged Replication Forks. Cell.

Brem, R.B., Yvert, G., Clinton, R., Kruglyak, L., DeRisi, J.L., Iyer, V.R., Brown, P.O., Wodicka, L., Dong, H., Mittmann, M., et al. (2002). 190. Genetic dissection of transcriptional regulation in budding yeast. Science.

Brown, D.T., Izard, T., and Misteli, T. (2006). 203. Mapping the interaction surface of linker histone H10with the nucleosome of native chromatin in vivo. Nat. Struct. Mol. Biol.

Bugreev, D. V., Mazina, O.M., and Mazin, A. V. (2006). Rad54 protein promotes branch migration of Holliday junctions. Nature.

Bugreev, D. V., Yu, X., Egelman, E.H., and Mazin, A. V. (2007a). 151. Novel pro- and anti-

recombination activities of the Bloom's syndrome helicase. Genes Dev.

Bugreev, D. V., Hanaoka, F., and Mazin, A. V. (2007b). Rad54 dissociates homologous recombination intermediates by branch migration. Nat. Struct. Mol. Biol.

Burgess, R.C., Rahman, S., Lisby, M., Rothstein, R., and Zhao, X. (2007). 125. The Slx5-Slx8 Complex Affects Sumoylation of DNA Repair Proteins and Negatively Regulates Recombination. Mol. Cell. Biol.

Burma, S., Chen, B.P., Murphy, M., Kurimasa, A., and Chen, D.J. (2001). 41. ATM phosphorylates histone H2AX in response to DNA double-strand breaks. J. Biol. Chem.

Buschbeck, M., and Hake, S.B. (2017). 213. Variants of core histones and their roles in cell fate decisions, development and cancer. Nat. Rev. Mol. Cell Biol.

Bustin, M., and Reeves, R. (1996). 381. High-Mobility-Group Chromosomal Proteins: Architectural Components That Facilitate Chromatin Function. Prog. Nucleic Acid Res. Mol. Biol.

Cai, Y., Geacintov, N.E., and Broyde, S. (2012). 319. Nucleotide excision repair efficiencies of bulky carcinogen-DNA adducts are governed by a balance between stabilizing and destabilizing interactions. Biochemistry.

Caldecott, K.W. (2008). 14. Single-strand break repair and genetic disease. Nat. Rev. Genet.

Campos-Doerfler, L., Syed, S., and Schmidt, K.H. (2018). 566. Sgs1 binding to Rad51 stimulates homology-directed DNA repair in saccharomyces cerevisiae. Genetics.

Campos, E.I., and Reinberg, D. (2009). 214. Histones: Annotating Chromatin. Annu. Rev. Genet.

Cannavo, E., and Cejka, P. (2014). 496. Sae2 promotes dsDNA endonuclease activity within Mre11-Rad50-Xrs2 to resect DNA breaks. Nature.

Caron, P., Aymard, F., Iacovoni, J.S., Briois, S., Canitrot, Y., Bugler, B., Massip, L., Losada, A., and Legube, G. (2012). 401. Cohesin protects genes against γH2AX induced by DNA double-strand breaks. PLoS Genet.

Carpy, A., Krug, K., Graf, S., Koch, A., Popic, S., Hauf, S., and Macek, B. (2014). 311. Absolute proteome and phosphoproteome dynamics during the cell cycle of Schizosaccharomyces pombe (Fission Yeast). Mol. Cell. Proteomics.

Carr, A.M., and Lambert, S. (2013). 154. Replication stress-induced genome instability: The dark side of replication maintenance by homologous recombination. J. Mol. Biol.

Carr, a M., Schmidt, H., Kirchhoff, S., Muriel, W.J., Sheldrick, K.S., Griffiths, D.J., Basmacioglu, C.N., Subramani, S., Clegg, M., and Nasim, A. (1994a). 492. The rad16 gene of Schizosaccharomyces pombe: a homolog of the RAD1 gene of Saccharomyces cerevisiae. Mol. Cell. Biol.

Carr, A.M., Dorrington, S.M., Hindley, J., Phear, G.A., Aves, S.J., and Nurse, P. (1994b). 223. Analysis of a histone H2A variant from fission yeast: evidence for a role in chromosome stability. MGG Mol. Gen. Genet.

Carvalho, C.M.B., Pehlivan, D., Ramocki, M.B., Fang, P., Alleva, B., Franco, L.M., Belmont, J.W., Hastings, P.J., and Lupski, J.R. (2013). 557. Replicative mechanisms for CNV formation are error prone. Nat. Genet.

Cejka, P., Cannavo, E., Polaczek, P., Masuda-Sasa, T., Pokharel, S., Campbell, J.L., and Kowalczykowski, S.C. (2010). 130. DNA end resection by Dna2-Sgs1-RPA and its stimulation by Top3-Rmi1 and Mre11-Rad50-Xrs2. Nature.

Chafin, D.R., Vitolo, J.M., Henricksen, L.A., Bambara, R.A., and Hayes, J.J. (2000). 430. Human DNA ligase I efficiently seals nicks in nucleosomes. EMBO J.

Chanet, R., Heude, M., Adjiri, A., Maloisel, L., and Fabre, F. (1996). Semidominant mutations in the yeast Rad51 protein and their relationships with the Srs2 helicase. Mol. Cell. Biol.

Chang, H.H.Y., Pannunzio, N.R., Adachi, N., and Lieber, M.R. (2017). 61. Non-homologous DNA end joining and alternative pathways to double-strand break repair. Nat. Rev. Mol. Cell Biol.

Chen, L., Trujillo, K., Sung, P., and Tomkinson, A.E. (2000). 66. Interactions of the DNA ligase IV-XRCC4 complex with DNA ends and the DNA-dependent protein kinase. J. Biol. Chem.

Chi, P., Van Komen, S., Sehorn, M.G., Sigurdsson, S., and Sung, P. (2006). 132. Roles of ATP binding and ATP hydrolysis in human Rad51 recombinase function. DNA Repair (Amst).

Chiolo, I., Minoda, A., Colmenares, S.U., Polyzos, A., Costes, S. V., and Karpen, G.H. (2011). 416. Double-strand breaks in heterochromatin move outside of a dynamic HP1a domain to complete recombinational repair. Cell.

Cho, N.W., Dilley, R.L., Lampson, M.A., and Greenberg, R.A. (2014). 362. Interchromosomal homology searches drive directional ALT telomere movement and synapsis. Cell.

Choi, E.H., Yoon, S., Park, K.S., and Kim, K.P. (2017). 158. The Homologous Recombination Machinery Orchestrates Post-replication DNA Repair during Self-renewal of Mouse Embryonic Stem Cells. Sci. Rep.

Chou, C.C., and Wang, A.H.J. (2015). 568. Structural D/E-rich repeats play multiple roles especially in gene regulation through DNA/RNA mimicry. Mol. Biosyst.

Chow, K.H., and Courcelle, J. (2004). 164. RecO Acts with RecF and RecR to Protect and Maintain Replication Forks Blocked by UV-induced DNA Damage in Escherichia coli. J. Biol. Chem.

Chu, W.K., and Hickson, I.D. (2009). 533. RecQ helicases: Multifunctional genome caretakers. Nat. Rev. Cancer.

Chuang, C.H., Carpenter, A.E., Fuchsova, B., Johnson, T., de Lanerolle, P., and Belmont, A.S. (2006). 361. Long-Range Directional Movement of an Interphase Chromosome Site. Curr. Biol.

Ciccia, A., and Elledge, S.J. (2010). 366. The DNA Damage Response: Making It Safe to Play with Knives. Mol. Cell.

Clapier, C.R., and Cairns, B.R. (2009). 351. The Biology of Chromatin Remodeling Complexes. Annu. Rev. Biochem.

Clapier, C.R., Iwasa, J., Cairns, B.R., and Peterson, C.L. (2017). 363. Mechanisms of action and regulation of ATP-dependent chromatin-remodelling complexes. Nat. Rev. Mol. Cell Biol.

Claussin, C., and Chang, M. (2015). 106.The many facets of homologous recombination at telomeres. Microb. Cell.

Clément, C., and Almouzni, G. (2015). 232. MCM2 binding to histones H3-H4 and ASF1 supports a tetramer-to-dimer model for histone inheritance at the replication fork. Nat. Struct. Mol. Biol.

Clemente-Ruiz, M., and Prado, F. (2009). Chromatin assembly controls replication fork stability. EMBO Rep.

Clemente-Ruiz, M., González-Prieto, R., and Prado, F. (2011). Histone H3K56 acetylation, CAF1, and Rtt106 coordinate nucleosome assembly and stability of advancing replication forks. PLoS Genet.

Colavito, S., Macris-Kiss, M., Seong, C., Gleeson, O., Greene, E.C., Klein, H.L., Krejci, L., and Sung, P. (2009). 523. Functional significance of the Rad51-Srs2 complex in Rad51 presynaptic filament disruption. Nucleic Acids Res.

Costantino, L., Sotiriou, S.K., Rantala, J.K., Magin, S., Mladenov, E., Helleday, T., Haber, J.E., Iliakis, G.,

Kallioniemi, O.P., and Halazonetis, T.D. (2014). 556. Break-induced replication repair of damaged forks induces genomic duplications in human cells. Science (80-.).

Costes, A., and Lambert, S.A.E. (2013). 545. Homologous recombination as a replication fork escort: Fork-protection and recovery. Biomolecules.

Courcelle, J., Donaldson, J.R., Chow, K.H., and Courcelle, C.T. (2003). 542. DNA damage-induced replication fork regression and processing in Escherichia coli. Science (80-.).

Dabin, J., Fortuny, A., and Polo, S.E. (2016). 367. Epigenome Maintenance in Response to DNA Damage. Mol. Cell.

Daboussi, F., Courbet, S., Benhamou, S., Kannouche, P., Zdzienicka, M.Z., Debatisse, M., and Lopez, B.S. (2008). 541. A homologous recombination defect affects replication-fork progression in mammalian cells. J. Cell Sci.

Das, C., Tyler, J.K., and Churchill, M.E.A. (2010). 246. The histone shuffle: Histone chaperones in an energetic dance. Trends Biochem. Sci.

Davey, C.A., Sargent, D.F., Luger, K., Maeder, A.W., and Richmond, T.J. (2002). 195. Solvent mediated interactions in the structure of the nucleosome core particle at 1.9 Å resolution. J. Mol. Biol.

Davies, S.L., North, P.S., and Hickson, I.D. (2007). 546. Role for BLM in replication-fork restart and suppression of origin firing after replicative stress. Nat. Struct. Mol. Biol.

Davis, L., and Smith, G.R. (2001). 565. Meiotic recombination and chromosome segregation in Schizosaccharomyces pombe. Proc. Natl. Acad. Sci. U. S. A.

Deans, A.J., and West, S.C. (2011). 11. DNA interstrand crosslink repair and cancer. Nat. Rev. Cancer.

Decottignies, A. (2013). 82. Alternative end-joining mechanisms: A historical perspective. Front. Genet.

Deem, A., Keszthelyi, A., Blackgrove, T., Vayl, A., Coffey, B., Mathur, R., Chabes, A., and Malkova, A. (2011). 156. Break-induced replication is highly inaccurate. PLoS Biol.

Deriano, L., and Roth, D.B. (2013). 76. Modernizing the Nonhomologous End-Joining Repertoire: Alternative and Classical NHEJ Share the Stage. Annu. Rev. Genet.

Deshpande, A.M., and Newlon, C.S. (1996). 31. DNA replication fork pause sites dependent on transcription. Science (80-.).

Dexheimer, T.S. (2013). 44. DNA Repair Pathways and Mechanisms. In DNA Repair of Cancer Stem Cells, p.

Diffley, J.F.X. (2011). Quality control in the initiation of eukaryotic DNA replication. Philos. Trans. R. Soc. Lond. B. Biol. Sci.

Dinant, C., Ampatziadis-Michailidis, G., Lans, H., Tresini, M., Lagarou, A., Grosbart, M., Theil, A.F., VanCappellen, W.A., Kimura, H., Bartek, J., et al. (2013). 425.Enhanced chromatin dynamics by fact promotes transcriptional restart after UV-induced DNA damage. Mol. Cell.

Doe, C.L., Ahn, J.S., Dixon, J., and Whitby, M.C. (2002). 500. Mus81-Eme1 and Rqh1 involvement in processing stalled and collapsed replication forks. J. Biol. Chem.

Dohke, K., Miyazaki, S., Tanaka, K., Urano, T., Grewal, S.I.S., and Murakami, Y. (2008). 257. Fission yeast chromatin assembly factor 1 assists in the replication-coupled maintenance of heterochromatin. Genes to Cells.

Dong, X., and Weng, Z. (2013). 393. The correlation between histone modifications and gene expression. Epigenomics.

Dou, H., Huang, C., Singh, M., Carpenter, P.B., and Yeh, E.T.H. (2010). 124. Regulation of DNA Repair through DeSUMOylation and SUMOylation of replication protein A complex. Mol. Cell.

Downs, J.A., and Jackson, S.P. (2004). 562. A means to a DNA end: The many roles of Ku. Nat. Rev. Mol. Cell Biol.

Downs, J.A., Lowndes, N.F., and Jackson, S.P. (2000). A role for Saccharomyces cerevisiae histone H2A in DNA repair. Nature.

Doyon, Y., Selleck, W., Lane, W.S., Tan, S., and Côté, J. (2004). 460. Structural and functional conservation of the NuA4 histone acetyltransferase complex from yeast to humans. Mol. Cell. Biol.

Dunleavy, E.M., Roche, D., Tagami, H., Lacoste, N., Ray-Gallet, D., Nakamura, Y., Daigo, Y., Nakatani, Y., and Almouzni-Pettinotti, G. (2009). 384. HJURP Is a Cell-Cycle-Dependent Maintenance and Deposition Factor of CENP-A at Centromeres. Cell.

Dunleavy, E.M., Almouzni, G., and Karpen, G.H. (2011). 413. H3.3 is deposited at centromeres in S phase as a placeholder for newly assembled CENP-A in G phase. Nucleus.

Dupaigne, P., Le Breton, C., Fabre, F., Gangloff, S., Le Cam, E., and Veaute, X. (2008). 524. The Srs2 Helicase Activity Is Stimulated by Rad51 Filaments on dsDNA: Implications for Crossover Incidence during Mitotic Recombination. Mol. Cell.

Egel, R., and Egel-Mitani, M. (1974). 463. Premeiotic DNA synthesis in fission yeast. Exp. Cell Res.

Eickbush, T.H., and Moudrianakis, E.N. (1978). 209. The Histone Core Complex: An Octamer Assembled by Two Sets of Protein-Protein Interactions. Biochemistry.

Eissenberg, J.C., and Elgin, S.C. (2014). 187. Heterochromatin and Euchromatin. In ELS, p.

Emil, H. (1928). Das Heterochromatin der Moose. Jahrbücher Für Wissenschaftliche Bot.

Endo, M., Ishikawa, Y., Osakabe, K., Nakayama, S., Kaya, H., Araki, T., Shibahara, K.I., Abe, K., Ichikawa, H., Valentine, L., et al. (2006a). 444. Increased frequency of homologous recombination and T-DNA integration in Arabidopsis CAF-1 mutants. EMBO J.

Endo, M., Ishikawa, Y., Osakabe, K., Nakayama, S., Kaya, H., Araki, T., Shibahara, K.I., Abe, K., Ichikawa, H., Valentine, L., et al. (2006b). Increased frequency of homologous recombination and T-DNA integration in Arabidopsis CAF-1 mutants. EMBO J.

Entian, K.D., Schuster, T., Hegemann, J.H., Becher, D., Feldmann, H., Güldener, U., Götz, R., Hansen, M., Hollenberg, C.P., Jansen, G., et al. (1999). Functional analysis of 150 deletion mutants in Saccharomyces cerevisiae by a systematic approach. Mol. Gen. Genet.

Eriksson, P.R., Ganguli, D., Nagarajavel, V., and Clark, D.J. (2012). 364. Regulation of histone gene expression in budding yeast. Genetics.

Etheridge, T.J., Boulineau, R.L., Herbert, A., Watson, A.T., Daigaku, Y., Tucker, J., George, S., Jönsson, P., Palayret, M., Lando, D., et al. (2014). Quantification of DNA-associated proteins inside eukaryotic cells using single-molecule localization microscopy. Nucleic Acids Res.

Fabre, F., Chan, A., Heyer, W.-D., and Gangloff, S. (2002). Alternate pathways involving Sgs1/Top3, Mus81/ Mms4, and Srs2 prevent formation of toxic recombination intermediates from single-stranded gaps created by DNA replication. Proc. Natl. Acad. Sci.

Falbo, K.B., and Shen, X. (2006). 19. Chromatin remodeling in DNA replication. J. Cell. Biochem.

Falck, J., Coates, J., and Jackson, S.P. (2005). 340. Conserved modes of recruitment of ATM, ATR and DNA-PKcs to sites of DNA damage. Nature.

Fan, Y., Nikitina, T., Zhao, J., Fleury, T.J., Bhattacharyya, R., Bouhassira, E.E., Stein, A., Woodcock, C.L.,

and Skoultchi, A.I. (2005). 206. Histone H1 depletion in mammals alters global chromatin structure but causes specific changes in gene regulation. Cell.

Fantes, P.A., and Hoffman, C.S. (2016). 461. A brief history of Schizosaccharomyces pombe research: A perspective over the past 70 years. Genetics.

Fekairi, S., Scaglione, S., Chahwan, C., Taylor, E.R., Tissier, A., Coulon, S., Dong, M.Q., Ruse, C., Yates, J.R., Russell, P., et al. (2009). 504. Human SLX4 Is a Holliday Junction Resolvase Subunit that Binds Multiple DNA Repair/Recombination Endonucleases. Cell.

Ferguson, D.O., and Holloman, W.K. (1996). 120. Recombinational repair of gaps in DNA is asymmetric in Ustilago maydis and can be explained by a migrating D-loop model. Proc Natl Acad Sci U S A.

Ferreira, M.G., and Cooper, J.P. (2004). 57. Two modes of DNA double-strand break repair are reciprocally regulated through the fission yeast cell cycle. Genes Dev.

Fishman-Lobell, J., and Haber, J.E. (1992). 493. Removal of nonhomologous DNA ends in double-strand break recombination: The role of the yeast ultraviolet repair gene RAD1. Science (80-.).

Fishman-Lobell, J., Rudin, N., and Haber, J.E. (1992). 477. Two alternative pathways of double-strand break repair that are kinetically separable and independently modulated. Mol. Cell. Biol.

Flynn, R.L., and Zou, L. (2010). 131. Oligonucleotide/oligosaccharide-binding fold proteins: A growing family of genome guardians. Crit. Rev. Biochem. Mol. Biol.

Foltz, D.R., Jansen, L.E.T., Bailey, A.O., Yates, J.R., Bassett, E.A., Wood, S., Black, B.E., and Cleveland, D.W. (2009). 385. Centromere-Specific Assembly of CENP-A Nucleosomes Is Mediated by HJURP. Cell.

Forsburg, S.L., and Rhind, N. (2006). 464. Basic methods for fission yeast. Yeast.

Fortin, G.S., and Symington, L.S. (2002). 144. Mutations in yeast Rad51 that partially bypass the requirement for Rad55 and Rad57 in DNA repair by increasing the stability of Rad51-DNA complexes. EMBO J.

Franklin, S.G., and Zweidler, A. (1977). Non-allelic variants of histones 2a, 2b and 3 in mammals [25]. Nature.

Fung, C.W., Mozlin, A.M., and Symington, L.S. (2009). 146. Suppression of the double-strand-break-repair defect of the Saccharomyces cerevisiae rad57 mutant. Genetics.

Gaillard, H., García-Muse, T., and Aguilera, A. (2015). Replication stress and cancer. Nat. Rev. Cancer.

Gaillard, P.H., Martini, E.M., Kaufman, P.D., Stillman, B., Moustacchi, E., and Almouzni, G. (1996). 420. Chromatin assembly coupled to DNA repair: a new role for chromatin assembly factor I. Cell.

Gaillard, P.H.L., G.moggs, J., Roche, D.M.J., Quivy, J.P., Becker, P.B., Wood, R.D., and Almouzni, G. (1997). 421. Initiation and bidirectional propagation of chromatin assembly from a target site for nucleotide excision repair. EMBO J.

Gaines, W.A., Godin, S.K., Kabbinavar, F.F., Rao, T., VanDemark, A.P., Sung, P., and Bernstein, K.A. (2015). 517. Promotion of presynaptic filament assembly by the ensemble of S. cerevisiae Rad51 paralogues with Rad52. Nat. Commun.

Game, J.C., and Kaufman, P.D. (1999). 443. Role of Saccharomyces cerevisiae chromatin assembly factor-I in repair of ultraviolet radiation damage in vivo. Genetics.

Gangloff, S., Soustelle, C., and Fabre, F. (2000). Homologous recombination is responsible for cell death in the absence of the Sgs1 and Srs2 helicases. Nat. Genet.

Gari, K., Décaillet, C., Stasiak, A.Z., Stasiak, A., and Constantinou, A. (2008). 526. The Fanconi Anemia

Protein FANCM Can Promote Branch Migration of Holliday Junctions and Replication Forks. Mol. Cell.

Ge, X.Q., Jackson, D.A., and Blow, J.J. (2007). 24. Dormant origins licensed by excess Mcm2-7 are required for human cells to survive replicative stress. Genes Dev.

Gérard, A., Koundrioukoff, S., Ramillon, V., Sergère, J.C., Mailand, N., Quivy, J.P., and Almouzni, G. (2006a). 255. The replication kinase Cdc7-Dbf4 promotes the interaction of the p150 subunit of chromatin assembly factor 1 with proliferating cell nuclear antigen. EMBO Rep.

Gérard, A., Polo, S.E., Roche, D., and Almouzni, G. (2006b). 422. Methods for Studying Chromatin Assembly Coupled to DNA Repair. Methods Enzymol.

Giglia-Mari, G., Zotter, A., and Vermeulen, W. (2011). 2. DNA damage response. Cold Spring Harb. Perspect. Biol.

Godin, S., Wier, A., Kabbinavar, F., Bratton-Palmer, D.S., Ghodke, H., Van Houten, B., Vandemark, A.P., and Bernstein, K.A. (2013). 515. The Shu complex interacts with Rad51 through the Rad51 paralogues Rad55-Rad57 to mediate error-free recombination. Nucleic Acids Res.

Goldstein, M., Derheimer, F.A., Tait-Mulder, J., and Kastan, M.B. (2013). 375. Nucleolin mediates nucleosome disruption critical for DNA double-strand break repair. Proc. Natl. Acad. Sci.

Göttlich, B., Reichenberger, S., Feldmann, E., and Pfeiffer, P. (1998). 75. Rejoining of DNA double-strand breaks in vitro by single-strand annealing. Eur. J. Biochem.

Gravel, S., Chapman, J.R., Magill, C., and Jackson, S.P. (2008). 535. DNA helicases Sgs1 and BLM promote DNA double-strand break resection. Genes Dev.

Green, C.M., and Almouzni, G. (2002). 394. When repair meets chromatin. First in series on chromatin dynamics. EMBO Rep.

Green, C.M., and Almouzni, G. (2003). 423.Local action of the chromatin assembly factor CAF-1 at sites of nucleotide excision repair in vivo. EMBO J.

Greenall, A., Williams, E.S., Martin, K.A., Palmer, J.M., Gray, J., Liu, C., and Whitehall, S.K. (2006). 575. Hip3 interacts with the HIRA proteins Hip1 and Slm9 and is required for transcriptional silencing and accurate chromosome segregation. J. Biol. Chem.

Groth, A. (2009). 298. Replicating chromatin: a tale of histones. Biochem. Cell Biol.

Groth, A., Corpet, A., Cook, A.J.L., Roche, D., Bartek, J., Lukas, J., and Almouzni, G. (2007a). Regulation of replication fork progression through histone supply and demand. Science (80-.).

Groth, A., Rocha, W., Verreault, A., and Almouzni, G. (2007b). 395. Chromatin Challenges during DNA Replication and Repair. Cell.

Gruss, C., Wu, J., Koller, T., and Sogo, J.M. (1993). 235. Disruption of the nucleosomes at the replication fork. EMBO J.

Guillemette, B., Bataille, A.R., Gévry, N., Adam, M., Blanchette, M., Robert, F., and Gaudreau, L. (2005). Variant histone H2A.z is globally localized to the promoters of inactive yeast genes and regulates nucleosome positioning. PLoS Biol.

Gurard-Levin, Z.A., Quivy, J.-P., and Almouzni, G. (2014). 241. Histone Chaperones: Assisting Histone Traffic and Nucleosome Dynamics. Annu. Rev. Biochem.

Haince, J.F., McDonald, D., Rodrigue, A., Déry, U., Masson, J.Y., Hendzel, M.J., and Poirier, G.G. (2008). 81. PARP1-dependent kinetics of recruitment of MRE11 and NBS1 proteins to multiple DNA damage sites. J. Biol. Chem.

Hajjoul, H., Mathon, J., Ranchon, H., Goiffon, I., Mozziconacci, J., Albert, B., Carrivain, P., Victor, J.M.,

Gadal, O., Bystricky, K., et al. (2013). 357. High-throughput chromatin motion tracking in living yeast reveals the flexibility of the fiber throughout the genome. Genome Res.

Hake, S.B., and Allis, C.D. (2006). 215. Histone H3 variants and their potential role in indexing mammalian genomes: The “H3 barcode hypothesis.” Proc. Natl. Acad. Sci.

Hall, M.A., Shundrovsky, A., Bai, L., Fulbright, R.M., Lis, J.T., and Wang, M.D. (2009). 237. High-resolution dynamic mapping of histone-DNA interactions in a nucleosome. Nat. Struct. Mol. Biol.

Hammond, C.M., Strømme, C.B., Huang, H., Patel, D.J., and Groth, A. (2017). 245. Histone chaperone networks shaping chromatin function. Nat. Rev. Mol. Cell Biol.

Han, P., and Chang, C.-P. (2015). 352. Long non-coding RNA and chromatin remodeling. RNA Biol.

Han, J., Zhou, H., Li, Z., Xu, R.M., and Zhang, Z. (2007). 301. Acetylation of lysine 56 of histone H3 catalyzed by RTT109 and regulated by ASF1 is required for replisome integrity. J. Biol. Chem.

Han, J., Zhang, H., Zhang, H., Wang, Z., Zhou, H., and Zhang, Z. (2013). 303. XA Cul4 E3 ubiquitin ligase regulates histone hand-off during nucleosome assembly. Cell.

Harami, G.M., Gyimesi, M., and Kovács, M. (2013). 567. From keys to bulldozers: Expanding roles for winged helix domains in nucleic-acid-binding proteins. Trends Biochem. Sci.

Harami, G.M., Seol, Y., In, J., Ferencziová, V., Martina, M., Gyimesi, M., Sarlós, K., Kovács, Z.J., Nagy, N.T., Sun, Y., et al. (2017). 532. Shuttling along DNA and directed processing of D-loops by RecQ helicase support quality control of homologous recombination. Proc. Natl. Acad. Sci.

Harshman, S.W., Young, N.L., Parthun, M.R., and Freitas, M.A. (2013). 186. H1 histones: Current perspectives and challenges. Nucleic Acids Res.

Hashiguchi, K., Matsumoto, Y., and Yasui, A. (2007). Recruitment of DNA repair synthesis machinery to sites of DNA damage/repair in living human cells. Nucleic Acids Res.

Hashimoto, Y., Chaudhuri, A.R., Lopes, M., and Costanzo, V. (2010). 160. Rad51 protects nascent DNA from Mre11-dependent degradation and promotes continuous DNA synthesis. Nat. Struct. Mol. Biol.

Hashimoto, Y., Puddu, F., and Costanzo, V. (2012). 170. RAD51-and MRE11-dependent reassembly of uncoupled CMG helicase complex at collapsed replication forks. Nat. Struct. Mol. Biol.

Hatakeyama, A., Hartmann, B., Travers, A., Nogues, C., and Buckle, M. (2016). High-resolution biophysical analysis of the dynamics of nucleosome formation. Sci. Rep.

Hauer, M.H., and Gasser, S.M. (2017). 388. Chromatin and nucleosome dynamics in DNA damage and repair. Genes Dev.

Hauer, M.H., Seeber, A., Singh, V., Thierry, R., Sack, R., Amitai, A., Kryzhanovska, M., Eglinger, J., Holcman, D., Owen-Hughes, T., et al. (2017). 359. Histone degradation in response to DNA damage enhances chromatin dynamics and recombination rates. Nat. Struct. Mol. Biol.

Hays, S.L., Firmenich, A.A., and Berg, P. (1995). 141. Complex formation in yeast double-strand break repair: participation of Rad51, Rad52, Rad55, and Rad57 proteins. Proc. Natl. Acad. Sci.

Van Der Heijden, G.W., Derijck, A.A.H.A., Pósfai, E., Giele, M., Pelczar, P., Ramos, L., Wansink, D.G., Van Der Vlag, J., Peters, A.H.F.M., and De Boer, P. (2007). 580. Chromosome-wide nucleosome replacement and H3.3 incorporation during mammalian meiotic sex chromosome inactivation. Nat. Genet.

Helleday, T., Eshtad, S., and Nik-Zainal, S. (2014). 53. Mechanisms underlying mutational signatures in human cancers. Nat. Rev. Genet.

Heller, R.C., and Marians, K.J. (2006). 480. Replisome assembly and the direct restart of stalled

replication forks. Nat. Rev. Mol. Cell Biol.

Hentges, P., Van Driessche, B., Tafforeau, L., Vandenhaute, J., and Carr, A.M. (2005). 307. Three novel antibiotic marker cassettes for gene disruption and marker switching in Schizosaccharomyces pombe. Yeast.

Heo, K., Kim, H., Choi, S.H., Choi, J., Kim, K., Gu, J., Lieber, M.R., Yang, A.S., and An, W. (2008). 403. FACT-Mediated Exchange of Histone Variant H2AX Regulated by Phosphorylation of H2AX and ADP-Ribosylation of Spt16. Mol. Cell.

Herbert, S., Brion, A., Arbona, J., Lelek, M., Veillet, A., Lelandais, B., Parmar, J., Fernández, F.G., Almayrac, E., Khalil, Y., et al. (2017). 360. Chromatin stiffening underlies enhanced locus mobility after DNA damage in budding yeast. EMBO J.

Heun, P., Laroche, T., Shimada, K., Furrer, P., and Gasser, S.M. (2001). 356. Chromosome dynamics in the yeast interphase nucleus. Science (80-.).

Hicks, W.M., Yamaguchi, M., and Haber, J.E. (2011). Real-time analysis of double-strand DNA break repair by homologous recombination. Proc. Natl. Acad. Sci.

Hoek, M., Myers, M.P., and Stillman, B. (2011). 451. An analysis of CAF-1-interacting proteins reveals dynamic and direct interactions with the KU complex and 14-3-3 proteins. J. Biol. Chem.

Hoffman, C.S., Wood, V., and Fantes, P.A. (2015). 462. An ancient yeast for young geneticists: A primer on the Schizosaccharomyces pombe model system. Genetics.

Holland, S., Ioannou, D., Haines, S., and Brown, W.R.A. (2005). 365. Comparison of Dam tagging and chromatin immunoprecipitation as tools for the identification of the binding sites for S. pombe CENP-C. In Chromosome Research, p.

Holliday, R. (1964). 499. A mechanism for gene conversion in fungi. Genet. Res.

Hollingsworth, N.M., and Brill, S.J. (2004). 115. The Mus81 solution to resolution: Generating meiotic crossovers without Holliday junctions. Genes Dev.

Holt, L.J., Tuch, B.B., Villen, J., Johnson, A.D., Gygi, S.P., and Morgan, D.O. (2009). 582. Global analysis of cdk1 substrate phosphorylation sites provides insiqhts into evolution. Science (80-.).

Hu, Z., and Tee, W.-W. (2017). 347. Enhancers and chromatin structures: regulatory hubs in gene expression and diseases. Biosci. Rep.

Hu, L., Kim, T.M., Son, M.Y., Kim, S.A., Holland, C.L., Tateishi, S., Kim, D.H., Yew, P.R., Montagna, C., Dumitrache, L.C., et al. (2013). 537. Two replication fork maintenance pathways fuse inverted repeats to rearrange chromosomes. Nature.

Huang, Y., and Li, L. (2013). 10. DNA crosslinking damage and cancer - a tale of friend and foe. Transl. Cancer Res.

Huang, H., Strømme, C.B., Saredi, G., Hödl, M., Strandsby, A., González-Aguilera, C., Chen, S., Groth, A., and Patel, D.J. (2015). 230. A unique binding mode enables MCM2 to chaperone histones H3-H4 at replication forks. Nat. Struct. Mol. Biol.

Huang, M.-E., Rio, A.-G., Nicolas, A., and Kolodner, R.D. (2003). 344. A genomewide screen in Saccharomyces cerevisiae for genes that suppress the accumulation of mutations. Proc. Natl. Acad. Sci. U. S. A.

Huang, T.H., Fowler, F., Chen, C.C., Shen, Z.J., Sleckman, B., and Tyler, J.K. (2018). 454. The Histone Chaperones ASF1 and CAF-1 Promote MMS22L-TONSL-Mediated Rad51 Loading onto ssDNA during Homologous Recombination in Human Cells. Mol. Cell.

Huang, Y.-T., Lin, X., Liu, Y., Chirieac, L.R., McGovern, R., Wain, J., Heist, R., Skaug, V., Zienolddiny, S., Haugen, A., et al. (2011). 6. Cigarette smoking increases copy number alterations in nonsmall-cell lung cancer. Proc. Natl. Acad. Sci. U. S. A.

Hubscher, U., Jonsson, Z.O., and Hindges, R. (1998). 261. Regulation of DNA replication and repair proteins through interaction with the front side of proliferating cell nuclear antigen. Embo J.

Huggins, C.F., Chafin, D.R., Aoyagi, S., Henricksen, L.A., Bambara, R.A., and Hayes, J.J. (2002). 429. Flap endonuclease 1 efficiently cleaves base excision repair and DNA replication intermediates assembled into nucleosomes. Mol. Cell.

Iacovoni, J.S., Caron, PierreLassadi, I., Nicolas, E., Massip, L., Trouche, D., and Legube, G. (2010). 400. High-resolution profiling of gammaH2AX around DNA double strand breaks in the mammalian genome. EMBO J.

Ikura, T., Tashiro, S., Kakino, A., Shima, H., Jacob, N., Amunugama, R., Yoder, K., Izumi, S., Kuraoka, I., Tanaka, K., et al. (2007). 402. DNA Damage-Dependent Acetylation and Ubiquitination of H2AX Enhances Chromatin Dynamics. Mol. Cell. Biol.

Ip, S.C.Y., Rass, U., Blanco, M.G., Flynn, H.R., Skehel, J.M., and West, S.C. (2008). 116. Identification of Holliday junction resolvases from humans and yeast. Nature.

Ira, G., Malkova, A., Liberi, G., Foiani, M., and Haber, J.E. (2003). 180. Srs2 and Sgs1-Top3 Suppress Crossovers during Double-Strand Break Repair in Yeast. Cell.

Iraqui, I., Chekkal, Y., Jmari, N., Pietrobon, V., Fréon, K., Costes, A., and Lambert, S.A.E. (2012). 155. Recovery of Arrested Replication Forks by Homologous Recombination Is Error-Prone. PLoS Genet.

Ishii, S., Koshiyama, A., Hamada, F.N., Nara, T.Y., Iwabata, K., Sakaguchi, K., and Namekawa, S.H. (2008). 450. Interaction between Lim15/Dmc1 and the homologue of the large subunit of CAF-1 - A molecular link between recombination and chromatin assembly during meiosis. FEBS J.

Ivanov, E.L., and Haber, J.E. (1995). 491. RAD1 and RAD10, but not other excision repair genes, are required for double-strand break-induced recombination in Saccharomyces cerevisiae. Mol. Cell. Biol.

Ivanov, E.L., Sugawara, N., Fishman-Lobell, J., and Haber, J.E. (1996). 87. Genetic requirements for the single-strand annealing pathway of double-strand break repair in Saccharomyces cerevisiae. Genetics.

Jackson, S.P. (2002). 18. Sensing and repairing DNA double-strand breaks. Carcinogenesis.

Jackson, V. (1988). 229. Deposition of Newly Synthesized Histones: Hybrid Nucleosomes Are Not Tandemly Arranged on Daughter DNA Strands. Biochemistry.

Jasencakova, Z., Scharf, A.N.D., Ask, K., Corpet, A., Imhof, A., Almouzni, G., and Groth, A. (2010). 234. Replication Stress Interferes with Histone Recycling and Predeposition Marking of New Histones. Mol. Cell.

Jeffery, D.C.B., Kakusho, N., You, Z., Gharib, M., Wyse, B., Drury, E., Weinreich, M., Thibault, P., Verreault, A., Masai, H., et al. (2015). 581. CDC28 phosphorylates Cac1p and regulates the association of chromatin assembly factor i with chromatin http://www.tandfonline.com/doi/pdf/10.4161/15384101.2014.973745. Cell Cycle.

Jiao, R., Bachrati, C.Z., Pedrazzi, G., Kuster, P., Petkovic, M., Li, J.L., Egli, D., Hickson, I.D., and Stagljar, I. (2004). 258. Physical and functional interaction between the Bloom's syndrome gene product and the largest subunit of chromatin assembly factor 1. Mol Cell Biol.

Jiao, R., Harrigan, J.A., Shevelev, I., Dietschy, T., Selak, N., Indig, F.E., Piotrowski, J., Janscak, P., Bohr, V.A., and Stagljar, I. (2007). 452. The Werner syndrome protein is required for recruitment of

chromatin assembly factor 1 following DNA damage. Oncogene.

Kabotyanski, E.B., Gomelsky, L., Han, J.O., Stamato, T.D., and Roth, D.B. (1998). 73. Double-strand break repair in Ku86- and XRCC4-deficient cells. Nucleic Acids Res.

Kadyrova, L.Y., Blanko, E.R., and Kadyrov, F. a (2011). 436. CAF-I-dependent control of degradation of the discontinuous strands during mismatch repair. Proc. Natl. Acad. Sci. U. S. A.

Kadyrova, L.Y., Blanko, E.R., and Kadyrov, F.A. (2013). 437. Human CAF-1-dependent nucleosome assembly in a defined system. Cell Cycle.

Kadyrova, L.Y., Dahal, B.K., and Kadyrov, F.A. (2016). 438. The major replicative histone chaperone CAF-1 suppresses the activity of the DNA mismatch repair system in the cytotoxic response to a DNA-methylating agent. J. Biol. Chem.

Kalocsay, M., Hiller, N.J., and Jentsch, S. (2009). 405. Chromosome-wide Rad51 Spreading and SUMO-H2A.Z-Dependent Chromosome Fixation in Response to a Persistent DNA Double-Strand Break. Mol. Cell.

Kanoh, J., and Russell, P. (2000). 572. Slm9, a novel nuclear protein involved in mitotic control in fission yeast. Genetics.

Kato, T., Sato, N., Hayama, S., Yamabuki, T., Ito, T., Miyamoto, M., Kondo, S., Nakamura, Y., and Daigo, Y. (2007). 387. Activation of Holliday junction-recognizing protein involved in the chromosomal stability and immortality of cancer cells. Cancer Res.

Kaufman, P.D., Kobayashi, R., Kessler, N., and Stillman, B. (1995). 267. The p150 and p60 subunits of chromatin assembly factor I: a molecular link between newly synthesized histones and DNA replication. Cell.

Kaufman, P.D., Kobayashi, R., and Stillman, B. (1997). 288. Ultraviolet radiation sensitivity and reduction of telomeric silencing in Saccharomyces cerevisiae cells lacking chromatin assembly factor-I. Genes Dev.

Kaufman, P.D., Cohen, J.L., and Osley, M.A. (1998). 571. Hir Proteins Are Required for Position-Dependent Gene Silencing in Saccharomyces cerevisiae in the Absence of Chromatin Assembly Factor I. Mol. Cell. Biol.

Kawabata, T., Luebben, S.W., Yamaguchi, S., Ilves, I., Matise, I., Buske, T., Botchan, M.R., and Shima, N. (2011). 23. Stalled Fork Rescue via Dormant Replication Origins in Unchallenged S Phase Promotes Proper Chromosome Segregation and Tumor Suppression. Mol. Cell.

Kawamoto, T., Araki, K., Sonoda, E., Yamashita, Y.M., Harada, K., Kikuchi, K., Masutani, C., Hanaoka, F., Nozaki, K., Hashimoto, N., et al. (2005). 520. Dual roles for DNA polymerase eta in homologous DNA recombination and translesion DNA synthesis. Mol. Cell.

Kearsey, S.E., Brimage, L., Namdar, M., Ralph, E., and Yang, X. (2005). 309. In situ assay for analyzing the chromatin binding of proteins in fission yeast. Methods Mol. Biol.

Keeney, S., Giroux, C.N., and Kleckner, N. (1997). 564. Meiosis-specific DNA double-strand breaks are catalyzed by Spo11, a member of a widely conserved protein family. Cell.

Keller, C., and Krude, T. (2000). 285. Requirement of Cyclin/Cdk2 and protein phosphatase 1 activity for chromatin assembly factor 1-dependent chromatin assembly during DNA synthesis. J Biol Chem.

Khanna, K.K., and Jackson, S.P. (2001). 334. DNA double-strand breaks: Signaling, repair and the cancer connection. Nat. Genet.

Kiianitsa, K., Solinger, J. a, and Heyer, W.-D. (2006). 510. Terminal association of Rad54 protein with the Rad51-dsDNA filament. Proc. Natl. Acad. Sci. U. S. A.

Kim, J.-A., and Haber, J.E. (2009). 408. Chromatin assembly factors Asf1 and CAF-1 have overlapping roles in deactivating the DNA damage checkpoint when DNA repair is complete. Proc. Natl. Acad. Sci.

Kim, D., Setiaputra, D., Jung, T., Chung, J., Leitner, A., Yoon, J., Aebersold, R., Hebert, H., Yip, C.K., and Song, J.J. (2016). 287. Molecular architecture of yeast chromatin assembly factor 1. Sci. Rep.

Kim, J.A., Kruhlak, M., Dotiwala, F., Nussenzweig, A., and Haber, J.E. (2007). 399. Heterochromatin is refractory to γ-H2AX modification in yeast and mammals. J. Cell Biol.

Kirik, A., Pecinka, A., Wendeler, E., and Reiss, B. (2006). 445. The Chromatin Assembly Factor Subunit FASCIATA1 Is Involved in Homologous Recombination in Plants. PLANT CELL ONLINE.

Kirst, M., Basten, C.J., Myburg, A.A., Zeng, Z.B., and Sederoff, R.R. (2005). 191.bGenetic architecture of transcript-level variation in differentiating xylem of a eucalyptus hybrid. Genetics.

Kobayashi, J. (2004). 218. Molecular mechanism of the recruitment of NBS1/hMRE11/hRAD50 complex to DNA double-strand breaks: NBS1 binds to gamma-H2AX through FHA/BRCT domain. J. Radiat. Res.

Van Komen, S., Petukhova, G., Sigurdsson, S., Stratton, S., Sung, P., Komen, S. Van, Petukhova, G., Sigurdsson, S., Stratton, S., Sung, P., et al. (2000). 179. Superhelicity-driven homologous DNA pairing by yeast recombination factors Rad51 and Rad54. Mol Cell.

Van Komen, S., Petukhova, G., Sigurdsson, S., and Sung, P. (2002). 126. Functional cross-talk among Rad51, Rad54, and replication protein A in heteroduplex DNA joint formation. J. Biol. Chem.

Kornberg, R.D. (1974). 185. Chromatin structure: A repeating unit of histones and DNA. Science (80-.).

Kowalczykowski, S.C., and Krupp, R.A. (1987). 507. Effects of Escherichia coli SSB protein on the single-stranded DNA-dependent ATPase activity of Escherichia coli RecA protein. Evidence that SSB protein facilitates the binding of RecA protein to regions of secondary structure within single-stranded . J. Mol. Biol.

Kraus, E., Leung, W.-Y., and Haber, J.E. (2001). 479. Break-induced replication: A review and an example in budding yeast. Proc. Natl. Acad. Sci.

Krawitz, D.C., Kama, T., and Kaufman, P.D. (2002). 265. Chromatin assembly factor I mutants defective for PCNA binding require Asf1/Hir proteins for silencing. Mol. Cell. Biol.

Krejci, L., Chen, L., Komen, S. Van, Sung, P., and Tomkinson, A. (2003). 173. Mending the Break: Two DNA Double-Strand Break Repair Machines in Eukaryotes. Prog. Nucleic Acid Res. Mol. Biol.

Krejci, L., Altmannova, V., Spirek, M., and Zhao, X. (2012). 135. Homologous recombination and its regulation. Nucleic Acids Res.

Krokan, H.E., and Bjørås, M. (2013). 45. Base excision repair. Cold Spring Harb. Perspect. Biol.

Kruhlak, M.J., Celeste, A., Dellaire, G., Fernandez-Capetillo, O., Müller, W.G., McNally, J.G., Bazett-Jones, D.P., and Nussenzweig, A. (2006). 372. Changes in chromatin structure and mobility in living cells at sites of DNA double-strand breaks. J. Cell Biol.

Kukimoto, I., Elderkin, S., Grimaldi, M., Oelgeschläger, T., and Varga-Weisz, P.D. (2004). 239. The Histone-Fold Protein Complex CHRAC-15/17 Enhances Nucleosome Sliding and Assembly Mediated by ACF. Mol. Cell.

Kunkel, T.A., and Burgers, P.M. (2008). 548. Dividing the workload at a eukaryotic replication fork. Trends Cell Biol.

Kunoh, T., and Habu, T. (2014). 312. Pcf1, a large subunit of CAF-1, required for maintenance of

checkpoint kinase Cds1 activity. Springerplus.

Kuo, M.H., Brownell, J.E., Sobel, R.E., Ranalli, T.A., Cook, R.G., Edmondson, D.G., Roth, S.Y., and Allis, C.D. (1996). 299. Transcription-linked acetylation by Gcn5p of histones H3 and H4 at specific lysines. Nature.

Kuzmichev, A., Nishioka, K., Erdjument-Bromage, H., Tempst, P., and Reinberg, D. (2002). 292. Histone methyltransferase activity associated with a human multiprotein complex containing the Enhancer of Zeste protein. Genes Dev.

Laat, W.L. de, Jaspers, N.G.J., and Hoeijmakers, J.H.J. (1999). 47. Molecular mechanism of nucleotide excision repair. Genes Dev.

Lambert, S., and Carr, A.M. (2013). 21. Impediments to replication fork movement: Stabilisation, reactivation and genome instability. Chromosoma.

Lambert, S., Mizuno, K., Blaisonneau, J., Martineau, S., Chanet, R., Fréon, K., Murray, J.M., Carr, A.M., and Baldacci, G. (2010). 162. Homologous recombination restarts blocked replication forks at the expense of genome rearrangements by template exchange. Mol. Cell.

Lando, D., Endesfelder, U., Berger, H., Subramanian, L., Dunne, P.D., McColl, J., Klenerman, D., Carr, A.M., Sauer, M., Allshire, R.C., et al. (2012). 224. Quantitative single-molecule microscopy reveals that CENP-ACnp1 deposition occurs during G2 in fission yeast. Open Biol.

Lane, D.P. (1992). 341. Cancer. p53, guardian of the genome. Nature.

Langerak, P., Mejia-Ramirez, E., Limbo, O., and Russell, P. (2011). 528. Release of Ku and MRN from DNA ends by Mre11 nuclease activity and Ctp1 is required for homologous recombination repair of double-strand breaks. PLoS Genet.

Lans, H., Marteijn, J.A., and Vermeulen, W. (2012). 378. ATP-dependent chromatin remodeling in the DNA-damage response. Epigenetics and Chromatin.

Laskey, R.A., Honda, B.M., Mills, A.D., and Finch, J.T. (1978). 240. Nucleosomes are assembled by an acidic protein which binds histones and transfers them to DNA. Nature.

Latreille, D., Bluy, L., Benkirane, M., and Kiernan, R.E. (2014). 441. Identification of histone 3 variant 2 interacting factors. Nucleic Acids Res.

Lederberg, J., and Tatum, E.L. (1946). 104. Gene recombination in Escherichia coli [23]. Nature.

Lee, C.S., Lee, K., Legube, G., and Haber, J.E. (2014). 369. Dynamics of yeast histone H2A and H2B phosphorylation in response to a double-strand break. Nat. Struct. Mol. Biol.

Lemaître, C., and Soutoglou, E. (2014). 398. Double strand break (DSB) repair in heterochromatin and heterochromatin proteins in DSB repair. DNA Repair (Amst).

Letessier, A., Millot, G.A., Koundrioukoff, S., Lachagès, A.M., Vogt, N., Hansen, R.S., Malfoy, B., Brison, O., and Debatisse, M. (2011). 336. Cell-type-specific replication initiation programs set fragility of the FRA3B fragile site. Nature.

Lewis, L.K., Karthikeyan, G., Cassiano, J., and Resnick, M.A. (2005). 446. Reduction of nucleosome assembly during new DNA synthesis impairs both major pathways of double-strand break repair. Nucleic Acids Res.

Li, G.-M. (2008a). 48. Mechanisms and functions of DNA mismatch repair. Cell Res.

Li, G.-M. (2008b). 432. Mechanisms and functions of DNA mismatch repair. Cell Res.

Li, H.Q., and Li, M.R. (2004). 530. RecQ helicase enhances homologous recombination in plants. FEBS Lett.

Li, X., and Tyler, J.K. (2016). 453. Nucleosome disassembly during human non-homologous end joining followed by concerted HIRA- and CAF-1-dependent reassembly. Elife.

Li, X., Zhang, X.P., Solinger, J.A., Kiianitsa, K., Yu, X., Egelman, E.H., and Heyer, W.D. (2007). Rad51 and Rad54 ATPase activities are both required to modulate Rad51-dsDNA filament dynamics. Nucleic Acids Res.

Li, Y., Pursell, Z.F., and Linn, S. (2000). 238. Identification and cloning of two histone fold motif-containing subunits of HeLa DNA polymerase ε. J. Biol. Chem.

Lieber, M.R. (2008). 63. The mechanism of human nonhomologous DNA end joining. J. Biol. Chem.

Lieber, M.R., Gu, J., Lu, H., Shimazaki, N., and Tsai, A.G. (2014). 58. Nonhomologous DNA end joining (NHEJ) and chromosomal translocations in humans. Subcell. Biochem.

Limbo, O., Chahwan, C., Yamada, Y., de Bruin, R.A.M., Wittenberg, C., and Russell, P. (2007). 489. Ctp1 Is a Cell-Cycle-Regulated Protein that Functions with Mre11 Complex to Control Double-Strand Break Repair by Homologous Recombination. Mol. Cell.

Lin, F.L., Sperle, K., and Sternberg, N. (1984). 91. Model for homologous recombination during transfer of DNA into mouse L cells: role for DNA ends in the recombination process. Mol. Cell. Biol.

Lindahl, T. (1993). 12. Instability and decay of the primary structure of DNA. Nature.

Linger, J., and Tyler, J.K. (2005). 289. The yeast histone chaperone chromatin assembly factor 1 protects against double-strand DNA-damaging agents. Genetics.

Linger, J.G., and Tyler, J.K. (2007). 428. Chromatin disassembly and reassembly during DNA repair. Mutat. Res. - Fundam. Mol. Mech. Mutagen.

Liu, J., Renault, L., Veaute, X., Fabre, F., Stahlberg, H., and Heyer, W.D. (2011). 143. Rad51 paralogues Rad55-Rad57 balance the antirecombinase Srs2 in Rad51 filament formation. Nature.

Liu, S., Xu, Z., Leng, H., Zheng, P., Yang, J., Chen, K., Feng, J., and Li, Q. (2017). 305. RPA binds histone H3-H4 and functions in DNA replication-coupled nucleosome assembly. Science.

Liu, W.H., Roemer, S.C., Zhou, Y., Shen, Z.J., Dennehey, B.K., Balsbaugh, J.L., Liddle, J.C., Nemkov, T., Ahn, N.G., Hansen, K.C., et al. (2016). 259. The Cac1 subunit of histone chaperone CAF-1 organizes CAF-1-H3/H4 architecture and tetramerizes histones. Elife.

Llorente, B., Smith, C.E., and Symington, L.S. (2008). 98. Break-induced replication: What is it and what is it for? Cell Cycle.

Lobachev, K.S., Rattray, A., and Narayanan, V. (2007). 29. Hairpin- and cruciform-mediated chromosome breakage: causes and consequences in eukaryotic cells. Front. Biosci.

Lomonosov, M., Anand, S., Sangrithi, M., Davies, R., and Venkitaraman, A.R. (2003). 544. Stabilization of stalled DNA replication forks by the BRCA2 breast cancer susceptibility protein. Genes Dev.

Lopes, M., Foiani, M., and Sogo, J.M. (2006). 561. Multiple mechanisms control chromosome integrity after replication fork uncoupling and restart at irreparable UV lesions. Mol. Cell.

Loppin, B., Bonnefoy, E., Anselme, C., Laurençon, A., Karr, T.L., and Couble, P. (2005). 577. The histone H3.3 chaperone HIRA is essential for chromatin assembly in the male pronucleus. Nature.

Lorenz, A., Osman, F., Sun, W., Nandi, S., Steinacher, R., and Whitby, M.C. (2012). 527. The fission yeast FANCM ortholog directs non-crossover recombination during meiosis. Science (80-.).

Luger, K., and Richmond, T.J. (1998). 197. DNA binding within the nucleosome core. Curr Opin Struct Biol.

Luger, K., Mäder, A.W., Richmond, R.K., Sargent, D.F., and Richmond, T.J. (1997). 196. Crystal structure of the nucleosome core particle at 2.8 Å resolution. Nature.

Luijsterburg, M.S., Dinant, C., Lans, H., Stap, J., Wiernasz, E., Lagerwerf, S., Warmerdam, D.O., Lindh, M., Brink, M.C., Dobrucki, J.W., et al. (2009). 419. Heterochromatin protein 1 is recruited to various types of DNA damage. J. Cell Biol.

Luijsterburg, M.S., Lindh, M., Acs, K., Vrouwe, M.G., Pines, A., van Attikum, H., Mullenders, L.H., and Dantuma, N.P. (2012). 371.DDB2 promotes chromatin decondensation at UV-induced DNA damage. J. Cell Biol.

Lydeard, J.R., Jain, S., Yamaguchi, M., and Haber, J.E. (2007). 494. Break-induced replication and telomerase-independent telomere maintenance require Pol32. Nature.

Lydeard, J.R., Lipkin-Moore, Z., Sheu, Y.J., Stillman, B., Burgers, P.M., and Haber, J.E. (2010). 481. Break-induced replication requires all essential DNA replication factors except those specific for pre-RC assembly. Genes Dev.

Maga, G., and Hübscher, U. (2003). 262. Proliferating cell nuclear antigen (PCNA): a dancer with many partners. J. Cell Sci.

Magdalou, I., Lopez, B.S., Pasero, P., and Lambert, S.A.E. (2014). 330. The causes of replication stress and their consequences on genome stability and cell fate. Semin. Cell Dev. Biol.

Mailand, N., Bekker-Jensen, S., Faustrup, H., Melander, F., Bartek, J., Lukas, C., and Lukas, J. (2007). 391. RNF8 Ubiquitylates Histones at DNA Double-Strand Breaks and Promotes Assembly of Repair Proteins. Cell.

Maison, C., and Almouzni, G. (2004). 418. HP1 and the dynamics of heterochromatin maintenance. Nat. Rev. Mol. Cell Biol.

De Majo, F., and Calore, M. (2018). 354. Chromatin remodelling and epigenetic state regulation by non-coding RNAs in the diseased heart. Non-Coding RNA Res.

Malay, A.D., Umehara, T., Matsubara-Malay, K., Padmanabhan, B., and Yokoyama, S. (2008). 279. Crystal structures of fission yeast histone chaperone Asf1 complexed with the Hip1 B-domain or the Cac2 C terminus. J. Biol. Chem.

Malik, P.S., and Symington, L.S. (2008). 145. Rad51 gain-of-function mutants that exhibit high affinity DNA binding cause DNA damage sensitivity in the absence of Srs2. Nucleic Acids Res.

Malkova, A., and Ira, G. (2013). 99. Break-induced replication: Functions and molecular mechanism. Curr. Opin. Genet. Dev.

Malkova, A., Naylor, M.L., Yamaguchi, M., Ira, G., and Haber, J.E. (2005). 484. RAD51-dependent break-induced replication differs in kinetics and checkpoint responses from RAD51-mediated gene conversion. Mol. Cell. Biol.

Mankouri, H.W., Craig, T.J., and Morgan, A. (2002). 181. SGS1 is a multicopy suppressor of srs2: Functional overlap between DNA helicases. Nucleic Acids Res.

Mao, Z., Bozzella, M., Seluanov, A., and Gorbunova, V. (2008). 343. DNA repair by nonhomologous end joining and homologous recombination during cell cycle in human cells. Cell Cycle.

De March, M., Merino, N., Barrera-Vilarmau, S., Crehuet, R., Onesti, S., Blanco, F.J., and De Biasio, A. (2017). 570. Structural basis of human PCNA sliding on DNA. Nat. Commun.

Maréchal, A., and Zou, L. (2013). 39. DNA damage sensing by the ATM and ATR kinases. Cold Spring Harb. Perspect. Biol.

Marheineke, K., and Krude, T. (1998). 283. Nucleosome assembly activity and intracellular localization of human CAF-1 changes during the cell division cycle. J. Biol. Chem.

Marshall, W.F., Straight, A., Marko, J.F., Swedlow, J., Dernburg, A., Belmont, A., Murray, A.W., Agard, D.A., and Sedat, J.W. (1997). 355. Interphase chromosomes undergo constrained diffusional motion in living cells. Curr. Biol.

Martín, V., Chahwan, C., Gao, H., Blais, V., Wohlschlegel, J., Yates, J.R., McGowan, C.H., and Russell, P. (2006). 512. Sws1 is a conserved regulator of homologous recombination in eukaryotic cells. EMBO J.

Martini, E., Roche, D.M., Marheineke, K., Verreault, A., and Almouzni, G. (1998). 424.Recruitment of phosphorylated chromatin assembly factor 1 to chromatin after UV irradiation of human cells. J. Cell Biol.

Martino, J., and Bernstein, K.A. (2016). 508. The Shu complex is a conserved regulator of homologous recombination. FEMS Yeast Res.

Martnez-Balbs, M.A., Tsukiyama, T., Gdula, D., and Wu, C. (1998). 290. Drosophila NURF-55, a WD repeat protein involved in histone metabolism. Biochemistry.

Maryon, E., and Carroll, D. (1991). 478. Involvement of single-stranded tails in homologous recombination of DNA injected into Xenopus laevis oocyte nuclei. Mol. Cell. Biol.

Masai, H., Matsumoto, S., You, Z., Yoshizawa-Sugata, N., and Oda, M. (2010). 22. Eukaryotic Chromosome DNA Replication: Where, When, and How? Annu. Rev. Biochem.

Masumoto, H., Hawke, D., Kobayashi, R., and Verreault, A. (2005). 300. A role for cell-cycle-regulated histone H3 lysine 56 acetylation in the DNA damage response. Nature.

Matheson, T.D., and Kaufman, P.D. (2017). 273. The p150N domain of chromatin assembly factor-1 regulates Ki-67 accumulation on the mitotic perichromosomal layer. Mol. Biol. Cell.

Matsumoto, S., and Yanagida, M. (1985). 225. Histone gene organization of fission yeast: a common upstream sequence. EMBO J.

Mattiroli, F., Gu, Y., Yadav, T., Balsbaugh, J.L., Harris, M.R., Findlay, E.S., Liu, Y., Radebaugh, C.A., Stargell, L.A., Ahn, N.G., et al. (2017a). 269. DNA-mediated association of two histone-bound complexes of yeast chromatin assembly factor-1 (CAF-1) drives tetrasome assembly in the wake of DNA replication. Elife.

Mattiroli, F., Gu, Y., Balsbaugh, J.L., Ahn, N.G., and Luger, K. (2017b). 277. The Cac2 subunit is essential for productive histone binding and nucleosome assembly in CAF-1. Sci. Rep.

Mayle, R., Campbell, I.M., Beck, C.R., Yu, Y., Wilson, M., Shaw, C.A., Bjergbaek, L., Lupski, J.R., and Ira, G. (2015). 552. Mus81 and converging forks limit the mutagenicity of replication fork breakage. Science (80-.).

Mazin, A. V., Alexeev, A.A., and Kowalczykowski, S.C. (2003). 147. A novel function of Rad54 protein: Stabilization of the Rad51 nucleoprotein filament. J. Biol. Chem.

Mazina, O.M., and Mazin, A. V. (2004). Human Rad54 protein stimulates DNA strand exchange activity of hRad51 protein in the presence of Ca2+. J. Biol. Chem.

Mazina, O.M., Rossi, M.J., Thomä, N.H., and Mazin, A. V. (2007). Interactions of human Rad54 protein with branched DNA molecules. J. Biol. Chem.

McGinty, R.K., and Tan, S. (2015). 200. Nucleosome structure and function. Chem. Rev.

McIlwraith, M.J., and West, S.C. (2008). 506. DNA Repair Synthesis Facilitates RAD52-Mediated Second-End Capture during DSB Repair. Mol. Cell.

McKenzie, R.L., Björn, L.O., Bais, A., and Ilyasd, M. (2003). 316. Changes in biologically active ultraviolet radiation reaching the Earth's surface. Photochem. Photobiol. Sci.

Mcllwraith, M.J., Vaisman, A., Liu, Y., Fanning, E., Woodgate, R., and West, S.C. (2005). 519.Human DNA polymerase η promotes DNA synthesis from strand invasion intermediates of homologous recombination. Mol. Cell.

McNally, R., Bowman, G.D., Goedken, E.R., O'Donnell, M., and Kuriyan, J. (2010). 569. Analysis of the role of PCNA-DNA contacts during clamp loading. BMC Struct. Biol.

Mello, J.A., Silljé, H.H.W., Roche, D.M.J., Kirschner, D.B., Nigg, E.A., and Almouzni, G. (2002). 439. Human Asf1 and CAF-1 interact and synergize in a repair-coupled nucleosome assembly pathway. EMBO Rep.

Mijic, S., Zellweger, R., Chappidi, N., Berti, M., Jacobs, K., Mutreja, K., Ursich, S., Ray Chaudhuri, A., Nussenzweig, A., Janscak, P., et al. (2017). 551. Replication fork reversal triggers fork degradation in BRCA2-defective cells. Nat. Commun.

Mimitou, E.P., and Symington, L.S. (2008). 112. Sae2, Exo1 and Sgs1 collaborate in DNA double-strand break processing. Nature.

Mimitou, E.P., and Symington, L.S. (2009). 109. Nucleases and helicases take center stage in homologous recombination. Trends Biochem. Sci.

Miné-Hattab, J., Recamier, V., Izeddin, I., Rothstein, R., and Darzacq, X. (2017). 358. Multi-scale tracking reveals scale-dependent chromatin dynamics after DNA damage. Mol. Biol. Cell.

Mirkin, E. V., and Mirkin, S.M. (2007). 27. Replication Fork Stalling at Natural Impediments. Microbiol. Mol. Biol. Rev.

Mirzabekov, A.D. (1981). 194. Nucleosome structure. Trends Biochem. Sci.

Miyabe, I., Kunkel, T.A., and Carr, A.M. (2011). 549. The major roles of DNA polymerases epsilon and delta at the eukaryotic replication fork are evolutionarily conserved. PLoS Genet.

Miyabe, I., Mizuno, K., Keszthelyi, A., Daigaku, Y., Skouteri, M., Mohebi, S., Kunkel, T.A., Murray, J.M., and Carr, A.M. (2015a). 539. Polymerase Î replicates both strands after homologous recombination-dependent fork restart. Nat. Struct. Mol. Biol.

Miyabe, I., Mizuno, K., Keszthelyi, A., Daigaku, Y., Skouteri, M., Mohebi, S., Kunkel, T.A., Murray, J.M., and Carr, A.M. (2015b). 550. Polymerase Î replicates both strands after homologous recombination-dependent fork restart. Nat. Struct. Mol. Biol.

Mizuguchi, G., Shen, X., Landry, J., Wu, W.H., Sen, S., and Wu, C. (2004). 404. ATP-Driven Exchange of Histone H2AZ Variant Catalyzed by SWR1 Chromatin Remodeling Complex. Science (80-.).

Mizuguchi, T., Barrowman, J., and Grewal, S.I.S. (2015). 468. Chromosome domain architecture and dynamic organization of the fission yeast genome. FEBS Lett.

Mizuno, K., Lambert, S., Baldacci, G., Murray, J.M., and Carr, A.M. (2009). 163. Nearby inverted repeats fuse to generate acentric and dicentric palindromic chromosomes by a replication template exchange mechanism. Genes Dev.

Mizuno, K., Miyabe, I., Schalbetter, S.A., Carr, A.M., and Murray, J.M. (2013). 157. Recombination-restarted replication makes inverted chromosome fusions at inverted repeats. Nature.

Moggs, J.G., Grandi, P., Quivy, J.-P., Jonsson, Z.O., Hubscher, U., Becker, P.B., and Almouzni, G. (2000). 297. A CAF-1-PCNA-Mediated Chromatin Assembly Pathway Triggered by Sensing DNA Damage. Mol. Cell. Biol.

Moreau, S., Ferguson, J.R., and Symington, L.S. (1999). 486. The Nuclease Activity of Mre11 Is Required for Meiosis but Not for Mating Type Switching, End Joining, or Telomere Maintenance. Mol. Cell. Biol.

Moreau, S., Morgan, E.A., and Symington, L.S. (2001). 487. Overlapping functions of the Saccharomyces cerevisiae Mre11, Exo1 and Rad27 nucleases in DNA metabolism. Genetics.

Moreno, S., Klar, A., and Nurse, P. (1991). 308. Molecular genetic analysis of fission yeast Schizosaccharomyces pombe. Methods Enzymol.

Moriel-Carretero, M., and Aguilera, A. (2010). 172. A Postincision-Deficient TFIIH Causes Replication Fork Breakage and Uncovers Alternative Rad51- or Pol32-Mediated Restart Mechanisms. Mol. Cell.

Morley, M., Molony, C.M., Weber, T.M., Devlin, J.L., Ewens, K.G., Spielman, R.S., and Cheung, V.G. (2004). 192. Genetic analysis of genome-wide variation in human gene expression. Nature.

Mortensen, U.H., Bendixen, C., Sunjevaric, I., and Rothstein, R. (1996). 476. DNA strand annealing is promoted by the yeast Rad52 protein. Proc. Natl. Acad. Sci.

Mortusewicz, O., and Leonhardt, H. (2007). XRCC1 and PCNA are loading platforms with distinct kinetic properties and different capacities to respond to multiple DNA lesions. BMC Mol. Biol.

Mosig, G. (1998). 96. RECOMBINATION AND RECOMBINATION-DEPENDENT DNA REPLICATION IN BACTERIOPHAGE T4. Annu. Rev. Genet.

Moynahan, M.E., Cui, T.Y., and Jasin, M. (2001). 327. Homology-directed DNA repair, mitomycin-C resistance, and chromosome stability is restored with correction of a Brca1 mutation. Cancer Res.

Murakami, H., and Keeney, S. (2008). 15. Regulating the formation of DNA double-strand breaks in meiosis. Genes Dev.

Murr, R., Loizou, J.I., Yang, Y.G., Cuenin, C., Li, H., Wang, Z.Q., and Herceg, Z. (2006). 389. Histone acetylation by Trrap-Tip60 modulates loading of repair proteins and repair of DNA double-strand breaks. Nat. Cell Biol.

Murzina, N., Verreault, A., Laue, E., and Stillman, B. (1999). 295. Heterochromatin dynamics in mouse cells: Interaction between chromatin assembly factor 1 and HP1 proteins. Mol. Cell.

Myung, K., Pennaneach, V., Kats, E.S., and Kolodner, R.D. (2003). Saccharomyces cerevisiae chromatin-assembly factors that act during DNA replication function in the maintenance of genome stability. Proc. Natl. Acad. Sci.

Nabatiyan, A., Szüts, D., and Krude, T. (2006). 431. Induction of CAF-1 expression in response to DNA strand breaks in quiescent human cells. Mol. Cell. Biol.

Nakano, S., Stillman, B., and Horvitz, H.R. (2011). 304. Replication-coupled chromatin assembly generates a neuronal bilateral asymmetry in C. elegans. Cell.

Namsaraev, E.A., and Berg, P. (1998). 134. Binding of RAD51p to DNA. Interaction of RAD51p with single and double- stranded DNA. J. Biol. Chem.

Nassif, N., Penney, J., Pal, S., Engels, W.R., and Gloor, G.B. (1994). 121. Efficient copying of nonhomologous sequences from ectopic sites via P-element-induced gap repair. Mol. Cell. Biol.

Natsume, R., Eitoku, M., Akai, Y., Sano, N., Horikoshi, M., and Senda, T. (2007). 233. Structure and function of the histone chaperone CIA/ASF1 complexed with histones H3 and H4. Nature.

New, J.H., Sugiyama, T., Zaitseva, E., and Kowalczykowski, S.C. (1998). 564. Rad52 protein stimulates DNA strand exchange by Rad51 and replication protein A. Nature.

Newrock, K.M., Cohen, L.H., Hendricks, M.B., Donnelly, R.J., and Weinberg, E.S. (1978). Stage-specific

mRNAs coding for subtypes of H2A and H2B histones in the sea urchin embryo. Cell.

Nick McElhinny, S.A., Snowden, C.M., McCarville, J., and Ramsden, D.A. (2000). 65. Ku recruits the XRCC4-ligase IV complex to DNA ends. Mol. Cell. Biol.

Nicolette, M.L., Lee, K., Guo, Z., Rani, M., Chow, J.M., Lee, S.E., and Paull, T.T. (2010). 495. Mre11gRad50gXrs2 and Sae2 promote 5′ strand resection of DNA double-strand breaks. Nat. Struct. Mol. Biol.

Nimonkar, A. V., Sica, R.A., and Kowalczykowski, S.C. (2009). 505. Rad52 promotes second-end DNA capture in double-stranded break repair to form complement-stabilized joint molecules. Proc. Natl. Acad. Sci.

Niu, H., Chung, W.H., Zhu, Z., Kwon, Y., Zhao, W., Chi, P., Prakash, R., Seong, C., Liu, D., Lu, L., et al. (2010). 129. Mechanism of the ATP-dependent DNA endresection machinery from Saccharomyces cerevisiae. Nature.

Noll, D.M., McGregor Mason, T., and Miller, P.S. (2006). 320. Formation and repair of interstrand cross-links in DNA. Chem. Rev.

Nowsheen, S., and Yang, E.S. (2012). 342. The intersection between DNA damage response and cell death pathways. Exp. Oncol.

O'Donovan, A., Davies, A.A., Moggs, J.G., West, S.C., and Wood, R.D. (1994). 322. XPG endonuclease makes the 3′ Incision in human DNA nucleotide excision repair. Nature.

O'Driscoll, M., Cerosaletti, K.M., Girard, P.M., Dai, Y., Stumm, M., Kysela, B., Hirsch, B., Gennery, A., Palmer, S.E., Seidel, J., et al. (2001). 60. DNA ligase IV mutations identified in patients exhibiting developmental delay and immunodeficiency. Mol. Cell.

Ogawa, T., Yu, X., Shinohara, A., and Egelman, E.H. (1993). 176. Similarity of the yeast RAD51 filament to the bacterial RecA filament. Science (80-.).

Oh, S.D., Lao, J.P., Hwang, P.Y.H., Taylor, A.F., Smith, G.R., and Hunter, N. (2007). BLM Ortholog, Sgs1, Prevents Aberrant Crossing-over by Suppressing Formation of Multichromatid Joint Molecules. Cell.

Orsi, G.A., Couble, P., and Loppin, B. (2009). Epigenetic and replacement roles of histone variant H3.3 in reproduction and development. Int. J. Dev. Biol.

Osley, M.A., Tsukuda, T., and Nickoloff, J.A. (2007). 222. ATP-dependent chromatin remodeling factors and DNA damage repair. Mutat. Res. - Fundam. Mol. Mech. Mutagen.

Osman, F., Dixon, J., Doe, C.L., and Whitby, M.C. (2003). 502. Generating crossovers by resolution of nicked Holliday junctions: A role for Mus81-Eme1 in meiosis. Mol. Cell.

Palakodeti, A., Lucas, I., Jiang, Y., Young, D.J., Fernald, A.A., Karrison, T., and Le Beau, M.M. (2009). 337. Impaired replication dynamics at the FRA3B common fragile site. Hum. Mol. Genet.

Palmer, D.K., O'Day, K., Wener, M.H., Andrews, B.S., and Margolis, R.L. (1987). A 17-kD centromere protein (CENP-A) copurifies with nucleosome core particles and with histones. J. Cell Biol.

Papamichos-Chronakis, M., Watanabe, S., Rando, O.J., and Peterson, C.L. (2011). 406. Global regulation of H2A.Z localization by the INO80 chromatin-remodeling enzyme is essential for genome integrity. Cell.

Pâques, F., Leung, W.Y., and Haber, J.E. (1998). 122. Expansions and contractions in a tandem repeat induced by double-strand break repair. Mol. Cell. Biol.

Paull, T.T., Rogakou, E.P., Yamazaki, V., Kirchgessner, C.U., Gellert, M., and Bonner, W.M. (2000). 221. A critical role for histone H2AX in recruitment of repair factors to nuclear foci after DNA damage.

Curr. Biol.

Petermann, E., Orta, M.L., Issaeva, N., Schultz, N., and Helleday, T. (2010). 331. Hydroxyurea-Stalled Replication Forks Become Progressively Inactivated and Require Two Different RAD51-Mediated Pathways for Restart and Repair. Mol. Cell.

Petrini, J.H.J., and Stracker, T.H. (2003). 497. The cellular response to DNA double-strand breaks: Defining the sensors and mediators. Trends Cell Biol.

Petryk, N., Dalby, M., Wenger, A., Stromme, C.B., Strandsby, A., Andersson, R., and Groth, A. (2018). MCM2 promotes symmetric inheritance of modified histones during DNA replication. Science (80-.).

Petukhova, G., Stratton, S., and Sung, P. (1998). Catalysis of homologous DNA pairing by yeast Rad51 and Rad54 proteins. Nature.

Phair, R.D., and Misteli, T. (2000). High mobility of proteins in the mammalian cell nucleus. Nature.

De Piccoli, G., Katou, Y., Itoh, T., Nakato, R., Shirahige, K., and Labib, K. (2012). 540. Replisome Stability at Defective DNA Replication Forks Is Independent of S Phase Checkpoint Kinases. Mol. Cell.

Pidoux, A., Greenall, A., Blackwell, C., Martin, K.A., Allshire, R.C., and Whitehall, S.K. (2004). 574. The Schizosaccharomyces pombe HIRA-like protein Hip1 is required for the periodic expression of histone genes and contributes to the function of complex centromeres. Mol. Cell. Biol.

Pierce, A.J., and Jasin, M. (2001). 55. NHEJ deficiency and disease. Mol. Cell.

Pietrobon, V., Fréon, K., Hardy, J., Costes, A., Iraqui, I., Ochsenbein, F., and Lambert, S.A.E. (2014). 150. The Chromatin Assembly Factor 1 Promotes Rad51-Dependent Template Switches at Replication Forks by Counteracting D-Loop Disassembly by the RecQ-Type Helicase Rqh1. PLoS Biol.

Pitt, C.W., and Cooper, J.P. (2010). 85. Pot1 inactivation leads to rampant telomere resection and loss in one cell cycle. Nucleic Acids Res.

Plate, I., Hallwyl, S.C.L., Shi, I., Krejci, L., Müller, C., Albertsen, L., Sung, P., and Mortensen, U.H. (2008). 177. Interaction with RPA is necessary for Rad52 repair center formation and for its mediator activity. J. Biol. Chem.

Polo, S.E., and Almouzni, G. (2015). 396. Chromatin dynamics after DNA damage: The legacy of the access-repair-restore model. DNA Repair (Amst).

Polo, S.E., Roche, D., and Almouzni, G. (2006a). New Histone Incorporation Marks Sites of UV Repair in Human Cells. Cell.

Polo, S.E., Roche, D., and Almouzni, G. (2006b). 407. New Histone Incorporation Marks Sites of UV Repair in Human Cells. Cell.

Polo, S.E., Theocharis, S.E., Grandin, L., Gambotti, L., Antoni, G., Savignoni, A., Asselain, B., Patsouris, E., and Almouzni, G. (2010). Clinical significance and prognostic value of chromatin assembly factor-1 overexpression in human solid tumours. Histopathology.

Prakash, R., Krejci, L., Van Komen, S., Schürer, K.A., Kramer, W., and Sung, P. (2005). Saccharomyces cerevisiae MPH1 gene, required for homologous recombination-mediated mutation avoidance, encodes a 3′ to 5′ DNA helicase. J. Biol. Chem.

Prakash, R., Satory, D., Dray, E., Papusha, A., Scheller, J., Kramer, W., Krejci, L., Klein, H., Haber, J.E., Sung, P., et al. (2009). Yeast Mphl helicase dissociates Rad51-made D-loops: Implications for crossover control in mitotic recombination. Genes Dev.

Prieto, E., Hizume, K., Kobori, T., Yoshimura, S.H., and Takeyasu, K. (2012). 193. Core histone charge and linker histone H1 effects on the chromatin structure of Schizosaccharomyces pombe. Biosci.

Biotechnol. Biochem.

Qian, M.X., Pang, Y., Liu, C.H., Haratake, K., Du, B.Y., Ji, D.Y., Wang, G.F., Zhu, Q.Q., Song, W., Yu, Y., et al. (2013). 374. Acetylation-mediated proteasomal degradation of core histones during DNA repair and spermatogenesis. Cell.

Quivy, J.P., Grandi, P., and Almouzni, G. (2001). 268. Dimerization of the largest subunit of chromatin assembly factor 1: Importance in vitro and during Xenopus early development. EMBO J.

Ramirez-Parra, E., and Gutierrez, C. (2007). 242. The many faces of chromatin assembly factor 1. Trends Plant Sci.

Ramsperger, U., and Stahl, H. (1995). 236. Unwinding of chromatin by the SV40 large T antigen DNA helicase. EMBO J.

Ransom, M., Dennehey, B.K., and Tyler, J.K. (2010). 442. Chaperoning Histones during DNA Replication and Repair. Cell.

Räschle, M., Knipsheer, P., Enoiu, M., Angelov, T., Sun, J., Griffith, J.D., Ellenberger, T.E., Schärer, O.D., and Walter, J.C. (2008). Mechanism of Replication-Coupled DNA Interstrand Crosslink Repair. Cell.

Ravanat, J.-L., Douki, T., and Cadet, J. (2001). 5. Direct and indirect effects of UV radiation on DNA and its components. J. Photochem. Photobiol. B Biol.

Ray-Gallet, D., Quivy, J.P., Scamps, C., Martini, E.M.D., Lipinski, M., and Almouzni, G. (2002a). HIRA is critical for a nucleosome assembly pathway independent of DNA synthesis. Mol. Cell.

Ray-Gallet, D., Quivy, J.P., Scamps, C., Martini, E.M.D., Lipinski, M., and Almouzni, G. (2002b). 578. HIRA is critical for a nucleosome assembly pathway independent of DNA synthesis. Mol. Cell.

Ray-Gallet, D., Woolfe, A., Vassias, I., Pellentz, C., Lacoste, N., Puri, A., Schultz, D.C., Pchelintsev, N.A., Adams, P.D., Jansen, L.E.T., et al. (2011a). Dynamics of Histone H3 Deposition In Vivo Reveal a Nucleosome Gap-Filling Mechanism for H3.3 to Maintain Chromatin Integrity. Mol. Cell.

Ray-Gallet, D., Woolfe, A., Vassias, I., Pellentz, C., Lacoste, N., Puri, A., Schultz, D.C., Pchelintsev, N.A., Adams, P.D., Jansen, L.E.T., et al. (2011b). 412. Dynamics of Histone H3 Deposition In Vivo Reveal a Nucleosome Gap-Filling Mechanism for H3.3 to Maintain Chromatin Integrity. Mol. Cell.

Raynaud, C., Mallory, A.C., Latrasse, D., Jégu, T., Bruggeman, Q., Delarue, M., Bergounioux, C., and Benhamed, M. (2014). 20. Chromatin meets the cell cycle. J. Exp. Bot.

Reeves, R. (2015). 382. High mobility group (HMG) proteins: Modulators of chromatin structure and DNA repair in mammalian cells. DNA Repair (Amst).

Reis, C.C., Batista, S., and Ferreira, M.G. (2012). 56. The fission yeast MRN complex tethers dysfunctional telomeres for NHEJ repair. EMBO J.

Renkawitz, J., Lademann, C.A., Kalocsay, M., and Jentsch, S. (2013). 368.Monitoring Homology Search during DNA Double-Strand Break Repair In Vivo. Mol. Cell.

Rich, T., Allen, R.L., and Wyllie, A.H. (2000). 16. Defying death after DNA damage. Nature.

Richet, N., Liu, D., Legrand, P., Velours, C., Corpet, A., Gaubert, A., Bakail, M., Moal-Raisin, G., Guerois, R., Compper, C., et al. (2015). 231. Structural insight into how the human helicase subunit MCM2 may act as a histone chaperone together with ASF1 at the replication fork. Nucleic Acids Res.

Riley, T., Sontag, E., Chen, P., and Levine, A. (2008). 37. Transcriptional control of human p53-regulated genes. Nat. Rev. Mol. Cell Biol.

Rippe, K., Schrader, A., Riede, P., Strohner, R., Lehmann, E., and Langst, G. (2007). 350. DNA

sequence- and conformation-directed positioning of nucleosomes by chromatin-remodeling complexes. Proc. Natl. Acad. Sci.

Ristic, D., Wyman, C., Paulusma, C., and Kanaar, R. (2001). 178. The architecture of the human Rad54-DNA complex provides evidence for protein translocation along DNA. Proc. Natl. Acad. Sci. U. S. A.

Robert, T., Dervins, D., Fabre, F., and Gangloff, S. (2006). Mrc1 and Srs2 are major actors in the regulation of spontaneous crossover. EMBO J.

Robertson, A.B., Klungland, A., Rognes, T., and Leiros, I. (2009). 427. DNA repair in mammalian cells: Base excision repair: the long and short of it. Cell. Mol. Life Sci.

Rog, O., Miller, K.M., Ferreira, M.G., and Cooper, J.P. (2009). 310. Sumoylation of RecQ Helicase Controls the Fate of Dysfunctional Telomeres. Mol. Cell.

Rogakou, E.P., Pilch, D.R., Orr, A.H., Ivanova, V.S., and Bonner, W.M. (1998). 219. DNA double-stranded breaks induce histone H2AX phosphorylation on serine 139. J. Biol. Chem.

Rogakou, E.P., Boon, C., Redon, C., and Bonner, W.M. (1999). 220. Megabase chromatin domains involved in DNA double-strand breaks in vivo. J. Cell Biol.

Rogers, S., Wells, R., and Rechsteiner, M. (1986). 294. Amino acid sequences common to rapidly degraded proteins: The PEST hypothesis. Science (80-.).

Roseaulin, L., Yamada, Y., Tsutsui, Y., Russell, P., Iwasaki, H., and Arcangioli, B. (2008). 171. Mus81 is essential for sister chromatid recombination at broken replication forks. EMBO J.

Rossi, M.J., and Mazin, A. V. (2008). Rad51 protein stimulates the branch migration activity of Rrad54 protein. J. Biol. Chem.

Rothfuss, A., and Grompe, M. (2004). 326. Repair Kinetics of Genomic Interstrand DNA Cross-Links: Evidence for DNA Double-Strand Break-Dependent Activation of the Fanconi Anemia/BRCA Pathway. Mol. Cell. Biol.

Ruiz, J.F., Gomez-Gonzalez, B., and Aguilera, A. (2009). 483. Chromosomal Translocations Caused by Either Pol32-Dependent or Pol32-Independent Triparental Break-Induced Replication. Mol. Cell. Biol.

Saini, N., Ramakrishnan, S., Elango, R., Ayyar, S., Zhang, Y., Deem, A., Ira, G., Haber, J.E., Lobachev, K.S., and Malkova, A. (2013). 485. Migrating bubble during break-induced replication drives conservative DNA synthesis. Nature.

Saintigny, Y., Delacôte, F., Varès, G., Petitot, F., Lambert, S., Averbeck, D., and Lopez, B.S. (2001). 332. Characterization of homologous recombination induced by replication inhibition in mammalian cells. EMBO J.

Sakofsky, C.J., and Malkova, A. (2017). 94. Break induced replication in eukaryotes: mechanisms, functions, and consequences. Crit. Rev. Biochem. Mol. Biol.

Sakofsky, C.J., Roberts, S.A., Malc, E., Mieczkowski, P.A., Resnick, M.A., Gordenin, D.A., and Malkova, A. (2014). 555. Break-induced replication is a source of mutation clusters underlying kataegis. Cell Rep.

Sale, J.E. (2013). 7. Translesion DNA synthesis and mutagenesis in eukaryotes. Cold Spring Harb. Perspect. Biol.

San Filippo, J., Sung, P., and Klein, H. (2008). 123. Mechanism of Eukaryotic Homologous Recombination. Annu. Rev. Biochem.

Sarkar, S., Davies, A.A., Ulrich, H.D., and McHugh, P.J. (2006). 323. DNA interstrand crosslink repair

during G1 involves nucleotide excision repair and DNA polymerase zeta. EMBO J.

Sasaki, M.S., and Tonomura, A. (1973). 329. A High Susceptibility of Fanconi's Anemia to Chromosome Breakage by DNA Cross-linking Agents. Cancer Res.

Sasanuma, H., Tawaramoto, M.S., Lao, J.P., Hosaka, H., Sanda, E., Suzuki, M., Yamashita, E., Hunter, N., Shinohara, M., Nakagawa, A., et al. (2013). 514. A new protein complex promoting the assembly of Rad51 filaments. Nat. Commun.

Sauer, P.V., Timm, J., Liu, D., Sitbon, D., Boeri-Erba, E., Velours, C., Mücke, N., Langowski, J., Ochsenbein, F., Almouzni, G., et al. (2017). 272. Insights into the molecular architecture and histone H3-H4 deposition mechanism of yeast chromatin assembly factor 1. Elife.

Schadt, E.E., Monks, S.A., Drake, T.A., Lusis, A.J., Che, N., Colinayo, V., Ruff, T.G., Milligan, S.B., Lamb, J.R., Cavet, G., et al. (2003). 189. Genetics of gene expression surveyed in maize, mouse and man. Nature.

Schärer, O.D. (2013). 46. Nucleotide excision repair in Eukaryotes. Cold Spring Harb. Perspect. Biol.

Schatz, D.G., and Swanson, P.C. (2011). 17. V(D)J Recombination: Mechanisms of Initiation. Annu. Rev. Genet.

Schlacher, K., Christ, N., Siaud, N., Egashira, A., Wu, H., and Jasin, M. (2011). 100. Double-strand break repair-independent role for BRCA2 in blocking stalled replication fork degradation by MRE11. Cell.

Schopf, B., Bregenhorn, S., Quivy, J.-P., Kadyrov, F.A., Almouzni, G., and Jiricny, J. (2012). 440. Interplay between mismatch repair and chromatin assembly. Proc. Natl. Acad. Sci.

Schubert, I., Schubert, V., and Fuchs, J. (2011). 92. No Evidence for "Break-Induced Replication" in a Higher Plant – But Break-Induced Conversion May Occur. Front. Plant Sci.

Schürer, K.A., Rudolph, C., Ulrich, H.D., and Kramer, W. (2004). Yeast MPH1 Gene Functions in an Error-Free DNA Damage Bypass Pathway That Requires Genes from Homologous Recombination, but Not from Postreplicative Repair. Genetics.

Schwartz, E.K., and Heyer, W.D. (2011). 536. Processing of joint molecule intermediates by structure-selective endonucleases during homologous recombination in eukaryotes. Chromosoma.

Schwartzentruber, J., Korshunov, A., Liu, X.Y., Jones, D.T.W., Pfaff, E., Jacob, K., Sturm, D., Fontebasso, A.M., Quang, D.A.K., Tönjes, M., et al. (2012). 411. Driver mutations in histone H3.3 and chromatin remodelling genes in paediatric glioblastoma. Nature.

Sebesta, M., Burkovics, P., Haracska, L., and Krejci, L. (2011). 521. Reconstitution of DNA repair synthesis in vitro and the role of polymerase and helicase activities. DNA Repair (Amst).

Seong, C., Sehorn, M.G., Plate, I., Shi, I., Song, B., Chi, P., Mortensen, U., Sung, P., and Krejci, L. (2008). 136. Molecular anatomy of the recombination mediator function of Saccharomyces cerevisiae Rad5. J. Biol. Chem.

Serra-Cardona, A., and Zhang, Z. (2017). 244. Replication-Coupled Nucleosome Assembly in the Passage of Epigenetic Information and Cell Identity. Trends Biochem. Sci.

Sharma, A., Singh, K., and Almasan, A. (2012). 40. Histone H2AX phosphorylation: A marker for DNA damage. Methods Mol. Biol.

Sharma, G.G., So, S., Gupta, A., Kumar, R., Cayrou, C., Avvakumov, N., Bhadra, U., Pandita, R.K., Porteus, M.H., Chen, D.J., et al. (2010). 390. MOF and Histone H4 Acetylation at Lysine 16 Are Critical for DNA Damage Response and Double-Strand Break Repair. Mol. Cell. Biol.

Sharpless, N.E., Ferguson, D.O., O'hagan, R.C., Castrillon, D.H., Lee, C., Farazi, P.A., Alson, S., Fleming, J., Morton, C.C., Frank, K., et al. (2001). 59. Impaired nonhomologous end-joining provokes soft tissue sarcomas harboring chromosomal translocations, amplifications, and deletions. Mol. Cell.

Sherwood, P.W., Tsang, S. V, and Osley, M.A. (1993). 579. Characterization of HIR1 and HIR2, two genes required for regulation of histone gene transcription in Saccharomyces cerevisiae. Mol. Cell. Biol.

Shibahara, K.I., and Stillman, B. (1999). 296. Replication-dependent marking of DNA by PCNA facilitates CAF-1-coupled inheritance of chromatin. Cell.

Shinohara, A., and Ogawa, T. (1998). Stimulation by Rad52 of yeast Rad51-mediated recombination. Nature.

Shinohara, A., Ogawa, H., and Ogawa, T. (1992). 137. Rad51 protein involved in repair and recombination in S. cerevisiae is a RecA-like protein. Cell.

Shor, E., Weinstein, J., and Rothstein, R. (2005). 513. A genetic screen for top3 suppressors in Saccharomyces cerevisiae identifies SHU1, SHU2, PSY3 and CSM2: Four genes involved in error-free DNA repair. Genetics.

Shroff, R., Arbel-Eden, A., Pilch, D., Ira, G., Bonner, W.M., Petrini, J.H., Haber, J.E., and Lichten, M. (2004). 370.Distribution and dynamics of chromatin modification induced by a defined DNA double-strand break. Curr. Biol.

Shuaib, M., Ouararhni, K., Dimitrov, S., and Hamiche, A. (2010). 386. HJURP binds CENP-A via a highly conserved N-terminal domain and mediates its deposition at centromeres. Proc. Natl. Acad. Sci.

Siersbfk, R., Nielsen, R., John, S., Sung, M.H., Baek, S., Loft, A., Hager, G.L., and Mandrup, S. (2011). 348. Extensive chromatin remodelling and establishment of transcription factor hotspots during early adipogenesis. EMBO J.

Sigurdsson, S., Van Komen, S., Petukhova, G., and Sung, P. (2002). 511. Homologous DNA pairing by human recombination factors Rad51 and Rad54. J. Biol. Chem.

Simsek, D., and Jasin, M. (2010). 79. Alternative end-joining is suppressed by the canonical NHEJ component Xrcc4-ligase IV during chromosomal translocation formation. Nat. Struct. Mol. Biol.

Singh, D.K., Ahn, B., and Bohr, V.A. (2009). 503. Roles of RECQ helicases in recombination based DNA repair, genomic stability and aging. Biogerontology.

Singh, D.K., Ghosh, A.K., Croteau, D.L., and Bohr, V.A. (2012). 534. RecQ helicases in DNA double strand break repair and telomere maintenance. Mutat. Res.

Sinha, R.P., and Häder, D.-P. (2002). 4. UV-induced DNA damage and repair: a review. Photochem. Photobiol. Sci.

Smith, S., and Stillman, B. (1989). 253. Purification and characterization of CAF-I, a human cell factor required for chromatin assembly during DNA replication in vitro. Cell *58*, 15–25.

Smith, S., and Stillman, B. (1991a). Stepwise assembly of chromatin during DNA replication in vitro. EMBO J.

Smith, S., and Stillman, B. (1991b). 284. Immunological characterization of chromatin assembly factor I, a human cell factor required for chromatin assembly during DNA replication in vitro. J. Biol. Chem.

Smith, C.E., Llorente, B., and Symington, L.S. (2007). 554. Template switching during break-induced replication. Nature.

Smith, E.M., Lajoie, B.R., Jain, G., and Dekker, J. (2016). 346. Invariant TAD Boundaries Constrain Cell-

Type-Specific Looping Interactions between Promoters and Distal Elements around the CFTR Locus. Am. J. Hum. Genet.

Smith, T.F., Gaitatzes, C., Saxena, K., Neer, E.J., Duronio, R.J., Gordon, J.L., Boguski, M.S., Voorn, L. van der, Ploegh, H.L., Neer, E.J., et al. (1999). 275. The WD repeat: a common architecture for diverse functions. Trends Biochem. Sci.

Solinger, J.A., Kiianitsa, K., and Heyer, W.D. (2002). 148. Rad54, a Swi2/Snf2-like recombinational repair protein, disassembles Rad51: dsDNA filaments. Mol. Cell.

Song, Y., He, F., Xie, G., Guo, X., Xu, Y., Chen, Y., Liang, X., Stagljar, I., Egli, D., Ma, J., et al. (2007). 447. CAF-1 is essential for Drosophila development and involved in the maintenance of epigenetic memory. Dev. Biol.

Soria, G., Polo, S.E., and Almouzni, G. (2012). 379. Prime, Repair, Restore: The Active Role of Chromatin in the DNA Damage Response. Mol. Cell.

Stewart, E., Chapman, C.R., Al-Khodairy, F., Carr, A.M., and Enoch, T. (1997). rqh1+, a fission yeast gene related to the Bloom's and Werner's syndrome genes, is required for reversible S phase arrest. EMBO J.

Stillman, B. (1986). 252. Chromatin assembly during SV40 DNA replication in vitro. Cell.

Story, R.M., Bishop, D.K., Kleckner, N., and Steitz, T.A. (1993). 175. Structural relationship of bacterial RecA proteins to recombination proteins from bacteriophage T4 and yeast. Science (80-.).

Strahl, B.D., and Allis, C.D. (2000). 210. The language of covalent histone modifications. Nature.

Strickfaden, H., McDonald, D., Kruhlak, M.J., Haince, J.F., Th'Ng, J.P.H., Rouleau, M., Ishibashi, T., Corry, G.N., Ausio, J., Underhill, D.A., et al. (2016). 373.Poly(ADP-ribosyl)ation-dependent transient chromatin decondensation and histone displacement following laser microirradiation. J. Biol. Chem.

Sugawara, N., Ira, G., and Haber, J.E. (2000). 93. DNA length dependence of the single-strand annealing pathway and the role of Saccharomyces cerevisiae RAD59 in double-strand break repair. Mol. Cell. Biol.

Sugiyama, T., and Kowalczykowski, S.C. (2002). 138. Rad52 protein associates with replication protein A (RPA)-single-stranded DNA to accelerate Rad51-mediated displacement of RPA and presynaptic complex formation. J. Biol. Chem.

Sugiyama, T., New, J.H., and Kowalczykowski, S.C. (1998). 140. DNA annealing by Rad52 Protein is stimulated by specific interaction with the complex of replication protein A and single-stranded DNA. Proc. Natl. Acad. Sci.

Sullivan, S.A., and Landsman, D. (2003). 226. Characterization of sequence variability in nucleosome core histone folds. Proteins Struct. Funct. Bioinforma.

Sullivan, K.F., Hechenberger, M., and Masri, K. (2013). Human CENP-A contains a histone H3 related histone fold domain that is required for targeting to the centromere. Cancer Discov.

Sun, W., Nandi, S., Osman, F., Ahn, J.S., Jakovleska, J., Lorenz, A., and Whitby, M.C. (2008). The FANCM Ortholog Fml1 Promotes Recombination at Stalled Replication Forks and Limits Crossing Over during DNA Double-Strand Break Repair. Mol. Cell.

Sung, P. (1997a). 139. Function of yeast Rad52 protein as a mediator between replication protein A and the Rad51 recombinase. J. Biol. Chem.

Sung, P. (1997b). 142. Yeast Rad55 and Rad57 proteins form a heterodimer that functions with replication protein A to promote DNA strand exchange by Rad51 recombinase. Genes Dev.

Sung, P., Krejci, L., Van Komen, S., and Sehorn, M.G. (2003). 128. Rad51 Recombinase and Recombination Mediators. J. Biol. Chem.

Sutton, A., Bucaria, J., Osley, M.A., and Sternglanz, R. (2001). 573. Yeast ASF1 protein is required for cell cycle regulation of histone gene transcription. Genetics.

Šviković, S., and Sale, J.E. (2017). 243. The Effects of Replication Stress on S Phase Histone Management and Epigenetic Memory. J. Mol. Biol.

Swaney, D.L., Beltrao, P., Starita, L., Guo, A., Rush, J., Fields, S., Krogan, N.J., and Villén, J. (2013). 584. Global analysis of phosphorylation and ubiquitylation cross-talk in protein degradation. Nat. Methods.

Swenberg, J.A., Richardson, F.C., Boucheron, J.A., and Dyroff, M.C. (1985). 8. Relationships between DNA adduct formation and carcinogenesis. Environ. Health Perspect.

Swenberg, J.A., Lu, K., Moeller, B.C., Gao, L., Upton, P.B., Nakamura, J., and Starr, T.B. (2011). 9. Endogenous versus exogenous DNA adducts: Their role in carcinogenesis, epidemiology, and risk assessment. Toxicol. Sci.

Symington, L.S. (2002). 102. Role of RAD52 epistasis group genes in homologous recombination and double-strand break repair. Microbiol. Mol. Biol. Rev.

Symington, L.S. (2014). 488. End resection at double-strand breaks: Mechanism and regulation. Cold Spring Harb. Perspect. Biol.

Symington, L.S., and Gautier, J. (2011). 68. Double-Strand Break End Resection and Repair Pathway Choice. Annu. Rev. Genet.

Szostak, J.W., Orr-Weaver, T.L., Rothstein, R.J., and Stahl, F.W. (1983). 111. The double-strand-break repair model for recombination. Cell.

Szymkowski, D.E., Yarema, K., Essigmann, J.M., Lippard, S.J., and Wood, R.D. (1992). 321. An intrastrand d(GpG) platinum crosslink in duplex M13 DNA is refractory to repair by human cell extracts. Proc. Natl. Acad. Sci. U. S. A.

Tacconi, E.M.C., and Tarsounas, M. (2015). 107. How homologous recombination maintains telomere integrity. Chromosoma.

Tagami, H., Ray-Gallet, D., Almouzni, G., and Nakatani, Y. (2004). 278. Histone H3.1 and H3.3 Complexes Mediate Nucleosome Assembly Pathways Dependent or Independent of DNA Synthesis. Cell.

Talbert, P.B., and Henikoff, S. (2010). 212. Histone variants--ancient wrap artists of the epigenome. Nat Rev Mol Cell Biol.

Talbert, P.B., and Henikoff, S. (2017). 217. Histone variants on the move: Substrates for chromatin dynamics. Nat. Rev. Mol. Cell Biol.

Le Tallec, B., Dutrillaux, B., Lachages, A.-M., Millot, G.A., Brison, O., and Debatisse, M. (2011). 335. Molecular profiling of common fragile sites in human fibroblasts. Nat. Struct. Mol. Biol.

Tan, B.C.M., Chien, C.T., Hirose, S., and Lee, S.C. (2006). 250. Functional cooperation between FACT and MCM helicase facilitates initiation of chromatin DNA replication. EMBO J.

Tanae, K., Horiuchi, T., Matsuo, Y., Katayama, S., and Kawamukai, M. (2012). 315. Histone chaperone Asf1 plays an essential role in maintaining genomic stability in fission yeast. PLoS One.

Tanaka, K., Nishide, J., Okazaki, K., Kato, H., Niwa, O., Nakagawa, T., Matsuda, H., Kawamukai, M., and Murakami, Y. (1999). 313. Characterization of a fission yeast SUMO-1 homologue, pmt3p,

required for multiple nuclear events, including the control of telomere length and chromosome segregation. Mol. Cell. Biol.

Tang, Y., Poustovoitov, M. V., Zhao, K., Garfinkel, M., Canutescu, A., Dunbrack, R., Adams, P.D., and Marmorstein, R. (2006). 276. Structure of a human ASF1a-HIRA complex and insights into specificity of histone chaperone complex assembly. Nat. Struct. Mol. Biol.

Tang, Y., Wang, J., Lian, Y., Fan, C., Zhang, P., Wu, Y., Li, X., Xiong, F., Li, X., Li, G., et al. (2017). 353. Linking long non-coding RNAs and SWI/SNF complexes to chromatin remodeling in cancer. Mol. Cancer.

Taunton, J., Hassig, C.A., and Schreiber, S.L. (1996). 293. A mammalian histone deacetylase related to the yeast transcriptional regulator Rpd3p. Science (80-.).

Teixeira-Silva, A., Ait Saada, A., Hardy, J., Iraqui, I., Nocente, M.C., Fréon, K., and Lambert, S.A.E. (2017). 498. The end-joining factor Ku acts in the end-resection of double strand break-free arrested replication forks. Nat. Commun.

Terui, R., Nagao, K., Kawasoe, Y., Taki, K., Higashi, T.L., Tanaka, S., Nakagawa, T., Obuse, C., Masukata, H., and Takahashi, T.S. (2018). 434. Nucleosomes around a mismatched base pair are excluded via an Msh2-dependent reaction with the aid of SNF2 family ATPase Smarcad1. Genes Dev.

Thorslund, T., Ripplinger, A., Hoffmann, S., Wild, T., Uckelmann, M., Villumsen, B., Narita, T., Sixma, T.K., Choudhary, C., Bekker-Jensen, S., et al. (2015). 392. Histone H1 couples initiation and amplification of ubiquitin signalling after DNA damage. Nature.

Tombline, G., and Fishel, R. (2002). 133. Biochemical characterization of the human RAD51 protein. I. ATP hydrolysis. J. Biol. Chem.

Trojer, P., and Reinberg, D. (2007). 188. Facultative Heterochromatin: Is There a Distinctive Molecular Signature? Mol. Cell.

Tsang, E., Miyabe, I., Iraqui, I., Zheng, J., Lambert, S.A.E., and Carr, A.M. (2014). 475. The extent of error-prone replication restart by homologous recombination is controlled by Exo1 and checkpoint proteins. J. Cell Sci.

Tsunaka, Y., Fujiwara, Y., Oyama, T., Hirose, S., and Morikawa, K. (2016). 248. Integrated molecular mechanism directing nucleosome reorganization by human FACT. Genes Dev.

Tuduri, S., Tourrière, H., and Pasero, P. (2010). 547. Defining replication origin efficiency using DNA fiber assays. Chromosom. Res.

Turner, B.M. (2000). 211. Histone acetylation and an epigenetic code. BioEssays.

Tyagi, M., Imam, N., Verma, K., and Patel, A.K. (2016). 349. Chromatin remodelers: We are the drivers!! Nucleus.

Tyler, J.K., Adams, C.R., Chen, S.R., Kobayashi, R., Kamakaka, R.T., and Kadonaga, J.T. (1999). The RCAF complex mediates chromatin assembly during DNA replication and repair. Nature.

Tyler, J.K., Collins, K.A., Prasad-Sinha, J., Amiott, E., Bulger, M., Harte, P.J., Kobayashi, R., and Kadonaga, J.T. (2001). 280. Interaction between the Drosophila CAF-1 and ASF1 Chromatin Assembly Factors. Mol. Cell. Biol.

Uetz, P., Giot, L., Cagney, G., Mansfield, T. a, Judson, R.S., Knight, J.R., Lockshon, D., Narayan, V., Srinivasan, M., Pochart, P., et al. (2000). 518. A comprehensive analysis of protein-protein interactions in Saccharomyces cerevisiae. Nature.

Uwada, J., Tanaka, N., Yamaguchi, Y., Uchimura, Y., Shibahara, K. ichi, Nakao, M., and Saitoh, H. (2010). 271. The p150 subunit of CAF-1 causes association of SUMO2/3 with the DNA replication foci.

Biochem. Biophys. Res. Commun.

VanDemark, A.P., Blanksma, M., Ferris, E., Heroux, A., Hill, C.P., and Formosa, T. (2006). 251. The Structure of the yFACT Pob3-M Domain, Its Interaction with the DNA Replication Factor RPA, and a Potential Role in Nucleosome Deposition. Mol. Cell.

Vanoli, F., Fumasoni, M., Szakal, B., Maloisel, L., and Branzei, D. (2010). 558. Replication and recombination factors contributing to recombination-dependent bypass of DNA lesions by template switch. PLoS Genet.

Varas, J., Santos, J.L., and Pradillo, M. (2017). The Absence of the Arabidopsis Chaperone Complex CAF-1 Produces Mitotic Chromosome Abnormalities and Changes in the Expression Profiles of Genes Involved in DNA Repair. Front. Plant Sci.

Veaute, X., Jeusset, J., Soustelle, C., Kowalczykowski, S.C., Le Cam, E., and Fahre, F. (2003). The Srs2 helicase prevents recombination by disrupting Rad51 nucleoprotein filaments. Nature.

Verreault, A., Kaufman, P.D., Kobayashi, R., and Stillman, B. (1996). 254. Nucleosome assembly by a complex of CAF-1 and acetylated histones H3/H4. Cell.

Vesela, E., Chroma, K., Turi, Z., and Mistrik, M. (2017). 52. Common chemical inductors of replication stress: Focus on cell-based studies. Biomolecules.

Vogler, C., Huber, C., Waldmann, T., Ettig, R., Braun, L., Izzo, A., Daujat, S., Chassignet, I., Lopez-Contreras, A.J., Fernandez-Capetillo, O., et al. (2010). 199. Histone H2A C-terminus regulates chromatin dynamics, remodeling, and histone H1 binding. PLoS Genet.

Voineagu, I., Narayanan, V., Lobachev, K.S., and Mirkin, S.M. (2008). 28. Replication stalling at unstable inverted repeats: Interplay between DNA hairpins and fork stabilizing proteins. Proc. Natl. Acad. Sci.

Volk, A., and Crispino, J.D. (2015). 274. The role of the chromatin assembly complex (CAF-1) and its p60 subunit (CHAF1b) in homeostasis and disease. Biochim. Biophys. Acta - Gene Regul. Mech.

Walker, J.R., Corpina, R.A., and Goldberg, J. (2001). 563. Structure of the Ku heterodimer bound to dna and its implications for double-strand break repair. Nature.

Wang, H., Perrault, A.R., Takeda, Y., Qin, W., Wang, H., and Iliakis, G. (2003). 74. Biochemical evidence for Ku-independent backup pathways of NHEJ. Nucleic Acids Res.

Wang, H., Zhang, X., Teng, L., and Legerski, R.J. (2015). 43. DNA damage checkpoint recovery and cancer development. Exp. Cell Res.

Wang, Z.G., Wu, X.H., and Friedberg, E.C. (1991). 397. Nucleotide excision repair of DNA by human cell extracts is suppressed in reconstituted nucleosomes. J. Biol. Chem.

Warbrick, E. (1998). 264. PCNA binding through a conserved motif. BioEssays.

Ward, I.M., and Chen, J. (2001). 42. Histone H2AX Is Phosphorylated in an ATR-dependent Manner in Response to Replicational Stress. J. Biol. Chem.

Watts, F.Z., Skilton, A., Ho, J.C.-Y., Boyd, L.K., Trickey, M.A.M., Gardner, L., Ogi, F.-X., and Outwin, E.A. (2007). 314. The role of Schizosaccharomyces pombe SUMO ligases in genome stability. Biochem. Soc. Trans.

Weeden, C.E., and Asselin-Labat, M.-L. (2018). 3. Mechanisms of DNA damage repair in adult stem cells and implications for cancer formation. Biochim. Biophys. Acta - Mol. Basis Dis.

Wiedemann, G., van Gessel, N., Köchl, F., Hunn, L., Schulze, K., Maloukh, L., Nogué, F., Decker, E.L., Hartung, F., and Reski, R. (2018). 531. RecQ helicases function in development, DNA repair, and gene

targeting in Physcomitrella patens. Plant Cell.

Wierzbicki, A.T., and Jerzmanowski, A. (2005). 205. Suppression of histone H1 genes in arabidopsis results in heritable developmental defects and stochastic changes in DNA methylation. Genetics.

Wilkins, A.S. (2000). 263. The puzzle of PCNA's many partners. BioEssays.

Williams, R.S., Moncalian, G., Williams, J.S., Yamada, Y., Limbo, O., Shin, D.S., Groocock, L.M., Cahill, D., Hitomi, C., Guenther, G., et al. (2008). 490. Mre11 Dimers Coordinate DNA End Bridging and Nuclease Processing in Double-Strand-Break Repair. Cell.

Wilson, M.A., Kwon, Y., Xu, Y., Chung, W.H., Chi, P., Niu, H., Mayle, R., Chen, X., Malkova, A., Sung, P., et al. (2013). 553.Pif1 helicase and Polδ promote recombination-coupled DNA synthesis via bubble migration. Nature.

Winkler, D.D., Zhou, H., Dar, M.A., Zhang, Z., and Luger, K. (2012). 270. Yeast CAF-1 assembles histone (H3-H4)2tetramers prior to DNA deposition. Nucleic Acids Res.

Wittmeyer, J., and Formosa, T. (1997). 249. The Saccharomyces cerevisiae DNA polymerase alpha catalytic subunit interacts with Cdc68/Spt16 and with Pob3, a protein similar to an HMG1-like protein. Mol. Cell. Biol.

Wood, R.D. (2010). 324. Mammalian nucleotide excision repair proteins and interstrand crosslink repair. Environ. Mol. Mutagen.

Wood, V., Gwilliam, R., Rajandream, M.A., Lyne, M., Lyne, R., Stewart, A., Sgouros, J., Peat, N., Hayles, J., Baker, S., et al. (2002). 464.?The genome sequence of Schizosaccharomyces pombe. Nature.

Woodcock, C.L., and Ghosh, R.P. (2010). Chromatin higher-order structure and dynamics. Cold Spring Harb. Perspect. Biol.

Woodward, A.M., Göhler, T., Luciani, M.G., Oehlmann, M., Ge, X., Gartner, A., Jackson, D.A., and Blow, J.J. (2006). 25. Excess Mcm2-7 license dormant origins of replication that can be used under conditions of replicative stress. J. Cell Biol.

Wu, L., and Hickson, I.O. (2003). 183. The Bloom's syndrome helicase suppresses crossing over during homologous recombination. Nature.

Wu, L., Davies, S.L., Levitt, N.C., and Hickson, I.D. (2001). 565. Potential Role for the BLM Helicase in Recombinational Repair via a Conserved Interaction with RAD51. J. Biol. Chem.

Xhemalce, B., Miller, K.M., Driscoll, R., Masumoto, H., Jackson, S.P., Kouzarides, T., Verreault, A., and Arcangioli, B. (2007). 302. Regulation of histone H3 lysine 56 acetylation in Schizosaccharomyces pombe. J Biol Chem.

Xu, X., Ball, L., Chen, W., Tian, X., Lambrecht, A., Hanna, M., and Xiao, W. (2013). 516. The yeast Shu complex utilizes homologous recombination machinery for error-free lesion bypass via physical interaction with a Rad51 paralogue. PLoS One.

Yagi, T., Fujikawa, Y., Sawai, T., Takamura-Enya, T., Ito-Harashima, S., and Kawanishi, M. (2017). 318. Error-prone and error-free translesion DNA synthesis over site-specifically created dna adducts of aryl hydrocarbons (3-nitrobenzanthrone and 4-aminobiphenyl). Toxicol. Res.

Yanagida, M. (2002). 467. The model unicellular eukaryote, Schizosaccharomyces pombe. Genome Biol.

Yaneva, M., Kowalewski, T., and Lieber, M.R. (1997). 64. Interaction of DNA-dependent protein kinase with DNA and with Ku: Biochemical and atomic-force microscopy studies. EMBO J.

Yang, C., Sengupta, S., Hegde, P.M., Mitra, J., Jiang, S., Holey, B., Sarker, A.H., Tsai, M.-S., Hegde, M.L., and Mitra, S. (2016). 433. Regulation of oxidized base damage repair by chromatin assembly factor 1 subunit A. Nucleic Acids Res.

Ye, X., Franco, A.A., Santos, H., Nelson, D.M., Kaufman, P.D., and Adams, P.D. (2003). 281. Defective S phase chromatin assembly causes DNA damage, activation of the S phase checkpoint, and S phase arrest. Mol. Cell.

Yu, V.P.C.C., Koehler, M., Steinlein, C., Schmid, M., Hanakahi, L.A., Van Gool, A.J., West, S.C., and Venkitaraman, A.R. (2000). 328. Gross chromosomal rearrangements and genetic exchange between nonhomologous chromosomes following BRCA2 inactivation. Genes Dev.

Yuan, J., Adamski, R., and Chen, J. (2010). 383. Focus on histone variant H2AX: To be or not to be. FEBS Lett.

Zeitlin, S.G., Baker, N.M., Chapados, B.R., Soutoglou, E., Wang, J.Y.J., Berns, M.W., and Cleveland, D.W. (2009). 410. Double-strand DNA breaks recruit the centromeric histone CENP-A. Proc. Natl. Acad. Sci.

Zentner, G.E., and Henikoff, S. (2013). Regulation of nucleosome dynamics by histone modifications. Nat. Struct. Mol. Biol.

Zhang, H., Hua, Y., Li, R., and Kong, D. (2016a). 529. Cdc24 is essential for long-range end resection in the repair of double-stranded DNA breaks. J. Biol. Chem.

Zhang, K., Gao, Y., Li, J., Burgess, R., Han, J., Liang, H., Zhang, Z., and Liu, Y. (2016b). 266. A DNA binding winged helix domain in CAF-1 functions with PCNA to stabilize CAF-1 at replication forks. Nucleic Acids Res.

Zhang, W., Tyl, M., Ward, R., Sobott, F., Maman, J., Murthy, A.S., Watson, A.A., Fedorov, O., Bowman, A., Owen-Hughes, T., et al. (2013). 286. Structural plasticity of histones H3-H4 facilitates their allosteric exchange between RbAp48 and ASF1. Nat. Struct. Mol. Biol.

Zhang, Y., Ng, H.H., Erdjument-Bromage, H., Tempst, P., Bird, A., and Reinberg, D. (1999). 291. Analysis of the NuRD subunits reveals a histone deacetylase core complex and a connection with DNA methylation. Genes Dev.

Zheng, X.F., Prakash, R., Saro, D., Longerich, S., Niu, H., and Sung, P. (2011). Processing of DNA structures via DNA unwinding and branch migration by the S. cerevisiae Mph1 protein. DNA Repair (Amst).

Zhou, B.R., Jiang, J., Feng, H., Ghirlando, R., Xiao, T.S., and Bai, Y. (2015). 204. Structural Mechanisms of Nucleosome Recognition by Linker Histones. Mol. Cell.

Zhu, C., Mills, K.D., Ferguson, D.O., Lee, C., Manis, J., Fleming, J., Gao, Y., Morton, C.C., and Alt, F.W. (2002). 80. Unrepaired DNA breaks in p53-deficient cells lead to oncogenic gene amplification subsequent to translocations. Cell.

Zhu, Z., Chung, W.H., Shim, E.Y., Lee, S.E., and Ira, G. (2008). 113. Sgs1 Helicase and Two Nucleases Dna2 and Exo1 Resect DNA Double-Strand Break Ends. Cell.

Ziv, Y., Bielopolski, D., Galanty, Y., Lukas, C., Taya, Y., Schultz, D.C., Lukas, J., Bekker-Jensen, S., Bartek, J., and Shiloh, Y. (2006). 376. Chromatin relaxation in response to DNA double-strand breaks is modulated by a novel ATM- and KAP-1 dependent pathway. Nat. Cell Biol.

Annex

Annex 1

Manuscript

Histone deposition promotes recombination-dependent replication at arrested forks

Histone deposition promotes recombination-dependent replication at arrested forks

Julien Hardy[1,2], Dingli Dai[1,2], Anissia Ait Saada[1,2], Ana Teixeira-Silva[1,2], Louise Dupoiron[1,2], Fatemeh Mojallali[1,2], Karine Fréon[1,2], Francoise Ochsenbein[3], Brigitte Hartmann[4] and Sarah Lambert[1,2*].

[1] Institut Curie, PSL Research University, CNRS, UMR3348, F-91405, Orsay, France.

[2] University Paris Sud, Paris-Saclay University, CNRS, UMR3348, F-91405, Orsay, France.

[3] CEA, DRF, SB2SM, Laboratoire de Biologie Structurale et Radiobiologie, Gif-sur-Yvette, France.

[4] Laboratoire de Biologie et Pharmacologie Appliquée (LBPA) UMR 8113, CNRS / ENS de Cachan 61, avenue du Président Wilson, 94235 Cachan cedex.

*corresponding author and lead contact: Sarah Lambert

E-mail: sarah.lambert@curie.fr

Phone: 0033 169867191

Running title: Histone deposition promotes fork-restart

Keywords: Homologous recombination, Chromatin Assembly Factor 1, Histones, Rqh1 helicase, replication stress.

Abstract

Replication stress poses a serious threat to genome and epigenome stability. Recombination-Dependent-Replication (RDR) promotes DNA synthesis resumption from arrested forks. Despite the identification of chromatin restoration pathways during DNA repair processes, crosstalk coupling RDR and chromatin assembly is largely unexplored. Here, we addressed the contribution of chromatin assembly to replication stress in fission yeast. We expressed a mutated histone (H3-H113D) to genetically impair replication-dependent chromatin assembly by destabilizing $(H3\text{-}H4)_2$ tetramer. We established that DNA synthesis-dependent histone deposition, by CAF-1 and Asf1, promotes RDR by preventing Rqh1-mediated disassembly of joint molecules. This crosstalk contributes to cell survival upon replication stress but favors deletion type events. The recombination factor Rad52 is required for CAF-1 binding to the chromatin upon replication stress and to repair-synthesis during RDR. These results demonstrate that histone deposition plays an active role in fine-tuning RDR, a benefit counterbalanced by stabilizing at-risk joint molecules for genome stability.

- **H3-H113D impairs nucleosome stability and deposition**
- **Histone deposition, Asf1 and CAF-1 play an active role in RDR**
- **RDR-coupled histone deposition impacts genome stability at arrested forks.**
- **Rad52 promotes CAF-1 association to repair synthesis during RDR.**

Introduction

The maintenance of genome integrity occurs in the context of DNA packaged into chromatin. Chromatin constitutes a barrier to DNA replication and repair machineries, that should be first lifted and then restored behind the replication fork or once the repair event is achieved[1]. Genomes are routinely exposed to a variety of DNA damages that induce profound chromatin rearrangements and pose serious threat to epigenome integrity during DNA replication[2]. Despite the recent identification of chromatin restoration pathways upon DNA repair, the crosstalk and coordination between both processes, that is likely key to safeguard genome integrity, remain poorly understood[3].

The basic unit of chromatin is the nucleosome which consists of 147 bp of double stranded DNA wrapped around a histone octamer containing one $(H3\text{-}H4)_2$ tetramer and two H2A-H2B dimers[4]. During DNA replication, nucleosomes ahead of the replication fork are evicted and both parental and newly synthetized histones are assembled onto newly replicated DNA through a process called replication-coupled chromatin assembly. This process requires a network of chromatin factors that operate sequential reactions to handle histone dynamics at ongoing forks. Nucleosome assembly occurs as a stepwise process in which the $(H3\text{-}H4)_2$ tetramer is deposited before two H2A-H2B dimers[5,6]. Deposition of $(H3\text{-}H4)_2$ tetramer requires specific histone modifications and H3-H4 chaperones, such as the Chromatin Assembly Factor 1, CAF-1, the Anti-Silencing Factor 1, Asf1 and Rtt106[7].

CAF-1 plays a key role in nucleosome assembly coupled to DNA synthesis during DNA replication and repair. It associates with the proliferating cell nuclear antigen (PCNA), the processivity factor for DNA polymerases, to facilitate nucleosome deposition onto DNA *in vitro*[8,9]. CAF-1 is a tri-subunit complex in which the large subunit (human p150, *S. cerevisiae* Cac1 and *S. pombe* Pcf1), scaffolds interaction with H3-H4 and DNA to allow nucleosome assembly. Recent *in vitro* studies have elucidated how CAF-1 promotes $(H3\text{-}H4)_2$ tetramer deposition onto DNA[10-14]. One CAF-1 complex binds a single H3-H4 heterodimer, allowing unmasking the C-terminus winged helix domain of p150 to bind DNA. Then, DNA-mediated dimerization of two CAF-1 complexes allows $(H3\text{-}H4)_2$ tetramer formation and deposition onto DNA. $(H3\text{-}H4)_2$ tetramerization is required to achieve deposition onto DNA and then release H3-H4 from CAF-1. An histone H3 mutant that destabilizes H3-H3' interface impairs *in vitro* tetramer deposition[12]. Asf1 binds a H3-H4 heterodimer and acts by transferring H3-H4 to CAF-1 and Rtt106[15]. In yeast models, Asf1 is required for acetylation of H3 at lysine K56 (H3K56Ac), a mark of newly synthetized H3, by the acetyl transferase Rtt109[16,17]. Also, Asf1 associates with components of the replication machinery and facilitates CAF-1-mediated histone deposition *in vitro*[7,18].

Flaws in the DNA replication process are a source of genome and epigenome instability. Numerous Replication Fork Barriers (RFBs) and replication-blocking agents interrupt fork elongation, causing recurrent temporary pauses to a single replisome and occasional terminal fork arrest. Stressed forks are fragile structures prone to chromosomal aberrations which may result from faulty replication-based DNA repair events[19]. Chromatin establishment and maturation takes place during DNA replication, a critical step to the inheritance of the epigenome [20]. Histone supply and chromatin assembly regulate fork stability and elongation[21,22]. Fork obstacles interfere with histone dynamics, including histone recycling and inheritance of histone marks, resulting in adjacent loci liable to epigenetic changes[2,23]. Thus, stressed forks are instrumental in triggering chromosomal aberrations and chromatin changes by mechanisms that remain to be fully understood.

A variety of DNA repair factors are engaged in the timely resumption of fork elongation. Homologous recombination (HR) is a key DNA repair pathway that preserves fork integrity and replication competence through a process called Recombination-Dependent Replication (RDR) [24]. At the pre-synaptic step, the recombinase Rad51 is recruited onto single stranded DNA (ssDNA) exposed at arrested forks, to form a filament with the assistance of mediators such as yeast Rad52 and mammalian BRCA2. After homology search, the Rad51 filament promotes strand invasion into an intact homologous DNA template, usually the sister chromatid or the parental DNA ahead of the fork, to form a displacement loop (D-loop). The invading 3' end then primes DNA synthesis to restart the fork and complete DNA replication. D-loops can be disassembled by DNA helicases such as the human RecQ helicase BLM and its fission yeast orthologue Rqh1[25]. Because eukaryotic genomes contain several types of dispersed and repeated sequences, RDR can occasionally generate chromosomal rearrangements. In these circumstances, RecQ helicases are instrumental to limit the likelihood of faulty RDR creating chromosomal aberrations[26,27].

The access-prime-restore model has put forward the role of chromatin factors to handle histone dynamics at DNA lesions and to initiate DNA repair, with mammalian Asf1 and CAF-1 being involved in the early step of DSB repair by HR[1]. Subsequent to DNA repair, chromatin restoration is a necessary step to engage physiological processes such as transcription restart and turning-off the checkpoint response[28,29]. Crosstalk to couple DNA repair and chromatin re-assembly are poorly understood and it is unknown whether RDR remains coupled to histone deposition in S-phase. We previously reported that fission yeast CAF-1 is required to complete the process of RDR in a PCNA-dependent manner[30]. By counteracting Rqh1-dependent disassembly of D-loops, CAF-1 channels RDR events towards a chromosomal rearrangement pathway. However, the mechanism by which CAF-1 counteracts Rqh1 activity at site of replication stress is unknown.

Here, we uncovered that RDR is coupled to Asf1 and CAF-1-mediated histone deposition, a step necessary to promote RDR completion. RDR-coupled histone deposition prevents the disassembly of D-loops by Rqh1, a crosstalk promoting cell resistance to replication stress but channeling HR events towards deleterious recombinants types. Rad52 is necessary for Pcf1 binding to the chromatin upon replication stress and its binding to sites of DNA synthesis associated to RDR. Our data indicates that CAF-1 counteracts Rqh1 activity by promoting histone deposition during RDR. Therefore, we revealed a novel and replication-specific crosstalk between DNA repair factors and chromatin assembly to ensure repair-synthesis and balance genome stability at sites of fork-arrest.

Results

Asf1 is required to complete RDR.

We previously reported that CAF-1 acts during the DNA synthesis step of RDR, in a way that D-loops are protected from disassembly by Rqh1. Here, we asked whether Asf1 is also involved in RDR. To this end, we employed a previously described site-specific fork arrest assay in which replication of a specific genomic locus is dependent on HR[26]. The assay consists of two polar Replication Fork Barrier (RFB), called *RTS1*, integrated as inverted repeats at both sides of the *ura4*$^{+}$ gene, abbreviated as the *t>ura4<ori* locus (Fig. 1a). Upon activation of the RFB, the binding of Rad51 and its Rad52 loader allows blocked forks to be restarted to overcome the RFB. Occasionally, Rad51 promotes newly replicated strands to switch template and invades the opposite *RTS1* sequence to form a D-loop which primes the restarted DNA synthesis on a non-contiguous DNA template. This faulty restart pathway results in the formation of stable joint-molecules (JMs), referred to as D-loop and Holliday junction-like intermediates, whose resolution generates at least two RDR products: an acentric and a dicentric chromosome[30]. The formation of acentric and dicentric is strictly dependent on Rad52 and serves as a marker for RDR completion[26].

We applied the RDR assay to a thermo-sensitive allele of the essential *asf1* gene, *asf1-33*, which was reported to be defective for H3 deposition at restrictive temperature (36°C)[31]. Cells were cultured at semi-permissive temperature (32°C) at which *asf1-33* mutated cells exhibit sensitivity to methyl methane sulfonate (MMS, an alkylated DNA agent that impedes replication fork progression) and a reduced Asf1-H3 interaction (Supplementary Fig. 1a-b). Chromosome analysis by Pulsed Field Gel Electrophoresis (PFGE) coupled with Southern-blot hybridization showed that the amount of acentric fragment, a RDR product, was reduced in *asf1-33* cells, as well as in a mutant lacking CAF-1 (*i.e.* in *pcf1* deleted cells), indicating that Asf1 promotes RDR (Fig. 1b-c). The analysis of replication intermediates by two-dimensional gel electrophoresis (2DGE) showed that signals corresponding to arrested forks were similar in all analyzed strains, indicating that defect in RDR is not a consequence of a less efficient RFB activity in strains lacking CAF-1 or Asf1. JMs intensity was similarly reduced in *asf1-33* and *pcf1-d* mutants (Fig. 1D), showing that Asf1 preserves JMs during RDR, as proposed for CAF-1. It is worth noting that the *asf1-33* mutated cells form Rad52 foci, indicating that Asf1 is dispensable to the early step of HR[31]. Thus, as proposed for the lack of CAF-1[30], these data suggest that JMs are faster disassembled upon loss of Asf1 function rather than being less efficiently formed. We concluded that Asf1 and CAF-1 are necessary to RDR completion, possibly by promoting histone deposition during the DNA synthesis step of RDR, thus creating a substrate less favorable to Rqh1-dependent D-loop disassembly.

We investigated the role of other histone chaperones in RDR by analyzing the level of acentric chromosome upon RFB induction. We found no impact on acentric level in cells lacking the HIRA complex (involved in replication-independent H3-H4 deposition), the FACT complex, Rtt106, the two orthologues of the *S. cerevisiae* H2A-H2B histone chaperone Nap1 and Nap2, and Chz1, a histone variant H2AZ chaperone (Supplementary Fig. S1c-d). Thus, RDR requires the two key histone chaperones Asf1 and CAF-1 which mediate histone deposition in a DNA-synthesis dependent manner.

The mutated histone H3-H113D disrupts $(H3\text{-}H4)_2$ tetramer formation

To address the role of histone deposition during RDR, we decided to genetically disrupt replication-dependent chromatin assembly by altering the stability of $(H3\text{-}H4)_2$ tetramer to inhibit their stable deposition onto DNA. To this end, we employed a mutated form of H3 containing a single substitution of histidine to aspartic acid (H3-H113D). This mutation was reported to impair CAF-1-mediated nucleosome deposition *in vitro*[32].

The interface between the two H3-H4 dimers involves the C-terminal region (residues 106 to 131) of the two histones H3, called here H3 and H3'[4,33] (Fig. 2a-b and supplementary Fig. 2a). We examined X-ray structures of nucleosomes, chosen among the numerous available experimental models on the basis of homology with *S. pombe* histone H3 (see details in materials and methods). The H113 emerges as a key residue in the H3:H3' interface with H113 of one histone H3 being anchored to the second histone H3' by a dense network of contacts involving six residues (supplementary Fig. 2B). Each H113 forms two intermolecular hydrogen bonds with C110 and D123, reinforced by Van der Waals contacts with four residues: A114, R116, K122 and L126. By replacing a neutral or positively charged histidine residue by a negatively charged aspartate that is positioned in front to another aspartate, D123, the H113D mutation generates a prohibitive electrostatic repulsion in the intact H3:H3' organization. Previous works reported that a series of mutation (C110E, L12R-I130R, H113A, L126A and A114Y) prevent the H3:H3' interface formation because of an overwhelming energetic penalty and such mutations are lethal in budding yeast[12,34,35]. By analogy with these cases, the H113D mutation likely drastically destabilizes the H3:H3' interface, precluding the $(H3\text{-}H4)_2$ tetramer formation.

In *S. pombe* cells, 3 genes (*hht1*, *hht2* and *hht3*) encode a single histone H3 protein. The H113D mutation was introduced in the *hht2* gene and the resulting H3-H113D expressing cells were viable with no apparent growth defect (Fig. 2c). The deletion of *hht1* and *hht3* is viable (*hht1-d hht3-d*) and cells maintain histone H3 protein levels similar to those in *wt* strain [36]. To obtain a strain expressing only H3-H113D, the *hht2-H113D* mutated strain was crossed with an *hht1-d hht3-d* strain. Combining the *hht2-H113D* mutation with both deletions resulted in a synthetic lethality (Fig. 2c). Thus, when H3-H113D is the sole cellular histone H3 expressed, cells are not viable, in agreement with this mutation

inhibiting $(H3\text{-}H4)_2$ tetramer formation. Still, we observed that combining *hht2-H113D* with either single *htt1* or *hht3* deletion preserves cell viability but causes a severe synthetic growth defect (Fig. 2C). This strongly suggests that *wt* H3 is abundant enough to allow *wt* $(H3\text{-}H4)_2$ tetramer to be formed and to preserve cell viability but mixed (H3-H113D-H4-H3-H4) tetramer are also unstable.

We probed H3-H113D associations with histones H3 and H4 in *hht2-H113D* mutated cells ($hht1^+$ $hht3^+$). Although, the protein level of H3-H113D-HA (an HA tagged version of the mutated histone) was lower than the one of *wt* H3-HA (Fig. 2d and Supplementary Fig. 2c), immuno-precipitation experiments from total protein extracts clearly showed that H3-H113D-HA association with *wt* H3 and H4 were severely reduced, compared to H3-HA (Fig. 2d-e). These data indicate that mixed (H3-H113D-H4-H3-H4) tetramers are highly unstable. We asked if H3-H113D is incorporated into chromatin using chromatin fraction assays. As expected, the *wt* H3-HA was found to be chromatin-bound whereas H3-H113D-HA was not detected in the chromatin fraction, indicating that this mutated histone is very poorly incorporated into nucleosomes assembled onto DNA (Fig. 2f). *Wt* H3 (expressed from *hht1* and *hht3* gene) was equally detected in the chromatin fraction of *hht2-HA* and *hht2-H113D-HA* cells, indicating that *wt* H3 is *in fine* incorporated within *wt* nucleosomes in H3-H113D expressing cells. Our data indicate that in *hht2-H113D* mutated cells, H3-H113D inhibits stable tetramer formation and is therefore not deposited onto chromatin, while *wt* $(H3\text{-}H4)_2$ tetramers are formed and assembled onto chromatin.

H3-H113D impairs replication-coupled nucleosome assembly

We investigated the consequences of inhibiting tetramers formation and deposition on replication-coupled chromatin assembly. Asf1-MYC associated with *wt* H3 and H3-HA but not with H3-H113D-HA (Fig. 3a and Supplementary Fig. 3a), arguing that the histone chaperone function of Asf1 is preserved in *hht2-H113D* mutated cells. We found that H3-H113D-HA binds to Pcf1-YFP, without preventing Pcf1-YFP to associate with Pcf2-MYC (the second CAF-1 subunit), PCNA and *wt* H3 and H4; these protein-protein interactions being necessary for optimal CAF-1-mediated histone deposition (Fig. 3a and Supplementary Fig. 3b-d). Thus, in *hht2-H113D* mutated cells, CAF-1 forms complexes with H3-H4, H3-H113D, and PCNA. Because H3-H113D inhibits tetramer formation and that tetramerization is necessary to CAF-1-mediated histone deposition *in vitro*[12], H3-H113D may impair CAF-1-dependent chromatin assembly *in vivo*.

We further investigated the impact of H3-H113D on chromatin structure. We analyzed the MNase sensitivity of chromatin from *wt*, *pcf1-d* and *hht2-H113D* cells. Compared to *wt* strain, the proportion of mono-nucleosome population was increased in *pcf1-d* and *hht2-H113D* cells, showing a higher sensitivity to MNase as an indication of decreased global nucleosomal density (Fig. 3b-c and

Supplementary Fig. 4a-b). To test if this chromatin changes are caused by defective replication-coupled chromatin assembly, we analyzed the MNase sensitivity of the replicated chromatin in strains able to incorporate BrdU, a thymidine analogue[37]. Cells were blocked in early S-phase by hydroxyurea treatment and released in BrdU-containing media for 20 minutes to label the replicated chromatin. BrdU incorporation was detected in MNase-digested chromatin only when cells were released from HU block, showing that BrdU-labelling marks the replicated chromatin (Supplementary Fig. 4c). Compared to *wt* strain, the proportion of BrdU-positive mono-nucleosome was increased in *hht2-H113D* and *pcf1-d* mutated cells, indicating that the chromatin associated to newly replicated strands is more sensitive to MNase digestion (Fig. 3d-e and Supplementary Fig. 4d-e). These data are consistent with H3-H113D mutation impairing replication-coupled histone deposition to an extent at least similar to a CAF-1 defect. Defective histone deposition behind replication forks results in DSBs in budding yeast[38]. Consistent with this, *pcf1-d* and *hht2-H113D* mutated cells exhibited a high frequency of cells showing Rad52 foci, a marker of DNA lesion (Fig. 3f-g). Of note, H3-H113D expressing cells are competent to form Rad52 foci, indicating that the presynaptic steps of the HR process are likely unaffected when inhibiting $(H3\text{-}H4)_2$ tetramer formation and deposition. Although other histone deposition pathways might be affected, our data are consistent with CAF-1-mediated chromatin assembly pathway being impaired in H3-H113D expressing cells.

Histone deposition acts in RDR to prevent D-loop disassembly

The H3-H113D offers the possibility to question the role of replication-coupled chromatin assembly during RDR. We thus applied the RDR assay to *hht2-H113D* mutated cells and found that JMs intensity was reduced as well as the subsequent accumulation of acentric chromosome, one RDR product (Fig. 4a-c). These data indicate that histone deposition is required to RDR completion by preserving JMs. No additive effect was observed in the *pcf1-d hht2-H113D* strain (Fig. 4a-b), showing that CAF-1 and histone deposition act in a same pathway of promoting RDR. We reported that in the absence of CAF-1, JMs are faster disassembled by Rqh1[30]. Remarkably, similar interactions were observed in *hht2-H113D* cells in which the deletion of *rqh1* restored the intensity of JMs signal (Fig. 4c). Since the presynaptic steps of the HR process appear functional in *hht2-H113D* cells (Fig. 3f-g), these data strongly support that inhibiting $(H3\text{-}H4)_2$ tetramer assembly onto DNA favors D-loop disassembly by Rqh1. No defect in RDR were observed in strains in which genes encoded H3 are deleted (either *hht2-d* or *hht1-d hht3-d* cells, Fig. 4a-b and Supplementary Fig. 5), indicating that H3-H113D favors D-loop disassembly as a consequence of impairing replication-coupled histone deposition. These data establish that histone deposition promotes RDR by preventing D-loops disassembly by Rqh1.

Rqh1 and RDR-coupled histone deposition promotes resistance to replication stress

Our data reveal a novel crosstalk between Rqh1 and CAF-1-mediated histone deposition in JMs resolution during RDR. We addressed the consequences of this crosstalk by exanimating cell survival upon genotoxic stress. The H3-H113D mutation increased the cell sensitivity of *rqh1-d* deleted cells to MMS and campthotecin (CPT, a topoisomerase I inhibitor), thus mimicking CAF-1 defect as previously reported[30] (Fig. 5). This was not a consequence of a loss of Rqh1-Pcf1 interaction as Rqh1-MYC associated with Pcf1-YFP in *hht2-H113D* mutated cells (Supplementary Fig. 3c). Also, MMS treatment did not stimulate chromatin-bound H3-H113D-HA, suggesting that unstable tetramers are unlikely to be assembled during repair synthesis (Fig. 2f). Interestingly, such synthetic interactions were not observed in response to bleomycin, a DSB-inducing agent, indicating that the antagonistic activities of CAF-1-mediated histone deposition and Rqh1 in JMs resolution during RDR is pivotal to promote cell resistance to replication stress but not to DSBs.

RDR-coupled histone deposition favors deletion type recombinant

We investigated the consequences of RDR-coupled histone deposition on HR outcomes, by monitoring spontaneous HR events using an assay for intra-allelic recombination between direct *ade6* (Fig. 6a)[39]. Gene conversion (GC) and synthesis dependent strand annealing (SDSA) result in conversion type, whereas crossover (CO) and single strand annealing (SSA, a DNA repair pathway independent of Rad51-mediated strand exchange) give rise to deletion type. In *rqh1-d* cells, conversion and deletion events were increased by 2- and 3-fold, respectively, which is consistent with known Rqh1 anti-recombinase activity (Fig. 6b)[40]. The H3-H113D mutation had little impact on HR outcomes but when combined with *rqh1-d*, it partially rescued the deletion rate, and suppressed bias towards deletion type. These data are consistent with antagonistic activities of Rqh1 and histone deposition in controlling HR outcomes: Rqh1 promotes D-loop disassembly to favor a conservative pathway whereas histone deposition promotes D-loop stability to channel HR event towards deletion events such as CO.

H3K56Ac is dispensable to RDR

The H3K56Ac modification marks newly synthetized histone and was proposed to regulate nucleosome assembly and to contribute to the DNA damage response[41]. Hence the importance of acetylation in addition to histone deposition has to be considered. We found that in contrast to *wt* H3 which was efficiently acetylated by Rtt109 in *hht2-H113D* cells, H3-H113D that is unable to associate with Asf1-MYC (Fig. 3a) lost the H3K56Ac mark (Supplementary Fig. 5a). We thus tested the role of H3K56Ac in RDR. We analyzed two strains: one expressing a single H3 protein which cannot be acetylated on K56 (*hht1-d hht3-d hht2-K56R*) and a *rtt109* deleted strain. Consistent with previous reports[17], both strains were defective for H3K56Ac (Supplementary Fig. 5b) and were proficient for the formation of acentric

chromosome, a RDR product (Supplementary Fig. 5c-d). Thus, H3K56Ac is dispensable to RDR completion.

Rad52 promotes CAF-1 binding to chromatin upon replication stress

Our data indicate that RDR is coupled to histone deposition mediated by Asf1 and CAF-1. We investigated how CAF-1 associates to RDR events. First, we observed that the chromatin-bound Pcf1 fraction was enriched after treatment with MMS, but not with bleomycin or hydroxyurea (an agent that slows down fork progression) (Fig. 7a). Consistent with CAF-1 being a scarce complex (~ 500 to 900 molecules/cells[42]), Pcf1-YFP was hardly detectable in the total fraction, but was clearly enriched in the chromatin fraction from 1-2 hours upon MMS treatment, concomitantly with PCNA that links CAF-1 function to the DNA synthesis step during RDR [30] (Fig. 7b). It is worth noting that in *rad52-d* mutant, upon MMS treatment, the chromatin-bound PCNA and H3 fractions were reduced (Supplementary Fig. 6a), indicating that the HR process is necessary for PCNA recruitment and the retention/restoration of histone on damaged chromatin. However, neither H3-H4 nor PCNA enrichment to damaged chromatin were affected by the lack of CAF-1 (Supplementary Fig. S6b), suggesting that multiple histone chaperones likely contribute to chromatin restoration in response to MMS.

Due to technical issues, we were unable to generate chromatin fractions of good quality in *rad52-d* cells, which precluded us from addressing whether or not HR factors are required for CAF-1 recruitment to damaged chromatin. To overcome this, we developed an *in vivo* chromatin binding assay using strains expressing a Pcf1-GFP[43] fusion protein to monitor the chromatin-bound Pcf1 fraction after removal of the soluble fraction by a detergent-containing buffer[44]. Whereas ~ 90 % of nuclear Pcf1-GFP signal was sensitive to triton extraction in untreated cells, MMS treatment resulted in twice more Pcf1-GFP bound to the chromatin (Fig. 7c-f). Although Rad52 was not necessary for Pcf1-GFP association to the chromatin in untreated conditions, Pcf1-GFP was not found enriched in the chromatin fraction *in rad52-d* cells after MMS (Fig. 7e-f). Thus, we revealed a novel mode of CAF-1 association to the chromatin upon replication stress requiring Rad52.

CAF-1 recruitment to repair DNA synthesis during RDR requires Rad52

We then asked whether CAF-1-mediated histone deposition is recruited to restarted DNA synthesis associated to RDR. We took advantage of the RDR assay in which the replication of the *ura4* gene occurs by RDR. Pcf1-YFP was recruited at the two active RFBs (Fig. 8a, primer pairs 1 and 3, left panel) and, remarkably to ura4 only in "ON" condition (primer pair 2, left panel). This Pcf1 binding was no longer observed in *rad52-d* cells in which RDR and JMs cannot occur (Fig. 8a, right panel)[26]. We concluded that CAF-1 recruitment to restarted DNA synthesis associated to RDR occurs downstream from Rad52.

Discussion

Fork-obstacles open up the risk of genome and epigenome instability. We established that RDR, a major fork-restart pathway, is coupled to histone deposition, mediated by the chromatin assembly factors CAF-1 and Asf1 (Fig. 8b). We made the surprising finding that histone deposition coupled to restarted DNA synthesis impacts the subsequent resolution of JMs at site of fork arrest and thus fines tune RDR. We reveal a novel crosstalk between chromatin restoration and DNA repair factors; a crosstalk necessary to cell survival to replication stress and that balances genome stability at arrested forks. Our finding highlight that chromatin restoration is entirely part of the RDR process. We proposed a scenario in which histone deposition plays an active role in RDR to avoid discontinuity in chromatin assembly upon replication stress, a benefit counterbalanced by stabilizing at-risk joint molecules for genome stability.

We establish that Asf1, CAF-1 and histone deposition act in RDR at the step of DNA synthesis. Despite recent advances in understating the mechanism of CAF-1-mediated histone deposition *in vitro,* it remains challenging to define point mutations to generate mutated forms of CAF-1 unable to interact with H3-H4 *in vivo*[12]. To overcome this, we took advantage of the H3-H113D mutated form, reported to inhibit CAF-1-mediated histone deposition *in vitro*[32]. We show here that the H3-H113D precludes $(H3\text{-}H4)_2$ tetramer formation, and is thus poorly incorporated into nucleosomes deposited onto DNA and inhibits replication-coupled chromatin assembly. Remarkably, the H3-H113D mutation mimics the absence of CAF-1 in impairing RDR. RDR requires Asf1, the three CAF-1 subunits and the ability of CAF-1 to interact with PCNA[30], supporting the view that Asf1 and CAF-1 fine-tune RDR by coupling histone deposition to the step of DNA synthesis. Consistent with this, CAF-1 binds to repair synthesis during RDR in a Rad52-dependent manner, indicating that the early steps of RDR must be engaged for the subsequent recruitment of CAF-1.

Mammalian CAF-1 and ASF1 are necessary for the early steps of recombinational repair of DSBs by facilitating the loading of HR factors[45,46]. Our data favors a model in which fission yeast CAF-1 and histone deposition act in the later steps of RDR. Firstly, Rad52 was able to bind arrested forks in the absence of CAF-1 [30]. Secondly, the binding of CAF-1 to the sites of DNA synthesis occurs downstream from Rad52. Thirdly, RDR defects are rescued by deleting *rqh1.* This indicates that, in cells lacking the pathway of histone deposition coupled to RDR, D-loops are faster disassembled rather than unable to form. We proposed that CAF-1-mediated histone deposition acts as a chromatin restoration pathway during the DNA synthesis step of RDR. In this scenario, histone deposition would occur onto the DNA duplex of the extended D-loop (Fig. 8b). However, we cannot exclude that histone deposition occurs onto the displaced strand of the D-loop, as it has been proposed that nucleosome can be deposited onto ssDNA[47]. RDR requires two histones chaperones that mediate chromatin assembly in a DNA

synthesis manner and requires the ability of CAF-1 to interact with PCNA. Therefore, we favor the first hypothesis in which histone deposition is coupled to DNA synthesis to extend the D-loop thus creating a substrate less favorable to Rqh1-dependent D-loop disassembly. Extensive works have address the role of chromatin factors in regulating genome accessibility to DNA repair machineries but how chromatin restoration is coupled to the DNA repair event is poorly understood[3]. Our data put forward a crosstalk between the DNA repair machinery and the step of chromatin restoration that plays an active role in fine-tuning RDR.

Histone deposition coupled to RDR impacts genome stability at site of replication stress. CAF-1 counteracts Rqh1 activity at sites of replication stress by promoting repair synthesis-coupled histone deposition. Possibly, histone deposition onto extended D-loops creates a substrate less favorable to the Rqh1 activity. RecQ helicases act as motor proteins/helicases to migrate DNA junctions which may be prevented by assembled nucleosomes. It remains challenging to address whether histone are deposited onto D-loops as these structures are very transient. JMs visualization by 2DGE requires a step of enrichment in replication intermediates, technically incompatible with chromatin immuno-precipitation approaches to address histone binding to JMs. Nonetheless, we established that inhibiting replication-coupled histone deposition favors D-loops disassembly. We provide insights into the nature of the chromatin required to protect D-loops.

Asf1 acts as an histone chaperone to present H3-H4 to Rtt109 and establish the H3K56Ac mark and then transfer H3-H4 to CAF-1 [7]. We found H3K56Ac dispensable to promote RDR. Possibly, Asf1 is required for RDR by acting as a donor histone to CAF-1. However, H3-H113D binds to CAF-1, likely as a H3-H4 dimer, but not to Asf1, indicating that, during RDR-coupled histone deposition, H3-H4 can be handed off to CAF-1 independently of Asf1, a pathway that remains to be clarified.

Nucleosome deposition onto extended D-loops may impose topological constraints. D-loops disassembly is a topoisomerase-mediated mechanism[48]. Thus, topological constraints resulted from DNA wrapped around nucleosome may be easily relieved by topoisomerase 3. When seeking for additional chromatin factors required for RDR, we found Nap1 and Nap2, two histone H2A-H2B chaperones, to be dispensable to protect D-loops. This suggests that the deposition of $(H3\text{-}H4)_2$ tetramer, but not the formation of a nucleosome, is sufficient by itself to counteract Rqh1 activity and to limit topological constraints.

During HR-mediated DSB repair, disassembly of D-loops extended by DNA polymerase ensures a non-crossover outcome[25]. Our data indicate that histone deposition during RDR stabilizes JMs and favors deletion events and a chromosomal rearrangement pathway. Similarly, in the absence of Rqh1, spontaneous HR events are channeled towards deletion type recombinants in an histone deposition

manner. Interestingly, spontaneous rates of gene conversion were unaffected by the defect in repair synthesis-histone deposition. This suggests that DNA synthesis associated to GC and SDSA is too short in length to favor histone deposition. Nonetheless, our data reveal that the antagonistic activities of RDR-coupled histone deposition and Rqh1 in D-loops resolution are pivotal to balance genome stability at arrested forks and to promote cell resistance upon replication stress.

During unchallenged replication, the concerted action of multiple histone chaperones coordinates the assembly of chromatin behind the fork to achieve recycling of parental histones and deposition of newly synthetized histones [20]. RDR results in the progression of non-canonical forks in which both strands are synthetized by the DNA polymerase delta, which contrasts with the division of labor between DNA polymerase delta and epsilon within origin-born replication forks [49]. Such restarted forks are liable to replication errors such as multiple template switches, replication slippage and U-turn. Despite these unusual features, our data established that a restarted fork remains coupled to histone deposition and thus may help to ensure continuous chromatin assembly upon replication stress.

Fork obstacles and replication stress interfere with the inheritance of epigenetic marks, [23,50,51]. On the one hand, the post-replicative repair of DNA lesions/structures, left un-replicated behind the fork, is uncoupled from chromatin assembly and recycling of parental histones. On the other hand, it was proposed that the bypass of DNA secondary structures, such as G quadruplexes, by PrimPol allows the repriming of DNA synthesis very closly to the fork obstacle and thus reassuring the maintenance of replication-coupled chromatin maturation [52]. The choice of the pathway employed to overcome fork obstacles may impact on the maintenance of histone deposition coupled to restarted forks. Our data indicate that RDR, a main pathway to bypass fork obstacles, is coupled to histone deposition with D-loops offering the possibility to prime repair synthesis-coupled histone deposition. In the view that replisomes are often interrupted by numerous obstacles, RDR-coupled histone deposition contributes to cell resistance to replication stress and may ensure continuity in assembling chromatin upon replication stress.

We propose that histone deposition coupled to RDR comes at the expense of stabilizing JMs which can be detrimental to genome stability. Overexpression of Asf1b, one isoform of human Asf1, and CAF-1 was found to be associated with poor prognosis in various cancer types[53,54]. Since cancer cells exhibit signs of replication stress, we speculate that upregulating chromatin assembly factors may favor the stability of at-risk JMs at site of replication stress, channeling RDR events towards a chromosomal rearrangement pathway that fuels cancer development.

Materials and Methods

Standards yeast genetics

Yeast strains used in this work are listed in Supplementary Table 1. Gene deletion and gene tagging were performed by classical and molecular genetics techniques[55]. Strains containing the *RTS1*-RFB were grown in supplemented EMM-glutamate media containing 60µM of thiamine. To induce the *RTS1*-RFB, cells were washed twice in water and grown in supplemented EMM-glutamate media containing thiamine (Rtf1 repressed, RFB OFF condition) or not (Rtf1 expressed, RFB ON condition) for 24 hours or 48 hours.

Chromatin Fraction Assay

Chromatin fractionation was performed as described previously[56] with the following modifications. Cells were harvested, digested with 100µg of zymolyase 20T (Amsbio, 120491-1) to obtain spheroplasts, and resuspended in lysis buffer (50mM potassium acetate, 2mM MgCl2, 20mM HEPES pH7.9, 1% Triton X-100, 1mM PMSF, 60mM β-glycerophosphate, 0.2mM Na_3VO_4, 1µg/ml AEBSF and Complete Protease Inhibitor EDTA-Free Tablet (Roche, 04 693 159 001). After lysis, extracts were subsequently fractionated into soluble and pellet fractions by centrifugation. The insoluble chromatin-enriched pellet fraction was washed twice with the lysis buffer without 1 % Triton X-100 and digested with 100Units of DNase I HC (ThermoScientific, EN0523) on ice for 15min followed by 15min at RT. The DNase I-digested chromatin-enriched fraction was centrifuged for 5 min at 16,000g. Supernatant was designated as the chromatin fraction. Samples corresponding to total soluble and chromatin fractions were migrated and transferred on nitrocellulose membrane. Proteins of interest were revealed by anti-GFP (1/1000^e, Roche, 11 814 460 001), anti-MYC (1/300^e, SantaCruz, 9E10), anti-HA (1/500^e, SantaCruz, 12CA5), anti-PCNA (1/500^e, SantaCruz, PC10), anti-Tubulin (1/4000^e, Abcam, ab6160) and anti-H3 (1/2000^e, Abcam, ab1791) antibodies.

Analysis of replication intermediates by 2DGE.

Replication Intermediates (RIs) were analyzed by 2DGE as previously described [57]. RIs were migrated in 0.35% agarose gel in 1X TBE for the first dimension. The second dimension was migrated in 0.9% agarose gel 1XTBE supplemented with EtBr (Brewer 1992). DNA was transferred onto a nylon membrane (Perkin Elmer, NEF988001PK) in 10X SSC. Membranes were incubated with a ^{32}P radiolabeled *ura4* probe, and RIs were detected using phosphor-imager software (Typhoon-trio) and quantified with ImageQuantTL.

Co-immunoprecipitation.

5.10^8 cells were harvested with 0.1% sodium azide, washed in cold water and resuspended in 400 µl of EB buffer (50mM HEPES High salt, 50mM KOAc pH7.5, 5mM EGTA, 1% Triton X-100, 1mM PMSF, and Complete Protease Inhibitor EDTA-Free Tablet (Roche, 04 693 159 001). Cell lysis was performed with a Precellys24 homogenizer (Bertin instruments). The lysate was treated with 250mU/µl of benzonase (Novagen, NOVG 70664-3) for 30min. After centrifugation, the supernatant was recovered and an aliquot of 50 µl was saved as the INPUT control. To 300µl of lysate, 2µl for anti-GFP (Life Technologies, A11122) were added and incubated for 1.5 hours at 4°C on a wheel. Then, 20µl of Dynabeads protein-G (Life Technologies, 10004D) prewashed in PBS were added and then incubated at 4°C overnight. Alternatively, lysates were incubated overnight with 20µl of anti-MYC (Life Technologies, 88842) or anti-HA (Life Technologies, 88836) antibody coupled to magnetic beads. Proteins of interest were detected using anti-HA high affinity (1/500e, Roche, clone 3F10), anti-GFP (1/1000e Roche, 11 814 460 001), anti-MYC (1/300e, SantaCruz, A-14), anti-HA (1/500e, SantaCruz, 12CA5), anti-PCNA (1/500e, SantaCruz, PC10), and anti-H3 (1/2000e, Abcam, ab1791) antibodies.

Chromatin immunoprecipitation of Pcf1-YFP.

ChIP experiments were performed as previously reported [58]. Cells were crosslinked with fresh 1% formaldehyde (Sigma, F-8775) for 15 minutes. Cells were lysed using Precellys24 homogenizer (Bertin instruments) in lysis buffer (50mM Hepes-KOH pH7.5, 140mM NaCl, 1mM EDTA, 1% Triton X-100, 0.1% sodium deoxycholate, 1mM phenylmethylsulfonyl fluoride, and Protease Inhibitor Cocktail (Sigma P8215)). The crude cell lysate was sonicated (using a Diagenod Bioruptor at high setting for 15 cycles: 30 seconds ON + 30 seconds OFF) and clarified by centrifugation for 15min at 16,000g. Prior to immunoprecipitation, 1/100 volume of the cell lysate was saved for an input control. Immunoprecipitations were performed with 2µl of anti-GFP antibody (Life Technologies, A11122) for 2 hours. After 30min incubation with 20µl magnetic beads (Life Technologies, 10004D), immunoprecipitates were successively washed with 2x1ml lysis buffer, 2x1ml lysis buffer/500mM NaCl, 2x1ml wash buffer (10mM Tris-HCl pH8, 0.25M LiCl, 0.5% NP-40, 0.5% sodium deoxycholate, 1mM EDTA) and 1ml TE buffer (10mM Tris-HCl, 1mM EDTA pH8). Crosslink was reversed by incubating the samples at 65°C overnight. Samples were then treated with 0.5mg/ml Proteinase K (Euromedex, EU0090) and DNA was purified using Qiagen PCR purification kit and eluted in 100µl of water. The relative amount of DNA was quantified by qPCR (primers are listed in supplementary Table 2). Pcf1-YFP enrichment was normalized to an internal control locus (*ade6*).

Pulse-Field Gel Electrophoresis.

PFGE were performed as previously described[26]. Membranes were then incubated with a ^{32}P radiolabeled *rng3* probe. Quantification of acentric chromosomes visualized by PFGE was performed as previously described[30].

Microccocal digestion and BrdU incorporation

Microccocal digestions were performed as previously described[59]. After crosslink with 1% formaldehyde, 1.10^9 Cells were spheroplasted in 2ml of CES buffer (50mM Citric acid/50mM $Na2HPO_4$ pH 5.6, 40mM EDTA pH8, 1.2M Sorbitol, 20mM β-mercaptoethanol) containing 1 mg/ml Zymolyase 100T (Amsbio, 120493-1) for 20min at 30°C. Spheroplasts were washed twice with 1ml of iced cold 1.2M Sorbitol buffer. Cells were resuspended in 1ml of NP-S buffer (1.2M Sorbitol; 10mM $CaCl_2$, 100mM NaCl, 1mM EDTA pH8, 14mM β -mercaptoethanol, 50mM Tris-HCl pH8, 0.075% NP-40, 5mM spermidine, 0.1mM PMSF, Complete Protease Inhibitor EDTA-Free Tablet (Roche, 04 693 159 001)) containing the indicated units of Micrococcal Nuclease (Worthington Biochemical, LS004798) for 10 min at 37°C. Reactions were stopped by addition of 50mM EDTA pH8 and SDS 0,2%. Crosslinking was reversed overnight at 65°C in the presence of 20µg of RNAseA (Sigma, R5503) and 0.2mg/ml Proteinase K (Euromedex, EU0090). DNA was purified by phenol/chloroform extraction and ethanol precipitation. Purified DNA was resolved on 1.5% agarose gel (1X TBE).

For BrdU incorporation, we used cells expressing *Drosophila melanogaster* deoxyribonucleoside kinase (DmdNK) under the control of the fission yeast a*dh* promoter, together with the human equilibrative nucleoside transporter (hENT1) (*adh-dmdNK-adh-hENT1*)[37]. Cells were arrested 4 hours with 40mM HU (Sigma, H8627) and released in fresh media containing BrdU (Sigma, B5002) for 20min. After MNase digestion, DNA was analyzed by Southern-blot using anti BrdU antibody (1/4000^e, Abcam, ab12219).

Spontaneous Recombination assay

Spontaneous recombination rate was assayed using strains containing a direct repeat of two nonfunctional *ade6* alleles flanking a functional *ura4* gene[39]. Strains were kept on low adenine EMM plates lacking uracil to prevent selection for Ade^+ and Ura^- recombinants. Dark pink colonies were streaked on supplemented YE plates and at least 11 independent single colonies for each strain were used to calculate Ade+ recombinant rate. Appropriate dilutions were plated on supplemented YE plates (to determine cell survival), EMM plates lacking adenine (to score spontaneous recombination rate, Ade+ recombinants) and EMM plates lacking adenine and uracil (to score gene conversion rate, Ade+ Ura+ recombinants). Colonies were counted after 5-7 days of incubation at 30°C.The rates of Ade+ and Ade+ Ura+ recombinant were calculated as described in[60].

Analyzed X-ray structures of nucleosome

There is no experimental model of nucleosome containing histones from *S. pombe*. Among the numerous available structures of nucleosome, only three of them include yeast histones, all from *S. cerevisiae (*PDB codes 1ID3, 4JJN and 4KUD), with resolutions of ~3 Å. Indeed, the highest resolution was obtained for a nucleosome containing histones from *Xenopus laevis* (PDB code 1KX5, resolution of 1.9 Å). Since the histone sequences are extremely conserved, *S. cerevisiae* and *Xenopus laevis* H3 histones share 92% of residues with H3 of *S. pombe*. More specifically, the region surrounding H113 is well preserved across *S. pombe, S. cerevisiae* and *Xenopus laevis*, with a very good score being observed for the couple *S. pombe / Xenopus laevis* (Figure S2A). Given the reasonable sequence agreement, 1ID3, 4JJN, 4KUD and 1KX5 were analyzed using PDBsum (de Beer *et al*, 2014) to describe the interface between two H3-H4 dimers[61].

Chromatin Binding Assay

Chromatin binding assay was performed as previously described[44] with the following modifications. $1.5.10^8$ cells were harvested with 0.1% sodium azide, washed in cold EMM sorbitol buffer (1.2M sorbitol, 15mM KH phallate, 15mM Na_2HPO_4, 90mM NH_4Cl, pH7). Cells were spheroplasted at 32°C in 500 µl EMM sorbitol buffer containing 10mM DTT and 2mg of zymolyase 20T (Amsbio, 120491-1) then washed twice with cold EMM sorbitol buffer and once with cold extraction buffer (20 mM PIPES-KOH, pH 6.8, 0.4M sorbitol, 150mM KAc, 2mM MgAc). Cells were resuspended in extraction buffer containing or not 1% triton and incubated at 20°C for 5min, with gentle inversion. Finally, cells were pelleted then incubated in cold methanol for 5min before being stocked in cold acetone at -20°C.
Cells were harvested, resuspended in H_2O containing 0.1µg/ml Hoechst and mounted into 1.4ml EMM-agar covered slide. Image acquisition and analysis were performed with MetaMorph software (Molecular Devices). The images were analyzed by quantifying the average nuclear Pcf1-GFP signal using ImageJ/Fiji software. To analyze, a z-project was first made based on the z-stack obtained from DAPI or FITC channel. Based on the z-project of DAPI channel, the area of nuclear staining was selected by using the "freehand selection tool"; the size of the area was measured (S) and the selected nuclear staining area was saved (mask). The mask was then applied to the z-project of FITC channel to measure the fluorescence intensity of Pcf1-GFP signal (FI); the mask was next dragged to cytoplasmic area of the same cell to measure the background fluorescence intensity (BG). To calculate the average nuclear Pcf1-GFP signal, the formula: (FI-BG)/S was used. At least 50 cells were analyzed for each sample. Quantifications and statistical analysis were made using Graphpad Prism software.

References

1. Soria, G., Polo, S.E. & Almouzni, G. Prime, repair, restore: the active role of chromatin in the DNA damage response. *Mol Cell* **46**, 722-34 (2012).
2. Svikovic, S. & Sale, J.E. The Effects of Replication Stress on S Phase Histone Management and Epigenetic Memory. *J Mol Biol* **429**, 2011-2029 (2017).
3. Dabin, J., Fortuny, A. & Polo, S.E. Epigenome Maintenance in Response to DNA Damage. *Mol Cell* **62**, 712-27 (2016).
4. Luger, K., Mader, A.W., Richmond, R.K., Sargent, D.F. & Richmond, T.J. Crystal structure of the nucleosome core particle at 2.8 A resolution. *Nature* **389**, 251-60 (1997).
5. Smith, S. & Stillman, B. Stepwise assembly of chromatin during DNA replication in vitro. *EMBO J* **10**, 971-80 (1991).
6. Hatakeyama, A., Hartmann, B., Travers, A., Nogues, C. & Buckle, M. High-resolution biophysical analysis of the dynamics of nucleosome formation. *Sci Rep* **6**, 27337 (2016).
7. Burgess, R.J. & Zhang, Z. Histone chaperones in nucleosome assembly and human disease. *Nat Struct Mol Biol* **20**, 14-22 (2013).
8. Moggs, J.G. et al. A CAF-1-PCNA-mediated chromatin assembly pathway triggered by sensing DNA damage. *Mol Cell Biol* **20**, 1206-18 (2000).
9. Shibahara, K. & Stillman, B. Replication-dependent marking of DNA by PCNA facilitates CAF-1-coupled inheritance of chromatin. *Cell* **96**, 575-85 (1999).
10. Mattiroli, F., Gu, Y., Balsbaugh, J.L., Ahn, N.G. & Luger, K. The Cac2 subunit is essential for productive histone binding and nucleosome assembly in CAF-1. *Sci Rep* **7**, 46274 (2017).
11. Zhang, K. et al. A DNA binding winged helix domain in CAF-1 functions with PCNA to stabilize CAF-1 at replication forks. *Nucleic Acids Res* **44**, 5083-94 (2016).
12. Sauer, P.V. et al. Insights into the molecular architecture and histone H3-H4 deposition mechanism of yeast Chromatin assembly factor 1. *Elife* **6**(2017).
13. Mattiroli, F. et al. DNA-mediated association of two histone-bound complexes of yeast Chromatin Assembly Factor-1 (CAF-1) drives tetrasome assembly in the wake of DNA replication. *Elife* **6**(2017).
14. Liu, W.H. et al. The Cac1 subunit of histone chaperone CAF-1 organizes CAF-1-H3/H4 architecture and tetramerizes histones. *Elife* **5**(2016).
15. English, C.M., Adkins, M.W., Carson, J.J., Churchill, M.E. & Tyler, J.K. Structural basis for the histone chaperone activity of Asf1. *Cell* **127**, 495-508 (2006).
16. Han, J., Zhou, H., Li, Z., Xu, R.M. & Zhang, Z. Acetylation of lysine 56 of histone H3 catalyzed by RTT109 and regulated by ASF1 is required for replisome integrity. *J Biol Chem* **282**, 28587-96 (2007).
17. Xhemalce, B. et al. Regulation of histone H3 lysine 56 acetylation in Schizosaccharomyces pombe. *J Biol Chem* **282**, 15040-7 (2007).
18. Franco, A.A., Lam, W.M., Burgers, P.M. & Kaufman, P.D. Histone deposition protein Asf1 maintains DNA replisome integrity and interacts with replication factor C. *Genes Dev* **19**, 1365-75 (2005).
19. Lambert, S. & Carr, A.M. Replication stress and genome rearrangements: lessons from yeast models. *Curr Opin Genet Dev* **23**, 132-9 (2013).
20. Alabert, C. & Groth, A. Chromatin replication and epigenome maintenance. *Nat Rev Mol Cell Biol* **13**, 153-67 (2012).
21. Prado, F. & Maya, D. Regulation of Replication Fork Advance and Stability by Nucleosome Assembly. *Genes (Basel)* **8**(2017).
22. Mejlvang, J. et al. New histone supply regulates replication fork speed and PCNA unloading. *J Cell Biol* **204**, 29-43 (2014).
23. Jasencakova, Z. et al. Replication stress interferes with histone recycling and predeposition marking of new histones. *Mol Cell* **37**, 736-43 (2010).

24. Carr, A.M. & Lambert, S. Replication stress-induced genome instability: the dark side of replication maintenance by homologous recombination. *J Mol Biol* **425**, 4733-44 (2013).
25. Mimitou, E.P. & Symington, L.S. Nucleases and helicases take center stage in homologous recombination. *Trends Biochem Sci* **34**, 264-72 (2009).
26. Lambert, S. et al. Homologous recombination restarts blocked replication forks at the expense of genome rearrangements by template exchange. *Mol Cell* **39**, 346-59 (2010).
27. Hu, L. et al. Two replication fork maintenance pathways fuse inverted repeats to rearrange chromosomes. *Nature* **501**, 569-72 (2013).
28. Adam, S., Polo, S.E. & Almouzni, G. Transcription recovery after DNA damage requires chromatin priming by the H3.3 histone chaperone HIRA. *Cell* **155**, 94-106 (2013).
29. Chen, C.C. et al. Acetylated lysine 56 on histone H3 drives chromatin assembly after repair and signals for the completion of repair. *Cell* **134**, 231-43 (2008).
30. Pietrobon, V. et al. The chromatin assembly factor 1 promotes Rad51-dependent template switches at replication forks by counteracting D-loop disassembly by the RecQ-type helicase Rqh1. *PLoS Biol* **12**, e1001968 (2014).
31. Tanae, K., Horiuchi, T., Matsuo, Y., Katayama, S. & Kawamukai, M. Histone chaperone Asf1 plays an essential role in maintaining genomic stability in fission yeast. *PLoS One* **7**, e30472 (2012).
32. Nakano, S., Stillman, B. & Horvitz, H.R. Replication-coupled chromatin assembly generates a neuronal bilateral asymmetry in C. elegans. *Cell* **147**, 1525-36 (2011).
33. Davey, C.A., Sargent, D.F., Luger, K., Maeder, A.W. & Richmond, T.J. Solvent mediated interactions in the structure of the nucleosome core particle at 1.9 a resolution. *J Mol Biol* **319**, 1097-113 (2002).
34. Banks, D.D. & Gloss, L.M. Folding mechanism of the (H3-H4)2 histone tetramer of the core nucleosome. *Protein Sci* **13**, 1304-16 (2004).
35. Ramachandran, S., Vogel, L., Strahl, B.D. & Dokholyan, N.V. Thermodynamic stability of histone H3 is a necessary but not sufficient driving force for its evolutionary conservation. *PLoS Comput Biol* **7**, e1001042 (2011).
36. Yadav, R.K. et al. Histone H3G34R mutation causes replication stress, homologous recombination defects and genomic instability in S. pombe. *Elife* **6**(2017).
37. Fleck, O. et al. Deoxynucleoside Salvage in Fission Yeast Allows Rescue of Ribonucleotide Reductase Deficiency but Not Spd1-Mediated Inhibition of Replication. *Genes (Basel)* **8**(2017).
38. Clemente-Ruiz, M. & Prado, F. Chromatin assembly controls replication fork stability. *EMBO Rep* **10**, 790-6 (2009).
39. Hartsuiker, E., Vaessen, E., Carr, A.M. & Kohli, J. Fission yeast Rad50 stimulates sister chromatid recombination and links cohesion with repair. *EMBO J* **20**, 6660-71 (2001).
40. Doe, C.L., Dixon, J., Osman, F. & Whitby, M.C. Partial suppression of the fission yeast rqh1(-) phenotype by expression of a bacterial Holliday junction resolvase. *EMBO J* **19**, 2751-62 (2000).
41. Driscoll, R., Hudson, A. & Jackson, S.P. Yeast Rtt109 promotes genome stability by acetylating histone H3 on lysine 56. *Science* **315**, 649-52 (2007).
42. Carpy, A. et al. Absolute proteome and phosphoproteome dynamics during the cell cycle of Schizosaccharomyces pombe (Fission Yeast). *Mol Cell Proteomics* **13**, 1925-36 (2014).
43. Kunoh, T. & Habu, T. Pcf1, a large subunit of CAF-1, required for maintenance of checkpoint kinase Cds1 activity. *Springerplus* **3**, 30 (2014).
44. Kearsey, S.E., Brimage, L., Namdar, M., Ralph, E. & Yang, X. In situ assay for analyzing the chromatin binding of proteins in fission yeast. *Methods Mol Biol* **296**, 181-8 (2005).
45. Baldeyron, C., Soria, G., Roche, D., Cook, A.J. & Almouzni, G. HP1alpha recruitment to DNA damage by p150CAF-1 promotes homologous recombination repair. *J Cell Biol* **193**, 81-95 (2011).
46. Huang, T.H. et al. The Histone Chaperones ASF1 and CAF-1 Promote MMS22L-TONSL-Mediated Rad51 Loading onto ssDNA during Homologous Recombination in Human Cells. *Mol Cell* **69**, 879-892 e5 (2018).

47. Adkins, N.L. et al. Nucleosome-like, Single-stranded DNA (ssDNA)-Histone Octamer Complexes and the Implication for DNA Double Strand Break Repair. *J Biol Chem* **292**, 5271-5281 (2017).
48. Fasching, C.L., Cejka, P., Kowalczykowski, S.C. & Heyer, W.D. Top3-Rmi1 dissolve Rad51-mediated D loops by a topoisomerase-based mechanism. *Mol Cell* **57**, 595-606 (2015).
49. Miyabe, I. et al. Polymerase delta replicates both strands after homologous recombination-dependent fork restart. *Nat Struct Mol Biol* **22**, 932-8 (2015).
50. Sarkies, P., Reams, C., Simpson, L.J. & Sale, J.E. Epigenetic instability due to defective replication of structured DNA. *Mol Cell* **40**, 703-13 (2010).
51. Li, W. et al. Replication stress affects the fidelity of nucleosome-mediated epigenetic inheritance. *PLoS Genet* **13**, e1006900 (2017).
52. Schiavone, D. et al. PrimPol Is Required for Replicative Tolerance of G Quadruplexes in Vertebrate Cells. *Mol Cell* **61**, 161-9 (2016).
53. Corpet, A. et al. Asf1b, the necessary Asf1 isoform for proliferation, is predictive of outcome in breast cancer. *EMBO J* **30**, 480-93 (2011).
54. Polo, S.E. et al. Clinical significance and prognostic value of chromatin assembly factor-1 overexpression in human solid tumours. *Histopathology* **57**, 716-24 (2010).
55. Moreno, S., Klar, A. & Nurse, P. Molecular genetic analysis of fission yeast Schizosaccharomyces pombe. *Methods Enzymol* **194**, 795-823 (1991).
56. Kai, M., Tanaka, H. & Wang, T.S. Fission yeast Rad17 associates with chromatin in response to aberrant genomic structures. *Mol Cell Biol* **21**, 3289-301 (2001).
57. Ait Saada, A. et al. Unprotected Replication Forks Are Converted into Mitotic Sister Chromatid Bridges. *Mol Cell* **66**, 398-410 e4 (2017).
58. Audry, J. et al. RPA prevents G-rich structure formation at lagging-strand telomeres to allow maintenance of chromosome ends. *EMBO J* **34**, 1942-58 (2015).
59. Pai, C.C. et al. A histone H3K36 chromatin switch coordinates DNA double-strand break repair pathway choice. *Nat Commun* **5**, 4091 (2014).
60. Lea, D.E. & Coulson, C.A. The distribution of the numbers of mutants in bacterial populations. *J Genet* **49**, 264-85 (1949).
61. de Beer, T.A., Berka, K., Thornton, J.M. & Laskowski, R.A. PDBsum additions. *Nucleic Acids Res* **42**, D292-6 (2014).

Acknowledgements:

We thank Makoto Kawamukai for the gift of the *asf1-myc* and *asf1-33-myc* strains, Edgar Hartsuiker for the gift of the *adh-dmdNK-adh-hENT1* strain and Tatsuki Kunoh and Toshiyuki Habu for the gift of Pcf1-GFP strain. We thank Jean-Pierre Quivy, Vincent Pennaneach and Kirill Lobachev for critical comments of the manuscript. We also thank the PICT-IBiSA@Orsay Imaging Facility of the Institut Curie. This study was supported by grants from the Institut Curie, the CNRS, the *Fondation ARC*, the *Fondation Ligue* (*comité Essonne*), *l'Agence Nationale de la Recherche* ANR-14-CE10-0010-01, the *Institut National du Cancer* 2016-1-PLBIO-03-ICR-1 and the *Fondation pour la Recherche Médicale* "Equipe FRM DEQ20160334889". ATS and AAS were funded by the Institut Curie international PhD program, and a French governmental fellowship, respectively. ATS was supported by a 4th year PhD fellowship from *Fondation pour la Recherche Medicale* (FDT20160435131). The funders had no role in study design, data collection and analysis, the decision to publish, or preparation of the manuscript.

Author contributions:

J.H., D.D., A.A.S., A.T.S., L.D., F.M. and K.F. performed the experiments.

B.H. and F.O. provided structural biology expertise.

J.H. and S.A.E.L. designed experiments and analyzed the data.

J.H. and S.A.E.L. wrote the paper.

Competing financial interests

The authors declare no competing financial interests.

Figure legends

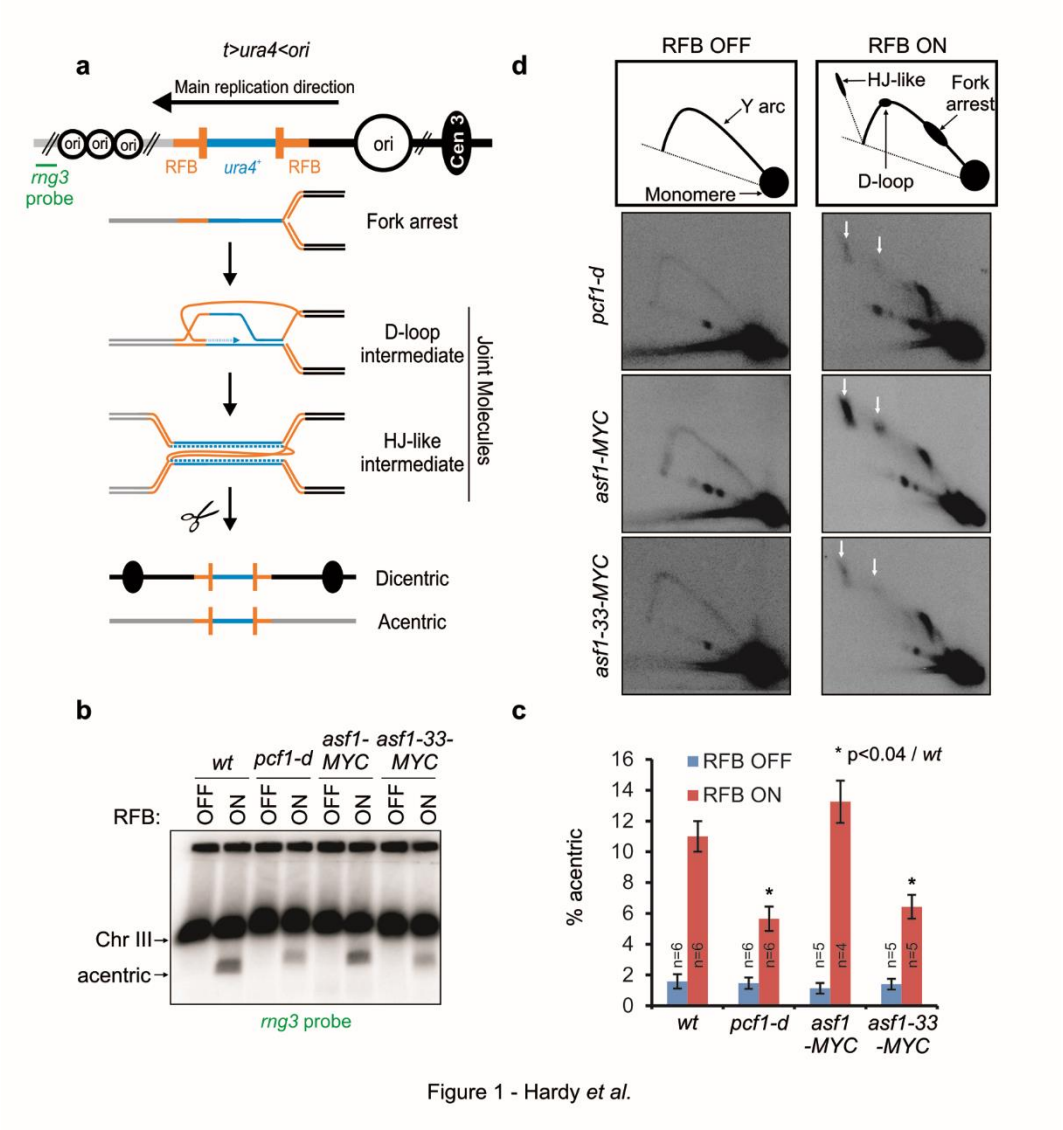

Figure 1 - Hardy *et al.*

Fig. 1: Loss of Asf1-function impairs RDR

a. Diagram of the *t>ura4<ori* locus, in which *t* refers to the telomere-proximal side (gray lines), *ura4* refers to the *wt* gene (blue line), *> and <* refers to the polarity of the two *RTS1*-RFBs (orange bars) and *ori* refers to the replication origin (opened black circle, the largest one being the most efficient origin). Green bar indicates the *rng3* probe. The RDR assay consists of a polar Replication Fork Barrier (RFB), called *RTS1*, integrated at the *ura4*$^{+}$ gene, 5Kb away from a strong replication origin at the centromere-proximal side. An inverted repeated *RTS1* sequence is integrated at the telomere-proximal side of *ura4*$^{+}$ to generate the *t>ura4<ori* locus. Due to the main replication direction, the barrier activity of the centromere-proximal *RTS1*-RFB is predominant over the activity of the telomere-proximal RFB. The RFB activity is mediated by the *RTS1*-bound protein Rtf1, the expression of which is regulated by the *nmt41* promoter repressed in the presence of thiamine. Upon Rtf1 expression, > 90% of forks are blocked at the centromere-proximal RFB. The binding of the Rad51 recombinase and its Rad52 loader allow the blocked fork to be restarted to overcome the RFB. Faulty restart events occur in ~ 2-3 % of cells/replication: Rad51 promotes newly replicated strands to switch template and to invade the opposite inverted *RTS1* sequence. DNA synthesis is then initiated from the 3' invading strand on a non-

contiguous DNA template, resulting in a stable early JM, referred to as a D-loop intermediate. Upon arrival of the converging fork, a second template switch event results in the formation of a later JM, referred to as Holliday junction (HJ)-like intermediate whose resolution generates at least two recombination products: acentric and dicentric which levels are a marker of RDR completion. **b.** Chromosome analysis in indicated strains and conditions by PFGE and Southern-blot using a radiolabeled *rng3* probe. **c.** Quantification of acentric level normalized to chromosome III level. Values are means of n independent biological replicates ± standard error of the mean (SEM). Statistical analysis was performed using Mann & Whitney U test. **d.** Top panel: schematics of replication intermediates (RIs) observed by 2DGE, in RFB OFF and ON conditions. Bottom panels: representative 2DGE experiments in indicated strains and conditions. White arrows indicate JMs.
See Figure S1 for RDR analysis in additional chromatin factor mutants.

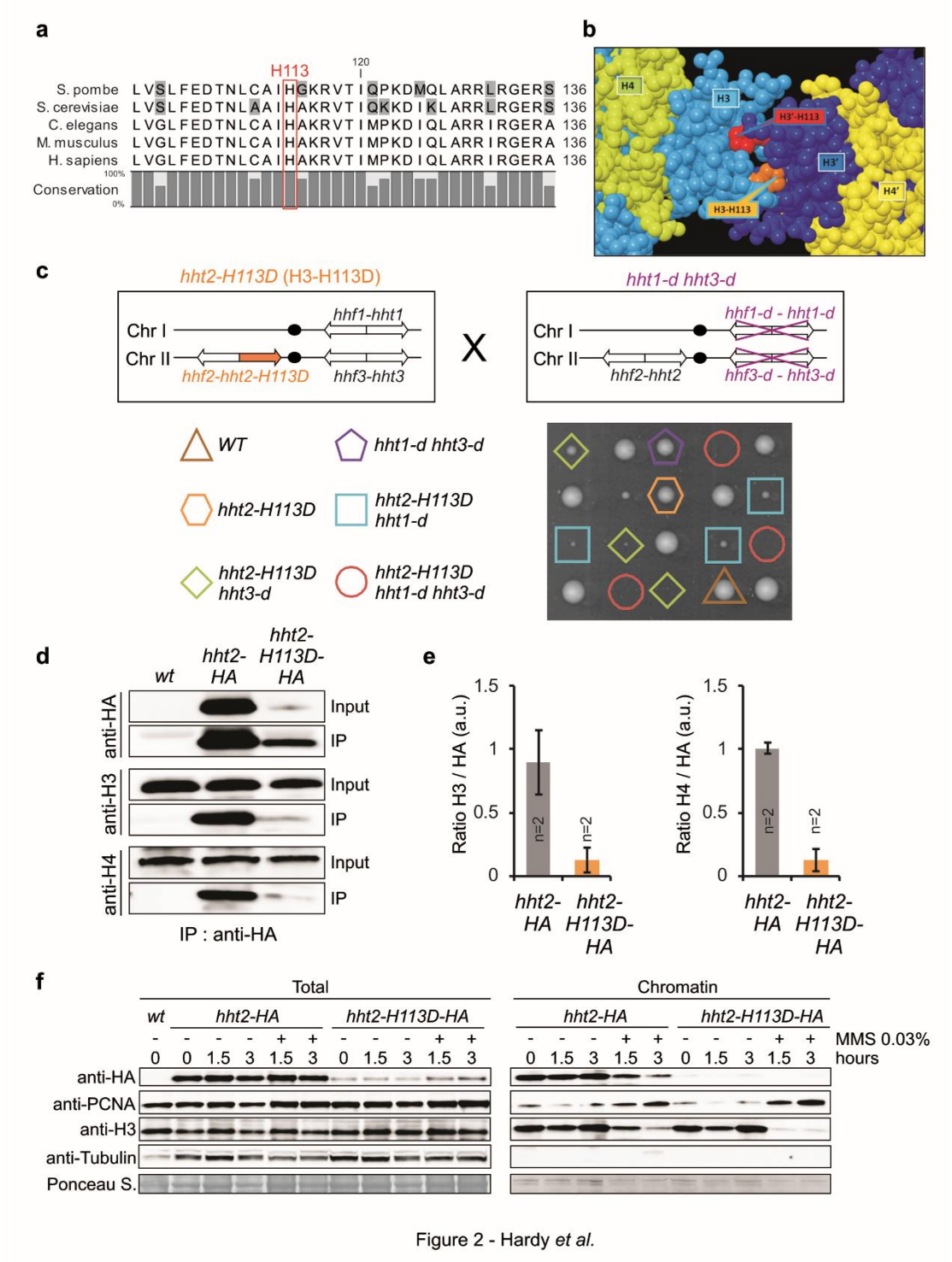

Figure 2 - Hardy *et al.*

Fig. 2: The mutated histone H3-H113D destabilizes $(H3\text{-}H4)_2$ tetramer

a. Alignment of yeast, worm, mouse and human histone H3. Red rectangle indicates the position of histidine 113. UniProtKB access codes used are *S.pombe*: P09988; *S. cerevisiae*: P61830; *C.elegans:* P08898; *M. musculus*: P84228 and *H. sapiens*: Q71DI3. **b.** View of the H3:H3' interface. The interface between the two histones H3, colored here in light (H3) and dark blue (H3'), maintains H3 and H4 in the tetramer form $(H3\text{-}H4)_2$. In the H3:H3' interface, H113 of each histone (orange for H113 in H3 and red for H113 in H3') is deeply buried in the adjacent histone partner. For clarity, the other histones H2A and H2B, as well as DNA, are not represented. **c.** Spore viability analysis of indicated genotypes.

d. Association of H3-HA and H3-H113D-HA with untagged H3 and H4 in indicated strains. **e.** Quantification of panel D expressed in arbitrary unit (a.u.). Values are means of n independent biological replicates ± standard deviation (SD). **f.** Chromatin association of analyzed proteins in indicated strains and conditions (hours upon MMS addition or not).
See Figure S2 for structural impact of H3-H113D.

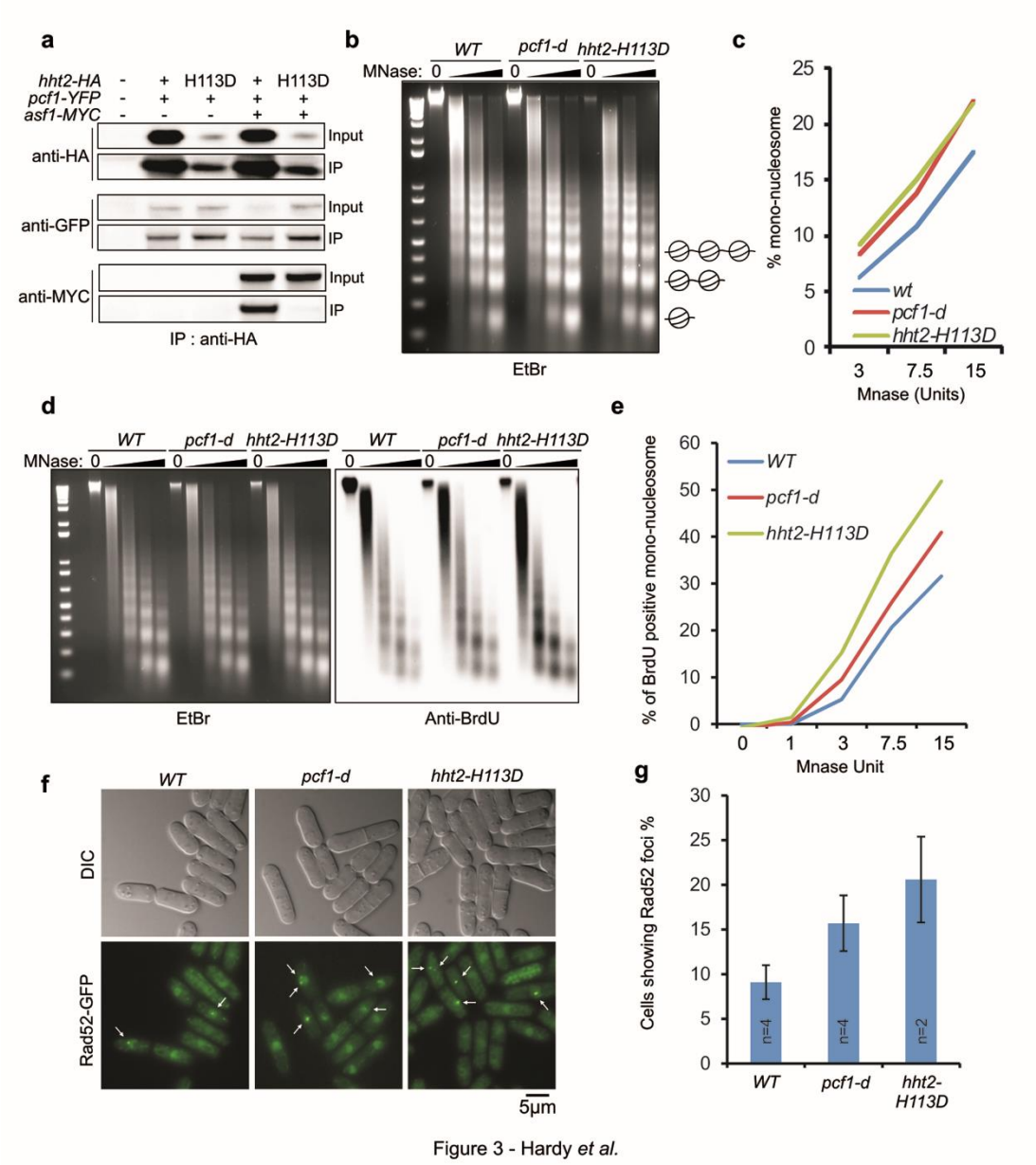

Figure 3 - Hardy *et al.*

Fig. 3: H3-H113D impairs replication-coupled chromatin assembly

a. Association of H3-HA and H3-H113D-HA with Pcf1-YFP and Asf1-MYC in indicated strains. **b.** Representative experiment of chromatin digestion by MNase. Genomic DNA of wild type and mutant strains was digested with increasing amount of MNase and migrated on ethidium bromide (EtBr)-containing agarose gel. **c.** Percentage of mono-nucleosome relative to total DNA. **d.** Representative experiment of replicated chromatin sensitivity to MNase treatment in indicated strains. Left panel: BrdU-incorporated genomic DNA was digested with increasing amount of MNase and migrated on ethidium bromide-containing agarose gel. Right panel: after transfer onto nitrocellulose membrane, incorporated BrdU was revealed using anti-BrdU antibody. **e.** Percentage of BrdU-positive mono-nucleosome relative to total BrdU signal. **f.** Representative examples of Rad52-GFP foci (white arrows) in indicated strains. **g.** Quantification of E. Values are means of n independent biological replicates ±SEM.

See Figure S3 for protein-protein interactions and S4 for biological replicates of sensitivity to MNase.

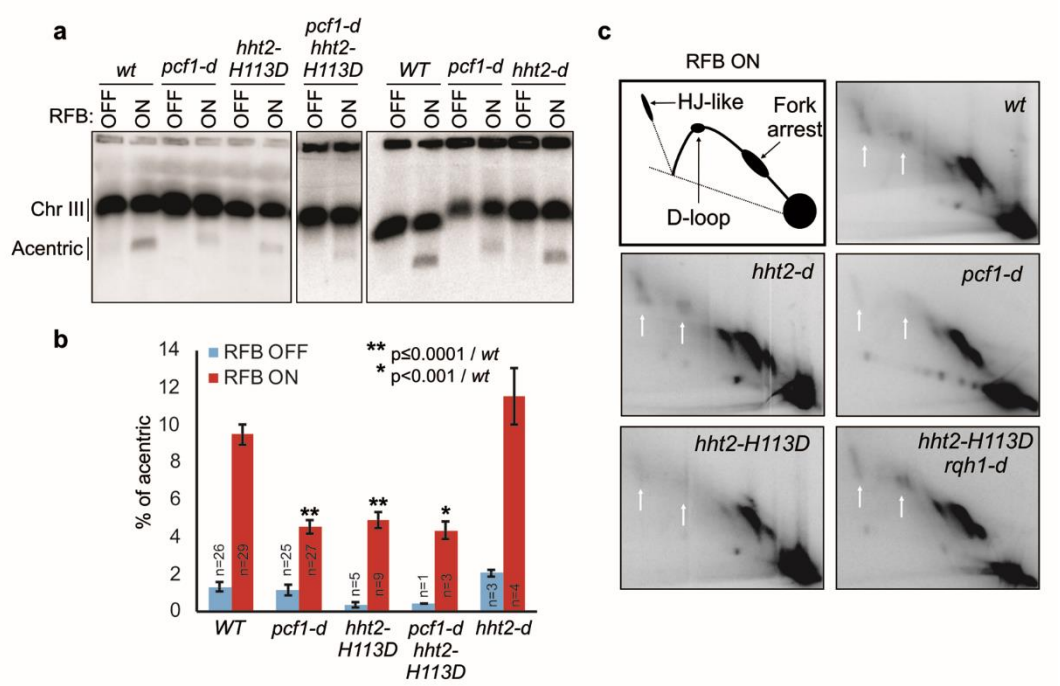

Figure 4 - Hardy *et al.*

Fig. 4: Histone deposition promotes RDR

a. Chromosome analysis in indicated strains and conditions as described on Figure 1. **b.** Quantification of acentric level as described on Figure 1. Values are means of n independent biological replicates ± SEM. Statistical analysis was performed using Mann & Whitney U test. **c.** Representative 2DGE analysis in indicated strains. White arrows indicate JMs. **d.** Survival assay in 10-fold serial dilution experiment of wild type and mutant strains in indicated conditions.

See Figure S5 for the role of H3K56Ac in RDR.

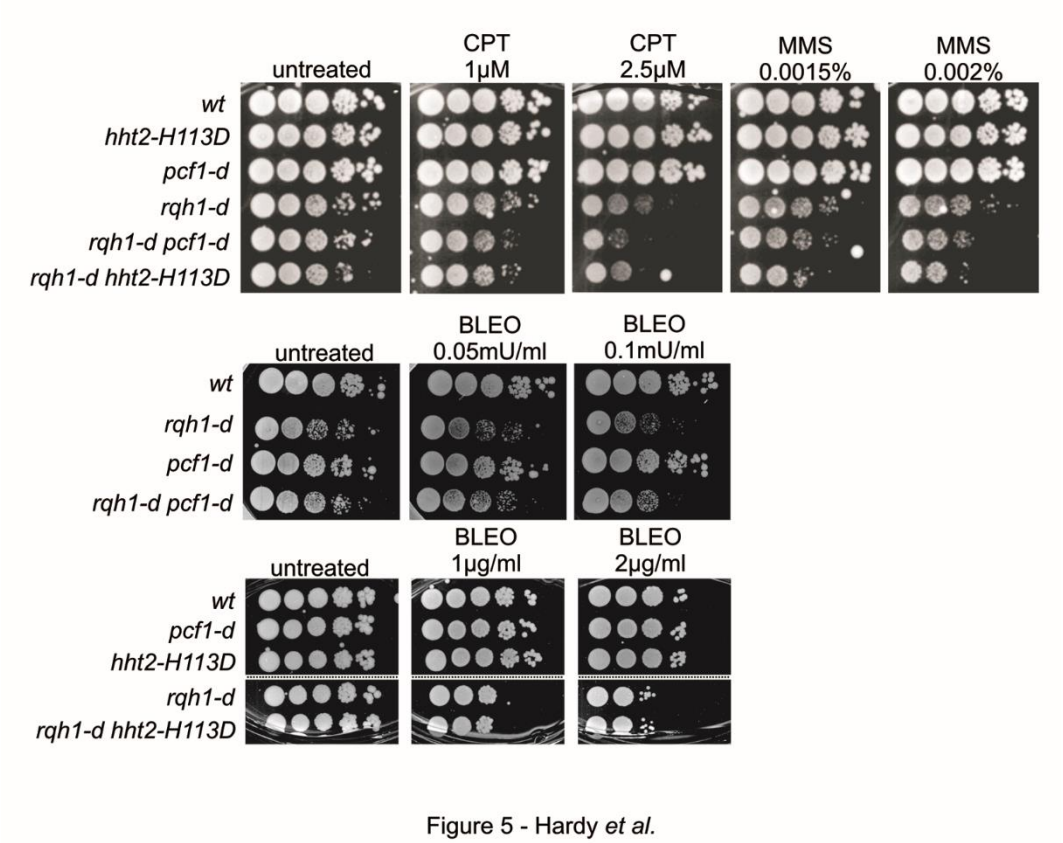

Figure 5 - Hardy *et al.*

Fig. 5: Crosstalk between Rqh1 and histone deposition is required to cell survival to replication stress

Survival assay in 10-fold serial dilution experiment of wild type and mutant strains in indicated conditions.

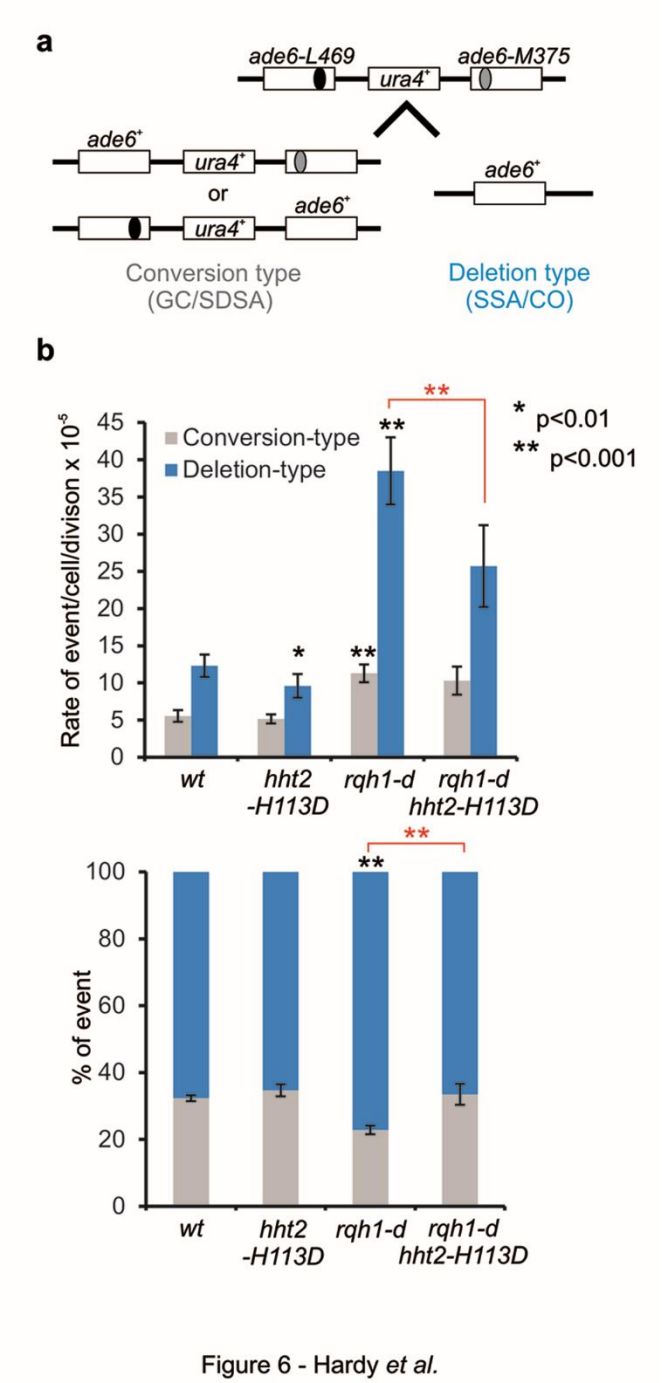

Figure 6 - Hardy *et al.*

Fig. 6: Histone deposition favors deletion-type events

a. Schematic representation of HR substrate and recombination outcomes. **b.** Top panel: rate of conversion and deletion type in indicated strains. Values are median rate calculated from at least 25 independent cultures ± 95 % confidence interval (CI). Bottom panel: ratio of deletion and conversion type in indicated strains. Error bars indicate SEM. Statistical analysis was performed using Mann & Whitney U test. Black and red stars indicate statistics compared to *wt* and compared to *rqh1-d*, respectively.

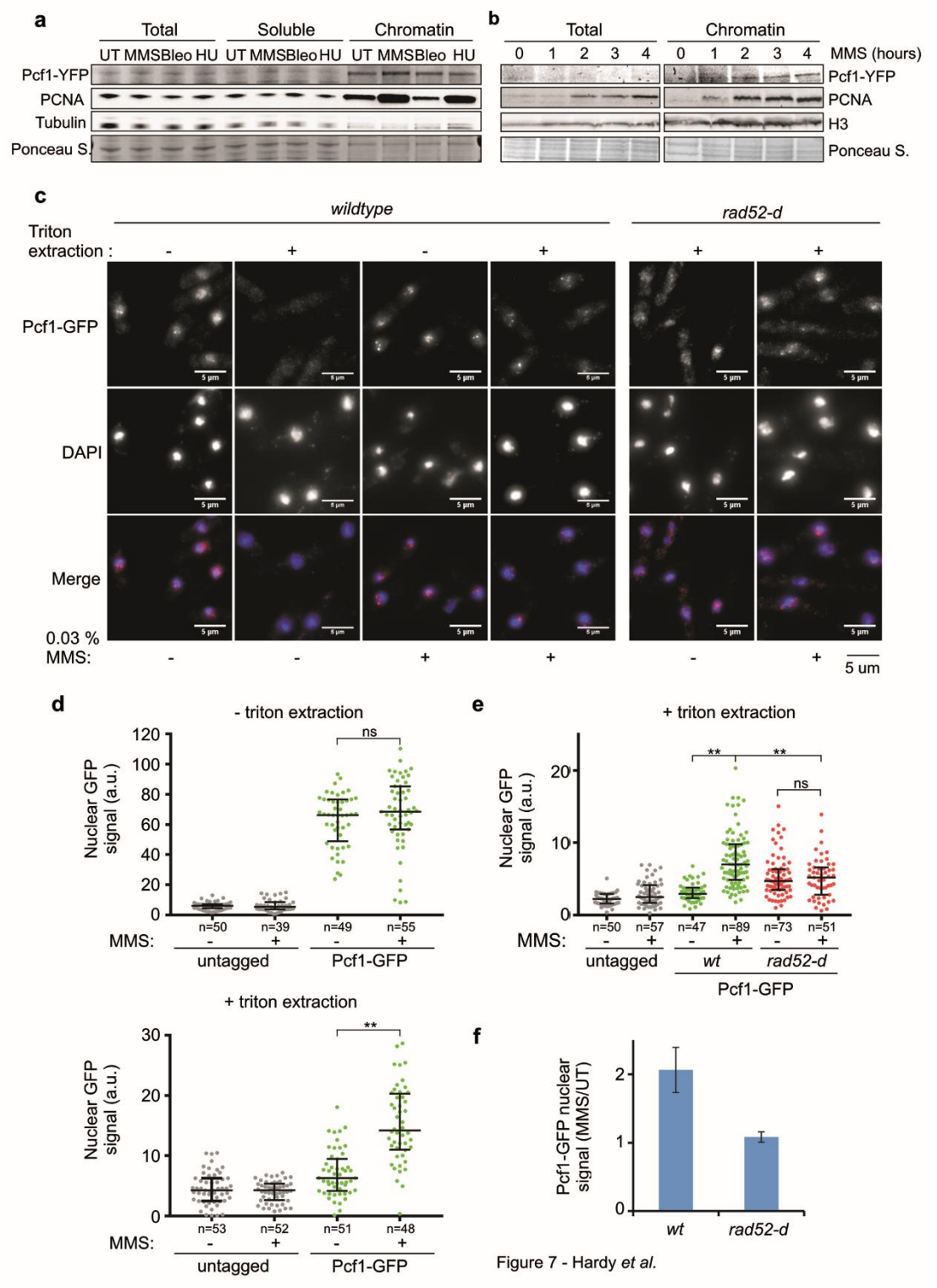

Figure 7 - Hardy *et al.*

Fig. 7: Rad52 promotes Pcf1 binding to the chromatin upon replication stress

a. Chromatin association of Pcf1-YFP in indicated conditions (MMS: 2 hours of 0.03 % MMS, Bleo: 2 hours of 3.5mU/ml of Bleomycin, HU: 2 hours of 20 mM of HU). These doses result in significant cell death in chronic treatment and were thus used in acute treatment. **b.** Kinetics of chromatin association of Pcf1-YFP after 0.03% MMS treatment. **C.** Examples of *in vivo* Chromatin Binding Assay (CBA) from cells expressing Pcf1-GFP in indicated strains and conditions (MMS: 0.03%, 3 hours). **c and e.** Quantification of nuclear GFP signal in arbitrary unit (a.u.) normalized to nucleus area and cytoplasmic

signal (see material and method) in indicated strains and conditions. Quantification Bars indicate the median and interquartile, n indicates the number of cell analyzed. Statistical analysis was performed using Mann & Whitney U test. ** indicates p<0.0001. **f.** Fold enrichment in Pcf1-GFP nuclear staining upon MMS treatment in indicated strains. Values are means of two independent experiments ± SD. See Figure S6 for PCNA and H3 association to chromatin in *rad52-d* mutant.

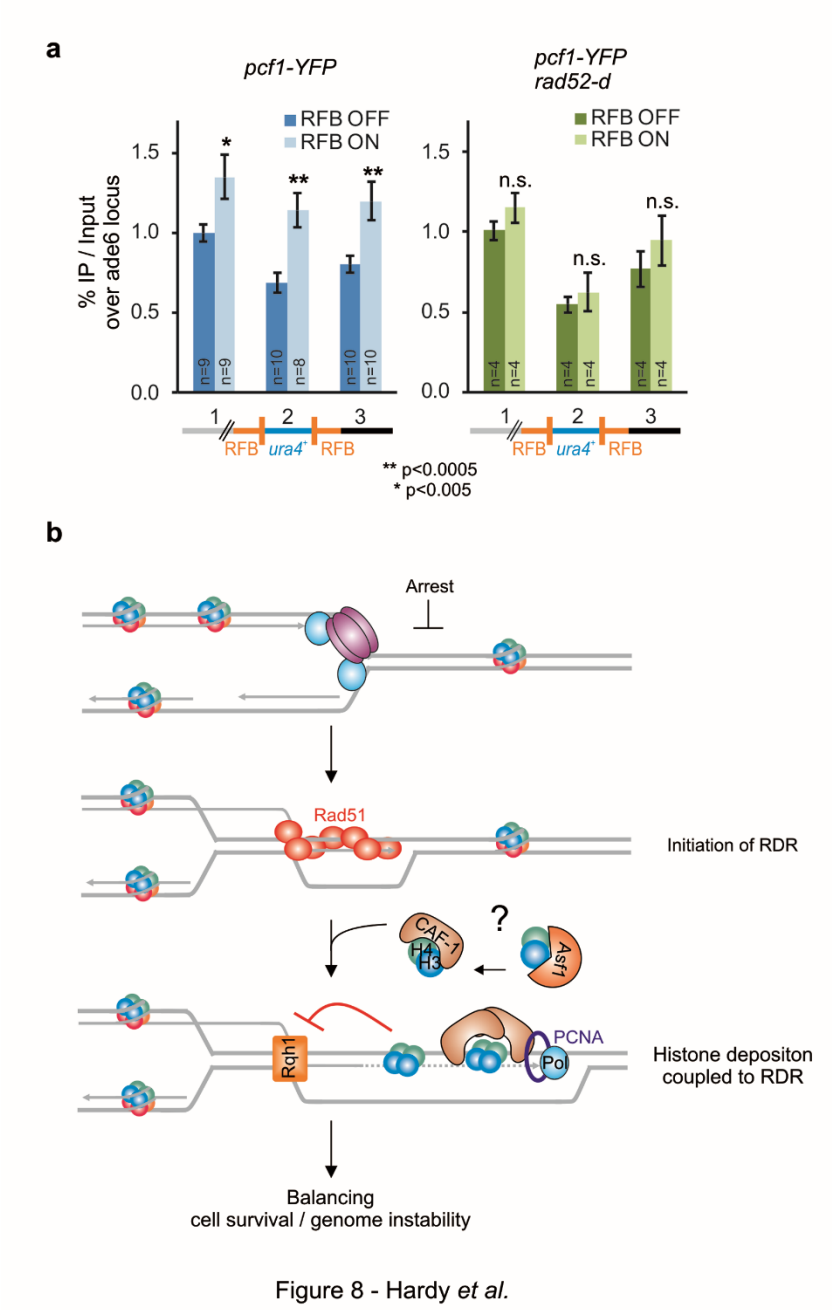

Figure 8 - Hardy *et al.*

Fig. 8: CAF-1 recruitment to RDR sites requires Rad52

a. Pcf1-YFP binding to the *t>ura4<ori* locus in RFB OFF and ON conditions (left panel: *wt strain,* right panel: *rad52-d strain*). Scheme at the bottom depicts the primers location within the *t>ura4<ori* locus: primer pair 1 are located 400 bp at the telomere-proximal side, primer pair 2 are within the *ura4* gene, primer pair 3 are located 150 bp at the centromere-proximal side. Values are means of n independent biological replicates from 2 independent clones ± 95 % CI. Statistical analysis was performed using Mann & Whitney U test. **b.** Model of histone deposition coupled to recombination-dependent replication. Upon fork arrest, HR factors promote D-loop formation which primes the restarted synthesis and histone deposition. Histone deposition coupled to RDR allows JMs to be protected from disassembly by Rqh1. This antagonistic activity of histone deposition and Rqh1 in JMs protection/disassembly contributes to cell resistance to replication stress and balance genome stability at site of replication stress.

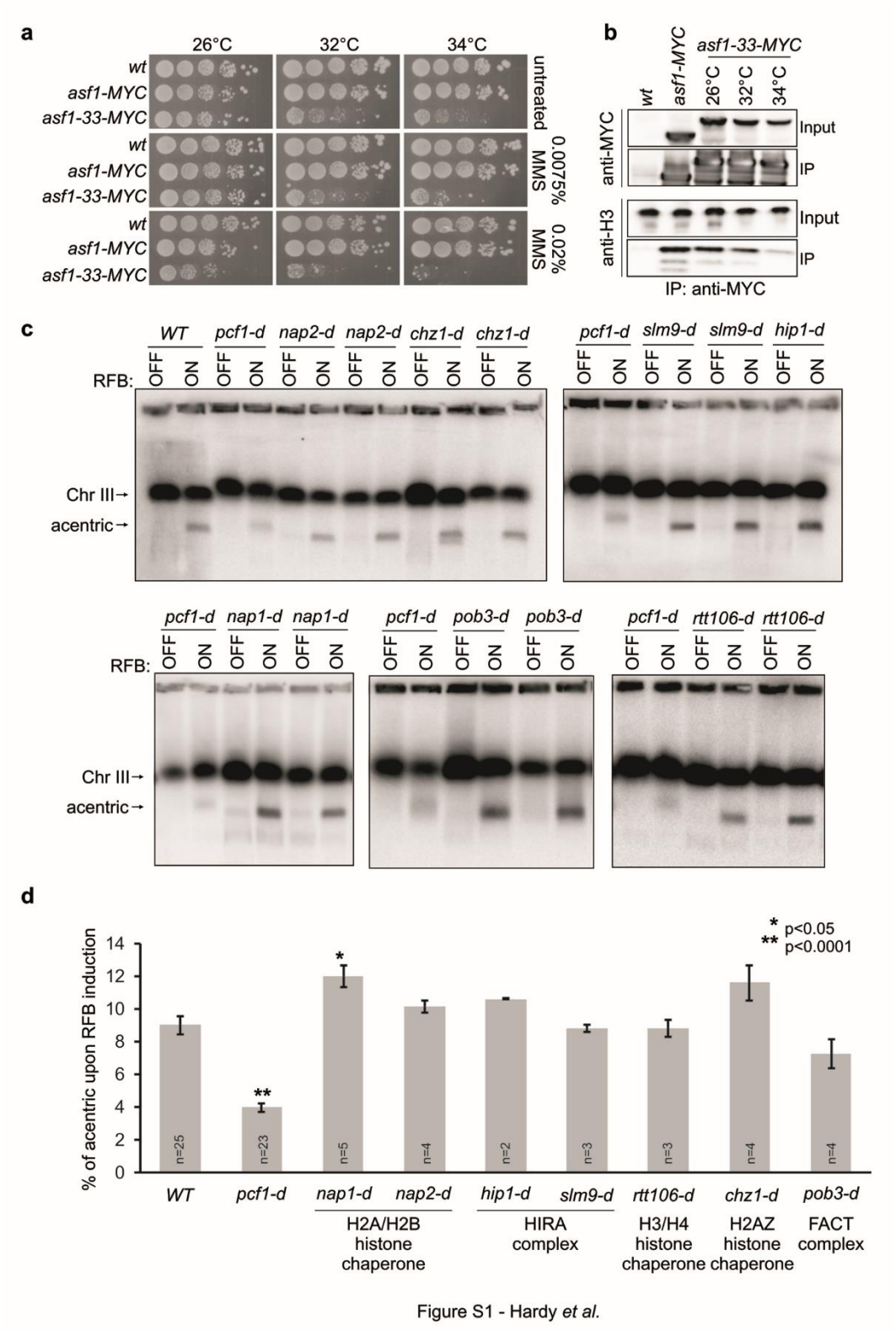

Figure S1 - Hardy *et al.*

Supplementary Fig. 1: Chromatin factors involved in RDR (related to Figure 1)

a. Survival assay of 10-fold serial dilutions of indicated strains in indicated conditions. **b.** Association of Asf1-MYC and Asf1-33-MYC with histone H3 at indicated temperatures. **c.** Chromosome analysis in indicated strains and conditions by PFGE and Southern-blot using a radiolabeled *rng3* probe. **d.** Quantification of acentric level normalized to chromosome III level. Values are means of n independent biological replicates ± standard error of the mean (SEM). Statistical analysis was performed using Mann & Whitney U test.

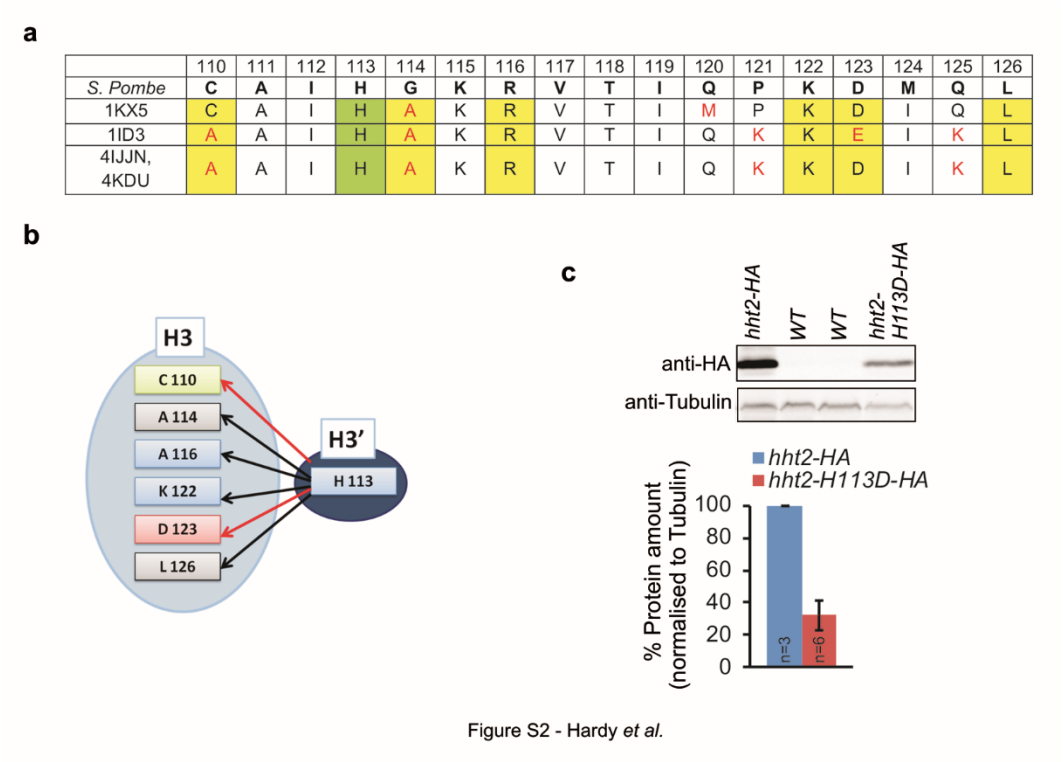

	110	111	112	113	114	115	116	117	118	119	120	121	122	123	124	125	126
S. Pombe	**C**	**A**	**I**	**H**	**G**	**K**	**R**	**V**	**T**	**I**	**Q**	**P**	**K**	**D**	**M**	**Q**	**L**
1KX5	C	A	I	H	A	K	R	V	T	I	M	P	K	D	I	Q	L
1ID3	A	A	I	H	A	K	R	V	T	I	Q	K	K	E	I	K	L
4IJJN, 4KDU	A	A	I	H	A	K	R	V	T	I	Q	K	K	D	I	K	L

Figure S2 - Hardy *et al.*

Supplementary Fig. 2: Impact of H3-H113D on interactions with *wt* H3 and H4 (related to Figure 2)

a. Amino acid sequences of the region containing H113 and its interacting partners in the H3:H3' nucleosomal interface. This table gives the amino acid sequences of the relevant part of H3 in *Schizosaccharomyces pombe* and the considered X-ray structures. The X-ray structures are referenced by their PDB codes. 1KX5 contains histones from *Xenopus laevis*; 1ID3, 4JJN and 4KUD include histones from *Saccharomyces Cerevisiae*. The residues in red differ from those of *Schizosaccharomyces pombe*. The residues on yellow background form a network of contact with H113 (green background) in the H3:H3' interface. **b.** Schematic representation of the contact network involving H113 in the H3:H3' interface. H3'-H113 interacts with 6 residues of H3. Two hydrogen bonds (red arrows) are reinforced by van der Waals contacts (grey arrows). Identical, symmetric interaction pattern is observed with H3-H113 and C110, H3'-D123, A114, R116, K122 and L126. The interface analysis was carried out with PDBsum (de Beer *et al*, 2014). **c.** Top panel: expression of H3-HA and H3-H113D-HA in indicated strains. Tubulin was used as loading control. Bottom panel: Quantification of left panel, the level of H3-H113D-HA was normalized to tubulin and H3-HA. Values are means of n independent biological replicates ± SD.

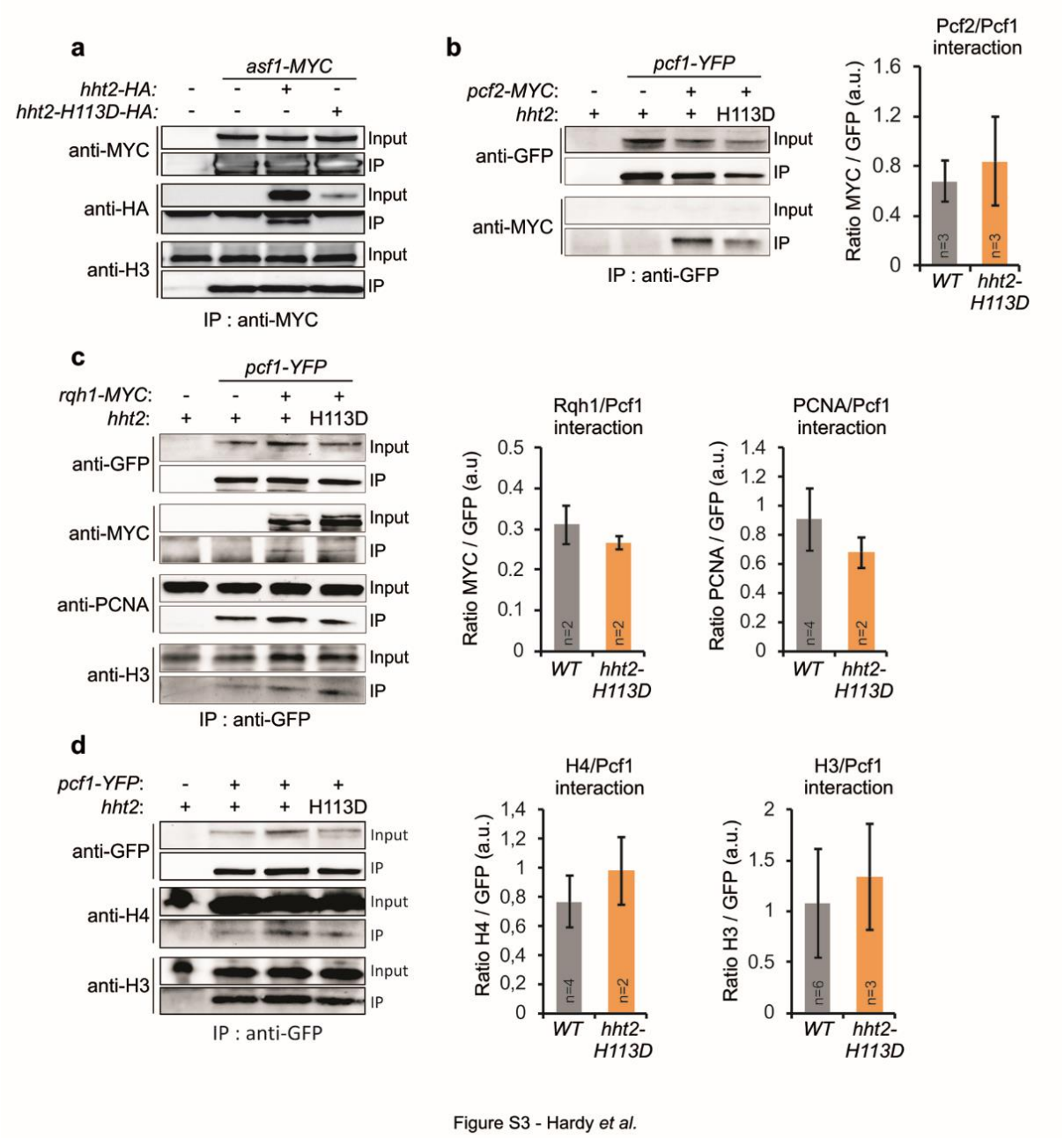

Figure S3 - Hardy *et al.*

Supplementary Fig. 3: Impact of H3-H113D on protein-protein interactions (related to Figure 3).

a. Association of Asf1-MYC with histone H3 (H3, H3-HA and H3-H113D-HA). **b.** Left panel: association of Pcf1-YFP with Pcf2-MYC in indicated strains. Right panel: quantification expressed in arbitrary unit (a.u.). Values are means of n independent biological replicates ± SD. **c.** Left panel: association of Pcf1-GFP with Rqh1-MYC and PCNA in indicated strains. Right panels: quantification. Values are means of n independent biological replicates ± SD. **d.** Left panel: association of Pcf1-GFP with histone H3 and H4 in indicated strains. Right panels: quantification. Values are means of n independent biological replicates ± SD.

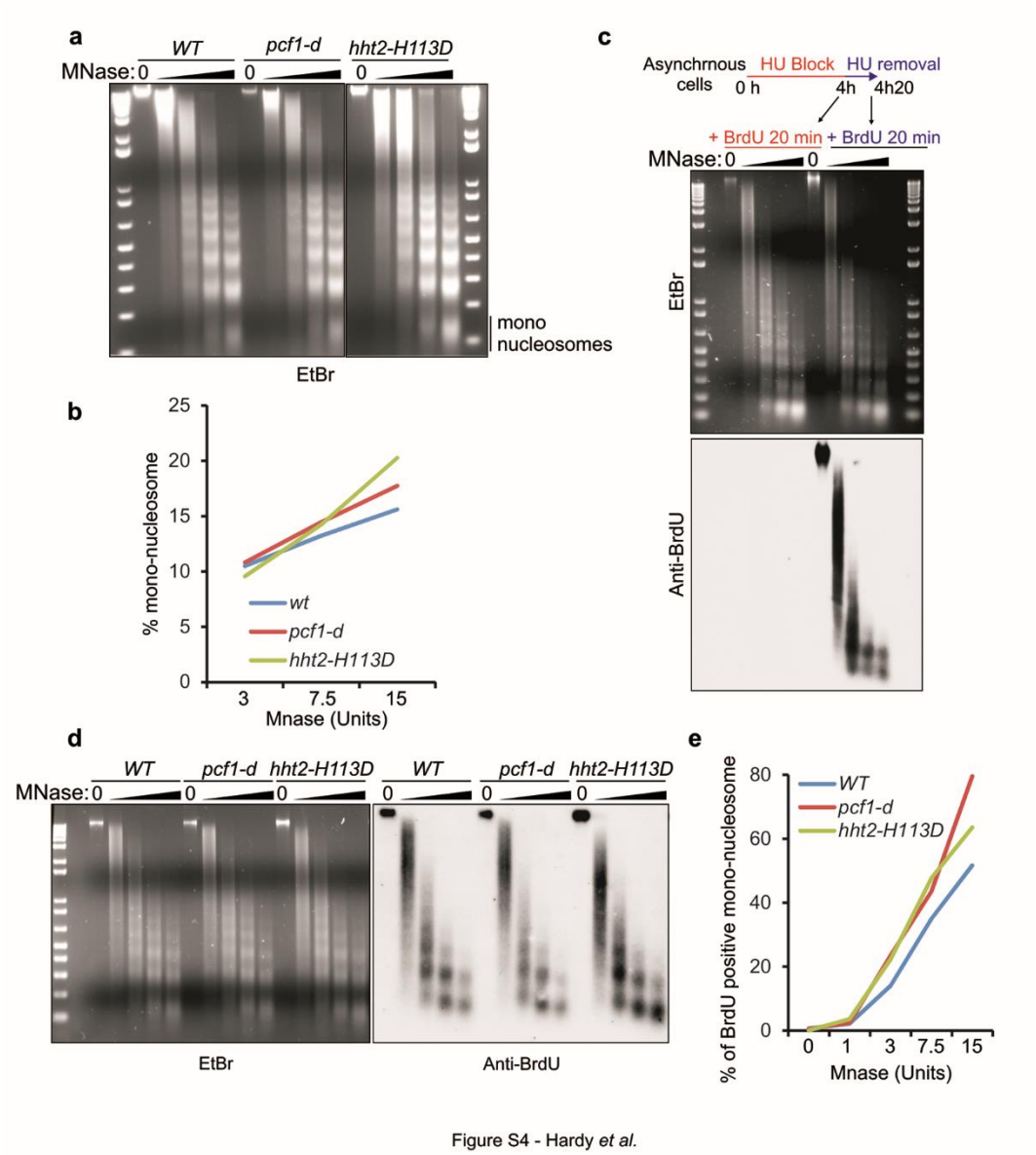

Figure S4 - Hardy *et al.*

Supplementary Fig. 4: H3-H113D impairs replication-coupled chromatin assembly (related to Figure 3)

a. Representative experiment of chromatin digestion by MNase in indicated strains. Genomic DNA of indicated strains was digested with increasing amount of MNase and migrated on ethidium bromide-containing agarose gel. **b.** Percentage of mono-nucleosome relative to total DNA. **c.** Logarithmic growing cells were arrested in early S-phase with HU treatment. Pulse of 20min BrdU (400µM) incorporation was done after 4 hours of HU block or after releasing cells in a fresh media. Top panel: BrdU-incorporated genomic DNA was digested with increasing amount of MNase and migrated on ethidium bromide-containing agarose gel. Bottom panel: after transfer onto nitrocellulose membrane, incorporated BrdU was revealed using anti-BrdU antibody. **d.** Representative experiment of replicated chromatin sensitivity to MNase treatment in indicated strains. Left panel: BrdU-incorporated genomic DNA was digested with increasing amount of MNase and migrated on ethidium bromide-containing agarose gel. Right panel: after transfer onto nitrocellulose membrane, incorporated BrdU was revealed using anti-BrdU antibody. **d.** Percentage of BrdU-positive mono-nucleosome relative to the total BrdU signal.

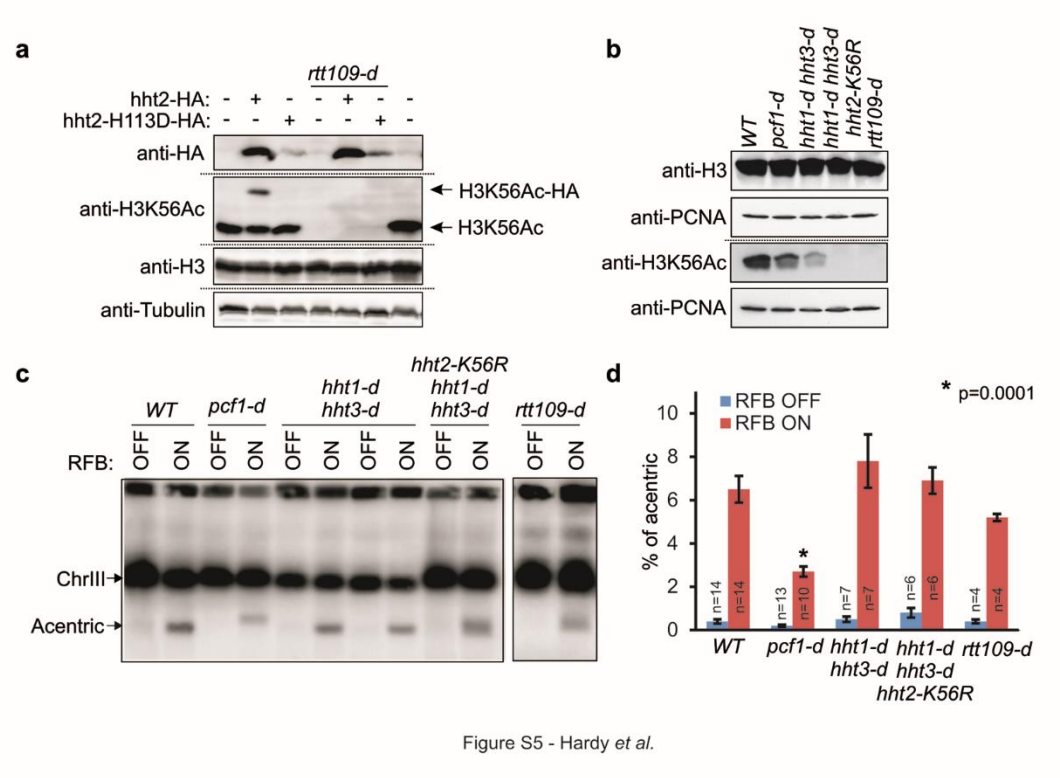

Figure S5 - Hardy *et al.*

Supplementary Fig. 5: H3K56Ac is dispensable to RDR (related to Figure 4)

a. Level of H3K56Ac, H3-HA and H3-H113D in indicated strains. H3 and tubulin were used as loading control. Each panel corresponds to replicate loading on the same gel. **b.** Level of H3 and H3-K56Ac in indicated strains. PCNA was used as a loading control. The two top and the two bottom panels correspond to the same membrane blotted with two different antibodies **c.** Chromosome analysis in indicated strains and conditions by PFGE and Southern-blot using a radiolabeled *rng3* probe. **d.** Quantification of acentric level normalized to chromosome III level. Values are means of 0 independent biological replicates ± 95% CI. Statistical analysis was performed using Mann & Whitney U test.

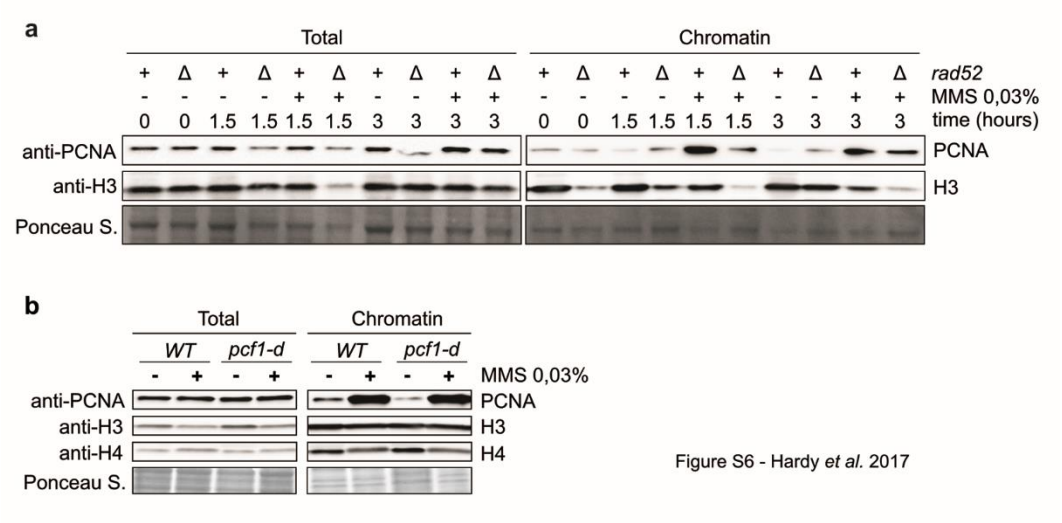

Supplementary Fig. S6: Chromatin-bound H3 and PCNA upon MMS requires Rad52 but not CAF-1 (related to Figure 6)

Chromatin association of H3 and PCNA in strains defective for *rad52-d* (**a**) and *pcf1-d* (**b**), after addition or not of 0.03% MMS.

Supplementary Table 1: Strains used in this study (related to all figures).

Name		*Genotype*	Reference	Experiment
II4	*h-smto*	*rad54::hphMX6, ade6-704, leu1-32, ura4-D18*	Lambert	Fig. S5C
JH059	*h- smto*	*hht2-H113D:hphMX, ade6-704, leu1-32, ura4-D18*	This study	Fig. 3A-B Fig. 4A Fig. S3A-B
JH086	*h- smto*	*hht2-hhf2::kanMX6 , rtf1:nmt41:sup35, t>ura4^{+}<ori, ade6-704, leu1-32*	This study	Fig. 4B-D
JH118	*h- smto*	*hht2-3HA:kanMX6, ade6-704, leu1-32, ura4-D18, his3-D1, arg3-D4*	This study	Fig. 2D-E and H Fig. S2C Fig. S4A
JH122	*h- smto*	*hht2-H113D-3HA:kanMX6, ade6-704, leu1-32, ura4-D18, his3-D1, arg3-D4*	This study	Fig. 2D-E and H Fig. S2C FigS4A
JH193	*h- smto*	*hht2-3HA:kanMX6, pcf1-YFP:kanMX6, ade6-704, leu1-32, ura4-D18, his3-D1, arg3-D4*	This study	Fig. 2F-G
JH197	*h- smto*	*hht2-H113D-3HA:kanMX6, pcf1-YFP:kanMX6, ade6-704, leu1-32, ura4-D18, his3-D1, arg3-D4*	This study	Fig. 2F-G
JH217	*h+*	*hht2-3HA:kanMX6, pcf1-YFP:kanMX6, asf1-MYC:kanMX6, leu1-32, ura4-D18, his3-D1, arg3-D4*	This study	Fig. 2F-G Fig. S2D
JH218	*h+*	*hht2-H113D-3HA:kanMX6, pcf1-YFP:kanMX6, asf1-MYC:kanMX6, ade6-704, leu1-32, ura4-D18, his3-D1*	This study	Fig. 2F-G Fig. S2D
JH242	*h- smto*	*hht2-H113D:hphMX, rqh1-MYC:kanMX6, pcf1-YFP:kanMX6, ade6-704, leu1-32, ura4-D18*	This study	Fig. S2F
JH245	*h-smto*	*hht2-H113D:hphMX, rqh1::kanMX6, ade6-704, leu1-32, ura4-D18*	This study	Fig. 4A
JH253	*h+*	*hht2-3HA:kanMX6, rtt109::kanMX6, ade6-704, leu1-32, ura4-D18*	This study	Fig. S4A
JH255	*h+*	*hht2-H113D-3HA:kanMX6, rtt109::kanMX6, ade6-704, leu1-32, ura4-D18, his3-D1, arg3-D4*	This study	Fig. S4A
JH274	*h- smto*	*hht2-H113D:hphMX6, pcf1-YFP:kanMX6, pcf2-4.5MYC:kanMX6, ade6-704, leu1-32, ura4-D18*	This study	Fig. S2E
JH300	*h- smto*	*rqh1::kanMX6, hht2-H113D:hphMX, rtf1:nmt41:sup35, t>ura4^{+}<ori, ade6-704, leu1-32*	This study	Fig. 4D
JH302	*h- smto*	*nap2::kanMX6, rtf1:nmt41:sup35, t>ura4^{+}<ori, ade6-704, leu1-32*	This study	Fig. S1
JH304	*h- smto*	*chz1::kanMX6, rtf1:nmt41:sup35, t>ura4^{+}<ori, ade6-704, leu1-32*	This study	Fig. S1
JH305		*pob3::kanMX6, rtf1:nmt41:sup35, t>ura4^{+}<ori, ade6-704, leu1-32*	This study	Fig. S1
JH308	*h- smto*	*pcf1::kanMX6, ura4::adh::dmdNK-natMX-adh::hENT1, ura4-aim*	This study	Fig. 3C-D Fig. S3D-E
JH314	*h+*	*hht2-H113D:hphMX, ura4::adh::dmdNK-natMX-adh::hENT1, ura4-aim*	This study	Fig. 3C-D Fig. S3D-E
JH336	*h-smto*	*rad52-GFP:kanMX6, pcf1::kanMX6, ade6-704, leu1-32, ura4-D18*	This study	Fig. 3E-F
JH341	*h-smto*	*rad52-GFP:kanMX6 hht2-H113D:hphMX6, ade6-704, leu1-32, ura4-D18*	This study	Fig. 3E-F

JH344	*h+*	*pcf1::kanMX6, hht2-H113D-hphMX6, rtf1:nmt41:sup35, t>ura4$^+$<ori, ade6-704, leu1-32*	This study	Fig. 4B-C
JH359		*ade6-M375 int:puc8/ura4$^+$/ade64-69, rqh1::kanMX6, ura4-D18*	This study	Fig. 4E-F
JH361		*ade6-M375 int:puc8/ura4+/ade64-69, hht2-H113D:hphMX6, ura4-D18*	This study	Fig. 4E-F
JH363		*ade6-M375 int:puc8/ura4+/ade64-69, rqh1::kanMX6, hht2-H113D:hphMX6, ura4-D18*	This study	Fig. 4E-F
JH403	*h- smto*	*pcf1-YFP:kanMX6 rad52::natMX6, rtf1::nmt41:sup35, t>ura4$^+$<ori, ade6-704, leu1-32*	This study	Fig. 5D
SL75	*h-*	*ade6-704, leu1-32, ura4-D18,*	Carr's lab	Fig. 1A-B Fig. 2D, F, H Fig. 3A-B Fig. 4A Fig.5C Fig. S2C-F Fig. S3A-B Fig. S4A-B Fig. S5
SL80	*h+*	*rqh1::kanMX6, ade6-704, leu1-32, ura4-D18*	Pietrobon *et al.* 2014	Fig. 4A
SL228	*h+*	*rtf1:nmt41:sup35, t>ura4+<ori, ade6-704, leu1-32*	Lambert *et al*. 2005	Fig. 1D Fig. 4B-D Fig. S1 Fig. S4C-D
SL261	*h- smto*	*rad51::kanMX6, ade6-704, leu1-32, ura4-D18*	Lambert *et al.* 2005	Fig. S5B
SL291	*h+*	*rad52-GFP:kanMX6, ade6-704, leu1-32, ura4-D18*	Tsang *et al.* 2014	Fig. 3E-F
SL413	*h+*	*rad52::kanMX6, ade6-704, leu1-32, ura4-D18*	Lambert *et al.* 2005	Fig. S5A
SL917	*h+*	*ade6-M375 int:puc8/ura4+/ade64-69*	Hartsuiker et al. 2001	Fig. 4E-F
SL990	*h-*	*asf1-MYC:kanMX6, ade6-704, leu1-32, ura4-D18*	Tanae *et al.* 2012	Fig. 1A-B Fig. S2D
SL991	*h+*	*asf1-33-MYC:kanMX6, ade6-704, leu1-32, ura4-D18*	Tanae *et al.* 2012	Fig. 1A-B
SL1077	*h+*	*ura4::adh::dmdNK-natMX-adh::hENT1, ura4-aim*	Fleck *et al.* 2017	Fig. 3C-D Fig. S3C-E
VP103	*h- smto*	*pcf1::kanMX6, rtf1:nmt41:sup35, t>ura4$^+$<ori, ade6-704, leu1-32*	Pietrobon *et al*. 2014	Fig. 1D-E Fig. 4B-D Fig. S1 Fig. S4B-C-D
VP247	*h- smto*	*pcf1-YFP:kanMX6, rtf1::nmt41:sup35, t>ura4$^+$<ori, ade6-704, leu1-32*	This study	Fig. 5D
VP285	*h+*	*pcf1::ura4$^+$, ade6-704, leu1-32, ura4-D18*	Pietrobon *et al*. 2014	Fig. 3A-B Fig. 4A Fig. S3A-B Fig. S5D
VP316	*h- smto*	*rqh1::kanMX6, pcf1::ura4$^+$, ade6-704, leu1-32, ura4-D18*	Pietrobon *et al*. 2014	Fig.4A
VP394	*h- smto*	*pcf1-YFP:kanMX6, ade6-704, leu1-32, ura4-D18*	Pietrobon *et al*. 2014	Fig. 5A-B Fig. S2E-F

VP399	*h-*	*hht1-hhf1::his3^{+} hht3-hhf3::arg3^{+}, hht2-K56R, ade6-210, leu1-32, ura4-D18, ade6-otr, his3-D1, arg3-D4*	Xhelmace et al. 2007	Fig. S4B
VP409	*h-smto*	*pcf2-4.5-MYC:kanMX6, ade6-704, leu1-32, ura4-D18*	Pietrobon *et al*. 2014	Fig. 5C
VP426	*h- smto*	*pcf1-YFP:kanMX6, pcf2-4.5-MYC:kanMX6, ade6-704, leu1-32, ura4-D18*	Pietrobon *et al*. 2014	Fig. S2E
VP453	*h-*	*hht1-hhf1::his3,$^{+}$ hht3-hhf3::arg3^{+}, rtf1:nmt41:sup35, t>ura4+<ori, leu1-32, ade6-704, ade6-otr, his3-D1, arg3-D4*	This study	Fig. 2C Fig. S4C-D
VP476	*h+*	*rtt109::kanMX6, ade6-M216, leu1-32, ura4-D18*	Bioneer	Fig. S4 A-B
VP478	*h+*	*hht1-hhf1::his3^{+}, hht3-hhf3::arg3^{+}, hht2-K56R, rtf1:nmt41:sup35, t>ura4^{+}<ori, leu1-32, ade6-210, ade6-otr, his3-D1, arg3-D4*	This study	Fig. S4 C-D
VP480	*h+*	*rtt109::kanMX6, rtf1:nmt41:sup35, t>ura4^{+}<ori, ade6-704, leu1-32*	This study	Fig. S4 C-D
VP481	*h-*	*slm9::kanMX6, rtf1:nmt41:sup35, t>ura4^{+}<ori, ade6-704, leu1-32*	This study	Fig. S1
VP484	*h+*	*asf1-MYC:kanMX6, rtf1:nmt41:sup35, t>ura4^{+}<ori, ade6-704, leu1-32*	This study	Fig. 1D-E
VP486	*h- smto*	*asf1-33-MYC:kanMX6, rtf1:nmt41:sup35, t>ura4^{+}<ori, ade6-704, leu1-32*	This study	Fig. 1D-E
VP488	*h+*	*rtt106::kanMX6, rtf1:nmt41:sup35, t>ura4^{+}<ori, ade6-704, leu1-32*	This study	Fig. S1
VP490	*h+*	*nap1::kanMX6, rtf1:nmt41:sup35, t>ura4^{+}<ori, ade6-704, leu1-32*	This study	Fig. S1
VP511	*h- smto*	*hht2-H113D:hphMX, rtf1:nmt41:sup35, t>ura4^{+}<ori, ade6-704, leu1-32*	This study	Fig. 4B-D
VP520	*h- smto*	*rqh1-MYC:kanMX6, pcf1-YFP:kanMX6, ura4-D18, ade6-704, leu1-32*	Pietrobon *et al*. 2014	Fig. S2F
VP543	*h+*	*hht2-H113D:hphMX, rtf1:nmt41:sup35, t>ura4^{+}<ori, ade6-704, leu1-32*	This study	Fig. 2C
VP562	*h-smto*	*hip1::kanMX6, rtf1:nmt41:sup35, t>ura4^{+}<ori, ade6-704, leu1-32*	This study	Fig. S1

Supplementary Table 2: List of primers used in this study

Name	Sequence (5'-3')	Experiment
#1 (R400F)	CACACTTGCTCTGTACACGTATTCT	ChIP Pcf1-YFP
#1 (R400R)	AGGATCCATGATGCACAGATT	ChIP Pcf1-YFP
#2 (Ura4-1F)	GACTCCACGACCAACAATGA	ChIP Pcf1-YFP
#2 (Ura4-1R)	CTGGTATCGGCTTGGATGTT	ChIP Pcf1-YFP
#3 (L3F)	TTTAAATCAAATCTTCCATGCG	ChIP Pcf1-YFP
#3 (L3R)	TGTACCCATGAGCAAACTGC	ChIP Pcf1-YFP
Ade6-23	GGCTGCCTCTACCATCATTC	ChIP Pcf1-YFP
Ade6-25	TTAAGCTGAGCTGCCAAGGT	ChIP Pcf1-YFP
RuraR probe 1F	CAAACGCAAACAAGGCATCGAC	^{32}p probe
RuraR probe 1R	GGCTCTTTGGCTACTGGTTC	^{32}p probe
RNG3 lo	AAGGACTGCGTTCTTCTAGC	^{32}p probe
RNG3 up	TGAATCCTCCGTTCAGTAGG	^{32}p probe

université PARIS-SACLAY
ÉCOLE DOCTORALE
Structure et dynamique des systèmes vivants (SDSV)

Titre : Caractérisation des interactions physiques et fonctionnelles entre le facteur d'assemblage de la chromatine, CAF-1, et des facteurs de la recombinaison homologue au cours de la réparation de l'ADN

Mots clés : recombinaison homologue, réparation de l'ADN, chromatine

L'ADN est constamment exposé à des insultes génotoxiques endogènes et exogènes. Plusieurs mécanismes de réparations de l'ADN sont mis en œuvre pour préserver la stabilité du génome et de l'épigénome. La recombinaison homologue (RH) joue un rôle central dans la réparation des cassures double brin de l'ADN (CDBs) et le redémarrage des fourches de réplication en réponse à un stress réplicatif. Ces deux processus sont tous deux couplés à l'assemblage de la chromatine. Le facteur d'assemblage de la chromatine 1 (CAF-1) est un chaperon d'histone conservé au cours de l'évolution qui fonctionne dans le processus d'assemblage des nucléosomes couplé à la réparation de l'ADN et à la réplication, en déposant sur l'ADN les tétramères d'histones $(H3\text{-}H4)_2$ nouvellement synthétisés. Chez la levure *Schizosaccharomyces pombe*, le complexe CAF-1 est constitué de trois sous-unités, Pcf1, Pcf2 et Pcf3. Il a été montré que CAF-1 agit dans l'étape de synthèse de l'ADN durant le processus de réplication dépendante de la recombinaison (RDR) et protège le désassemblage des D-loops par l'hélicase Rqh1, membre de la famille des hélicases RecQ. Dans cette étude, nous avons adressé le rôle de CAF-1 pendant la réparation de l'ADN par recombinaison homologue chez la levure *Schizosaccharomyces pombe*.

En utilisant des approches *in vivo* et *in vitro*, nous avons validé des interactions protéines-protéines au sein d'un complexe contenant Rqh1, CAF-1, PCNA, et l'Histone H3. Nous avons montré que Rqh1 interagit avec Pcf1 et avec Pcf2 indépendamment l'un de l'autre, et que l'interaction Rqh1-Pcf1 est stimulée par des dommages à l'ADN. Nous avons mis en place une méthode d'analyse d'association de CAF-1 à la chromatine en réponse aux dommages à l'ADN. Nous avons observé qu'un stress réplicatif, mais pas l'induction de cassures double brin de l'ADN, favorise l'association de CAF-1 à la chromatine. Nous avons identifié plusieurs facteurs de la RH nécessaire pour l'association de CAF-1 à la chromatine en réponse à un stress réplicatif. De plus, nous avons mis en évidence des interactions physiques entre Pcf1 et des facteurs de la recombinaison homologue, parmi lesquels RPA et Rad51. Nos données suggèrent que CAF-1 pourrait s'associer aux sites de synthèse d'ADN dépendent de la recombinaison via son interaction avec des facteurs de la RH. L'ensemble des données de cette étude contribuent à renforcer le rôle de CAF-1 couplé à la réparation de l'ADN, et révèlent une interconnexion entre les facteurs de la RH et l'assemblage de la chromatine.

Université Paris-Saclay

Espace Technologique / Immeuble Discovery

Route de l'Orme aux Merisiers RD 128 / 91190 Saint-Aubin, France

Title : Characterization of physical and functional interactions between the chromatin assembly factor 1, CAF-1, and homologous recombination factors during DNA repair

Keywords : homologous recombination, DNA repair, chromatin

Abstract : DNA is constantly exposed to both endogenous and exogenous genotoxic insults. Multiple DNA repair mechanisms are exploited to guard the genome and epigenome stability. Homologous recombination (HR) plays a major role in repairing DNA double strand breaks (DSBs) and restarting stalled replication forks under replicative stress. These two processes are both coupled to chromatin assembly. The chromatin assembly factor 1 (CAF-1) is a highly conserved histone chaperone known to function in a network of nucleosome assembly coupled to DNA repair and replication, by depositing newly synthesized histone $(H3\text{-}H4)_2$ tetramers onto the DNA. The fission yeast CAF-1 complex consists of three subunits: Pcf1, Pcf2 and Pcf3. CAF-1 has been previously reported to act at the DNA synthesis step during the process of recombination-dependent replication (RDR) and protects the D-loop from disassembly by the RecQ helicase family member, Rqh1. In this study, we addressed the role of CAF-1 during homologous recombination-mediated DNA repair in fission yeast. Using *in vivo* and *in vitro* approaches, we validated interactions within a complex containing Rqh1, CAF-1, PCNA, and Histone H3. We showed that Rqh1 interacts with both Pcf1 and Pcf2 independently of each other, and the Pcf1-Rqh1 interaction is stimulated by DNA damage. We developed an in vivo chromatin binding assay to monitor the association of CAF-1 to the chromatin upon DNA damage. We observed that replication stress but not double strand break favors CAF-1 association to the chromatin. We identified that several HR factors are required for CAF-1 association to the chromatin upon replication stress. In support of this, we have identified physical interactions between Pcf1 and HR factors, including RPA and Rad51. Our data suggest that CAF-1 would associate to the site of recombination-dependent DNA synthesis through physical interactions with HR factors. Put together, this work contributes to strengthening the role of CAF-1 coupled to DNA repair, and reveals the crosstalk between HR factors and chromatin assembly.

Université Paris-Saclay

Espace Technologique / Immeuble Discovery

Route de l'Orme aux Merisiers RD 128 / 91190 Saint-Aubin, France